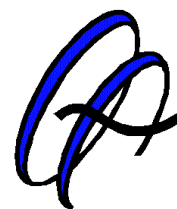




Universidad de Córdoba



Departamento de
Química Analítica

NANOPARTÍCULAS COMO HERRAMIENTAS ANALÍTICAS Y ESTUDIOS TOXICOLÓGICOS ASOCIADOS



NANOPARTICLES AS ANALYTICAL TOOLS AND ASSOCIATED TOXICITY STUDIES

Tesis Doctoral
Encarnación Caballero Díaz
Córdoba, 2014

TITULO: *Nanopartículas como herramientas analíticas y estudios toxicológicos asociados*

AUTOR: *Encarnación Caballero Díaz*

© Edita: Servicio de Publicaciones de la Universidad de Córdoba. 2014
Campus de Rabanales
Ctra. Nacional IV, Km. 396 A
14071 Córdoba

www.uco.es/publicaciones
publicaciones@uco.es

**NANOPARTÍCULAS COMO HERRAMIENTAS
ANALÍTICAS Y ESTUDIOS
TOXICOLÓGICOS ASOCIADOS**


EL DIRECTOR,



Fdo. Miguel Valcárcel Cases
Catedrático del Departamento
de Química Analítica de la
Universidad de Córdoba

*Trabajo presentado para aspirar al
grado de Doctor en Ciencias*

LA DOCTORANDA,



Fdo. Encarnación Caballero Díaz
Licenciada en Ciencias Ambientales

Miguel Valcárcel Cases, Catedrático del Departamento de Química Analítica de la Universidad de Córdoba,

EN CALIDAD DE:

Director de la Tesis Doctoral presentada por la Licenciada en Ciencias Ambientales ENCARNACIÓN CABALLERO DÍAZ, titulada “Nanopartículas como Herramientas Analíticas y Estudios Toxicológicos Asociados”,

CERTIFICA:

- 1) Que el trabajo experimental de la Tesis Doctoral ha sido desarrollado en los laboratorios del Departamento de Química Analítica de la Universidad de Córdoba (España) y en el Institut für Biophotonik (Fachbereich Physik) de la Philipps Universität Marburg (Alemania).
- 2) A mi juicio, reúne todos los requisitos exigidos a este tipo de trabajo.
- 3) Encarnación Caballero es la primera autora de todos los trabajos científicos desarrollados durante la fase experimental de la Tesis. De acuerdo a la normativa de la Universidad y los acuerdos internos de nuestro grupo de investigación, el primer autor es el responsable por completo de la implementación del trabajo experimental y de la producción de la primera versión del artículo. Además, ella ha participado activamente en las reuniones con el director para comprobar y discutir el progreso del trabajo doctoral.

Córdoba, a 28 de Enero de 2014.



Miguel Valcárcel Cases

Miguel Valcárcel Cases, Full Professor of Analytical Chemistry of the University of Córdoba,

IN QUALITY OF:

Supervisor of the Doctoral Thesis of ENCARNACIÓN CABALLERO DÍAZ, entitled “Nanoparticles as Analytical Tools and Associated Toxicity Studies”,

CERTIFIES THAT:

1) The experimental work of the PhD thesis has been developed in the laboratories of the Department of Analytical Chemistry of the University of Córdoba (Spain) and the Institute of Biophotonic (Department of Physics) of the Phillips University of Marburg (Germany).

2) According to my judgment the thesis meets all the requirements of this type of scientific work.

3) Encarnación Caballero is the first author of all the scientific works developed during the experimental phase of the Thesis. According to the University rules and the internal agreements in our research group, the first author of a paper is the full responsible for the implementation of the experimental work and also to produce the first draft of the paper. In addition, she has also actively participated in the meetings with the supervisor to check and discuss the progress of the doctoral work.

Córdoba, 28th January 2014

A handwritten signature in black ink, consisting of a large, stylized initial 'M' followed by a series of vertical and diagonal strokes, ending in a long horizontal line that extends to the right.

Miguel Valcárcel Cases



TÍTULO DE LA TESIS: NANOPARTÍCULAS COMO HERRAMIENTAS ANALÍTICAS Y ESTUDIOS TOXICOLÓGICOS ASOCIADOS

DOCTORANDO/A: Encarnación Caballero Díaz

INFORME RAZONADO DEL/DE LOS DIRECTOR/ES DE LA TESIS

La doctoranda Encarnación Caballero Díaz cursó brillantemente los estudios del Máster en Química Fina Avanzada, obteniendo excelentes calificaciones en las asignaturas del mismo. El trabajo fin de Máster se publicó en la revista Analytical Methods, situada en el tercer cuartil del área de conocimiento.

La temática de la tesis se encuadra en una línea de investigación puntera, como es la Nanociencia y Nanotecnología Analíticas. En este sentido, se han desarrollado métodos analíticos para la determinación de contaminantes emergentes en matrices ambientales que implican el empleo de nanopartículas como herramientas analíticas. Asimismo la investigación también estuvo enfocada a evaluar la toxicidad asociada a dos tipos de nanopartículas (nanopartículas de plata y nanotubos de carbono) bajo la influencia de diferentes factores determinantes en la misma.

La realización de la investigación recogida en la Memoria que se presenta, ha permitido a la doctoranda adquirir una sólida formación analítica, adiestrándose en el manejo de técnicas de separación electroforéticas, espectroscopias de absorción UV/Vis, fluorescencia y Raman, y microscopía electrónica de transmisión, entre otras. Asimismo, se han analizado contaminantes emergentes de distinta naturaleza en muestras ambientales, principalmente en agua de río, lo que ha permitido completar la formación integral de la doctoranda en el ámbito analítico. Todo ello ha dado lugar a seis trabajos científicos y dos trabajos de revisión publicados o en vías de publicación en revistas incluidas dentro de los tres primeros cuartiles del área de Química Analítica. También han sido fruto de esta Tesis Doctoral nueve comunicaciones a Congresos nacionales o internacionales, cuatro de ellas orales/flash.

La estancia realizada en el grupo de investigación del Prof. Parak (Universidad de Marburg, Alemania) durante el desarrollo de la Tesis Doctoral ha complementado de forma satisfactoria dicha formación, adquiriendo nuevos conocimientos relacionados con la evaluación de la toxicidad asociada a las nanopartículas de plata a través de la realización de ensayos *in vitro*.

Por todo ello, considero que la investigación desarrollada y recogida en esta Memoria, reúne todos los requisitos necesarios en cuanto a originalidad, innovación y calidad, y autorizo la presentación de la Tesis Doctoral de D^a Encarnación Caballero Díaz.

Córdoba, a 28 de Enero de 2014

Firma del/de los director/es

Fdo.: Miguel Valcárcel Cases

MENCIÓN DOCTORADO INTERNACIONAL

Mediante la defensa de esta Memoria de Tesis Doctoral se pretende optar a la obtención de la Mención de “Doctorado Internacional” habida cuenta de que el doctorando reúne los requisitos para tal mención (R.D. 99/2011, de 28 de Enero):

1. Cuenta con los informes favorables de dos doctores pertenecientes a instituciones de Enseñanza Superior de países distintos a España.
2. Uno de los miembros del tribunal que ha de evaluar la Tesis pertenece a un centro de Enseñanza Superior de otro país distinto a España.
3. Parte de la defensa de la Tesis Doctoral se realizará en una lengua distinta de las lenguas oficiales en España.
4. La doctoranda ha realizado una estancia de cuatro meses en el Institut für Biophotonik (Fachbereich Physik) de la Philipps Universität Marburg (Alemania), gracias a la concesión de una ayuda para estancias en el extranjero asociada a una beca de Formación de Profesorado Universitario del Ministerio de Educación, Cultura y Deporte, que ha contribuido a su formación y permitido desarrollar parte del trabajo experimental de esta Memoria.

Agradezco al Ministerio de Educación, Cultura y Deporte la concesión de una beca de Formación de Profesorado Universitario (FPU) que ha hecho posible mi dedicación a este trabajo durante los últimos cuatro años.

**“Al terminar de escalar una colina solo nos queda disfrutar el momento
y agradecer a todos los que lo hicieron posible”**
(E.Caballero)

A *Miguel*, por alumbrarme cada tramo de esta larga travesía, por transmitirme el afán por aprender y superarme. Valoro cada gesto, cada comentario de ánimo siempre oportuno que me revitalizaba y llenaba de fuerza para continuar. GRACIAS por darme un empujón constante de optimismo y confianza en mí misma de la que tanto carezco. Eres una persona de las que se puede aprender con creces tanto profesional como personalmente. Pero sobre todo, GRACIAS por recordarme constantemente que siempre caminaba acompañada, difícil expresar lo que ha significado tu apoyo para mí...esas son de las cosas que siempre recordaré... Las dificultades compartidas aparte de hacerse más llevaderas, unen tremendamente a las personas... GRACIAS POR HACERME SENTIR AFORTUNADA.

A los actuales integrantes del MAGNÍFICO grupo FQM-215, *Merche, Mayte, Guille, Maruchi, Laura C, Emi, Rocío, Azahara, Julia, M^a del Mar, Bea, Nati y Jeanette*. A otros que ya partieron, *Bricio, Yoli, Carolina, Eva, Marta, Fran, Juanma e Isa*. A mis forasteros, *M^a Ysabel, Sara, Carla, Patarollo, Sofi, Andrés, Flora y Raúl*. Sois unas personas formidables, me llevo lo mejor de cada uno que no es poco. He disfrutado cada momento compartido con vosotros, GRACIAS por hacerme sentir en casa y ayudarme a crecer como persona. Es un lujo sentir el cariño de la gente, GRACIAS por brindarme con él. El grupo FQM-215 seguirá manteniendo el encanto que lo caracteriza porque así lo hacéis posible cada uno de vosotros.

A mis chicas Proyecto INSTANT, *Celia y Laura S*, compañeras y confidentes, desde que os conocí pensé que érais unas excelentes personas y no me equivoqué, es más, lo sigo corroborando día a día, GRACIAS por vuestro apoyo y compañía.

A mis cuatro niñas, *Lola, Sandra, Mari y Ángela*, sois un recuerdo imborrable de mi paso por este lugar... amigas y casi hermanas, me habéis hecho reír, me habéis consolado y arropado en estos años... hombro con hombro... Tan simple de decir como que no hubiera pasado todo esto sin vosotras. Por compartir tantas vivencias y sentimientos..., OS QUIERO.

A *Jose Manuel*, como ya te advertí, aquí va tu merecida dedicatoria. Por tus emails recordatorios, por estar al pie del cañón, por tu ayuda día tras día; es de admirar tu esfuerzo por hacer que todo marche, GRACIAS.

A *Rafa, Marisol, Lourdes*, por acompañarme estos años. A *Juan Manuel* por su ayuda y consejos en prácticas de laboratorio. A *Diego* por sus “buenos días” acompañado de una sonrisa. *Al resto de profesores y PAS* del departamento, a los *compañeros de otras plantas*, GRACIAS.

I would like to thank Wolfgang Parak and all members of his research group, for their support and comradeship during my stay in the University of Marburg (Germany). This gave me the opportunity to open my mind and face new personal and professional challenges. Spaniards... *Jose, Susana, Dorleta* and *Pili*, you were THE LIFE and HAPPINESS of that laboratory, there is nothing like going abroad and feeling at home. A special mention for *Dominik, Moritz, Markus, Christian, Lena, Stefanie* and *Verena*, thanks for accepting me as one of your own, you are GREAT and I will NEVER FORGET YOU!

Dear friend *Wolfgang*, the life has a lot of good things but the most important one is to enjoy the little things and share them with the best people. It is admirable your honest and kind character towards your friends, and for being one of them is because I feel so lucky. Many people go through our life without leaving trace, but others like you, make one feels grateful that our paths crossed in the past. DANKE!

.....

Me gustaría también tener unas palabras para el Departamento de Biología Celular, Fisiología e Inmunología de la Universidad de Córdoba, con los que he tenido la gran suerte de hacer una colaboración durante mi Tesis Doctoral. A la profesora *M^a del Mar Malagón*, por su profesionalidad, disponibilidad, ayuda y ánimo prestado durante el trabajo. A *Rocío, Laura, Alberto* y *Antonio*, por su compañerismo con esta “analítica”, y por sus consejos y momentos de charla. Sin duda, aparte de enriquecer mi conocimiento en un ámbito que tanto me apasiona, he tenido la oportunidad de conocer a unas *grandes* personas. GRACIAS POR HACERME PARTÍCIPE DE ESTA EXPERIENCIA!

***“La mayor gloria no es nunca caer,
sino levantarse siempre”***

(Nelson Mandela)

Y he podido levantarme gracias a ellos...A mi FAMILIA

Mamá, Papá... apoyo continuo, sabéis como soy, sabéis que os estoy eternamente agradecida. No habría podido afrontar esto sin vuestra ayuda, sin vuestros consejos, sin vuestro saber escuchar. GRACIAS por entenderme, por animarme, por no fallarme nunca, sois mi vida y os lo debo todo. Disfruto cada momento que paso con vosotros, sois mis confidentes, cómplices de mis logros, indispensables en mi vida... he crecido de vuestra mano... OS ADORO!

Ali, Celia, Mariam, Toñín......mis pilares, mis ejemplos a seguir, siendo la más pequeña de la familia siempre me he sentido arropada por vosotros, hermanos... GRACIAS por entenderme y cuidarme.

Mª Ángeles, Lucía, Antonio C, Antonio G, Antonio R, David, Sofía...... mis tesoros, sois mi alegría aunque sé que sois demasiados pequeños para daros cuenta de esto, pero quiero que quede constancia de que soy la tita más afortunada del mundo por teneros! OS QUIERO!

Mayte, Carlos, Carmen, Raúl... amigos, siempre cercanos, os agradezco vuestra compañía y apoyo durante tantos años. Mayte y Carmen, en especial a vosotras, GRACIAS por mimarme, y ayudarme en tantos momentos!

Juan, cómo agradecerte... cada paso que he dado ha sido de tu mano, cada decisión tomada tenía un apoyo por tu parte, cada obstáculo que encontraba lo salvaba con tu ayuda, eres todo en lo que me he convertido, GRACIAS por hacerme mejor persona, por ayudarme a superar mis retos, por sacarme una sonrisa cuando parecía impensable, GRACIAS por apreciarme, por quererme como soy, y por recordármelo cada día. No hay nada más bonito que una persona que te acompañe y te deje ser como verdaderamente eres. TE QUIERO!

Nunca lo olvidaré... mucho de esto es vuestro

Si algo he aprendido es que la mayor flaqueza de una persona puede ser su miedo a defraudar a todos, en especial a uno mismo.

La barrera personal que nos imponemos puede ser más implacable y demoledora que cualquier error cometido.

***A**prende de la vida porque en errar consiste!,*

***A**vanza firme paso a paso! y*

***Á**rmate de valor frente a las adversidades!*

Éstas serán tus fortalezas!

(E.Caballero)

.....
Cada página escrita esconde una experiencia personal vivida...

Aquí os presento pues mi diario de vivencias...



ÍNDICE

INDEX

ACRÓNIMOS / <i>ABBREVIATIONS</i>	1
OBJETO / <i>AIM</i>	9
BLOQUE I. INTRODUCCIÓN	17
I.1. Aplicaciones analíticas de las nanopartículas	19
- Tratamiento de muestra	
- Separación instrumental	
- Detección	
I.2. Multiplexed Sensing and Imaging with Colloidal Nano- and Microparticles	43
I.3. Toxicidad asociada a las nanopartículas	93
- Rutas de liberación y exposición	
- Procesos de internalización celular	
- Mecanismos que inducen toxicidad	
- Métodos de evaluación de la <i>Nanotoxicidad</i>	
- Retos en la evaluación de la <i>Nanotoxicidad</i>	
I.4. The social responsibility of Nanoscience and Nanotechnology: an integral approach	117
BLOQUE II. HERRAMIENTAS ANALÍTICAS	147
II.1. Herramientas para los estudios de aplicaciones analíticas	149
- Analitos, reactivos y muestras	
- Nanopartículas	

- Síntesis de nanopartículas	
- Métodos de tratamiento de muestra	
- Instrumentación, aparatos y otros materiales	
II.2. Herramientas para los estudios de toxicidad	164
- Analitos y reactivos	
- Síntesis de nanopartículas de plata	
- Material biológico	
- Ensayos de viabilidad celular	
- Instrumentación	
II.3. Gestión de residuos generados	177
BLOQUE III. NANOPARTÍCULAS COMO HERRAMIENTAS ANALÍTICAS	179
.....	
Introducción	181
III.1. Nanodiamonds assisted-cloud point extraction for the determination of fluoranthene in river water	185
III.2. Liquid-liquid extraction assisted by a carbon nanoparticles interface. Electrophoretic determination of atrazine in environmental samples	209
III.3. Carbon nanotubes as SPE sorbents for extraction of salicylic acid from river water	231
III.4. Microextraction by packed sorbents combined with Surface-enhanced Raman spectroscopy for determination of musk ketone in river water	249
BLOQUE IV. ESTUDIOS TOXICOLÓGICOS DE NANOPARTÍCULAS	269
.....	
Introducción	271
IV.1. The toxicity of silver nanoparticles depends on their uptake by cells and thus on their surface chemistry	273

IV.2. Effects of the interaction of single-walled carbon nanotubes with 4-nonylphenol on their <i>in vitro</i> toxicity	315
BLOQUE V. RESULTADOS Y DISCUSIÓN	341
.....	
CONCLUSIONES / <i>CONCLUSIONS</i>	393
.....	
AUTOEVALUACIÓN / <i>SELF-ASSESSMENT</i>	401
.....	
ANEXOS. PRODUCCIÓN CIENTÍFICA	407
.....	
Anexo A. Publicaciones científicas derivadas de la Tesis Doctoral	407
Anexo B. Presentación de comunicaciones a congresos	419
Anexo C. Pósters	425



ACRÓNIMOS

ABBREVIATIONS

ACNTs	Membranas de nanotubos de carbono alineados / <i>Aligned carbon nanotube membranes</i>
AENOR	Asociación española de normalización y certificación / <i>Spanish association for standardization and certification</i>
AgNPs	Nanopartículas de plata / <i>Silver nanoparticles</i>
AuNPs	Nanopartículas de oro / <i>Gold nanoparticles</i>
BRET	Transferencia de energía de resonancia de bioluminiscencia / <i>Bioluminescence resonance energy transfer</i>
CE	Electroforesis capilar / <i>Capillary electrophoresis</i>
CMC	Concentración micelar crítica / <i>Critical micelle concentration</i>
CNIM	Membranas de nanotubos de carbono inmovilizados / <i>Carbon nanotube immobilized membranes</i>
CNPs	Nanopartículas de carbono / <i>Carbon nanoparticles</i>
CNTs	Nanotubos de carbono / <i>Carbon nanotubes</i>
CPE	Extracción punto de nube / <i>Cloud point extraction</i>
CPT	Temperatura punto de nube / <i>Cloud point temperature</i>
CRET	Transferencia de energía de resonancia de quimioluminiscencia / <i>Chemiluminescence resonance energy transfer</i>
CSP	Responsabilidad social de funcionamiento interno / <i>Corporate social performance</i>
CSR	Responsabilidad social corporativa / <i>Corporate social responsibility</i>
d_h	Diámetro hidrodinámico / <i>Hydrodynamic diameter</i>

Acrónimos / Abbreviations

DLS	Dispersión de luz dinámica / <i>Dynamic light scattering</i>
DMEM	Medio de cultivo Eagle modificado de Dulbecco / <i>Dulbecco's modified Eagle medium</i>
DMSO	Dimetilsulfóxido / <i>Dimethyl sulfoxide</i>
DSPE	Extracción en fase sólida dispersiva / <i>Dispersive solid-phase extraction</i>
EDC	1-Etil-3-(3-dimetilaminopropil)carbodiimida / <i>1-Ethyl-3-(3-dimethylaminopropyl)carbodiimide</i>
EF	Factor de enriquecimiento / <i>Enrichment factor</i>
EIIs	Inmunoensayos e inmunosensores electroquímicos / <i>Electrochemical immunosensors and immunoassays</i>
EKC	Cromatografía electrocinética / <i>Electrokinetic chromatography</i>
EPA	Agencia de protección ambiental de los Estados Unidos / <i>US Environmental protection agency</i>
FBS	Suero fetal bovino / <i>Fetal bovine serum</i>
FECYT	Fundación española para la ciencia y la tecnología / <i>Spanish foundation for science and technology</i>
FRET	Transferencia de energía de resonancia de Förster / <i>Förster resonance energy transfer</i>
GC	Cromatografía de gases / <i>Gas chromatography</i>
GC-MS	Cromatografía de gases-espectrometría de masas / <i>Gas chromatography-mass spectrometry</i>
ICP-MS	Espectrometría de masas con plasma de acoplamiento inductivo / <i>Inductively coupled plasma mass spectrometry</i>

ILO	Organización internacional del trabajo / <i>International labour organization</i>
IR	Infrarrojo / <i>Infrared</i>
ISO	Organización internacional de normalización / <i>International organization for standardization</i>
IUPAC	Unión internacional de química pura y aplicada / <i>International union of pure and applied chemistry</i>
LC	Cromatografía de líquidos / <i>Liquid chromatography</i>
LD₅₀	Dosis letal media / <i>Median lethal dose</i>
LDH	Lactato deshidrogenasa / <i>Lactate dehydrogenase</i>
LLE	Extracción líquido-líquido / <i>Liquid-liquid extraction</i>
LPME	Microextracción en fase líquida / <i>Liquid-phase microextraction</i>
LSPR	Resonancia de plasmón superficial localizado / <i>Localized surface plasmon resonance</i>
MEPS	Microextracción con adsorbentes empaquetados / <i>Microextraction by packed sorbent</i>
MiNDEKC	Cromatografía electrocinética micelar de nanopartículas dispersadas / <i>Micellar nanoparticle dispersed electrokinetic chromatography</i>
MIPs	Polímeros de impresión molecular / <i>Molecular imprinted polymers</i>
MK	Almizcle de cetona / <i>Musk ketone</i>
MMM	Membranas de matriz mixta / <i>Mixed matrix membranes</i>
MNPs	Nanopartículas magnéticas / <i>Magnetic nanoparticles</i>

Acrónimos / Abbreviations

MR	Resonancia magnética / <i>Magnetic resonance</i>
MRI	Imagen por resonancia magnética / <i>Magnetic resonance imaging</i>
MS	Espectrometría de masas / <i>Mass spectrometry</i>
MSPE	Extracción en fase sólida magnética / <i>Magnetic solid-phase extraction</i>
MTT	Bromuro de 3-(4,5-dimetiltiazol-2-il)-2,5 difeniltetrazolio / <i>3-(4,5-dimethylthiazol-2-yl)-2,5 diphenyl tetrazolium bromide</i>
MUA	Ácido mercaptoundecanoico / <i>Mercaptoundecanoic acid</i>
MWCNTs	Nanotubos de carbono multicapa / <i>Multi-walled carbon nanotubes</i>
MWCNTs-1	Nanotubos de carbono multicapa de la casa comercial Bayer / <i>Multi-walled carbon nanotubes provided by Bayer</i>
MWCNTs-2	Nanotubos de carbono multicapa de la casa comercial Nanocyl / <i>Multi-walled carbon nanotubes provided by Nanocyl</i>
MWCNTs-3	Nanotubos de carbono multicapa de la casa comercial MER / <i>Multi-walled carbon nanotubes provided by MER</i>
MWCNTs_{ox}	Nanotubos de carbono multicapa oxidados / <i>Oxidized multi-walled carbon nanotubes</i>
MWCO	Peso molecular de corte / <i>Molecular weight cut off</i>
ND_{ol}	Nanodiamantes oleofílicos / <i>Oleophilic nanodiamonds</i>
NDs	Nanodiamantes / <i>Nanodiamonds</i>
NDs-MWCNTs	Nanopartículas híbridas formadas por nanodiamantes y nanotubos de carbono multicapa / <i>Hybrid nanoparticles composed of nanodiamonds and multi-walled carbon nanotubes</i>

NIR	Infrarrojo cercano / <i>Near infrared</i>
N&N	Nanociencia & Nanotecnología / <i>Nanoscience & Nanotechnology</i>
NP	4-nonilfenol / <i>4-nonylphenol</i>
NPs	Nanopartículas / <i>Nanoparticles</i>
OECD	Organización para la cooperación y el desarrollo económicos / <i>Organization for economic cooperation and development</i>
PAHs	Hidrocarburos aromáticos policíclicos / <i>Polycyclic aromatic hydrocarbons</i>
PBS	Tampón fostato salino / <i>Phosphate buffered saline</i>
PEG	Polietilenglicol / <i>Polyethylene glycol</i>
PET	Transferencia electrónica fotoinducida / <i>Photoinduced electron-transfer</i>
PMA	Anhídrido maleico de poliisobutileno modificado con dodecilamina / <i>Dodecylamine modified poly(isobutylene-alt-maleic anhydride)</i>
QDs	Puntos cuánticos / <i>Quantum dots</i>
R&D	Investigación & Desarrollo / <i>Research & Development</i>
R&D&I	Investigación & Desarrollo & Innovación / <i>Research & Development & Innovation</i>
ROS	Especies reactivas de oxígeno / <i>Reactive oxygen species</i>
RSD	Desviación estándar relativa / <i>Relative standard deviation</i>
SA	Ácido salicílico / <i>Salicylic acid</i>
SDS	Dodecil sulfato de sodio / <i>Sodium dodecyl sulfate</i>

Acrónimos / Abbreviations

SEM	Microscopía electrónica de barrido / <i>Scanning electron microscopy</i>
SERS	Espectroscopía Raman amplificada por superficie / <i>Surface enhanced Raman spectroscopy</i>
SERRS	Dispersión Raman resonante amplificada por superficie / <i>Surface-enhanced resonance Raman scattering</i>
SPE	Extracción en fase sólida / <i>Solid-phase extraction</i>
SPME	Microextracción en fase sólida / <i>Solid-phase microextraction</i>
SPR	Resonancia de plasmón superficial / <i>Surface plasmon resonance</i>
SR	Responsabilidad social / <i>Social responsibility</i>
SWCNTs	Nanotubos de carbono de pared simple / <i>Single-walled carbon nanotubes</i>
SWCNTs-PEG	Nanotubos de carbono de pared simple recubiertos de polietilenglicol / <i>Polyethylene glycol coated single-walled carbon nanotubes</i>
TBE	Tris-Borato-EDTA / <i>Tris-Borate-EDTA</i>
TEM	Microscopía electrónica de transmisión / <i>Transmission electron microscopy</i>
UN	Naciones Unidas / <i>United Nations</i>
UV-Vis	Ultravioleta-Visible / <i>Ultraviolet-Visible</i>



OBJETO

AIM



El tamaño nanométrico de las nanopartículas (NPs) les confiere unas excelentes e inusuales propiedades fisicoquímicas que son explotadas en diversas áreas de aplicación como la Electrónica, Biomedicina, Farmacia o Ciencia de los Materiales. A su vez, los continuos avances en los métodos de síntesis de las NPs, así como en su aplicabilidad, proporcionan grandes beneficios al ámbito de la Química Analítica en tanto en cuanto suponen el desarrollo de nuevos procedimientos analíticos o bien la mejora de otros ya existentes. En este sentido, el tratamiento de muestra, la separación instrumental y la detección, constituyen las tres etapas dentro del procedimiento analítico que pueden verse claramente beneficiadas por el empleo de las NPs.

Sin embargo, las NPs también presentan una faceta negativa ya que, como consecuencia de su producción masiva y uso creciente en la sociedad actual, son liberadas continuamente al medio ambiente donde entran en contacto con el medio abiótico y biótico. Es por tanto necesario llevar a cabo una evaluación exhaustiva sobre los posibles efectos tóxicos inherentes a las NPs que se están sintetizando y empleando actualmente.

También cabe mencionar que el comportamiento de las NPs en el medio ambiente no es comparable al de otros contaminantes ya conocidos, y que además, los protocolos de evaluación toxicológica disponibles actualmente no han sido convenientemente adaptados para su aplicación al ámbito de las partículas a escala nanométrica. Si además tenemos en cuenta el amplio espectro de NPs existentes con propiedades fisicoquímicas variables, llegamos a la conclusión de que la investigación en cuanto a toxicidad de los nanomateriales aún requiere mucho esfuerzo a día de hoy.

Teniendo en cuenta lo anteriormente expuesto, los objetivos genéricos de la Tesis Doctoral aquí presentada se centran, por un lado, en el desarrollo de

Objeto

nuevas metodologías analíticas basadas en el empleo de NPs como herramientas en las etapas de tratamiento de muestra y detección, y por otro lado, en evaluar la toxicidad *in vitro* asociada a las NPs de plata y los nanotubos de carbono bajo la influencia de diferentes factores condicionantes en la misma.

Estos objetivos genéricos se desglosan a su vez en las siguientes líneas de investigación más específicas:

- ⊕ Investigar el papel desempeñado por las NPs de carbono (CNPs) cuando son introducidas como fase adicional en las técnicas de extracción convencionales (en concreto, las extracciones punto de nube y líquido-líquido) aplicadas a la determinación de contaminantes de interés medioambiental.
- ⊕ Diseñar un procedimiento analítico sencillo basado en el empleo de CNPs como adsorbentes de extracción en fase sólida para determinar un compuesto farmacéutico en muestras de agua.
- ⊕ Desarrollar nuevas metodologías analíticas que impliquen el uso de NPs metálicas para mejorar considerablemente la sensibilidad de la etapa de detección mediante Espectroscopía Raman.
- ⊕ Esclarecer la influencia de la química superficial de las NPs de plata sobre diversos factores que determinan su grado de citotoxicidad.
- ⊕ Estudiar la citotoxicidad de los nanotubos de carbono en presencia de un contaminante ambiental común, con el propósito de identificar posibles mecanismos de toxicidad combinada (adición, antagonismo o sinergia) cuando ambas especies entran en contacto.

Aparte de la labor investigadora desempeñada durante la Tesis Doctoral y que ha contribuido indiscutiblemente a la formación de la doctoranda, otras actividades complementarias como la asistencia a cursos formativos y la presentación de comunicaciones/pósters en congresos (tanto de ámbito nacional como internacional) también le han permitido ampliar sus conocimientos y adquirir nuevas destrezas. La producción científica derivada de la Tesis Doctoral, así como las contribuciones a congresos son recogidas en su totalidad en los Anexos de esta Memoria.

Aim

The nanometric size of nanoparticles (NPs) confers them excellent and unusual physicochemical properties that are exploited in diverse application fields such as Electronics, Biomedicine, Pharmacy or Materials Science. Moreover, continuous advances in the methods for nanoparticle synthesis, as well as in their applicability, benefit the Analytical Chemistry field inasmuch as they lead to the development of novel analytical procedures or the improvement of other already existing. In this regard, sample treatment, instrumental separation and detection, constitute the three stages within the analytical procedure which may clearly benefit from the use of NPs.

Nevertheless, NPs also exhibit a negative side since, as a result of their mass production and growing use in today's society, they are continuously released into the environment where interact with biotic and abiotic media. It is therefore mandatory to carry out a thorough assessment of the possible toxic effects inherent to NPs which are synthesized and used currently.

It is also noteworthy that the behavior of NPs in the environment is not comparable to that of other already known contaminants, and in addition, the toxicological assessment protocols currently available have not been properly adapted for their application to nanoscale particles. If we also take into account the broad spectrum of existing NPs with tunable physicochemical features, we come to the conclusion that research on toxicity of nanomaterials still requires a great deal of effort as of today.

Based on the foregoing, the general objectives of the Doctoral Thesis presented herein are, on the one hand, to develop new analytical methodologies involving the use of NPs as tools in sample treatment and detection stages and, on the other hand, to assess the in vitro toxicity associated to silver NPs and carbon nanotubes under the influence of several determining factors.

These general goals are specified in the following research lines:

- ⊕ *Investigating the role of carbon NPs (CNPs) when they are introduced as additional phase in conventional extraction techniques (viz., cloud point and liquid-liquid extractions) applied to the determination of contaminants of environmental concern.*
- ⊕ *Designing a simple analytical procedure based on the use of CNPs as solid-phase extraction adsorbents for determining a pharmaceutical compound in water samples.*
- ⊕ *Developing new analytical methodologies that entail the utilization of metallic NPs to considerably improve the sensitivity of the detection by Raman spectroscopy.*
- ⊕ *Clarifying the influence of surface chemistry of silver NPs on several determining factors that influence their degree of cytotoxicity.*
- ⊕ *Studying the cytotoxicity of carbon nanotubes in presence of a known environmental contaminant, with the purpose of identifying possible mechanisms of combined toxicity (i.e. addition, antagonism or synergy) when both species come into contact.*

Apart from the research work performed during the Doctoral Thesis, which has undoubtedly contributed to the training of the PhD student, other supplementary activities including the attendance at various training courses and the presentation of oral communications and posters in conferences (both national and international ones) have also enabled doctoral student to broaden her knowledge and acquire new skills. The scientific production arising from the Doctoral Thesis along with the contributions to conferences are collected entirely in the Annexes of this Report.



BLOQUE I

Introducción

I.1. Aplicaciones analíticas de las nanopartículas	19
- Tratamiento de muestra	
- Separación instrumental	
- Detección	
I.2. Multiplexed Sensing and Imaging with Colloidal Nano- and Microparticles	43
I.3. Toxicidad asociada a las nanopartículas	93
- Rutas de liberación y exposición	
- Procesos de internalización celular	
- Mecanismos que inducen toxicidad	
- Métodos de evaluación de la Nanotoxicidad	
- Retos en la evaluación de la Nanotoxicidad	
I.4. The social responsibility of Nanoscience and Nanotechnology: an integral approach	117

I.1 Aplicaciones analíticas de las nanopartículas

En el marco de la Química Analítica, las nanopartículas (NPs) han sido ampliamente utilizadas como herramientas para mejorar o desarrollar métodos analíticos que permitan la determinación de nuevos analitos en diferentes y complejas matrices de estudio [1]. La Figura I.1.1 resume las principales aplicaciones analíticas de las NPs haciendo mención especial a los nanotubos de carbono (CNTs). Como se aprecia, las NPs pueden emplearse en las tres etapas del procedimiento analítico; tratamiento de muestra, separación instrumental y detección.

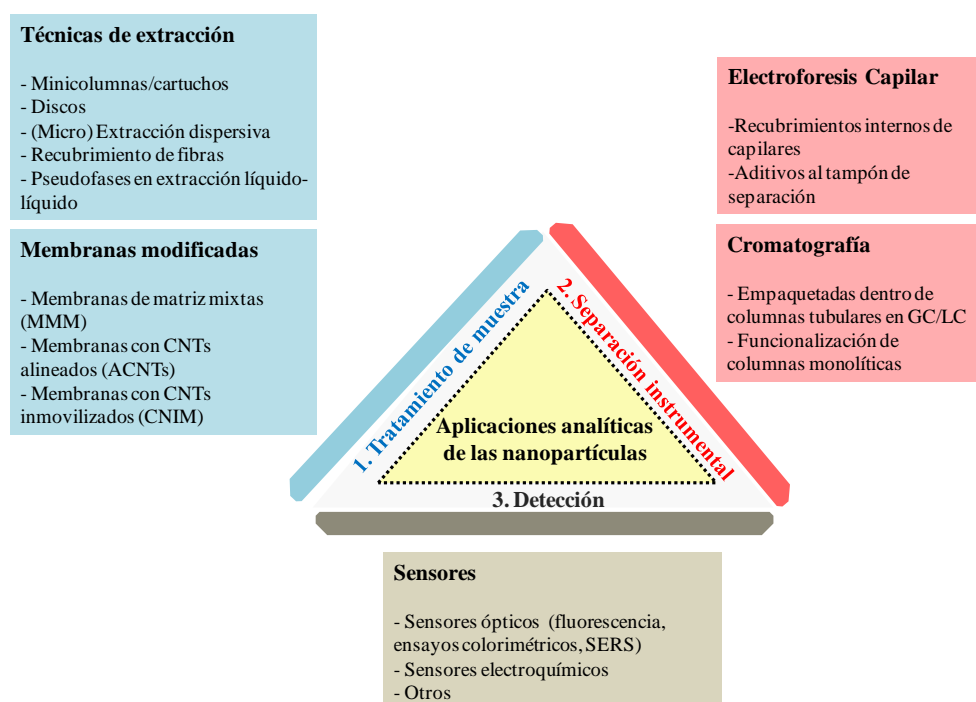


Figura I.1.1. Aplicaciones analíticas de las NPs, principalmente de los CNTs.

Durante el transcurso de este apartado, profundizaremos en mayor detalle en las nanopartículas de carbono (CNPs) empleadas en la etapa de

BLOQUE I. INTRODUCCIÓN

tratamiento de muestra por su mayor peso en la investigación desarrollada durante la Tesis Doctoral.

TRATAMIENTO DE MUESTRA

Las NPs son utilizadas en el tratamiento de muestra para extraer y preconcentrar los analitos de la matriz. Con este fin, estas partículas pueden introducirse en las técnicas de extracción convencionales como fases sorbentes, o bien como componentes de las membranas de extracción (ver Figura I.1.1). En esta sección discutiremos principalmente el empleo de los CNTs como sorbentes aunque también se hará alusión a otro tipo de NPs.

Nanotubos de carbono en (micro)extracción en fase sólida

Los CNTs han sido muy investigados como materiales sorbentes en la extracción en fase sólida (SPE) debido a su elevada área superficial específica y densidad de espacios intersticiales dentro de los agregados, características que les confieren una mayor interacción con los analitos [2]. Estas interacciones son de tipo no covalente, tales como enlaces de hidrógeno, interacciones π - π , fuerzas electrostáticas, fuerzas de van der Waals o interacciones hidrofóbicas. La habilidad de adsorción de los CNTs depende entre otros factores de su longitud y del número de láminas de grafeno que componen su estructura [3].

La aplicabilidad de los CNTs en SPE se ha centrado en la extracción de metales [4] y compuestos orgánicos [5], especialmente aquellos que presentan una estructura aromática o grupos funcionales superficiales de tipo -OH y -NH₂ que favorecen un mayor grado de interacción con las NPs. Una ventaja añadida es que la selectividad en la extracción puede lograrse mediante la funcionalización superficial de las NPs con ligandos de diversa naturaleza.

I.1. Aplicaciones analíticas de las nanopartículas

A continuación, se especifican las distintas estrategias que han sido descritas sobre SPE con el empleo de CNTs como fase sorbente.

▪ *Minicolumnas o cartuchos empaquetados*

En esta modalidad, los CNTs son empaquetados dentro de minicolumnas o cartuchos a través de los cuales se hace pasar la muestra con la consecuente separación del analito de la matriz gracias a su interacción con la fase estacionaria. La preconcentración se consigue posteriormente al eluir el analito con un volumen mínimo de disolvente. La principal limitación de esta estrategia radica en la posible obstrucción del cartucho cuando se analizan matrices muy complejas o cuando los CNTs son compactados en exceso. Esta obstrucción reduce la interacción potencial entre el analito y los CNTs, y como consecuencia, la eficiencia de extracción empeora. La Figura I.1.2 representa esta modalidad de SPE la cual ha sido aplicada a la extracción de diferentes compuestos [6,7].

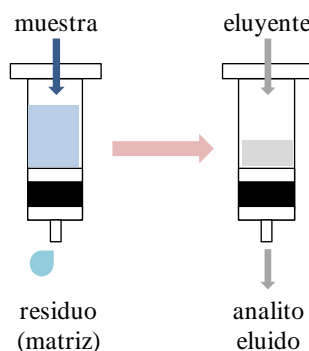


Figura I.1.2. Extracción con minicolumnas o cartuchos empaquetados.

▪ *Discos*

En este caso, la muestra se hace pasar a través de filtros modificados con CNTs. La preparación de estos filtros o discos consiste en filtrar dispersiones

BLOQUE I. INTRODUCCIÓN

homogéneas de CNTs obtenidas por sonicación. A diferencia de la modalidad anterior, la disposición más extendida de los CNTs por el filtro favorece una interacción reforzada con el analito, y puesto que aquí no hay problemas de compactación, también se permite un mayor flujo de muestra. Uno de los inconvenientes de esta modalidad tiene su origen en la irreproducibilidad derivada de la posible disposición no homogénea de las NPs por el soporte. El empleo de varios filtros conjuntamente es una estrategia bastante útil para maximizar la eficiencia de extracción tal y como ya se ha descrito en bibliografía relacionada [8]. La Figura I.1.3 ilustra la estrategia de extracción con discos.

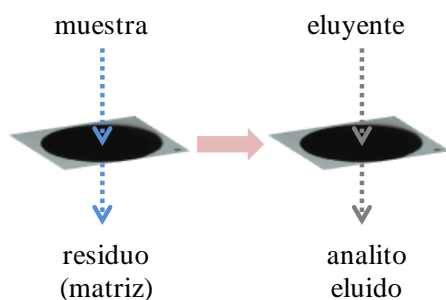


Figura I.1.3. Extracción con filtros modificados. Imagen de filtro perteneciente a [8].

▪ Extracción en fase sólida dispersiva (DSPE)

La extracción en fase sólida dispersiva o DSPE se produce en el seno de la muestra por la adición directa de las NPs a la disolución, y posterior retirada de las mismas por centrifugación o filtración principalmente. Posteriormente, la elución se efectúa sobre las NPs aisladas que interaccionaron previamente con el analito de la muestra. La Figura I.1.4 muestra de forma general el procedimiento de DSPE.

I.1. Aplicaciones analíticas de las nanopartículas

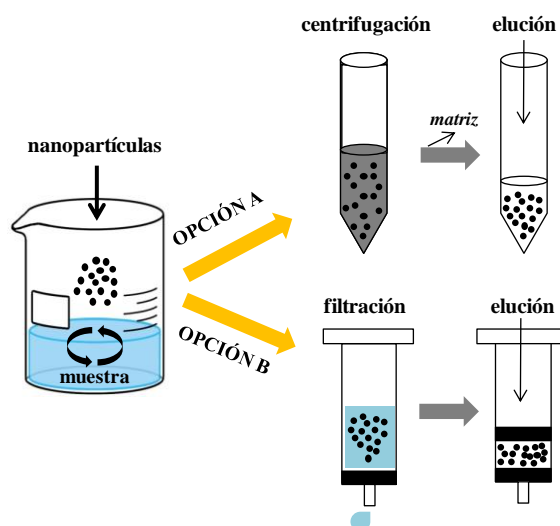


Figura I.1.4. Proceso de extracción y opciones de retirada de NPs en DSPE.

Por otro lado, las NPs magnéticas son buenas candidatas para su uso en DSPE gracias a su facilidad de retirada de la disolución por simple aplicación de un campo magnético externo [9]. Ejemplos de esta metodología han sido descritos para la extracción de pesticidas [10] y antibióticos [11]. La Figura I.1.5 muestra el procedimiento de DSPE con NPs magnéticas [12].

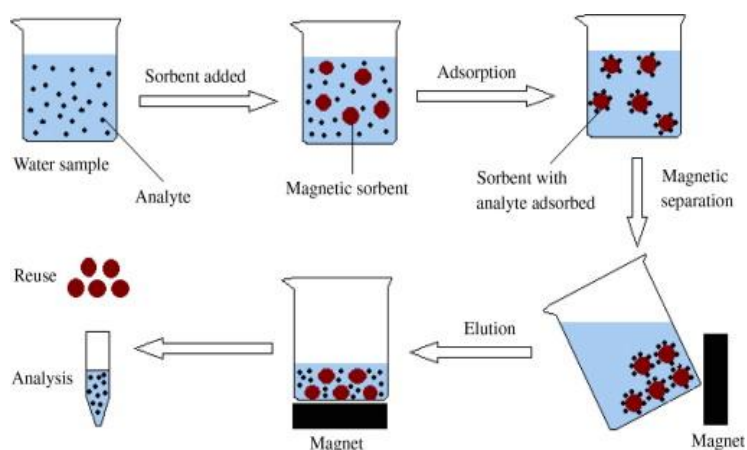


Figura I.1.5. DSPE con NPs magnéticas. Figura perteneciente a [12].

▪ Recubrimiento de fibras en microextracción en fase sólida (SPME)

La miniaturización ha ganado importancia dentro del ámbito de la SPE. La técnica de microextracción en fase sólida (SPME) se basa en el reparto del analito entre la muestra y, el espacio de cabeza o una fase estacionaria que recubre una fibra. La Figura I.1.6 representa las dos modalidades existentes de SPME. Las fibras de SPME modificadas con CNTs han sido investigadas para la extracción de aminas aromáticas [13], pesticidas [14], compuestos orgánicos volátiles [15], fenoles [16] y drogas [17]. A su vez, las NPs de óxidos metálicos también se han empleado como recubrimientos de fibras en SPME [18,19].

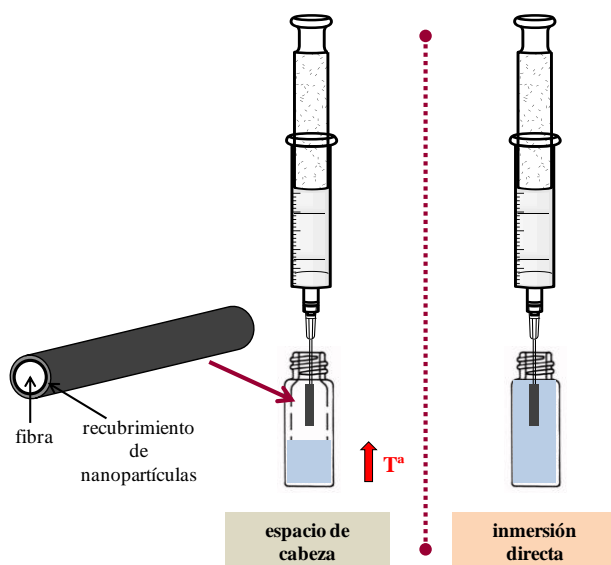


Figura I.1.6. Modalidades de SPME mediante generación de espacio de cabeza (izquierda) o por inmersión directa (derecha).

Como alternativa a los recubrimientos de fibras, también se han desarrollado unidades de extracción magnéticas en cuyo interior se almacenan las NPs sorbentes. Bajo aplicación de un campo magnético externo, la unidad magnética permite la agitación de la muestra y al mismo tiempo se produce la extracción mediada por las NPs de su interior [20-22].

Otras nanopartículas e híbridos empleados en SPE/SPME

Si bien es cierto que los CNTs tienen una mayor repercusión en el tratamiento de muestra, también existen otras NPs cuya aplicación a este ámbito conviene destacar.

La Figura I.1.7 muestra un diagrama de sectores con los porcentajes relativos correspondientes al número de publicaciones científicas en las que se utilizan NPs como sorbentes de SPE.

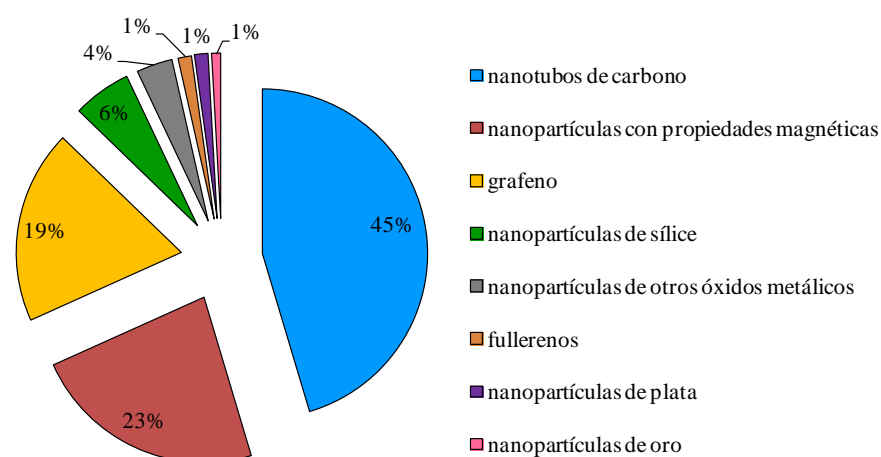


Figura I.1.7. Porcentajes relativos sobre artículos científicos que emplean diferentes NPs en SPE. (Fuente bibliográfica: SCOPUS).

Como se aprecia en el diagrama, los CNTs son las NPs más utilizadas en este ámbito. Les siguen en importancia, las NPs magnéticas y el grafeno. El resto de NPs sin embargo, no tienen mucha cabida en los procesos de tratamiento de muestra.

Dentro de las CNPs, los *fullerenos* muestran una excelente capacidad sorbente hacia los complejos metálicos y organometálicos, y consecuentemente,

BLOQUE I. INTRODUCCIÓN

han sido empleados para su extracción [23]. El *grafeno* se ha utilizado en la modalidad de minicolumnas o cartuchos empaquetados para la extracción de plomo [24], o como recubrimiento de fibras de SPME para extraer pesticidas organoclorados [25].

Dentro de las NPs metálicas, las *NPs de oro* muestran una elevada afinidad por los hidrocarburos aromáticos policíclicos (PAHs) y las especies de mercurio, y por ello se han empleado para la extracción de estos compuestos de diferentes matrices [26,27]. Las *NPs de plata* han sido investigadas como componentes de membranas para la extracción de uranio en agua de mar [28]. Las *NPs de óxidos metálicos* pueden ser utilizadas de forma aislada o formando hemimicelas/admicelas con surfactantes iónicos [29,30]. Las NPs magnéticas son las NPs de óxidos metálicos más empleadas en las técnicas de extracción y dan nombre a la técnica que se conoce como extracción en fase sólida magnética (MSPE) [31-34].

Las *NPs de sílice* son muy recomendables en el ámbito analítico ya que son químicamente inertes, de bajo coste y presentan una elevada estabilidad térmica. Además se pueden funcionalizar fácilmente gracias a la presencia de grupos silanol en su superficie. Por sus características, se han empleado principalmente como recubrimientos de fibras en SPME para la extracción de compuestos fenólicos y PAHs entre otros [35,36].

La combinación de diferentes NPs ha seguido al desarrollo de *sorbentes híbridos* que reúnen las características distintivas de las NPs involucradas. Aquí podemos citar la combinación de CNTs con, NPs magnéticas para la extracción de (fluoro)quinolonas en muestras de sangre, y con NPs de alúmina para la extracción de metales [37,38]. Estos híbridos facilitan la manipulación de la fase sorbente ya que son fáciles de extraer por aplicación de un campo magnético

externo. No obstante, presentan la desventaja de alterar la capacidad inherente de adsorción de los CNTs.

El empleo de los *CNTs en los polímeros de impresión molecular (MIPs)* se considera una de las estrategias de SPE de mayor selectividad. Además presenta una ventaja añadida sobre los MIPs convencionales y es que los sitios de unión con el analito se localizan en la capa más externa del composite. Estos composites se han descrito para la determinación de estrógenos y herbicidas en muestras de agua [39,40].

La combinación de *NPs con líquidos iónicos* ha resultado en la fabricación de sorbentes con una eficiencia de extracción mejorada en comparación con el uso exclusivo de NPs. Este tipo de sorbentes se han propuesto para la extracción de PAHs en muestras de agua [41,42].

Nanotubos de carbono en extracciones líquido-líquido

Mientras que las NPs han tenido una excelente acogida como materiales sorbentes en SPE, no han sido tantas las aplicaciones referentes a las extracciones líquido-líquido (LLE). En este sentido, solo se ha descrito en bibliografía un único procedimiento de tratamiento de muestra basado en una etapa de LLE asistida por NPs dispersas, para la extracción y preconcentración de compuestos aromáticos del aceite de oliva [43]. Como aportación a este ámbito, en esta Memoria se presenta un trabajo de investigación cuyo propósito fue modificar un sistema convencional de LLE mediante la inclusión de una interfase constituida por CNTs estabilizados en disolvente orgánico [44].

La mayoría de procedimientos de tratamiento de muestra que emplean la LLE en combinación con NPs (principalmente magnéticas), utilizan las NPs exclusivamente para retirar la fase extractante u orgánica una vez que ésta ha

extraído previamente el analito de la fase acuosa donadora. En otras palabras, la habilidad de adsorción de las NPs se aprovecha para retirar del medio la fase extractante orgánica que contiene el analito, pero las NPs no se emplean como extractantes del analito *per se* [45].

Nanopartículas en extracciones con surfactantes

A pesar de que se han desarrollado muchas metodologías analíticas que emplean medios micelares para la extracción y preconcentración de NPs, apenas se ha considerado el beneficio que las NPs pueden proporcionar como fase sorbente adicional en estas técnicas de extracción. Las NPs de alúmina, de oro, y magnéticas ya se han utilizado en combinación con algunos tensioactivos para la extracción de iones metálicos o compuestos orgánicos [46-48]. Como aportación científica a este ámbito de estudio, en esta Memoria se presenta un trabajo realizado que propone el empleo de nanodiamantes como fase adicional en un sistema de extracción punto de nube [49].

Nanotubos de carbono como componentes de membranas

Las propiedades sorbentes de las NPs también han sido explotadas en las extracciones con membranas. En este marco de aplicación, los CNTs son las NPs más investigadas.

Las membranas modificadas con CNTs, o también denominadas membranas nanoestructuradas, se han convertido en una alternativa bastante eficiente a las membranas poliméricas convencionales las cuales presentan los inconvenientes de una elevada tendencia a la obstrucción y bajas selectividad, permeabilidad y resistencias química y térmica. Los CNTs presentan una alta porosidad y área superficial, y además pueden ser funcionalizados superficialmente con ligandos específicos para permitir el transporte selectivo

I.1. Aplicaciones analíticas de las nanopartículas

de las moléculas de la fase donadora a la aceptora. El flujo de analito a través de una membrana incrementa cuanto mayor sea el área superficial efectiva y menor el espesor de ésta. Estas condiciones se dan cuando la membrana está constituida por una red de nanoporos. Si a esto le añadimos las propiedades sorbentes de los CNTs, podemos afirmar que estas NPs actúan como excelentes canales de transferencia de masa en los procesos con membranas [50].

La Figura I.1.8 representa los tres tipos de membranas nanoestructuradas modificadas con CNTs en función de su procedimiento de síntesis [50].

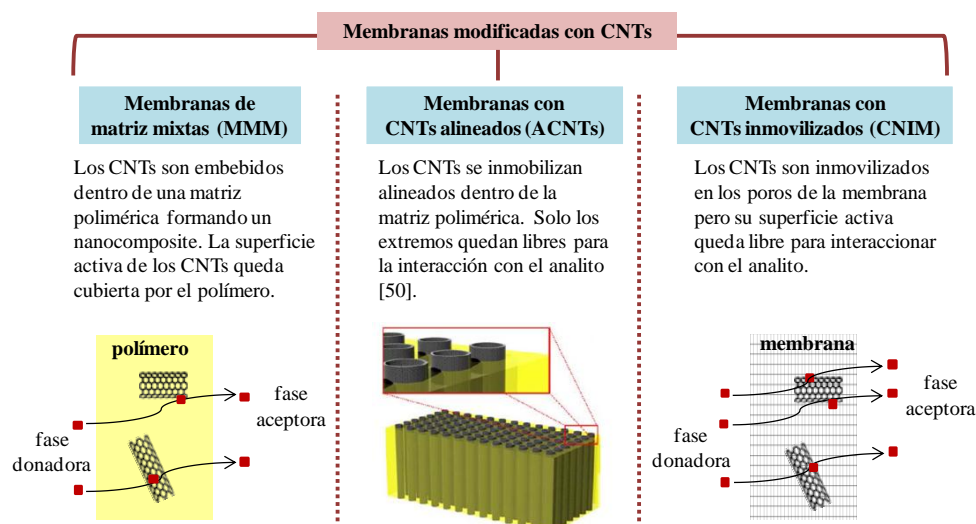


Figura I.1.8. Tipos de membranas modificadas con CNTs.

▪ Membranas de matriz mixtas (MMM)

Las membranas de matrix mixtas (MMM) se fabrican al fundir y mezclar un polímero con las NPs, de forma que se crea un composite con los CNTs embebidos dentro de la matriz polimérica. Esta estrategia conlleva algunos problemas derivados de la tendencia a la aglomeración de las NPs y su posible distribución no uniforme dentro de la matriz [51]. Las MMM se han utilizado

BLOQUE I. INTRODUCCIÓN

para la filtración de aguas [52], la separación de gases [53-56] y la extracción de pesticidas organofosforados de aguas residuales [57].

- *Membranas con nanotubos de carbono alineados (ACNTs)*

Estas membranas son similares a las MMM con la única diferencia de que en este caso los CNTs se inmovilizan en la matriz polimérica de forma alineada con uno de sus extremos libres y oxidados para incrementar su reactividad química e interacción con el analito. Puesto que la alineación de las NPs dentro de la matriz polimérica no supone grandes ventajas que justifiquen la complejidad añadida que entraña su síntesis en comparación con la de las MMM, las ACNTs no presentan muchas aplicaciones a día de hoy [58].

- *Membranas con nanotubos de carbono inmovilizados (CNIM)*

Aunque las MMM muestran ventajas significativas respecto a aquellas membranas sin modificar, el encapsulamiento de las NPs dentro de un polímero reduce su superficie activa de interacción y supone por tanto una barrera para la transferencia del analito de la fase donadora a la aceptora. Para solventar este problema y maximizar así la superficie de NPs disponible, también se han propuesto membranas en las que las NPs no están embebidas dentro de un polímero sino que impregnan los poros de una membrana; se trata de las membranas con CNTs inmovilizados (CNIM). Las *membranas líquido soportadas modificadas con NPs* son un ejemplo de CNIM. Se trata de membranas impregnadas en disolvente orgánico que separan las fases donadora y aceptora (ambas acuosas) y que pueden incluir NPs con el propósito de mejorar la eficiencia de extracción del proceso. Las CNIM se han descrito para la extracción de naftaleno y tolueno de muestras acuosas y de ácido cafeico de extractos de plantas [59,60]. Otras estrategias que emplean puntas de pipeta modificadas con CNIM también se han investigado para la extracción de herbicidas [61].

SEPARACIÓN INSTRUMENTAL

La separación instrumental también se ha visto enriquecida gracias al empleo de las NPs ya sea como fases pseudoestacionarias en Electroforesis Capilar (CE) o como fases estacionarias en Cromatografía de Gases (GC) o de Líquidos (LC). Dentro de este ámbito de aplicación, las NPs permiten mejorar la resolución en las separaciones y por consiguiente, la selectividad de la técnica instrumental.

Electroforesis capilar

Una modalidad de CE es la conocida *Cromatografía electrocinética (EKC)* en la que la separación se produce por diferencias en los coeficientes de reparto de los analitos entre una fase pseudoestacionaria y el tampón electroforético. La separación es también resultado de la diferente migración de los analitos libres y aquellos que se encuentran interaccionando con la pseudofase bajo la aplicación de un campo eléctrico [51]. Las CNPs pueden actuar como pseudofases en forma de recubrimientos internos de los capilares o bien como aditivos en el tampón electroforético de separación [62]. El principal inconveniente asociado al empleo de NPs en CE es su baja estabilidad en medios acuosos y disolventes orgánicos, lo que hace necesaria la funcionalización superficial de las NPs o bien la adición de especies como tensioactivos, que faciliten su solubilización. La modalidad electroforética que emplea NPs recubiertas de surfactante como aditivos en el tampón electroforético se denomina *Cromatografía electrocinética micelar de nanopartículas dispersadas (MiNDECK)* [63]. Algunas aplicaciones en la separación de antiinflamatorios no esteroideos o vitaminas son ejemplos del empleo de las NPs en la separación instrumental por CE [64, 65].

Técnicas cromatográficas

Las propiedades excepcionales de las NPs también las hacen aptas para su implantación como fases estacionarias en GC y LC. Las NPs se pueden empaquetar en el interior de las columnas cromatográficas o bien inmovilizarse sobre las paredes internas de las mismas. La primera estrategia conlleva problemas de sobrepresión y una reducción significativa del área de interacción con el analito. Esta es la razón de que la segunda estrategia sea la más utilizada a día de hoy. Diferentes aplicaciones en GC han sido descritas en este sentido [66,67]. El empleo de las NPs en LC es mucho más restringido que en GC debido a las altas presiones generadas junto con el calentamiento provocado por la fricción [62]. No obstante, existen algunas aplicaciones descritas con el empleo de nanotubos de carbono monocapa (SWCNTs) y NPs de oro para la separación de diferentes compuestos aromáticos [68,69].

DETECCIÓN

Su elevada área superficial y reactividad química, junto con su eficiencia catalítica y excelente capacidad de adsorción, hacen que las NPs sean excelentes candidatos para su uso en (bio)sensores [70]. La posibilidad de unir ligandos específicos sobre su superficie incrementa la biocompatibilidad, la selectividad y la sensibilidad del sensor.

Las NPs se pueden emplear como modificadores de la superficie de transductores, o como componentes ópticos o electroactivos, para mejorar la sensibilidad, acelerar los tiempos de respuesta, permitir la multidetección o proporcionar respuestas más estables. A continuación describiremos brevemente los sensores basados en la detección óptica y electroquímica.

Sensores ópticos

Los sensores ópticos se basan en los cambios de las propiedades ópticas de las NPs como resultado de su interacción con el analito. Estos cambios pueden consistir en alteraciones del plasmón de resonancia superficial, tales como: *i*) modificación de su longitud de onda o intensidad (*Espectroscopía de resonancia de plasmón superficial localizado; LSPR*) [71,72]; *ii*) cambios visibles de color como resultado de la alteración del estado de agregación de las NPs en presencia del analito (*sensores colorimétricos en Espectrofotometría UV-Vis*) [73-75]; *iii*) incremento de la dispersión inelástica Raman (*Espectroscopía Raman amplificada por superficie; SERS*) [76,77]; o *iv*) incremento de la temperatura por decaimiento de la energía de forma no radiativa (aplicaciones en *imaging*) [78].

Asimismo, las NPs fluorescentes, como los puntos cuánticos y las NPs de oro y plata, pueden alterar su fluorescencia nativa en presencia del analito (*quenching* o desactivación fluorescente) lo que permite la detección de compuestos de diferente naturaleza [79-81]. Los SWCNTs son fluoróforos en la zona del infrarrojo cercano (NIR) aunque su aplicación práctica como sensores está bastante limitada ya que sus propiedades fluorescentes varían en función de su estabilidad. Sensores de glucosa basados en SWCNTs funcionalizados con fenoxidextrano ya han sido desarrollados [82]. Los nanodiamantes, por ejemplo, han permitido desarrollar nanosensores basados en la inmovilización de anticuerpos [83]. Además, su fluorescencia intrínseca, su elevado índice de refracción y su señal Raman característica los convierten en candidatos atractivos para las aplicaciones en *imaging* [84].

Sensores electroquímicos

Los sensores electroquímicos emplean las NPs para modificar la superficie de los transductores o como componentes electroactivos para mejorar la sensibilidad. Las NPs pueden actuar como catalizadores de reacciones electroquímicas favoreciendo una catálisis más efectiva, y proporcionando una mayor área superficial efectiva de interacción, un transporte de masa más rápido, y un mayor control del microambiente del electrodo. Permiten mejorar también los procesos de transferencia electrónica y mejorar/variación la conductividad entre el receptor del analito y el electrodo.

Los sensores electroquímicos basados en electrodos modificados con grafeno se han empleado con diversos fines, entre ellos la detección de iones Pb^{2+} , peróxido de hidrógeno o glucosa [85]. Algunos sensores modificados con CNTs y con híbridos (CNTs en combinación con NPs metálicas) han sido descritos para la detección de gases a bajas concentraciones [86,87]. No obstante, las NPs metálicas, concretamente las NPs de óxidos de metales, son actualmente las más explotadas en este campo [88-90].

Los nanomateriales también pueden actuar como superficies para la inmovilización de biomoléculas. En este sentido, se han desarrollado algunos sensores híbridos basados en la combinación de biomoléculas (proteínas, ADN, anticuerpos) con NPs con el propósito de generar o amplificar la respuesta analítica [91]. La biocompatibilidad y elevada estabilidad física y química de las NPs magnéticas las han convertido en excelentes plataformas de inmovilización, y ya se han utilizado para la detección de proteínas y ADN [70].

Referencias

- [1] M. Valcárcel, B.M. Simonet, S. Cárdenas, Analytical nanoscience and nanotechnology today and tomorrow, *Anal. Bioanal. Chem.* 391 (2008) 1881-1887.
- [2] M. Valcárcel, S. Cárdenas, B.M. Simonet, Y. Moliner-Martínez, R. Lucena, Carbon nanostructures as sorbent materials in analytical processes, *TrAC* 27 (2008) 34-43.
- [3] A.H. El-Sheikh, M.K. Al-Jafari, J.A. Sweileh, Solid phase extraction and uptake properties of multi-walled carbon nanotubes of different dimensions towards some nitro-phenols and chloro-phenols from water, *Int. J. Environ. Anal. Chem.* 92 (2012) 190-209.
- [4] R. Sitko, B. Zawisza, E. Malicka, Modification of carbon nanotubes for preconcentration, separation and determination of trace-metals ions, *TrAC* 37 (2012) 22-31.
- [5] K. Pyrzynska, Application of carbon nanotubes as a solid-phase extraction material for environmental samples, *Environanotechnology* capítulo B (2010) 199-212.
- [6] J. Ma, R. Xiao, J. Li, J. Yu, Y. Zhang, L. Chen, Determination of 16 polycyclic aromatic hydrocarbons in environmental water samples by solid-phase extraction using multi-walled carbon nanotubes as adsorbent coupled with gas chromatography-mass spectrometry, *J. Chromatogr. A* 1217 (2010) 5462-5469.
- [7] P. Guo, Z. Guan, W. Wang, B. Chen, Y. Huang, Determination of linear alkylbenzene sulfonates by ion-pair solid-phase extraction and high-performance liquid chromatography, *Talanta* 84 (2011) 587-592.
- [8] H. Niu, Y. Shi, Y. Cai, F. Wei, G. Jiang, Solid-phase extraction of sulfonylurea herbicides from water samples with single-walled carbon nanotubes disk, *Microchim. Acta* 164 (2009) 431-438.
- [9] S. Mukdasaai, C. Thomas, S. Srijaranai, Enhancement of sensitivity for the spectrophotometric determination of carbaryl using dispersive liquid microextraction combined with dispersive μ -solid phase extraction, *Anal. Method.* 5 (2013) 789-796.
- [10] M. Asensio-Ramos, G. D'Orazio, J. Hernández-Borges, A. Rocco, S. Fanali, Multi-walled carbon nanotubes-dispersive solid-phase extraction combined with nano-liquid chromatography for the analysis of pesticides in water samples, *Anal. Bioanal. Chem.* 400 (2011) 1113-1123.
- [11] A.V. Herrera-Herrera, J. Hernández-Borges, M.M. Afonso, J.A. Palenzuela, M.A. Rodríguez-Delgado, Comparison between magnetic and non magnetic multi-walled carbon nanotubes-dispersive solid-phase extraction combined with ultra-high performance liquid chromatography for the determination of sulfonamide antibiotics in water samples, *Talanta* 116 (2013) 695-703.

BLOQUE I. INTRODUCCIÓN

[12] L. Chen, T. Wang, J. Tong, Application of derivatized magnetic materials to the separation and the preconcentration of pollutants in water samples, *TrAC* 30 (2011) 1095-1108.

[13] A. Sarafraz-Yazdi, M.S. Ardaki, A. Amiri, Determination of monocyclic aromatic amines using headspace solid-phase microextraction based on sol-gel technique prior to GC, *J. Sep. Sci.* 36 (2013) 1629-1635.

[14] X.Y. Song, Y.P. Shi, J. Chen, Carbon nanotubes-reinforced hollow fibre solid-phase microextraction coupled with high performance liquid chromatography for the determination of carbamate pesticides in apples, *Food Chem.* 139 (2013) 246-252.

[15] A. Sarafraz-Yazdi, M. Mosadegh, A. Amiri, Determination of volatile organic compounds in environmental water samples using three solid-phase microextraction fibers based on sol-gel technique with gas chromatography-flame ionization detector, *Anal. Method.* 3 (2011) 1877-1886.

[16] J. Feng, M. Sun, L. Xu, J. Li, X. Liu, S. Jiang, Preparation of metal wire supported solid-phase microextraction fiber coated with multi-walled carbon nanotubes, *J. Sep. Sci.* 34 (2011) 2482-2488.

[17] A. Sarafraz-Yazdi, A. Amiri, G. Rounaghi, H. Eshtiagh-Hosseini, Determination of non-steroidal anti-inflammatory drugs in water samples by solid-phase microextraction based sol-gel technique using poly(ethylene glycol) grafted multi-walled carbon nanotubes coated fiber, *Anal. Chim. Acta* 720 (2012) 134-141.

[18] D. Cao, J. Lü, J. Liu, G. Jiang, In situ fabrication of nanostructured titania coating on the surface of titanium wire: A new approach for preparation of solid-phase microextraction fiber, *Anal. Chim. Acta* 611 (2008) 56-61.

[19] H.M. Liu, D.A. Wang, L. Ji, J.B. Li, S.J. Liu, X. Liu, S.X. Jiang, A novel TiO₂ nanotube array/Ti wire incorporated solid-phase microextraction fiber with high strength, efficiency and selectivity, *J. Chromatogr. A* 1217 (2010) 1898-1903.

[20] J.M.F. Nogueira, Novel sorption-based methodologies for static microextraction analysis: A review on SBSE and related techniques, *Anal. Chim. Acta* 757 (2012) 1-10.

[21] Z. Es'haghi, M.A.K. Khooni, T. Heidari, Determination of brilliant green from fish pond water using carbon nanotube assisted pseudo-stir bar solid/liquid microextraction combined with UV-vis spectroscopy-diode array detection, *Spectrochim. Acta A* 79 (2011) 603-607.

[22] M.C. Alcudia-León, R. Lucena, S. Cárdenas, M. Valcárcel, Magnetically confined hydrophobic nanoparticles for the microextraction of endocrine-disrupting phenols from environmental waters, *Anal. Bioanal. Chem.* 405 (2013) 2729-2734.

I.1. Aplicaciones analíticas de las nanopartículas

- [23] J. Muñoz, M. Gallego, M. Valcárcel, Speciation analysis of mercury and tin compounds in water and sediments by gas-chromatography-mass spectrometry following preconcentration in C60 fullerene, *Anal. Chim. Acta* 548 (2005) 66-72.
- [24] Y. Wang, Y. Zhang, X. Zhou, J. Li, J. Ma, Graphene-based solid phase extraction for a sensitive determination of trace amounts of lead in water samples, *Anal. Chem. Letters* 1 (2011) 337-348.
- [25] Y.B. Luo, B.F. Yuan, Q.W. Yu, Y.Q. Feng, Substrateless graphene fiber: A sorbent for solid-phase microextraction, *J. Chromatogr. A* 1268 (2012) 9-15.
- [26] H. Wang, A.D. Campiglia, Determination of polycyclic aromatic hydrocarbons in drinking water samples by solid-phase nanoextraction and high-performance liquid chromatography, *Anal. Chem.* 80 (2008) 8202-8209.
- [27] A. Zierhut, K. Leopold, L. Harward, P. Worsfold, M. Schuster, Activated gold surfaces for the direct preconcentration of mercury species from natural waters, *J. Anal. At. Spectrom.* 24 (2009) 767-774.
- [28] S. Das, A.K. Pandey, A.A. Athawale, M. Subramanian, T.K. Seshagiri, P.K. Khanna, V.K. Manchanada, Silver nanoparticles embedded polymer sorbent for preconcentration of uranium from bio-aggressive aqueous media, *J. Hazard. Mater.* 186 (2011) 2051-2059.
- [29] S. Gunduz, S. Akman, M. Kahraman, Slurry analysis of cadmium and copper collected on 11-mercaptoundecanoic acid modified TiO₂ core-Au shell nanoparticles by flame atomic absorption spectrometry, *J. Hazard. Mater.* 186 (2011) 212-217.
- [30] Q. Cheng, F. Qu, N.B. Li, H.Q. Luo, Mixed hemimicelles solid-phase extraction of chlorophenols in environmental water samples with 1-hexadecyl-3-methylimidazolium bromide-coated Fe₃O₄ magnetic nanoparticles with high-performance liquid chromatographic analysis, *Anal. Chim. Acta* 715 (2012) 113-119.
- [31] M. Faraji, Y. Yamini, M. Rezaei, Extraction of trace amounts of mercury with sodium dodecyl sulfate-coated magnetite nanoparticles and its determination by flow injection inductively coupled plasma-optical emission spectrometry, *Talanta* 81 (2010) 831-836.
- [32] Y. Wang, X. Luo, J. Tang, X. Hu, Q. Xu, C. Yang, Extraction and preconcentration of trace levels of cobalt using functionalized magnetic nanoparticles in a sequential injection lab-on-valve system with detection by electrothermal atomic absorption spectrometry, *Anal. Chim. Acta* 713 (2012) 92-96.
- [33] A.A. Ensafi, S. Rabiei, B. Rezaei, A.R. Allafchian, Magnetic solid-phase extraction to preconcentrate ultra trace amounts of lead(ii) using modified-carbon nanotubes decorated with NiFe₂O₄ magnetic nanoparticles, *Anal. Method.* 5 (2013) 3903-3908.

BLOQUE I. INTRODUCCIÓN

[34] L. Xie, R. Jiang, F. Zhu, H. Liu, G. Ouyang, Application of functionalized magnetic nanoparticles in sample preparation, *Anal. Bioanal. Chem.* (2013) doi: 10.1007/s00216-013-7302-6

[35] P. Hashemi, M. Shamizadeh, A. Badieli, P.Z. Poor, A.R. Ghiasvand, A. Yarahmadi, Amino ethyl-functionalized nanoporous silica as a novel fiber coating for solid-phase microextraction, *Anal. Chim. Acta* 646 (2009) 1-5.

[36] M.B. Gholivand, M.M. Abolghasemi, P. Fattahpour, A hexagonally ordered nanoporous silica-based fiber coating for SPME of polycyclic aromatic hydrocarbons from water followed by GC-MS, *Chromatographia* 74 (2011) 807-815.

[37] G. Morales-Cid, A. Fekete, B.M. Simonet, R. Lehmann, S. Cárdenas, X. Zhang, M. Valcárcel, P. Schmitt-Kopplin, In situ synthesis of magnetic multiwalled carbon nanotube composites for the clean-up of (fluoro)quinilones from human plasma prior to ultrahigh pressure liquid chromatography analysis, *Anal. Chem.* 82 (2010) 2743-2752.

[38] O. Yalcinkaya, O.M. Kalfa, A.R. Turker, Preconcentration of trace copper, cobalt and lead from various samples by hybrid nanosorbent and determination by FAAS, *Curr. Anal. Chem.* 7 (2011) 225-234.

[39] R. Gao, X. Su, X. He, L. Chen, Y. Zhang, Preparation and characterisation of core-shell CNTs@MIPs nanocomposites and selective removal of estrone from water samples, *Talanta* 83 (2011) 757-764.

[40] W. Yang, F. Jiao, L. Zhou, X. Chen, X. Jiang, Molecularly imprinted polymers coated on multi-walled carbon nanotubes through a simple indirect method for the determination of 2,4-dichlorophenoxyacetic acid in environmental water, *Appl. Surf. Sci.* 284 (2013) 692-699.

[41] M.L. Polo-Luque, B.M. Simonet, M. Valcárcel, Ionic liquid combined with carbon nanotubes: a soft material for the preconcentration of PAHs, *Talanta* 104 (2013) 169-172

[42] F. Galán-Cano, M.C. Alcudia-León, R. Lucena, S. Cárdenas, M. Valcárcel, Ionic liquid coated magnetic nanoparticles for the gas chromatography/mass spectrometric determination of polycyclic aromatic hydrocarbons in waters, *J. Chromatogr. A* 1300 (2013) 134-140.

[43] C. Carrillo-Carrión, R. Lucena, S. Cárdenas, M. Valcárcel, Liquid-liquid extraction/ headspace/ gas chromatographic/ mass spectrometric determination of benzene, toluene, ethylbenzene (*o*-, *m*-, *p*-) xylene and styrene in olive oil using surfactant-coated carbon nanotubes as extractant, *J. Chromatogr. A* 1171 (2007) 1-7.

[44] E. Caballero-Díaz, B. Simonet, M. Valcárcel, Liquid-liquid extraction assisted by a carbon nanoparticles interface. Electrophoretic determination of atrazine in environmental samples, *Analyst* 138 (2013) 5913-5919.

I.1. Aplicaciones analíticas de las nanopartículas

- [45] S. Mukdasai, C. Thomas, S. Srijaranai, Enhancement of sensitivity for the spectrophotometric determination of carbaryl using dispersive liquid microextraction combined with dispersive μ -solid phase extraction, *Anal. Methods* 5 (2013) 789-796.
- [46] Z.Q. Tan, J.F. Liu, R. Liu, Y.G. Yin, G.B. Jiang, Visual and colorimetric detection of Hg²⁺ by cloud point extraction with functionalized gold nanoparticles as a probe, *Chem. Commun.* 45 (2009) 7030-7032.
- [47] D.L. Giokas, Q. Zhu, Q. Pan, A. Chisvert, Cloud point-dispersive μ -solid phase extraction of hydrophobic organic compounds onto highly hydrophobic core-shell Fe₂O₃@C magnetic nanoparticles, *J. Chromatogr. A* 1251 (2012) 33-39.
- [48] S. Dadfarnia, F. Shakerian, A.M.H. Shabani, Suspended nanoparticles in surfactant media as a microextraction technique for simultaneous separation and preconcentration of cobalt, nickel, and copper ions for electrothermal atomic adsorption spectrometry determination, *Talanta* 106 (2013) 150-154.
- [49] E. Caballero-Díaz, B.M. Simonet, M. Valcárcel, Nanodiamonds assisted-cloud point extraction for the determination of fluoranthene in river water, *Anal. Method.* 5 (2013) 3864-3871.
- [50] M. Bhadra, S. Mitra, Nanostructured membranes in analytical chemistry, *TrAC* 45 (2013) 248-263.
- [51] A.V. Herrera-Herrera, M.A. González-Curbelo, J. Hernández Borges, M.A. Rodríguez-Delgado, Carbon nanotubes applications in separation science: A review, *Anal. Chim. Acta* 734 (2012) 1-30.
- [52] E. Celik, L. Liu, H. Choi, Protein fouling behavior of carbon nanotube/polyethersulfone composite membranes during water filtration, *Water Res.* 45 (2011) 5287-5294.
- [53] T.H. Weng, H.H. Tseng, M.Y. Wey, Preparation and characterization of multi-walled carbon nanotube/PBNPI nanocomposite membrane for H₂/CH₄ separation, *Int. J. Hydrogen Energ.* 34 (2009) 8707-8715.
- [54] A.V. Penkova, G.A. Polotskaya, V.A. Gavrilova, A.M. Toikka, J-C. Liu, M. Trchová, M. Slouf, Z. Pientka, Structure and pervaporation properties of poly(phenylene-isophthalamide) membranes modified by fullerene C₆₀, *Sep. Sci. Technol.* 45 (2009) 35-41.
- [55] S.M. Sanip, A.F. Ismail, P.S. Goh, T. Soga, M. Tanemura, H. Yasuhiko, Gas separation properties of functionalized carbon nanotubes mixed matrix membranes, *Sep. Purif. Technol.* 78 (2011) 208-213.
- [56] S. Kim, L. Chen, K. J. Johnson, E. Marand, Polysulfone and functionalized carbon nanotube mixed matrix membranes for gas separation: Theory and experiment, *J. Membr. Sci.* 294 (2007) 147-158.

BLOQUE I. INTRODUCCIÓN

[57] C. Basheer, A.A. Alnedhary, B.S. Madhava Rao, S. Valliyaveetil, H.K. Lee, Development and application of porous membrane-protected carbon nanotube micro-solid-phase extraction combined with gas chromatography/mass spectrometry, *Anal. Chem.* 78 (2006) 2853-2858.

[58] B.J. Hinds, N. Chopra, T. Rantell, R. Andrews, V. Gavalas, L.G. Bachas, Aligned multiwalled carbon nanotube membranes, *Science* 303 (2004) 62-65.

[59] K. Hylton, Y. Chen, S. Mitra, Carbon nanotube mediated microscale membrane extraction, *J. Chromatogr. A* 1211 (2008) 43-48.

[60] Z. Es'haghi, M. Ahmadi, A. Saify, A. Akbar, Z. Rezaeifar and Z. Alian-Nezhadi, Carbon nanotube reinforced hollow fiber solid/liquid phase microextraction: A novel extraction technique for the measurement of caffeic acid in *Echinacea purpurea* herbal extracts combined with high-performance liquid chromatography, *J. Chromatogr. A* 1217 (2010) 2768-2775.

[61] H.H. See, M. Sanagi, W.A.W. Ibrahim, A.A. Naim, Determination of triazine herbicides using membrane-protected carbon nanotubes solid phase membrane tip extraction prior to micro-liquid chromatography, *J. Chromatogr. A* 1217 (2010) 1767-1772.

[62] E. Guihen, Nanoparticles in modern separation science, *TrAC* 46 (2013) 1-14.

[63] Y. Moliner-Martínez, S. Cárdenas, M. Valcárcel, Surfactant coated fullerenes C60 as pseudostationary phase in electrokinetic chromatography, *J. Chromatogr. A* 1167 (2007) 210-216.

[64] Y.-J. Huang, G.-R. Wang, K.-P. Huang, Y.-F. Hsieh, C.-Y. Liu, Functionalized carbon nanotubes as the pseudostationary phase for capillary EKC separation of non-steroidal anti-inflammatory drugs, *Electrophoresis* 30 (2009) 3964-3970.

[65] J.M. Jiménez-Soto, Y. Moliner-Martínez, S. Cárdenas, M. Valcárcel, Evaluation of the performance of single-walled carbon nanohorns in capillary electrophoresis, *Electrophoresis* 31 (2010) 1681-1688.

[66] G.M. Gross, D.A. Nelson, J.W. Grate, R.E. Synovec, Monolayer-protected gold nanoparticles as a stationary phase for open tubular gas chromatography, *Anal. Chem.* 75 (2003) 4558-4564.

[67] L.M. Yuan, C.X. Ren, L. Li, P. Ai, Z.H. Yan, Z. Min, Z.Y. Li, Single-walled carbon nanotubes used as stationary phase in GC, *Anal. Chem.* 78 (2006) 6384-6390.

[68] K. Kobayashi, S. Kitagawa, H. Ohtani, Development of capillary column packed with thiol-modified gold-coated polystyrene particles and its selectivity for aromatic compounds, *J. Chromatogr. A* 1110 (2006) 95-101.

I.1. Aplicaciones analíticas de las nanopartículas

- [69] Y.X. Chang, L.L. Zhon, G.X. Li, J.Y. Wang, L.M. Yuan, Single-wall carbon nanotubes used as stationary phase in HPLC, *J. Liq. Chromatogr. Relat. Technol.* 30 (2007) 2953-2958.
- [70] B. Pérez-López, A. Merkoci, Nanoparticles for the development of improved (bio)sensing systems, *Anal. Bioanal. Chem* 399 (2011) 1577-1590.
- [71] N.A. Bakar, M.M. Salleh, A.A. Umar, M. Yahaya, Localized surface plasmon resonance sensor using gold nanoparticles for detection of bisphenol A, *Key Eng. Mat.* 543 (2010) 342-345.
- [72] D. Li, G. Zheng, X. Ding, J. Wang, J. Liu, L. Kong, DNA functionalized gold nanorods/nanoplates assembly as sensitive LSPR-based sensor for label-free detection of mercury ions, *Colloid. Surface. B* 110 (2013) 485-488.
- [73] P. Miao, T. Liu, X. Li, L. Ning, J. Yin, K. Han, Highly sensitive, label-free colorimetric assay of trypsin using silver nanoparticles, *Biosens. Bioelectron.* 49 (2013) 20-24.
- [74] H. Xing, S. Zhan, Y. Wu, L. He, P. Zhou, Sensitive colorimetric detection of melamine in milk with an aptamer-modified nanogold probe, *RSC Advances* 3 (2013) 17424-17430.
- [75] Y. Ma, L. Jiang, Y. mei, R. Song, D. Tian, H. Huang, Colorimetric sensing strategy for mercury(ii) and melamine utilizing cysteamine-modified gold nanoparticles, *Analyst* 138 (2013) 5338-5343.
- [76] E. Caballero-Díaz, B.M. Simonet, M. Valcárcel, Microextraction by packed sorbents combined with surface-enhanced Raman spectroscopy for determination of musk ketone in river water, *Anal. Bioanal. Chem.* 405 (2013) 7251-7257.
- [77] Y. Jin, P. Ma, F. Liang, D. Gao, X. Wang, Determination of malachite green in environmental water using cloud point extraction coupled with surface-enhanced Raman scattering, *Anal. Method.* 5 (2013) 5609-5614.
- [78] C.K. Lim, J. Shin, Y.D. Lee, J. Kim, K.S. Oh, S.H. Yuk, S.Y. Jeong, S. Kim, Phthalocyanine-aggregated polymeric nanoparticles as tumor-homing near-infrared absorbers for photothermal therapy of cancer, *Theranostics* 2 (2012) 871-879.
- [79] J. Zhao, Y. Yi, N. Mi, B. Yin, M. Wei, Q. Chen, H. Li, Y. Zhang, S. Yao, Gold nanoparticle coupled with fluorophore for ultrasensitive detection of protamine and heparin, *Talanta* 116 (2013) 951-957.
- [80] M.S. Hosseini, S. Nazemi, Preconcentration determination of arsenic species by sorption of As(V) on Amberlite IRA-410 coupled with fluorescence quenching of L-cysteine capped CdS nanoparticles, *Analyst* 138 (2013) 5769-5776.

BLOQUE I. INTRODUCCIÓN

- [81] C. Carrillo-Carrión, B.M. Simonet, M. Valcárcel, Determination of TNT explosive based on its selectively interaction with creatinine-capped CdSe/ZnS quantum dots, *Anal. Chim. Acta* 792 (2013) 93-100.
- [82] V.A. Karachevtsev, A.Y. Glamazda, V.S. Leontiev, O.S. Lytvyn, U. Dettlaff-Weglikowska, Glucose sensing based on NIR fluorescence of DNA-wrapped single-walled carbon nanotubes, *Chem. Phys. Lett.* 435 (2007) 104-108.
- [83] T.S. Huang, Y. Tzeng, Y.K. Liu, Y.C. Chen, K.R. Walker, R. Gutupalli, C. Liu, Immobilization of antibodies and bacterial binding on nanodiamond and carbon nanotubes for biosensor applications, *Diamond. Relat. Mater.* 13 (2004) 1098-1102.
- [84] R. Kaur, I. Badea, Nanodiamonds as novel nanomaterials for biomedical applications: drug delivery and imaging systems, *Int. J. Nanomed.* 8 (2013) 203-220.
- [85] M. Pumera, A. Ambrosi, A. Bonanni, E.L.K. Chng, H.L. Poh, Graphene for electrochemical sensing and biosensing, *TrAC* 29 (2010) 954-965.
- [86] S. Mubeen, T. Zhang, B. Yoo, M.A. Deshusses, N. Myung, Palladium nanoparticles decorated single-walled carbon nanotube hydrogen sensor, *J. Phys. Chem. C.* 111 (2007) 6321-6327.
- [87] P. Vichchulada, Q. Zhang, M.D. Lay, Recent progress in chemical detection with single-walled carbon nanotube networks, *Analyst* 132 (2007) 719-723.
- [88] L. Rassaei, M. Amiri, C.M. Cirtiu, M. Sillanpää, F. Marken, M. Sillanpää, Nanoparticles in electrochemical sensors for environmental monitoring, *TrAC* 30 (2011) 1704-1715.
- [89] P. Rameshkumar, R. Ramaraj, Gold nanoparticles deposited on amine functionalized silica sphere and its modified electrode for hydrogen peroxide sensing, *J. Appl. Electrochem.* 43 (2013) 1005-1010.
- [90] S. Bothra, J.N. Solanki, S.K. Sahoo, Functionalized silver nanoparticles as chemosensor for pH, Hg²⁺ and Fe³⁺ in aqueous medium, *Sensor Actuat. B-Chem.* 188 (2013) 937-943.
- [91] M.T. Castañeda, A. Merkoçi, M. Pumera, S. Alegret, Electrochemical genosensors for biomedical applications based on gold nanoparticles, *Biosens. Bioelectron.* 22 (2007) 1961-1969.



Multiplexed sensing and imaging with colloidal nano- and microparticles

S. Carregal-Romero^{1,2}, E. Caballero-Díaz^{1,3}, L. Beqa¹, A.M. Abdelmonem¹, M. Ochs¹, D. Hühn¹, B. Simonet³, M. Valcárcel³, W.J. Parak¹

¹Fachbereich Physik and WZMW, Philipps Universität Marburg, Marburg, Germany.

²BIONAND, Centro Andaluz de Nanomedicina y Biotecnología, Málaga, Spain.

³Department of Analytical Chemistry, Campus de Rabanales, University of Córdoba, Córdoba, Spain.

ABSTRACT

Sensing and imaging with fluorescent, plasmonic, and magnetic colloidal nano- and microparticles have been boosted in the last decade. In this review we describe concepts and their applications on how these techniques can be used in multiplexed mode, *i.e.* sensing of several analytes in parallel or imaging of several labels in parallel.

1. INTRODUCTION

During the past decade, the use of colloidal nano- and microparticles in biological sciences has attracted a great deal of attention. They have long been used as contrast agents for imaging [1–3] and transducers for molecular sensing [4]. Materials developed for these purposes range from single nanoparticles (NPs) and microparticles to complex hybrid nano- and microstructures. Nanoengineering allows for the integration of different functionalities into a single carrier system. Examples of multifunctional composites include the recently described nanocomposites based on silica, silver, and gold NPs (AuNPs), which have applications in photodynamic therapy, photothermolysis, and IR detection [5]. Our review focuses on the use of inorganic NPs as building blocks of multifunctional composites on the nano- and micrometer scales, and on their applications in biosensing and diagnostics. After briefly introducing the main detection modes, we discuss why and how the assembly of individual NPs into multifunctional composites allows for multiplexing. Multiplexed sensing and imaging mean that several analytes can be detected in parallel and that different types of particles can be imaged simultaneously. Finally, we discuss some issues and new challenges concerning sensing and imaging involving hybrid materials based on inorganic NPs.

2. DETECTION MODES

In sensing and imaging applications, NPs are used to provide readout. In sensing applications, the transduction principle, which provides readout in the presence of a specific analyte, can depend on either direct interaction between the NP and the analyte or interaction between the analyte and another entity supported on the NP, which then interacts with the NP. The NP ultimately changes the signal for readout in the presence of the analyte. In the case of imaging, NPs are typically used as markers that provide contrast (and thus

I.2. Multiplexed sensing and imaging with nano- and microparticles

readout) for different imaging techniques. Readout is usually based on optical, electrical, or magnetic detection, as we discuss in detail below. However, naturally there are also other detection schemes, such as detection with X-rays [6], radioactivity [7], or mass changes [8]; we do not focus on those techniques in this review.

2.1 Optical detection

The principle of optical detection is based on the interaction between continuous or pulsed light and the sample to be analyzed. This interaction causes changes in the initial incident light wave in terms of frequency, amplitude, phase, polarization state, or time dependence. Figure 1 summarizes some of the phenomena that are useful for analysis; these phenomena may occur when incident light interacts with a sample of dispersed colloidal particles [9]. In general, transmission, elastic and inelastic scattering, and absorption processes can occur. In the case of transmission, light passes through the object and is normally affected in terms of amplitude or intensity. In the case of scattering phenomena, the interaction between light and the particles changes the direction of the incident light wave. However, following elastic scattering, the energy of the incident light, and thus the wavelength, remains unchanged. The Rayleigh and Mie theories describe typical particle-based scattering for small (<5nm) and large (>5nm) particles, respectively. In contrast, following inelastic scattering, the energy of the incident light, and thus the wavelength, changes.

BLOQUE I. INTRODUCCIÓN

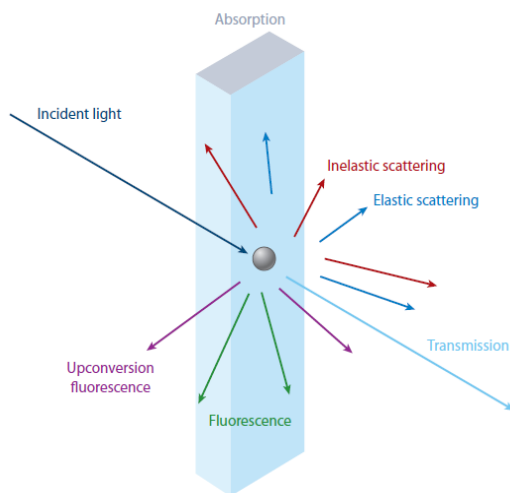


Figure 1. Possible interactions between a particle and light.

The inelastic scattering process (Raman scattering) is especially important for colloidal particles. The interaction between the incident light and the sample modifies the energy of the internal (typically rotational or vibronic) states of the particle, and the scattered light has either higher or lower energy, termed anti-Stokes or Stokes scattering, respectively. For luminescent particles, other interesting processes, such as the emission of light, may occur. This phenomenon is based on the excitation of energetic states by the charge carrier's absorption of the incident wave energy, which in general is possible only if the incident wave is in resonance with the excited electronic state. The light that is reemitted following relaxation of the excited states to the ground states is termed fluorescence if the emitted light is less energetic than the incident light (more conventional process) and upconversion fluorescence if the emitted light is more energetic (less conventional process). Other parts of the energy can be converted into heat. This nonradiative energetic contribution is referred to as absorption, which does not lead to the emission of light, and whereby the energy remains in the sample.

I.2. Multiplexed sensing and imaging with nano- and microparticles

Various techniques exist for the optical detection of particles on the basis of the above mentioned mechanisms. Hereafter, we distinguish between plasmonic [10] and fluorescent [11] particles [12].

NPs of several metals, such as platinum, copper, gold, and silver, or alloys such as Cu_{2-x}Se , demonstrate surface plasmon resonance (SPR) due to the collective oscillation of the free electrons stimulated by incident light of an appropriate wavelength [13]; they are therefore referred to as plasmonic NPs. This property has been exploited in many analytical techniques for sensing and imaging.

1. Localized surface plasmon resonance (LSPR) spectroscopy benefits from the high sensitivity of the plasmon resonance to changes in the local refractive index, and it can be applied to both individual NPs and periodic arrays of NPs. The light scattered by individual plasmonic NPs, for example, can be detected with dark-field microscopy [14]. Plasmon resonance wavelength and intensity can be modified by the temporal or irreversible presence of an analyte (bound or adsorbed) on the NP surface. LSPR is a very sensitive tool for quantitative analyte analysis [15], allowing for even single-molecule detection [16, 17].

2. Colorimetric sensors are also based on LSPR techniques, but they were developed on the basis of the visible color changes that plasmonic NPs undergo in the presence of a target analyte that triggers the agglomeration (or redispersion) of an assembly of NPs [18]. Although similar concepts have previously been used [19], the breakthrough in this technique was achieved by target DNA-mediated agglomeration of oligonucleotide-modified AuNPs, as introduced by the Mirkin group [4]. In that study, the presence of target DNA was observed by the naked eye following a color change of a AuNP solution from red to blue. This concept

has been further extended and has led to, for example, the development of scanometric sensors for DNA strands according to the specific binding of oligonucleotide functionalized AuNPs in a DNA array. The change of color due to analyte recognition was further amplified through the addition of a silver layer onto the AuNPs. This process causes visible darkening of the array surface only in the presence of a complementary target [20]. Colorimetric detection of analytes via analyte-induced agglomeration of plasmonic NPs is currently used for many different analytes [21, 22].

3. Surface-enhanced Raman spectroscopy (SERS) benefits from the intense electromagnetic field generated on some plasmonic nanostructures due to their LSPRs. Applications of this technique are expanding because of the possibility of ultrasensitive molecule detection without the need for special preparation of the sample. Imaging and sensing can be achieved with SERS labels in close contact with plasmonic NPs [23–26].

4. The nonradiative decay of plasmons can produce a localized increase of temperature on the plasmonic NP surface that can be exploited for imaging. Relevant techniques include photothermal microscopy [27, 28] and photoacoustic tomography [29, 30].

Fluorescence microscopy, spectroscopy, and flow cytometry are among the most powerful tools for imaging and analytical detection of molecules and ions. Several types of fluorescent particles can be used for sensing and imaging applications.

1. Quantum dots (QDs), namely semiconductor NPs, with tunable light emission. QDs composed by atoms in groups II–VI (CdSe, CdS, etc.) have been studied largely because of their higher stability against oxidation or

I.2. Multiplexed sensing and imaging with nano- and microparticles

agglomeration in biological fluids, compared with those of other semiconductor materials [31, 32]. However, QDs based on silicon or carbon are more interesting for biological applications due to their reduced toxicity. Efforts to synthesize, stabilize, and use silicon and carbon QDs as contrast agents and sensors are under way in clinical applications [33–36].

2. Noble-metal clusters. Silver NPs or AuNPs with diameters less than 2 nm do not exhibit SPR, but they can present fluorescence owing to their molecule-like properties [37, 38]. Such small NPs can be used as fluorescent labels within multifunctional nanostructures or individually if they are properly stabilized.

3. Upconversion NPs and complexes. Based mostly on lanthanide-doped materials, these materials are promising for in vivo imaging. Their range of excitation/emission wavelengths can be tuned to the near-IR region, in which tissue produces minimal absorption and scattering of light. Moreover, they have low cytotoxicity, a long lifetime, and a narrow emission bandwidth [39, 40].

4. Inorganic NPs acting as passive carriers. These NPs can accumulate organic dyes and bioluminescent or chemiluminescent molecules either on the surface of or within a particle [41].

5. Polymeric nanomatrices acting as passive carriers. Photonic explorers for bioanalysis with biologically localized embedding (PEBBLE) sensors are a prominent example. They can be loaded with several dyes, permitting ratiometric sensor preparation and multiplexing [42].

6. Microbeads and microcapsules. Due to their size, they can be simultaneously loaded with both organic dyes and fluorescent NPs. Multitasking can be readily achieved with such materials [43, 44].

Detection based on fluorescent particles depends on the physicochemical process involved in the modification of the emitted light upon analyte–particle interaction. The main applied concepts for fluorescence detection include the following.

1. Readout based on analyte-sensitive fluorophores. The presence of the analyte can directly modify the emission of the fluorophore [45].

2. Readout based on the quenching of QD fluorescence through the proximity of another NP, such as a AuNP [46].

3. Readout based on photoinduced electron-transfer (PET) sensors. They consist of one fluorescent species attached to a recognition group that acts as a quencher in the unbound dark state. The binding of the recognition component with the analyte (normally metal cations and protons) cancels the electron transfer and dequenches the fluorophore [47].

4. Readout based on Förster resonance energy transfer (FRET) between two fluorophores. Often, QDs act as donors and transfer energy to an analyte-sensitive fluorophore that acts as an acceptor, but FRET in which the QDs are acting as the acceptors can occur [48]. The lifetime of and the response to analytes of the acceptor fluorophore are modified due to the presence [within a short (<10nm) distance] of the donor fluorophore.

1.2. Multiplexed sensing and imaging with nano- and microparticles

5. Readout based on chemiluminescence resonance energy transfer (CRET). In CRET, a chemiluminescent probe is the donor; it excites the acceptor fluorophore, which can be a dye or a particle. The chemiluminescent probe should be analyte sensitive and should be formed by two species that react to produce emission of light only in the presence of the analyte [49].

6. Readout based on bioluminescence resonance energy transfer (BRET). Bioluminescent proteins are efficient energy donors for QDs [50]. Because CRET and BRET processes do not need light excitation, their sensitivity is high.

2.2 Electrical detection

Electrical detection modes deal mainly with NPs that conduct electricity, such as noble metals or semiconductors, which are typically supported by a flat electrode [51, 52]. However, oxide NPs and hybrid multifunctional NPs have also been used as electrochemical sensors and biosensors. The function of the NPs in such sensors varies not only according to the nature of the NP but also on the basis of how the analyte is detected. Luo et al. [53] provide some important examples of the functions of NPs in electrical sensors: *(a)* The NPs are reactants themselves [54], *(b)* they are catalysts of electrochemical reactions [55], *(c)* they provide an appropriate surface for immobilization of biomolecules (e.g., analyte receptors) [56], *(d)* they improve or vary the conductivity between the analyte receptor and the electrode [57, 58], *(e)* they enhance electron-transfer processes [59], and *(f)* they perform labeling [60]. The four main electroanalytical categories of detection involving NPs are *(a)* classic potentiometry (which involves potential measurements) [61], *(b)* coulometry (by measuring current, the amount of matter transformed during the electrolysis reaction is calculated) [62], *(c)* amperometry (wherein ions are

detected on the basis of current measurements) [54], and *(d)* voltammetry (in which current measurements are performed while the potential is changed) [55]. Electrochemical biosensing is often applied to the detection of biomolecules such as enzymes, antigens, and DNA, which are responsible for specifically recognizing the analyte and, in the case of enzymes, for converting the analyte in the signal that is actually detected (such as electrons, H⁺, and H₂O₂). Many comprehensive reviews summarizing the most significant improvements in nanomaterial-based electrical biosensing have been published, and we recommend reading them for further information [63, 64].

Hybrid systems that mix optical and electrical measurements for analyses involving NPs have been performed. Electrochemical-LSPR biosensors have been developed for label-free detection of peptide toxins through the use of core-shell NP arrays [65]. The substrate comprised silica NPs used as the core and a thin gold film used as the shell, which simultaneously acted as a working electrode and a LSPR sensor. The binding of the peptide toxin melittin to the hybrid electrode was optically detected by LSPR, and the membrane-disturbing properties were assessed electrochemically [65]. In the case of fluorescent NPs, optical excitation can be used to modulate the electrochemical signal. The illumination of QDs, immobilized on an electrode, generates charge carriers (electrons and holes) and gives rise to a photocurrent. This detection scheme has been employed in, for instance, the light-triggered electrochemical detection of aminophenyl phosphate [66].

2.3 Magnetic detection

Functionalized magnetic nanoparticles (MNPs) are widely used for sensing and imaging in the context of magnetic resonance (MR) [67–69]. When used as targeted contrast agents, molecules or functional groups on the MNP surface bind the targeted molecules, first producing local inhomogeneities in

1.2. Multiplexed sensing and imaging with nano- and microparticles

the applied magnetic field that affect the proton spin precession (decreasing the relaxation time) within the target molecules and then increasing the contrast. These changes in relaxation times have been extensively utilized for high-sensitivity detection. For example, a recently published study used polymerase chain reaction detection, which normally requires fluorescence readout methods [70].

Magnetic relaxation switches are MR-based assays that are associated with different spin-spin relaxation times between the dispersed and agglomerated states of MNPs [71]. SQUIDs (superconducting quantum interference devices) have been used for sensing on the basis of the change of the relaxation magnetic moment in the presence or absence of the corresponding analyte [72]. Moreover, magnetoresistance can be also applied to magnetic sensing [73]. In this case, the change of the sensor's electrical resistance is measured following analyte binding in the presence of a magnetic field. Superparamagnetic NPs are normally used as magnetic field concentrators, but they need to be functionalized with a molecule that specifically binds the corresponding analyte. Proteins, DNA, and enzyme reactions have been detected with this technique, given that it is one of the most sensitive magnetic sensing methods [71, 74].

3. MULTIPLEXED SENSING

Analyte detection involving colloidal NPs often requires the use of multifunctional NPs. In this context, the simplest sensing system would be formed by NPs that produce or enhance a signal (which can be detected optically, electrically, magnetically, etc.), coated with a recognition element such as an antibody or an analyte-sensitive fluorophore. Multianalyte sensing could be achieved simply by producing similarly functionalized NPs with different recognition elements according to the respective analytes and with individually

resolved readout (for example, by different wavelengths in the case of optical readout). However, practical problems, such as cross-reactivity between analytes to different recognition elements involving limited selectivity, signal overlap of the different readouts, and limitations related to the NP functionalization, have to be considered. Not only does multiplexed detection reduce costs, sample volume, and assay time, but it is convenient for the analysis of real samples, such as blood or river water, in which many different analytes can interfere with the signal of a specific sensor. Therefore, there is increasing interest in developing multiplexed sensors that can substitute individual analyte-detection assays, such as enzyme-linked immunosorbent assays (ELISAs) for tumor markers [75].

In this section, we discuss some recent nanotechnology strategies applied to multiplexed sensing. There are two different approaches: assays based on particles in suspension and assays based on planar arrays. Advantages of the use of particle sensors in suspension include *(a)* the higher surface-to-volume ratio for receptor conjugation and target analyte binding; *(b)* the better accessibility of the analyte to the sensing surface, given that sensor particles move in solution similarly to the analyte; and *(c)* the possibility of incorporation in vivo by targeted delivery. This approach also has some drawbacks: *(a)* particles in suspension are normally less sensitive (i.e., have higher detection limits) than planar array sensors; *(b)* their stability and reusability are often lower; *(c)* multiplexing due to spatial separation is more easily achieved for planar arrays of NPs; and *(d)* in the case of in vivo sensing, one must take into account the fact that NPs may stay in the body for a long time and thus have cytotoxic effects. We describe two scenarios: sensing based on dispersed particles in solution and sensing based on particles associated with planar arrays. In the first case, readout is typically carried out without the particles having to be ordered on specific positions; in other words, the particles are randomly dispersed in solution (after the binding of the analyte) or are

1.2. Multiplexed sensing and imaging with nano- and microparticles

randomly associated with a surface (without order). In the second case, readout is based on structured surfaces on which the particles are bound to specific locations (Figure 2).

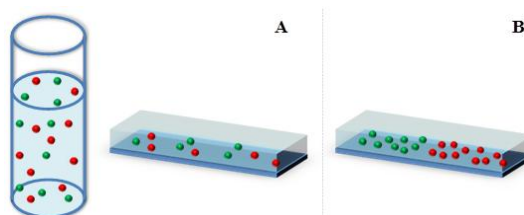


Figure 2. Classification of sensors on the basis of multifunctional particles. (a) Particles are dispersed in solution, and following analyte binding, readout can be performed in solution or on a planar surface, where sensor particles are randomly distributed. (b) Readout is based on structured surfaces on which the particles are bound to specific locations.

3.1. Multiplexed sensors based on dispersed particles in solution

For multiplexed detection in solution, particles must be designed to carry receptors for specific analytes. Also required are the corresponding transducer and an encoding scheme for use in determining which receptor is emitting the signal [76]. In this section, we focus on optical readout because it is the most frequently used technique for multiplexed sensing with dispersed particles.

Multiplexing can be achieved by spectral, spatial, and temporal separation of the readout originated from different particles (which are sensitive to different analytes) [77]. Before we describe the different principles for multiplexed sensing, we note that in all sensing applications involving particle-based sensors, one must be aware that the analyte concentration close to the (sensitive) particle surface in general differs from that in bulk [76]. This problem can be easily understood with the following examples. First, in the case of ion detection, electrostatic interaction between the corresponding ion and the particle surface occurs when the particles are charged. Debye-Hückel-

based screening on the particle charge with counterions thus involves ion concentrations close to the particle surface (where the actual detection takes place) that are different from those in bulk [78–80]. Second, in the case of protein detection, one has to be aware that proteins often (nonspecifically) adsorb to the surface of particles, forming the so-called protein corona [81, 82]. Thus, the protein concentration at particle surfaces is generally higher than in bulk. Third, the sensing element (for example, an analyte-sensitive fluorophore bound to the particle) can be influenced by the particle. If the sensing element, the actual probe, is bound inside a (porous) particle or to the particle surface, then the particle impregnates a different environment to the probe. The environment near the particle can be, for example, more apolar than the surrounding aqueous solution, which can affect the response of the probe [83]. One must therefore be aware that what particle-based sensors actually detect are local analyte concentrations, not bulk concentrations.

In case the spectrally resolved readout is based on fluorescent particles, multiplexing can be performed by using a set of particles emitting at different wavelengths, whereby the fluorescence readout of each particle-based sensor is sensitive to one analyte species. Spectrally resolved fluorescence measurements allow several analytes to be detected in parallel. The most significant problem with this approach is spectral overlap of the fluorescence from different particles. QDs are better suited to this purpose than particles that are decorated or filled with organic fluorophores, given that the emission spectra of QDs are generally narrower and do not have a red tail [1]. For example, investigators have simultaneously detected enzymatic activity from two different enzymes by using a simple assay procedure based on QDs with distinct emission spectra [46]. The enzymatic biomarkers uPA protease and Her2 kinase were detected at concentrations that were clinically relevant for the determination of breast cancer prognosis by use of two differently functionalized QDs with different emission spectra. The first QD dequenched following enzymatic degradation

1.2. Multiplexed sensing and imaging with nano- and microparticles

(Figure 3*a,b*). FRET occurred between the second QD (donor) and an organic dye (acceptor) when the residue of the enzymatic reaction was bound to a specific antibody functionalized with organic dyes on the surface of the QD (Figure 3*c,d*). Another example, also based on various QD emissions, involves a direct multiplexed sensor for Ag^+ and Hg^{2+} . The QDs were functionalized with different nucleic acids that specifically bound Ag^+ or Hg^{2+} (84). Thereafter, the presence of these ions in solution caused the formation of Ag^+ -cytosine or Hg^{2+} -thymine complexes and resulted in QD electron-transfer quenching.

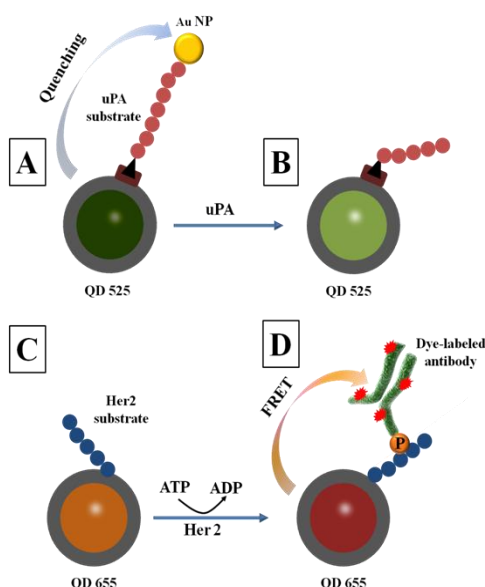


Figure 3. A multiplexed sensor for uPA protease and Her2 kinase. (**a,b**) The protease sensor is based on the quenching of quantum dots (QDs) emitting at 525 nm (**a**) and further dequenching in the presence of uPA that cleaves the substrate and releases the gold nanoparticles (AuNPs) responsible for the quenching. AuNPs absorb light very efficiently due to their surface plasmon resonance (**b**). (**c,d**) The kinase sensor is based on Förster resonance energy transfer (FRET) from QDs emitting at 655 nm to organic dyes that label the antibody bound to the analyte on the surface of the QDs following an enzymatic reaction. Modified from Reference 46 with permission.

Multiplexed, spectrally resolved optical readout can also take place with plasmonic NPs because the LSPR depends on the size and shape of the

BLOQUE I. INTRODUCCIÓN

plasmonic NPs [85]. Thus, plasmons of different types of NPs can be recorded at different wavelengths. This property has been used to create a multiplexed LSPR sensor involving gold nanorods (AuNRs) with different aspect ratios [86]. In this study, the ratio between the length and the thickness of the rods determined the respective readouts. NRs with different aspect ratios were modified with recognition molecules for various analytes. The binding of the analytes to the different AuNRs can shift the plasmon band position and modify its extent. In this context, investigators have carried out parallel detection of three different cell-surface markers and detection of two different types of bacteria [87, 88]. Although these sensors can detect only a few different analytes in parallel (given that the plasmonic peaks are relatively broad and thus suffer from spectral overlap), they are interesting because of their simple design and ease of use.

The principles discussed above are based on ensemble measurements that allow for simultaneous readout. Each particle is responsible for the detection of one analyte, giving rise to the corresponding signals at different wavelengths. Thus, readout can be spectrally resolved. However, there is an alternative way to read out particles one by one; in other words, readout can be spatially resolved. In this case, spectral overlap does not pose a problem because the particles are spatially separated and readout can be correlated with individual particles [77]. To read out particles one by one in solution, one can use either flow cytometry or microscopy.

In this context, there are two readout strategies both based on bar-coding. In the first strategy, analyte-sensitive readout can be combined with a bar code. The bar code identifies the analyte for each optical readout. Consider, for example, a class of fluorophores that are sensitive to Na^+ and another class sensitive to K^+ and that the emission spectra of both types of fluorophores overlap. If two types of particles that make up either the Na^+ - or K^+ -sensitive

I.2. Multiplexed sensing and imaging with nano- and microparticles

fluorophores, along with a corresponding bar code, are produced, then one can classify each particle by first reading the bar code, which reveals whether the fluorescence from the analyte-sensitive fluorophore corresponds to Na^+ or K^+ [77]. QDs are very useful for the production of fluorescent bar codes due to their narrow emission band. Compared with that of organic dyes, the emission of different QD species can be better spectrally resolved, so more codes can be generated. For instance, the inner cavities of porous microparticles (polyelectrolyte capsules) were loaded with analyte-sensitive fluorophores, and the surfaces of the fluorophores were tagged with a QD-based fluorescence bar code. This system allowed three ions (H^+ , Na^+ , and K^+) to be detected in parallel, despite the spectral overlap of the analyte-sensitive fluorophores (Figure 4) [44].

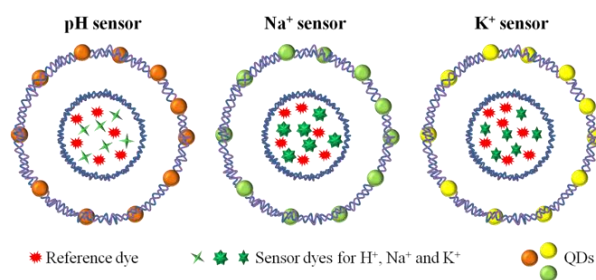


Figure 4. Simplified scheme of multiplexed sensors for H^+ , Na^+ , and K^+ based on quantum dot (QD) bar codes. Ion-sensitive dyes are encapsulated, together with a reference dye, in a permeable multiple-shell structure within the capsule to enable ratiometric measurements. The emission of the specific ion sensors may overlap, but the bar codes made with the different QDs allow for discrimination between signals.

The second bar code-based strategy is based not on active sensing (i.e., there is no molecule or particle of which the readout is altered following binding of the analyte), but on passive detection. On the basis of molecular recognition, analyte molecules in solution are tagged with a bar code; that is, bar codes need to be modified with analyte receptors. Consider a scenario in which different viruses are to be detected in solution. Antibodies for the different viruses would be modified with different bar codes. By observing one

BLOQUE I. INTRODUCCIÓN

by one the conjugates that form (as mentioned above in the context of flow cytometry or with microscopy), one can identify the different viruses. An important example is a multiplexed sensor for five different genetic biomarkers (human immunodeficiency virus, malaria, hepatitis B, hepatitis C, and syphilis) developed by Giri et al. [43]. These authors encoded microbeads with QDs of different emission wavelengths and intensities to produce a library of bar codes for multiplexed detection; this library exceeded the limit of 100 useful bar codes of similar systems involving organic dyes instead of QDs. The bar-coded particle bound the biomarker without causing any change in its fluorescent emission. A universal fluorescent probe that binds all biomarkers was used to discriminate between the unbound bar codes and the analyte–bar-coded particles. Only when there was colocalization between the emission of the bar code and the universal probe was the analyte bound to the bar code. Readout was performed with flow cytometry (Figure 5).

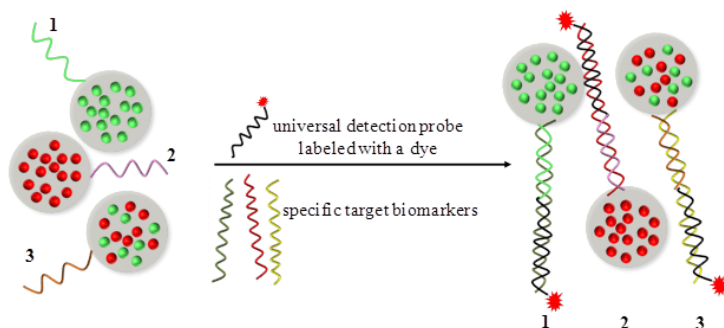


Figure 5. Microbeads labeled with different mixtures of quantum dots for multiplexed biomarker detection. Each sensor is functionalized with a capture DNA strand (steps 1 through 3). In solution, hybridization occurs between the specific target biomarkers and the universal detection probe. The universal labeled probe is used to differentiate between bar codes bound to the biomarkers and free ones. Finally, the sample is analyzed by flow cytometry, in which each particle is analyzed individually.

SERS-encoded NPs are a promising alternative to bar-coding [89]. Particles should contain organic molecules (SERS reporters) in close contact with or bound to the plasmonic surfaces, providing the signature of the particle

I.2. Multiplexed sensing and imaging with nano- and microparticles

[90]. The particle should be separately functionalized with an analyte receptor [91]. Due to the uncountable number of molecules, each of which has specific vibrational spectra, a multiplexed sensor based on SERS-encoded NPs can be considered limitless. However, the number of codes that can be experimentally produced is restricted by several factors involved in the synthesis of multifunctional particles, such as the binding of the SERS reporter on the metallic surface, the insufficient field enhancement necessary to raise the SERS signal up to detectable levels, and the stability of the particles. Many examples of the synthesis of encoded NPs for SERS sensing in solution exist [92, 93] but the multiplexed sensing of a large number of analytes is still in its infancy, so more universal strategies for the SERS-encoding and detection should be performed. In vivo multiplexed sensing has been demonstrated only recently [94].

Another example involves plasmonic NPs assembled on a surface for the design of SERS-based multiplexed sensing platforms [95]. So-called sandwich-type DNA coated silver NP arrays have been used to specifically hybridize various DNA strands labeled with different SERS probes [96]. Multiplexing can take place because different SERS labels can conveniently be spectrally resolved (Figure 6); thus, no structuring of the surface is required. The number of DNA strands that can be detected in parallel is limited by the number of SERS labels that can bind DNA and by the length of the DNA strand (with sufficient enhancement of the Raman signal, which depends on the number of labels and the distance between the labels and the surface). The creation of hot spots following DNA hybridization has also been exploited in multiplexed SERS-based sensors involving sandwich-type DNA arrays to reach a DNA detection limit of 10 pM [97].

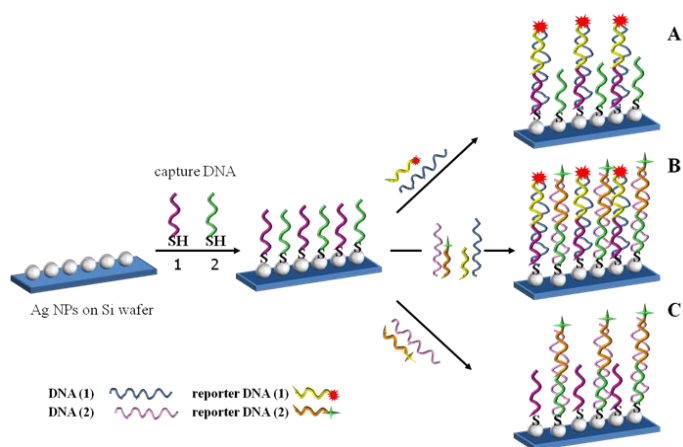


Figure 6. A multiplexed DNA sensor based on silver nanoparticles (AgNPs) deposited on silicon wafers and functionalized with thiolated DNA (1 and 2) strands for the specific hybridization of DNA (1) and DNA (2) and the corresponding surface-enhanced Raman spectroscopy-labeled DNA reporters. (a) Only DNA (1) in solution. (b) A mixture of DNA (1) and DNA (2) in solution. (c) Only DNA (2) in solution. Abbreviation: SH, thiol group termination. Modified from Reference 96 with permission.

Encoded hybrid materials can help improve the number of analytes detected in parallel, as discussed in the previous section. However, if a second encoding scheme is added to multifunctional NPs, then the number of parallel detected analytes can be multiplied. This idea was introduced by Wang et al. [98], who recently produced a hybrid system based on AuNRs coated with SiO₂ and encoded with different QDs with different emission and SERS labels. The resulting immunoassay has great potential for multiplexing.

In addition to spectral and spatial discrimination, temporal resolution of different optical sensors can also be performed. In the case of fluorescent particles, analyses of luminescence lifetime and the intensity-to-lifetime ratio allow for discrimination between signals that may be spectrally overlapped [99, 100]. Sensors based on lifetime measurements of QDs exist [101], but to the best of our knowledge, multiplexed sensors based on lifetime measurements are still uncommon. Techniques such as fluorescence lifetime imaging microscopy (FLIM) will probably extend the use of temporal discrimination in

1.2. Multiplexed sensing and imaging with nano- and microparticles

optical biosensing. Recently, cellular viscosity was studied with fluorescent ratiometry and FLIM [102], and multiplexed sensing is likely to evolve in this direction by simultaneously taking advantage of several measurements, either spectral and temporal or spatial and temporal [103]. An example of a promising technique in multiplexing wherein lifetime and spectral measurements of fluorophores can reveal information about analyte binding involves multiplexed FRET assays. If FRET occurs, not only the emission intensity and wavelength of the donor and acceptor fluorophore but also the lifetime can be changed (Section 2). Multiplexed FRET assays for biosensing have been developed on the basis of (a) FRET from luminescent lanthanide complexes to several different QDs (acceptors) following molecular recognition [104] or (b) FRET from several QDs (donors) to organic dyes for the detection of DNA [105].

Although most of the examples of multifunctional NPs used for multiplexed sensing in solution involve optical detection, there are remarkable examples that mix several detection modes. These include magnetofluorescent nanoparticles, which can be used for flow cytometry and diagnostic MR detection [106, 107].

3.2. Multiplexed sensors based on particles associated with planar arrays

Planar arrays, composed mainly of metallic and semiconductor NPs and arrays of biomolecules such as DNA and antibodies that bind NPs, have been extensively studied for use in NP-based optical or electrical biosensors [108–110]. Multiplexed sensing with NPs associated with (typically planar) arrays can easily be performed because of the possibility of positional encoding [111]. The general idea is to detect various analytes at different positions of the (generally structured) array. In this section, we discuss recent examples of multiplexed sensors based on NP planar arrays.

3.2.1. Localized surface plasmon resonance spectroscopy

LSPR-based multiplexed sensors detect, for example, changes in interparticle distance; modification of the refractive index; and changes in color in the LSPR of NPs due to the presence of analytes, whose individual signal can be differentiated by specific receptors, normally DNA or antibodies [112–114]. Colorimetric assays can be produced through functionalization of a microstructure chip with different antibodies in different regions. The addition of a solution with antigen produces specific antibody–antigen binding, and depending on the amount of antigen, the response in color (and absorbance) may differ. This method is sensitive and specific. Endo et al. [115] applied this method to eight different proteins. In a similar approach, investigators modified the above-mentioned scanometric assay by using antibodies instead of DNA microarrays and electroless deposition of gold instead of silver. The light was thereby scattered by antibody–oligonucleotide hybrid AuNPs, and the amplification of the signal was greater than that of precedent scanometric assays due to gold deposition (Figure 7). The assay detected very low concentrations of different proteins, in this case in serum, without the need to trap of the analyte in solution with two differently labeled NPs. This process eliminated several steps from the production of the multiplexed sensors [116]. Note that scanometric assays are US Food and Drug Administration–approved detection methods for biological samples. Therefore, they are among the most-studied and most widely used methods for multiplexed analyses involving NPs.

1.2. Multiplexed sensing and imaging with nano- and microparticles

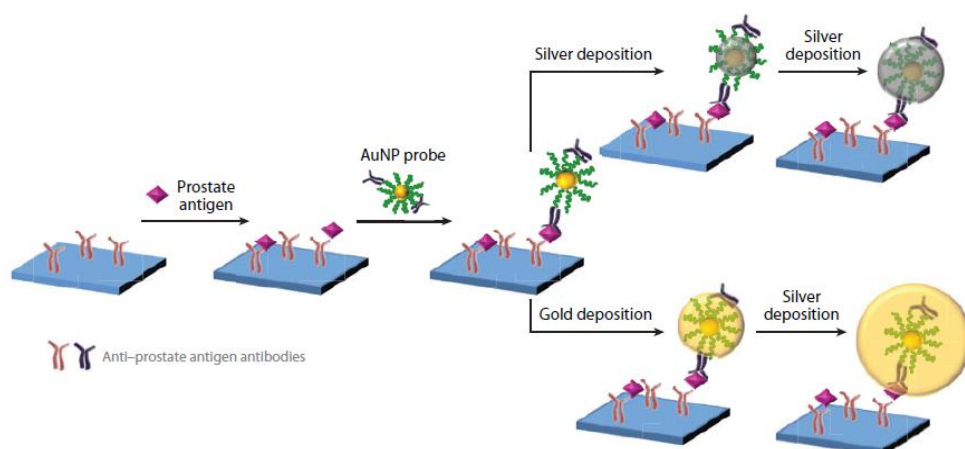


Figure 7. A scanometric immunoassay. Abbreviation: AuNPs, gold nanoparticle. Modified in part from Reference 116.

In addition to direct arrangement of the NPs via recognition of the analyte on the array surface, NPs that have captured an analyte can also be arranged via bar codes. Bar codes can be made, for example, with biological molecules. An interesting example is a multiplexed sensor based on bio-bar-coded AuNPs and scanometric detection (involving colorimetric detection) [117]. The analytes—in this case, protein cancer markers—are trapped by two different types of NPs, DNA bar-coded AuNPs and MNPs, which have different antibodies that bind the same protein in different epitopes. Magnetic separation is applied after the analytes are trapped in solution by the antibodies bound to the surface of the MNPs. The DNA used as a bar code is then released from the gold surface and quantified in a scanometric detector (LSPR-based detection). Again, the detector involves (smaller) AuNPs and a silver-layer coating that significantly amplified the signal and reduced the detection limits. Figure 8 depicts this multiplexed sensor, which is very sensitive and specific. However, it requires many functionalization steps for numerous different NPs.

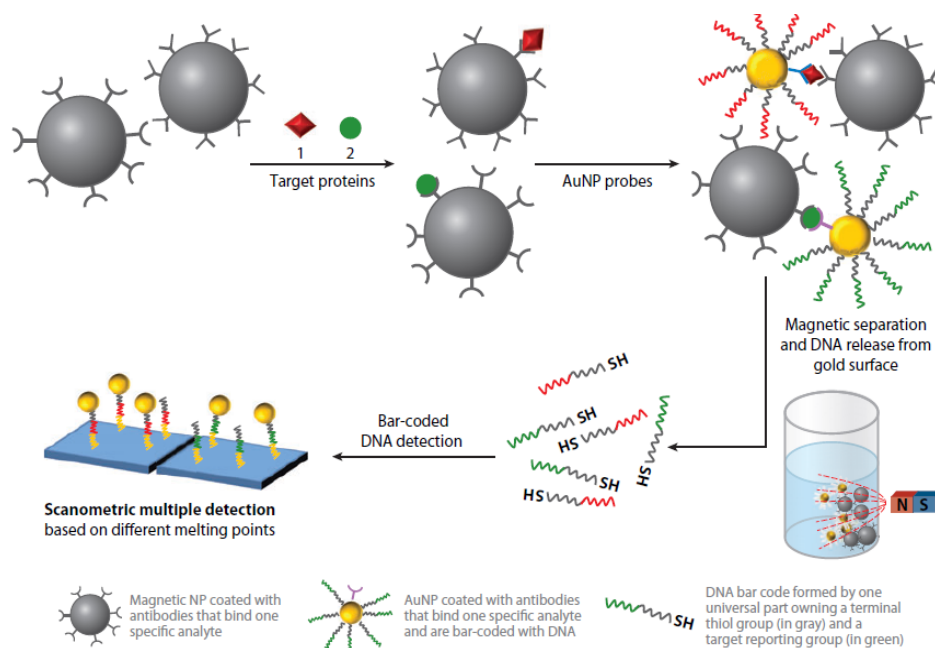


Figure 8. A bio-bar-coded gold nanoparticle (AuNP) assay for multiplexed protein detection. Scanometric detection also involves a silver coating to improve sensitivity (not shown for simplicity). Abbreviation: SH, thiol group termination. Modified from Reference 117 with permission.

Recently, copper-capped silica particles have been used to develop a cost-effective optical setup on disposable chips capable of multiplexed sensing of biomolecules; the chips have a detection limit of 10 fM. The assay is based on measurable changes in the refractive index in the presence of analytes (in this case, different DNA strands), which arise from the LSPR of the copper layer deposited on the silica NPs [118]. The combination of LSPR refractive-index sensing and the well-known ELISA assay has led to the development of another colorimetric multiplexed sensor with single-molecule sensitivity. This new technique takes advantage of the amplification of the shift of the LSPR scattering maximum following an enzymatic reaction that allows for the detection of one or a few enzymes [119]. The authors have not yet applied this new approach to multianalyte analyses, but due to the sensor configuration and

1.2. Multiplexed sensing and imaging with nano- and microparticles

the results from single-particle analyses, multiplexing is highly anticipated, along with the development of nonfluorescence single-molecule ELISA assays.

3.2.2. Electrochemical immunosensors and immunoassays

Electrochemical immunosensors and immunoassays (EIs) are electrochemical sensors in which antibody–antigen interactions occur on an electrochemical transducer (in immunosensors) or the immunological material is immobilized on a solid support, such as a nanomaterial. Following sandwich or competitive immunoreactions, the solid support containing the immunological material is attached to the transducer surface (in immunoassays) [120]. EIs are excellent candidates for multianalyte analysis in terms of clinical diagnosis, in which the biological agents to be detected are present in very low concentrations [121]. Multiplexed analysis can be performed in EIs when the sensing electrodes are sufficiently separated to prevent signal interference (cross talk) between neighboring electrodes. Very low analyte concentrations can be detected through amplification of the antibody–antigen interaction transduction signal with labels such as enzymes or NPs [122]. NPs can have different functions within the sensor (Section 2.2), such as trapping analytes and improving the transducer surface for better antibody adhesion.

Interesting examples of EIs involving multifunctional NPs have recently been provided [60, 123]. Mani et al. [124] produced a multiplexed sensor for four different oral cancer biomarkers that can be used with clinical samples. These authors achieved ultralow detection ($5\text{--}50\text{ fg ml}^{-1}$) on the basis of amperometric measurements. In another study, magnetic nanobeads were functionalized with both an antibody to capture a specific analyte and horseradish peroxidase to amplify the signal during the detection on the planar electrode. In the first step of the detection, the magnetic beads functionalized

BLOQUE I. INTRODUCCIÓN

with specific antibodies captured the corresponding analyte due to antibody-antigen interactions; then, these magnetic nanobeads were magnetically separated from the solution. The second step of the detection involved the binding of a second antibody with the corresponding antigen on a planar electrode. This time, the second antibody bound to another epitope of the same antigen, and the unbound magnetic nanobeads were washed out. Multiplexing was achieved through the use of several electrodes in parallel [125]. Figure 9 depicts this multiplexed sensor.

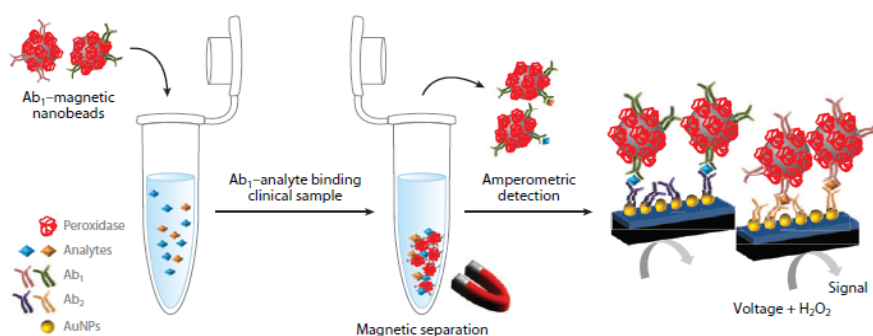


Figure 9. A gold nanoparticle (AuNP) array functionalized with antibodies (Ab_2) for the ultrasensitive detection of cancer biomarkers. The sensor also contains magnetic beads labeled with antibodies (Ab_1) and horseradish peroxidase for amplification and biomarker capture. Multiplexing is achieved through parallel detection in different electrodes.

AuNP arrays are useful in immunoassays for several reasons. First, they increase the electrode surface area. Second, they facilitate the attachment of numerous antibodies due to the easy functionalization of gold surfaces. The production of high-AuNP-coverage electrodes depends on both the stabilizing molecule on the gold surface and the electrode surface. Often, it is necessary to coat the electrode with a layer of molecules that increase the adhesion of the AuNP. For example, positively charged polyelectrolytes such as PDDA [poly(diallyldimethylammonium chloride)] can be used to increase the AuNP's adhesion. Similar electrodes have been produced for multiplexed protein detection by use of carbon nanotube arrays, but their detection limits,

I.2. Multiplexed sensing and imaging with nano- and microparticles

reproducibility, and stability were lower than those of the AuNPs arrays [124, 126, 127].

Multiplexing as discussed above, is based on the use of an array of differently functionalized electrodes. Geometrically, the number of electrodes that can be used in parallel is limited [128]. However, as an alternative to electrode arrays, spatial resolution and, thus, multiplexing capability can be achieved by use of a light pointer in connection with a semiconducting electrode surface to select defined points on an electrode surface [129–131]. The light pointer creates a local photocurrent whose amplitude is influenced by local redox reactions on the electrode surface. The semiconductor layer can be constructed from QDs [57, 58]. The first observations of enzymatic reactions have already been reported [55, 66, 132, 133]. Although multiplexed analysis has not yet been practically demonstrated, its spatial resolution capability clearly demonstrates its potential.

3.2.3. Giant magnetoresistive sensors

Giant magnetoresistive (GMR) sensors are a promising and low-cost alternative for the detection of proteins and nucleic acids. In the former case, antibody arrays must be prepared beforehand to specifically capture the corresponding analyte. Functionalized MNPs in solution that bind the same antigen are used to detect the presence of an analyte by measuring the small changes in resistance due to the binding event in the presence of a magnetic field. Multiplexed sensors have been developed using this technique, but their reproducibility and sensitivity remain compromised in extended sensing applications with real and untreated samples [134–138].

There are many other examples of the use of NP arrays or NPs as labels in immunoassays, such as chemiluminescence imaging immunoassays involving

horseradish peroxidase and AuNPs [139]. New strategies for multiplexing with planar arrays are continually being introduced due to their significant possibilities in multifunctional NP synthesis and the application of new materials, such as fluorescent nano-graphene oxide and ensemble aptamers instead of more specific DNAs for analyte recognition [140].

4. MULTIMODAL IMAGING

In recent years, many applications of NPs to bioimaging and diagnosis have been developed [141–143]. The most important example is undoubtedly the use of MNPs in magnetic resonance imaging (MRI) [144–147]. However, many other NP applications are expected to find clinical use in the near future. Advances in colloidal chemistry have enabled “a la carte” design of multifunctional particles. By combining elements such as radioactive isotopes, QDs [31, 148], and organic dyes in the same nanostructure or microparticle, one can easily obtain multimodal nano- or microcomposites. The use of multimodal labels is necessary to overcome the limits of any single technique, such as spatial resolution or bleaching. Cheon & Lee [149] explored these ideas on the basis of multimodal imaging probes consisting of MNPs with further functionalities, namely radionuclides enabling positron emission tomography and fluorescent moieties for optical tracking. These probes can be modified with anchor molecules such as antibodies, peptides, DNA, and RNA, permitting the investigators to address specific targets.

Liong et al. [150] provided an example of advantageous MNP-based multimodal systems. These authors applied multifunctional iron oxide–mesoporous silica NPs that were detectable both optically and by MRI. They rendered the particles suitable for live-cell imaging and therapeutic purposes by targeting them specifically to human cancer cells. Moreover, those particles

I.2. Multiplexed sensing and imaging with nano- and microparticles

were simultaneously used to deliver hydrophobic anticancer drugs (or other molecules) into cells.

Nahrendorf et al. [151] investigated a comparable trimodal imaging system comprising MRI (iron oxide core), PET sensors (chelator ligand complexing the radiotracer Cu^{64}), and fluorescence (VivoTag-680™) that enabled *in vivo* studies of the detection of macrophage markers, specifically, the detection of inflammatory atherosclerosis. Given the lower required concentration of NPs and their higher target-to-background ratio, the authors found this technique especially relevant for clinical use. The production of nano- or microprobes for multimodal imaging *in vivo* can be difficult, mainly because of targeting issues [152, 153], the colloidal stability and purity of the probes, the retention time *in vivo* [154], the long-term stability of the signal, degradability, possible toxicity, and the clearance mechanisms of the probes in humans. Degradation over the long term and dissolution of the nanoprobe within the body are very difficult to avoid, in particular in the case of corrosive NP materials such as CdSe or silver. Regarding *in vivo* applications, the use of toxic materials (e.g., radiotracers) or materials that deliver toxic ions during dissolution (e.g., CdSe QDs) should be minimized. Nevertheless, in specific instances, the lack of a diagnosis would be worse for the patient than the risk posed by the probe itself (e.g., a PET sensor).

Several types of multimodal particle platforms exist. On the NP level, for example, polymer coated NPs purified with gel electrophoresis and size-exclusion chromatography fulfill most of the above-mentioned requirements [80, 155]. They are very stable and pure [156–158]; their size is reasonably small; and in the size range for the longest blood circulation time (10–100 nm) [159], the surface charge can be varied [160], the polymer shell itself does not impose enhanced cytotoxicity [161], and the polymer protecting the core can be loaded with functional entities [162]. For these NPs, the inorganic core can be

BLOQUE I. INTRODUCCIÓN

used as the first label (for example, it can be made magnetic, fluorescent, or radioactive), and the second label can be incorporated within the amphiphilic polymer that stabilizes the NP surface [155, 157, 158]. Both labels are thereby protected from the biological environment, which helps improve signal stability and leaves the NP surface free for further functionalization by, for instance, cell-penetrating peptides, molecular receptors, or molecules that improve cell circulation such as poly(ethylene glycol) [154]. Figure 10 presents examples of such probes.

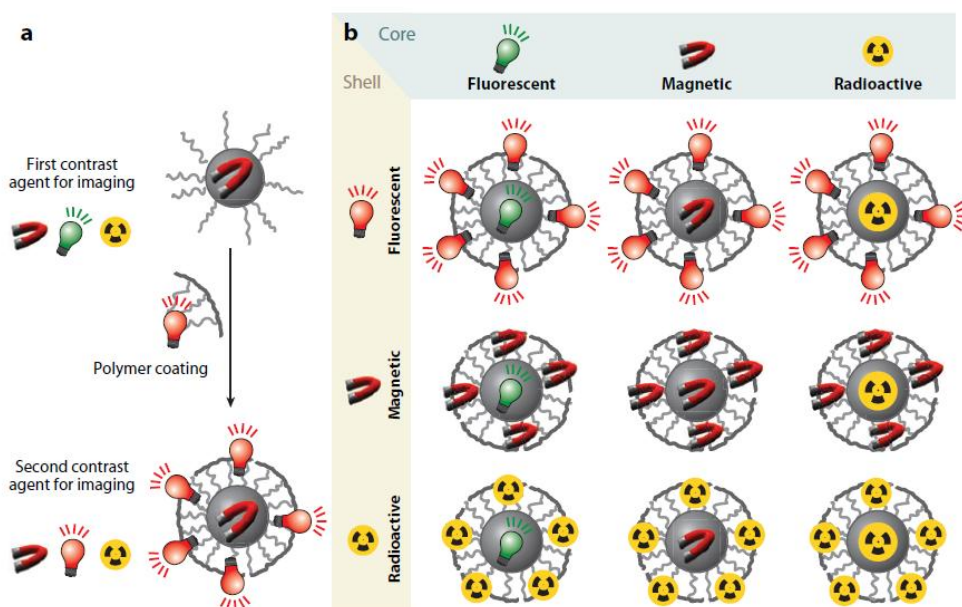


Figure 10. Strategy to produce multifunctional nanoparticles (NPs) for dual imaging. (a) Inorganic cores (gray) can be synthesized with different materials that are magnetic, fluorescent, or radioactive. Organic molecules are stabilized on the NP surface following core synthesis. The cores are coated with an amphiphilic polymer that makes them water soluble. The amphiphilic polymer is loaded prior to coating with the second label (fluorophore, radioactive atom, etc.), and the final NP is double labeled. (b) Table including the possibilities of NPs for dual imaging based on polymer-coated NPs.

Fluorescence microscopy can be conveniently combined with SERS imaging through the incorporation of dyes, SERS probes, and even surface-

I.2. Multiplexed sensing and imaging with nano- and microparticles

enhanced resonance Raman scattering (SERRS)-active labels in the same multifunctional particle. Core-shell particles made from a gold core and an organosilica shell are good platforms for the simultaneous entrapment of fluorophores and SERS probes. Cui et al. [163] produced ~100-nm-diameter core-shell particles loaded with fluorescein isothiocyanate and malachite green isothiocyanate (green dye and SERS label). In a further demonstration of multiplexing, the authors synthesized similar particles with fluorescein isothiocyanate and X-rhodamine-5-(6)-isothiocyanate (green dye and SERRS label) (Figure 11a). Multimodal imaging in living cells was thereby demonstrated with these two differently labeled types of particles.

Currently, SERS imaging is limited by light penetration. NPs can be detected at a maximum depth of 1 cm [164]. The combination of SERS with techniques such as spatially offset Raman spectroscopy could pave the way for clinical detection because the depth can be increased to up to 5 cm [165]. In SERS applications and, more importantly, in bioimaging, the metallic surface of the NPs should be protected with an appropriate shell that hinders the adsorption of molecular species that could interfere with the vibrational code of the SERS probe. Silica shells have been used primarily for SERS applications and for multimodal imaging based on colloidal NPs because of their (a) reduced agglomeration, (b) biocompatibility, (c) optical transparency, (d) tunable porosity, (e) chemical inertness, and (f) ease of further functionalization [166]. Figure 11 shows several examples of multimodal NP imaging probes built up with silica shells and different inorganic cores. Not only do silica shells act as protective shells, but also they can be loaded with fluorophores, SERS and SERRS labels, or other NPs (Figure 11a). For example, the surface of $\text{Fe}_3\text{O}_4@SiO_2$ core-shell particles was further functionalized with AuNRs for in vivo MRI and IR imaging [167]. Also, more than two imaging modalities can be used within one NP (Figure 11c). Hwang et al. [41] have produced quadruple-labeled particles by first coating cobalt ferrite NPs with a silica shell entrapping

BLOQUE I. INTRODUCCIÓN

rhodamine B isothiocyanate and then functionalizing the silica surface with an organic dye. The bioluminescent protein luciferase was added as the third label and radioactive $^{68}\text{GaCl}_3$ as the fourth. These particles were successfully used in five in vivo imaging techniques: fluorescence, bioluminescence, BRET, positron emission tomography, and MRI. The same authors monitored in vivo and in vitro uptake in target cells of similar particles that were functionalized with specific aptamers with fluorescence microscopy, radioactive detection, and MRI [168].

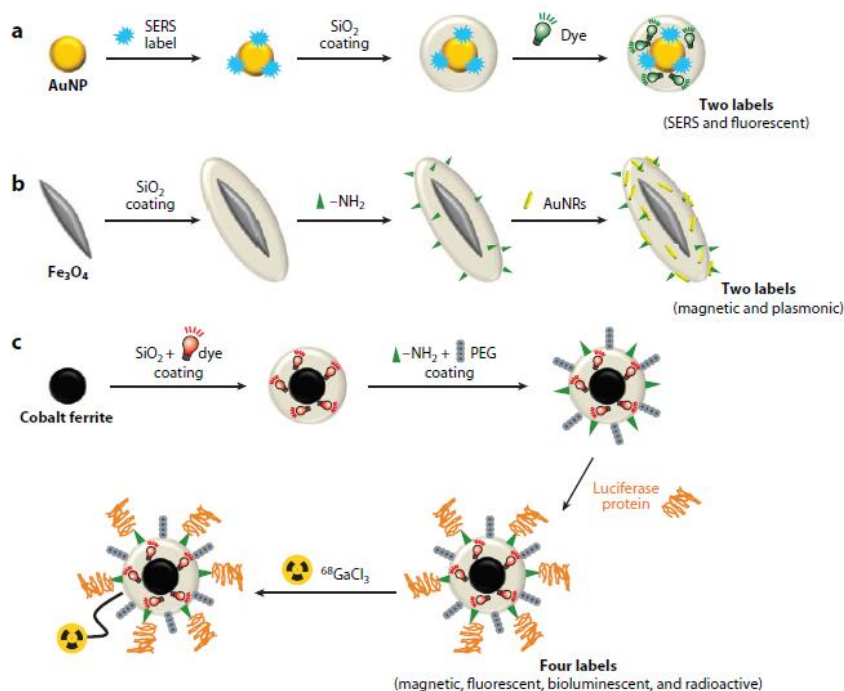


Figure 11. Different multimodal nanoparticle (NP) probes made with core-shell particles involving silica coating. (a) Particles for surface-enhanced Raman spectroscopy (SERS) and fluorescence imaging. Gold nanoparticles (AuNPs) are coated with a silica layer that entraps both the SERS probe and the fluorophore. Image adopted from Cui et al. [163]. (b) Particles for in vivo magnetic resonance imaging and IR thermal imaging. Fe_3O_4 ellipsoids are coated with silica and gold nanorods (AuNRs). Image adapted from Ma et al. [167]. (c) Quadruple imaging based on a magnetic core coated with a silica shell embedding a fluorophore, and further silica surface functionalization with a bioluminescent protein and a radioactive isotope. Abbreviation: PEG, poly(ethylene glycol). Data adapted from Hwang et al. [41].

I.2. Multiplexed sensing and imaging with nano- and microparticles

Silica shells have also helped produce lanthanide-based multifunctional NPs. Upconverting NPs are interesting for multimodal imaging due to their special 4f electron structure, their rich optical and magnetic properties, their biocompatibility, and the tunability of their emission wavelength [169]. More importantly, the upconversion of light due to anti-Stokes emission significantly minimized the background and simplified the discrimination of the signal from the target tissues or cells, compared with other optical techniques. Core-shell trimodal particles involving silica shells have recently been produced for X-ray computed tomography, MRI, and fluorescence imaging, demonstrating their suitability for further *in vitro* and *in vivo* applications [170, 171].

Multifunctional particles can also extend the application of certain imaging techniques, such as for magnetophotoacoustic (MPA) imaging. MPA imaging is based on the synergy of magnetomotive ultrasound, photoacoustic, and ultrasound imaging. It is a noninvasive technique that can be applied in diagnosis. To this end, Jin et al. [172] recently introduced a new class of core-shell NPs made from an iron oxide core and a gold shell separated by phospholipid-poly(ethylene) glycol and a layer of polyhistidine (Figure 12). Due to the hybrid nature of these NPs, their contrast, resolution, and sensitivity obtained in ultrasound imaging were acceptable. Otherwise, the technique is not yet good enough in terms of contrast, although it remains interesting due to its resolution at reasonable depths, nonionizing nature, cost-effectiveness, and portability. Moreover, the particles can be imaged with electron microscopy, MRI, and scattering-based techniques.

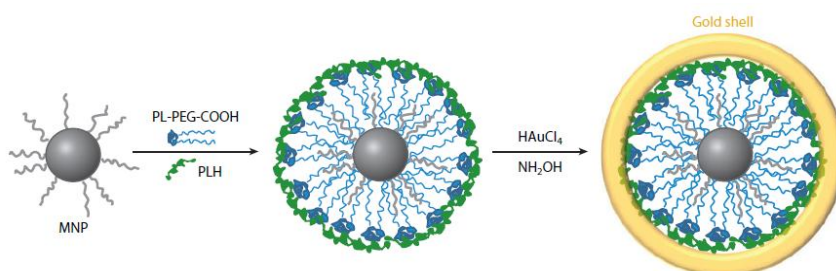


Figure 12. Core-shell iron oxide-gold nanoparticles. Magnetic nanoparticles (MNPs) were initially stabilized with oleic acid (gray), then coated with phospholipid-poly(ethylene glycol) (PL-PEG)-COOH and polyhistidine (PLH) to form a gold layer through the reduction of the salt HAuCl_4 by NH_2OH on the particle surface.

Multilayer polyelectrolyte capsules are promising candidates for multimodal imaging because they can simultaneously incorporate several labels that are spatially separated. In Section 3.1, we describe bar-coded capsules for multiplexed analysis [44]. Multimodal imaging can be easily achieved in the same manner by combining organic labels with inorganic NPs that act as contrast agents. In addition to optical detection with fluorescence microscopy, the magnetic properties of capsules loaded with superparamagnetic NPs are suitable for MRI [173]. Moreover, Johnston et al. [174] have demonstrated that it is possible to control the binding and uptake of such capsules on target cells by antibody labeling.

5. IMAGING AND SENSING

Many multifunctional NPs can be used for either imaging or sensing. The classical example is iron oxide-based NPs, which are useful in MRI as negative-contrast agents (image darkening) and in magnetoresistive immunoassays as nanotags [134, 144]. However, there are fewer examples of particles that can be applied simultaneously to in vivo or in vitro imaging and sensing. The application of multifunctional particles for such purposes could lead to great advances in diagnosis. The size of NPs is similar to that of ribosomes and some

I.2. Multiplexed sensing and imaging with nano- and microparticles

proteins; therefore, NPs may be able to simultaneously detect and localize changes in biomolecule or ion concentrations that are related to many diseases. In this context, nanoprobe based on organic polymers have been used to simultaneously image and estimate local concentrations of O₂ in vitro [175, 176]. Moreover, polymer matrices such as PEBBLE nanosensors have incorporated several fluorophores for imaging and ratiometric determination of in vitro ion concentrations [177]. Rare earth-doped NPs have been used as in vitro and in vivo luminescent tags and temperature sensors [178, 179]. Recently, SERS nanotags were simultaneously employed to image and detect cancer biomarkers in vivo [94].

Another alternative, similar to PEBBLE sensors, is the nanostructured production of polymer microcapsules that simultaneously incorporate NPs and fluorophores that are sensitive to different analytes [44, 180]. In vitro experiments to estimate pH changes in cells have been performed, but given the feasibility for multifunctionalization involving bar-coding, antibody functionalization, and ratiometric measurements, many future applications involving simultaneous imaging and sensing are likely [44, 174, 181].

6. OUTLOOK

This review describes many strategies for multiplexed sensing and multimodal imaging involving multifunctional nano- and microparticles. Although interesting examples have been published, most of these techniques have not yet been used for detection with real samples, such as blood serum, or for in vivo imaging. Some of these sensing techniques still lack reproducibility. With regard to in vitro detection, DNA arrays, for example, have been successfully used for multiplexed sensing of various analytes. However, the values obtained for the analyte concentrations are often only informative and not quantitative. Antibody arrays are promising substitutes for DNA arrays

BLOQUE I. INTRODUCCIÓN

because they can detect, in the case of gene expression, proteins directly from protein–antigen interactions, so quantification should be easier to perform. However, the use of antibodies for analyte trapping or recognition poses certain problems. The epitope where antibody–antigen binding takes part is only a small part of the analyte, and antibodies often aberrantly bind epitopes of nontargeted analytes. Some of the examples discussed above regarding antibody arrays involve several antibody–antigen binding events to reduce cross-reactivity. New amplification methods are currently being developed to improve sensitivity by improving analyte–receptor interaction specificity, as is the case in applications of orthogonal chemistries to diagnosis and imaging [107, 182]. Particle stability [76] still poses a problem for in vivo applications such as particle-based sensors and contrast agents for imaging. Circulation within the bloodstream and further uptake in target tissues remain the most critical challenges for nanomedicine [183].

Disclosure statement

The authors are not aware of any affiliations, memberships, funding, or financial holdings that might be perceived as affecting the objectivity of this review.

Acknowledgments

Parts of our work were supported by DFG (Germany; grant PA794/11-1 to W.J.P.) and the European Commission (a nanagnostics grant to W.J.P.). We acknowledge technical discussions with Dr. Gaëlle Charron.

I.2. Multiplexed sensing and imaging with nano- and microparticles

Literature cited

1. Bruchez MJ, Moronne M, GinP, Weiss S, Alivisatos AP. 1998. Semiconductor nanocrystals as fluorescent biological labels. *Science* 281:2013–16
2. Chan WCW, Nie S. 1998. Quantum dot bioconjugates for ultrasensitive nonisotopic detection. *Science* 281:2016–18
3. Alivisatos AP. 2004. The use of nanocrystals in biological detection. *Nat. Biotechnol.* 22:47–51
4. Elghanian R, Storhoff JJ, Mucic RC, Letsinger RL, Mirkin CA. 1997. Selective colorimetric detection of polynucleotides based on the distance-dependent optical properties of gold nanoparticles. *Science* 277:1078–81
5. Khlebtsov B, Panfilova E, Khanadeev V, Bibikova O, Terentyuk G, et al. 2012. Nanocomposites containing silica-coated gold–silver nanocages and Yb-2,4-dimethoxyhematoporphyrin: multifunctional capability of IR-luminescence detection, photosensitization, and photothermolysis. *Am. Chem. Soc. Nano* 5:7077–89
6. Jakhmola A, Anton N, Vandamme TF. 2012. Inorganic nanoparticles based contrast agents for X-ray computed tomography. *Adv. Healthc. Mater.* 1:413–31
7. Judenhofer MS, Wehrl HF, Newport DF, Catana C, Siegel SB, et al. 2008. Simultaneous PET-MRI: a new approach for functional and morphological imaging. *Nat. Med.* 14:459–65
8. Ross P, Hall L, Smirnov I, Haff L. 1998. High level multiplex genotyping by MALDI-TOF mass spectrometry. *Nat. Biotechnol.* 16:1347–51
9. Kotov N. 2011. Bioimaging: The only way is up. *Nat. Mater.* 10:903–4
10. Jans H, Huo Q. 2012. Gold nanoparticle-enabled biological and chemical detection and analysis. *Chem. Soc. Rev.* 41:2849–66
11. Freeman R, Willner I. 2012. Optical molecular sensing with semiconductor quantum dots (QDs). *Chem. Soc. Rev.* 41:4067–85
12. Jimenez de Aberasturi D, Montenegro JM, Ruiz de Larramendi I, Rojo T, Klar TA, et al. 2012. Optical sensing of small ions with colloidal nanoparticles. *Chem. Mater.* 24:738–45
13. Scotognella F, Della Valle G, Kandada ARS, Dorfs D, Zavelani-Rossi M, et al. 2011. Plasmon dynamics in colloidal Cu_{2-x}Se nanocrystals. *Nano Lett.* 11:4711–17
14. McFarland AD, Van Duyne RP. 2003. Single silver nanoparticles as real-time optical sensors with zeptomole sensitivity. *Nano Lett.* 3:1057–62

BLOQUE I. INTRODUCCIÓN

15. Rodríguez-Lorenzo L, de la Rica R, Álvarez-Puebla RA, Liz-Marzán LM, StevensMM. 2012. Plasmonic nanosensors with inverse sensitivity by means of enzyme-guided crystal growth. *Nat. Mater.* 11:604–7
16. Claridge SA, Schwartz JJ, Weiss PS. 2011. Electrons, photons, and force: quantitative single-molecule measurements from physics to biology. *Am. Chem. Soc. Nano* 5:693–729
17. Ament I, Prasad J, Henkel A, Schmachtel S, Soennichsen C. 2012. Single unlabeled protein detection on individual plasmonic nanoparticles. *Nano Lett.* 12:1092–95
18. Saha K, Agasti SS, Kim C, Li X, Rotello VM. 2012. Gold nanoparticles in chemical and biological sensing. *Chem. Rev.* 112:2739–79
19. Leuvering JHW, Thal P, Vanderwaart M, Schuurs A. 1981. A sol particle agglutination assay for human chorionic gonadotropin. *J. Immunol. Methods* 45:183–94
20. Taton TA, Mirkin CA, Letsinger RL. 2000. Scanometric DNA array detection with nanoparticle probes. *Science* 289:1757–60
21. Zhao W, Chiuman W, Lam JCF, McManus SA, Chen W, et al. 2008. DNA aptamer folding on gold nanoparticles: from colloid chemistry to biosensors. *J. Am. Chem. Soc.* 130:3610–18
22. Beqa L, Singh AK, Khan SA, Senapati D, Arumugam SR, Ray PC. 2011. Gold nanoparticle-based simple colorimetric and ultrasensitive dynamic light scattering assay for the selective detection of Pb (II) from paints, plastics, and water samples. *Am. Chem. Soc. Appl. Mater. Interfaces* 3:668–73
23. Aldeanueva-Potel P, Correa-Duarte MA, Álvarez-Puebla RA, Liz-Marzán LM. 2010. Free-standing carbon nanotube films as optical accumulators for multiplex SERRS attomolar detection. *Am. Chem. Soc. Appl. Mater. Interfaces* 2:19–22
24. Álvarez-Puebla RA, Agarwal A, Manna P, Khanal BP, Aldeanueva-Potel P, et al. 2011. Gold nanorods 3D supercrystals as surface enhanced Raman scattering spectroscopy substrates for the rapid detection of scrambled prions. *Proc. Natl. Acad. Sci. USA* 108:8157–61
25. Song J, Zhou J, Duan H. 2012. Self-assembled plasmonic vesicles of SERS-encoded amphiphilic gold nanoparticles for cancer cell targeting and traceable intracellular drug delivery. *J. Am. Chem. Soc.* 134:13458–69
26. Tsoutsi D, Montenegro JM, Dommershausen F, Koert U, Liz-Marzán LM, et al. 2011. Quantitative surface-enhanced Raman ultradetection of atomic inorganic ions: the case of chloride. *Am. Chem. Soc. Nano* 5:7539–46
27. Boyer D, Tamarat P, Maali A, Lounis B, Orrit M. 2002. Photothermal imaging of nanometer-sized metal particles among scatterers. *Science* 297:1160–63

I.2. Multiplexed sensing and imaging with nano- and microparticles

28. Lasne D, Blab GA, Berciaud S, Heine M, Groc L, et al. 2006. Single nanoparticle photothermal tracking (SNaPT) of 5-nm gold beads in live cells. *Biophys. J.* 91:4598–604
29. Dreaden EC, Alkilany AM, Huang X, Murphy CJ, El-Sayed MA. 2012. The golden age: gold nanoparticles for biomedicine. *Chem. Soc. Rev.* 41:2740–79
30. Ku G, Zhou M, Song S, Huang Q, Hazle J, Li C. 2012. Copper sulfide nanoparticles as a new class of photoacoustic contrast agent for deep tissue imaging at 1,064 nm. *Am. Chem. Soc. Nano* 6:7489–96
31. Michalet X, Pinaud FF, Bentolila LA, Tsay JM, Doose S, et al. 2005. Quantum dots for live cells, in vivo imaging, and diagnostics. *Science* 307:538–44
32. Jamieson T, Bakhshi R, Petrova D, Pocock R, Imani M, Seifalian AM. 2007. Biological applications of quantum dots. *Biomaterials* 28:4717–32
33. Erogbogbo F, Yong K-T, Roy I, Xu G, Prasad PN, Swihart MT. 2008. Biocompatible luminescent silicon quantum dots for imaging of cancer cells. *Am. Chem. Soc. Nano* 2:873–78
34. Erogbogbo F, Chang C-W, May JL, Liu L, Kumar R, et al. 2012. Bioconjugation of luminescent silicon quantum dots to gadolinium ions for bioimaging applications. *Nanoscale* 4:5483–89
35. Fowley C, McCaughan B, Devlin A, Yildiz I, Raymo FM, Callan JF. 2012. Highly luminescent biocompatible carbon quantum dots by encapsulation with an amphiphilic polymer. *Chem. Commun.* 48:9361–63
36. Dong Y, Wang R, Li G, Chen C, Chi Y, Chen G. 2012. Polyamine-functionalized carbon quantum dots as fluorescent probes for selective and sensitive detection of copper ions. *Anal. Chem.* 84:6220–24
37. Lin CAJ, Yang TY, Lee CH, Huang SH, Sperling RA, et al. 2009. Synthesis, characterization, and bioconjugation of fluorescent gold nanoclusters toward biological labeling applications. *Am. Chem. Soc. Nano* 3:395–401
38. Huang S, Pfeiffer C, Hollmann J, Friede S, Chen JJ-C, et al. 2012. Synthesis and characterization of colloidal fluorescent silver nanoclusters. *Langmuir* 28:8915–19
39. Hilderbrand SA, Shao F, Salthouse C, Mahmood U, Weissleder R. 2009. Upconverting luminescent nanomaterials: application to in vivo bioimaging. *Chem. Commun.* 2009:4188–90
40. Wang F, Banerjee D, Liu Y, Chen X, Liu X. 2010. Upconversion nanoparticles in biological labeling, imaging, and therapy. *Analyst* 135:1839–54
41. Hwang DW, Ko HY, Kim S-K, Kim D, Lee DS, Kim S. 2009. Development of a quadruple imaging modality by using nanoparticles. *Chem. Eur. J.* 15:9387–93

BLOQUE I. INTRODUCCIÓN

42. Park EJ, Brasuel M, Behrend C, Philbert MA, Kopelman R. 2003. Ratiometric optical PEBBLE nanosensors for real-time magnesium ion concentrations inside viable cells. *Anal. Chem.* 75:3784–91
43. Giri S, Sykes EA, Jennings TL, Chan WCW. 2011. Rapid screening of genetic biomarkers of infectious agents using quantum dot barcodes. *Am. Chem. Soc. Nano* 5:1580–87
44. del Mercato LL, Abbasi AZ, Ochs M, Parak WJ. 2011. Multiplexed sensing of ions with barcoded polyelectrolyte capsules. *Am. Chem. Soc. Nano* 5:9668–74
45. del Mercato LL, Abbasi AZ, Parak WJ. 2011. Synthesis and characterization of ratiometric ion-sensitive polyelectrolyte capsules. *Small* 7:351–63
46. Lowe SB, Dick JAG, Cohen BE, Stevens MM. 2012. Multiplex sensing of protease and kinase enzyme activity via orthogonal coupling of quantum dot–peptide conjugates. *Am. Chem. Soc. Nano* 6:851–57
47. Marin MJ, Galindo F, Thomas P, Russell DA. 2012. Localized intracellular pH measurement using a ratiometric photoinduced electron-transfer-based nanosensor. *Angew. Chem. Int. Ed.* 51:9657–61
48. Algar WR, Wegner D, Huston AL, Blanco-Canosa JB, Stewart MH, et al. 2012. Quantum dots as simultaneous acceptors and donors in time-gated Förster resonance energy transfer relays: characterization and biosensing. *J. Am. Chem. Soc.* 134:1876–91
49. Freeman R, Liu X, Willner I. 2011. Chemiluminescent and chemiluminescence resonance energy transfer (CRET) detection of DNA, metal ions, and aptamer–substrate complexes using Hemin/G-quadruplexes and CdSe/ZnS quantum dots. *J. Am. Chem. Soc.* 133:11597–604
50. Xia Z, Xing Y, So MK, Koh AL, Sinclair R, Rao J. 2008. Multiplex detection of protease activity with quantum dot nanosensors prepared by intein-mediated specific bioconjugation. *Anal. Chem.* 80:8649–55
51. Maltez-da Costa M, de la Escosura-Muñiz A, Nogués C, Barrios L, Ibáñez E, Merkoçi A. 2012. Simple monitoring of cancer cells using nanoparticles. *Nano Lett.* 12:4164–71
52. Yáñez-Sedeño P, Pingarrón JM, Riu J, Rius FX. 2010. Electrochemical sensing based on carbon nanotubes. *Trends Anal. Chem.* 29:939–53
53. Luo X, Morrin A, Killard AJ, Smyth MR. 2006. Application of nanoparticles in electrochemical sensors and biosensors. *Electroanalysis* 18:319–26
54. Xu J-J, Luo X-L, Du Y, Chen H-Y. 2004. Application of MnO₂ nanoparticles as an eliminator of ascorbate interference to amperometric glucose biosensors. *Electrochem. Commun.* 6:1169–73

I.2. Multiplexed sensing and imaging with nano- and microparticles

55. Khalid W, Helou ME, Murböck T, Yue Z, Montenegro J-M, et al. 2011. Immobilization of quantum dots via conjugated self-assembled monolayers and their application as a light-controlled sensor for the detection of hydrogen peroxide. *Am. Chem. Soc. Nano* 5:9870–76
56. Ko JW, Woo J-M, Jinhong A, Cheon JH, Lim JH, et al. 2011. Multi-order dynamic range DNA sensor using a gold decorated SWCNT random network. *Am. Chem. Soc. Nano* 5:4365–72
57. Stoll C, Kudera S, Parak WJ, Lisdat F. 2006. Quantum dots on gold: electrodes for photoswitchable cytochrome *c* electrochemistry. *Small* 2:741–43
58. Katz E, Zayats M, Willner I, Lisdat F. 2006. Controlling the direction of photocurrents by means of CdS nanoparticles and cytochrome *c*-mediated biocatalytic cascades. *Chem. Commun.* 2006:1395–97
59. Hočevár SB, Wang J, Deo RP, Musameh M, Ogorevc B. 2005. Carbon nanotube modified microelectrode for enhanced voltammetric detection of dopamine in the presence of ascorbate. *Electroanalysis* 17:417–22
60. Liu B, Zhang B, Cui Y, Chen H, Gao Z, Tang D. 2011. Multifunctional gold-silica nanostructures for ultrasensitive electrochemical immunoassay of streptomycin residues. *Am. Chem. Soc. Appl. Mater. Interfaces* 3:4668–76
61. Zelada-Guillén GA, Sebastián-Avila JL, Blondeau P, Riu J, Rius FX. 2012. Label-free detection of *Staphylococcus aureus* in skin using real-time potentiometric biosensors based on carbon nanotubes and aptamers. *Biosens. Bioelectron.* 31:226–32
62. Zhang J, Song S, Zhang L, Wang L, Wu H, et al. 2006. Sequence-specific detection of femtomolar DNA via a chronocoulometric DNA sensor (CDS): effects of nanoparticle-mediated amplification and nanoscale control of DNA assembly at electrodes. *J. Am. Chem. Soc.* 128:8575–80
63. Wang J. 2005. Nanomaterial-based electrochemical biosensors. *Analyst* 130:421–26
64. Willner I, Willner B, Tel-Vered R. 2011. Electroanalytical applications of metallic nanoparticles and supramolecular nanostructures. *Electroanalysis* 23:13–28
65. Hiep HM, Endo T, Saito M, Chikae M, Kim DK, et al. 2008. Label-free detection of melittin binding to a membrane using electrochemical-localized surface plasmon resonance. *Anal. Chem.* 80:1859–64
66. Khalid W, Göbel G, Hühn D, Montenegro JM, Rivera Gil P, et al. 2011. Light triggered detection of aminophenyl phosphate with a quantum dot based enzyme electrode. *J. Nanobiotechnol.* 9:46
67. Pankhurst QA, Connolly J, Jones SK, Dobson J. 2003. Applications of magnetic nanoparticles in biomedicine. *J. Phys. D* 36:R167–81

BLOQUE I. INTRODUCCIÓN

68. Colombo M, Carregal-Romero S, Casula MF, Gutiérrez L, Morales MP, et al. 2012. Biological applications of magnetic nanoparticles. *Chem. Soc. Rev.* 41:4306–34
69. Moros M, Pelaz B, López-Larrubia P, García-Martin ML, Grazú V, de la Fuente JM. 2010. Engineering biofunctional magnetic nanoparticles for biotechnological applications. *Nanoscale* 2:1746–55
70. Alcántara D, Guo Y, Yuan H, Goergen CJ, Chen HH, et al. 2012. Fluorochrome-functionalized magnetic nanoparticles for high-sensitivity monitoring of the polymerase chain reaction by magnetic resonance. *Angew. Chem. Int. Ed.* 51:6904–7
71. Koh I, Josephson L. 2009. Magnetic nanoparticle sensors. *Sensors* 9:8130–45
72. Hathaway HJ, Butler KS, Adolphi NL, Lovato DM, Belfon R, et al. 2011. Detection of breast cancer cells using targeted magnetic nanoparticles and ultra-sensitive magnetic field sensors. *Breast Cancer Res.* 13:R108
73. Gaster RS, Xu L, Han S-J, Wilson RJ, Hall DA, et al. 2011. Quantification of protein interactions and solution transport using high-density GMR sensor arrays. *Nat. Nanotechnol.* 6:314–20
74. Perez JM, Josephson L, O'Loughlin T, Högemann D, Weissleder R. 2002. Magnetic relaxation switches capable of sensing molecular interactions. *Nat. Biotechnol.* 20:816–20
75. Wang Y, Fang F, Shi C, Zhang X, Liu L, et al. 2012. Evaluation of a method for the simultaneous detection of multiple tumor markers using a multiplex suspension bead array. *Clin. Biochem.* 45:1394–98
76. Rivera-Gil P, Jimenez de Aberasturi D, Wulf V, Pelaz B, del Pino P, et al. 2013. The challenge to relate the physicochemical properties of colloidal nanoparticles to their cytotoxicity. *Acc. Chem. Res.* 46:743–49
77. Abbasi AZ, Amin F, Niebling T, Friede S, Ochs M, et al. 2011. How colloidal nanoparticles could facilitate multiplexed measurements of different analytes with analyte-sensitive organic fluorophores. *Am. Chem. Soc. Nano* 5:21–25
78. Zhang F, Ali Z, Amin F, Feltz A, Oheim M, Parak WJ. 2010. Ion and pH sensing with colloidal nanoparticles: influence of surface charge on sensing and colloidal properties. *ChemPhysChem* 11:730–35
79. Riedinger A, Zhang F, Dommershausen F, Röcker C, Brandholt S, et al. 2010. Ratiometric optical sensing of chloride ions with organic fluorophore–gold nanoparticle hybrids: a systematic study of distance dependency and the influence of surface charge. *Small* 6:2590–97
80. Zhang F, Lees E, Amin F, Rivera-Gil P, Yang F, et al. 2011. Polymer-coated nanoparticles: a universal tool for biolabelling experiments. *Small* 7:3113–27

I.2. Multiplexed sensing and imaging with nano- and microparticles

81. Cedervall T, Lynch I, Lindman S, Berggård T, Thulin E, et al. 2007. Understanding the nanoparticle–protein corona using methods to quantify exchange rates and affinities of proteins for nanoparticles. *Proc. Natl. Acad. Sci. USA* 104:2050–55
82. Jiang X, Weise S, Hafner M, Röcker C, Zhang F, et al. 2010. Quantitative analysis of the protein corona on FePt nanoparticles formed by transferrin binding. *J. R. Soc. Interface* 7:S5–13
83. Amin F, Yushchenko DA, Montenegro JM, Parak WJ. 2012. Integration of organic fluorophores in the surface of polymer-coated colloidal nanoparticles for sensing the local polarity of the environment. *ChemPhysChem* 13:1030–35
84. Freeman R, Finder T, Willner I. 2009. Multiplexed analysis of Hg²⁺ and Ag⁺ ions by nucleic acid functionalized CdSe/ZnS quantum dots and their use for logic gate operations. *Angew. Chem. Int. Ed.* 48:7818–21
85. Jin R, Cao Y, Mirkin CA, Kelly KL, Schatz GC, Zheng JG. 2001. Photoinduced conversion of silver nanospheres to nanoprisms. *Science* 294:1901–3
86. Yu C, Irudayaraj J. 2007. Multiplex biosensor using gold nanorods. *Anal. Chem.* 79:572–79
87. Yu C, Nakshatri H, Irudayaraj J. 2007. Identity profiling of cell surface markers by multiplex gold nanorod probes. *Nano Lett.* 7:2300–6
88. Wang C, Irudayaraj J. 2008. Gold nanorod probes for the detection of multiple pathogens. *Small* 4:2204–8
89. Fernández-López C, Mateo-Mateo C, Álvarez-Puebla RA, Pérez-Juste J, Pastoriza-Santos I, Liz-Marzán LM. 2009. Highly controlled silica coating of PEG-capped metal nanoparticles and preparation of SERS encoded particles. *Langmuir* 25:13894–99
90. Abalde-Cela S, Aldeanueva-Potel P, Mateo-Mateo C, Rodríguez-Lorenzo L, Álvarez-Puebla RA, Liz-Marzán LM. 2010. Surface-enhanced Raman scattering biomedical applications of plasmonic colloidal particles. *J. R. Soc. Interface* 7:S435–50
91. Ruez J, Blais DR, Zhang Y, Álvarez-Puebla RA, Bravo-Vasquez JP, et al. 2007. Spectroscopically encoded microspheres for antigen biosensing. *Langmuir* 23:6482–85
92. Sanles-Sobrido M, Exner W, Rodríguez-Lorenzo L, Rodríguez-Gonzalez B, Correa-Duarte MA, et al. 2009. Design of SERS-encoded, submicron, hollow particles through confined growth of encapsulated metal nanoparticles. *J. Am. Chem. Soc.* 131:2699–705
93. Kim K, Lee YM, Lee HB, Shin KS. 2009. Silver-coated silica beads applicable as core materials of dual-tagging sensors operating via SERS and MEF. *Am. Chem. Soc. Appl. Mater. Interfaces* 1:2174–80

BLOQUE I. INTRODUCCIÓN

94. Maiti KK, Dinish US, Samanta A, Vendrell M, Soh K-S, et al. 2012. Multiplex targeted in vivo cancer detection using sensitive near-infrared SERS nanotags. *Nano Today* 7:85–93
95. Sanchez-Iglesias A, Aldeanueva-Potel P, Ni WH, Pérez-Juste J, Pastoriza-Santos I, et al. 2010. Chemical seeded growth of Ag nanoparticle arrays and their application as reproducible SERS substrates. *Nano Today* 5:21–27
96. Jiang ZY, Jiang XX, Su S, Wei XP, Lee ST, He Y. 2012. Silicon-based reproducible and active surface enhanced Raman scattering substrates for sensitive, specific, and multiplex DNA detection. *Appl. Phys. Lett.* 100:203104
97. Kang T, Yoo SM, Yoon I, Lee SY, Kim B. 2010. Patterned multiplex pathogen DNA detection by Au particle-on-wire SERS sensor. *Nano Lett.* 10:1189–93
98. Wang Z, Zong S, Li W, Wang C, Xu S, et al. 2012. SERS-fluorescence joint spectral encoding using organic-metal-QD hybrid nanoparticles with a huge encoding capacity for high-throughput biodetection: putting theory into practice. *J. Am. Chem. Soc.* 134:2993–3000
99. Nagl S, Wolfbeis OS. 2007. Optical multiple chemical sensing: status and current challenges. *Analyst* 132:507–11
100. Grabolle M, Kapusta P, Nann T, Shu X, Ziegler J, Resch-Genger U. 2009. Fluorescence lifetime multiplexing with nanocrystals and organic labels. *Anal. Chem.* 81:7807–13
101. Ruedas-Rama MJ, Orte A, Hall EAH, Alvarez-Pez JM, Talavera EM. 2011. Quantum dot photoluminescence lifetime-based pH nanosensor. *Chem. Commun.* 47:2898–900
102. Peng X, Yang Z, Wang J, Fan J, He Y, et al. 2011. Fluorescence ratiometry and fluorescence lifetime imaging: using a single molecular sensor for dual mode imaging of cellular viscosity. *J. Am. Chem. Soc.* 133:6626–35
103. Kim J-H, Patra CR, Arkaigud JR, Boghossian AA, Zhang J, et al. 2011. Single-molecule detection of H₂O₂ mediating angiogenic redox signaling on fluorescent single-walled carbon nanotube array. *Am. Chem. Soc. Nano* 5:7848–57
104. Geissler D, Charbonnière L, Ziessel R, Butlin N, Löhmansröben HG, Hildebrandt N. 2010. Quantum dot biosensors for ultrasensitive multiplexed diagnostics. *Angew. Chem. Int. Ed.* 49:1396–401
105. Freeman R, Liu X, Willner I. 2011. Amplified multiplexed analysis of DNA by the exonuclease III-catalyzed regeneration of the target DNA in the presence of functionalized semiconductor quantum dots. *Nano Lett.* 11:4456–61

I.2. Multiplexed sensing and imaging with nano- and microparticles

106. Haun JB, Devaraj NK, Marinelli BS, Lee H, Weissleder R. 2012. Probing intracellular biomarkers and mediators of cell activation using nanosensors and bioorthogonal chemistry. *Am. Chem. Soc. Nano* 5:3204–13
107. Peterson VM, Castro CM, Lee H, Weissleder R. 2012. Orthogonal amplification of nanoparticles for improved diagnostic sensing. *Am. Chem. Soc. Nano* 6:3506–13
108. Shipway AN, Katz E, Willner I. 2000. Nanoparticle arrays on surfaces for electronic, optical, and sensor applications. *ChemPhysChem* 1:18–52
109. Katz E, Willner I. 2004. Integrated nanoparticle-biomolecule hybrid systems: synthesis, properties, and applications. *Angew. Chem. Int. Ed.* 43:6042–108
110. Ferguson JA, Steemers FJ, Walt DR. 2000. High-density fiber-optic DNA random microsphere array. *Anal. Chem.* 72:5618–24
111. Pregibon DC, Toner M, Doyle PS. 2007. Multifunctional encoded particles for high-throughput biomolecule analysis. *Science* 315:1393–96
112. Zamborini FP, Bao L, Dasari R. 2012. Nanoparticles in measurement science. *Anal. Chem.* 84:541–76
113. Mayer KM, Hafner JH. 2011. Localized surface plasmon resonance sensors. *Chem. Rev.* 111:3828–57
114. He S, Liu K-K, Su S, Yan J, Mao X, et al. 2012. Graphene-based high-efficiency surface-enhanced Raman scattering–active platform for sensitive and multiplex DNA detection. *Anal. Chem.* 84:4622–27
115. Endo T, Kerman K, Nagatani N, Hiepa HM, Kim D-K, et al. 2006. Multiple label-free detection of antigen–antibody reaction using localized surface plasmon resonance–based core-shell structured nanoparticle layer nanochip. *Anal. Chem.* 78:6465–75
116. Kim D, Daniel WL, Mirkin CA. 2009. Microarray-based multiplexed scanometric immunoassay for protein cancer markers using gold nanoparticle probes. *Anal. Chem.* 81:9183–87
117. Stoeva SI, Lee J-S, Smith JE, Rosen ST, Mirkin CA. 2006. Multiplexed detection of protein cancer markers with biobarcode nanoparticle probes. *J. Am. Chem. Soc.* 128:8378–79
118. Kim D-K, Yoo S-M, Park T-J, Yoshikawa H, Tamiya E-I, et al. 2011. Plasmonic properties of the multispot copper-capped nanoparticle array chip and its application to optical biosensors for pathogen detection of multiplex DNAs. *Anal. Chem.* 83:6215–22
119. Chen S, Svedendahl M, Van Duyne RP, Kaell M. 2011. Plasmon-enhanced colorimetric ELISA with single molecule sensitivity. *Nano Lett.* 11:1826–30

BLOQUE I. INTRODUCCIÓN

120. Skladal P. 1997. Advances in electrochemical immunosensors. *Electroanalysis* 9:737–45
121. Wilson MS, Nie W. 2006. Electrochemical multianalyte immunoassays using an array-based sensor. *Anal. Chem.* 78:2507–13
122. Akter R, Rahman MA, Rhee CK. 2012. Amplified electrochemical detection of a cancer biomarker by enhanced precipitation using horseradish peroxidase attached on carbon nanotubes. *Anal. Chem.* 84:6407–15
123. Lai G, Yan F, Wu J, Leng C, Ju H. 2011. Ultrasensitive multiplexed immunoassay with electrochemical stripping analysis of silver nanoparticles catalytically deposited by gold nanoparticles and enzymatic reaction. *Anal. Chem.* 83:2726–32
124. Mani V, Chikkaveeraiah BV, Patel V, Gutkind JS, Rusling JF. 2009. Ultrasensitive immunosensor for cancer biomarker proteins using gold nanoparticle film electrodes and multienzyme-particle amplification. *Am. Chem. Soc. Nano* 3:585–94
125. Malhotra R, Patel V, Chikkaveeraiah BV, Munge BS, Cheong SC, et al. 2012. Ultrasensitive detection of cancer biomarkers in the clinic by use of a nanostructured microfluidic array. *Anal. Chem.* 84:6249–55
126. Chikkaveeraiah BV, Bhirde A, Malhotra R, Patel V, Gutkind JS, Rusling JF. 2009. Single-wall carbon nanotube forest arrays for immunoelectrochemical measurement of four protein biomarkers for prostate cancer. *Anal. Chem.* 81:9129–34
127. Zarei H, Ghourchian H, Eskandari K, Zeinali M. 2012. Magnetic nanocomposite of anti-human IgG/COOH-multiwalled carbon nanotubes/Fe₃O₄ as a platform for electrochemical immunoassay. *Anal. Biochem.* 421:446–53
128. George M, Parak WJ, Gaub HE. 2000. Highly integrated surface potential sensors. *Sens. Actuators B* 69:266–75
129. Hafeman DG, Parce JW, McConnell HM. 1988. Light-addressable potentiometric sensor for biochemical systems. *Science* 240:1182–85
130. Lundström I, Erlandsson R, Frykman U, Hedborg E, Spetz A, et al. 1991. Artificial “olfactory” images from a chemical sensor using a light-pulse technique. *Nature* 352:47–50
131. Parak WJ, Hofmann UG, Gaub HE, Owicki JC. 1997. Lateral resolution of light addressable potentiometric sensors: an experimental and theoretical investigation. *Sens. Actuators A* 63:47–57
132. Tanne J, Schafer D, Khalid W, Parak WJ, Lisdat F. 2011. Light-controlled bioelectrochemical sensor based on CdSe/ZnS quantum dots. *Anal. Chem.* 83:7778–85

I.2. Multiplexed sensing and imaging with nano- and microparticles

133. Schubert K, Khalid W, Yue Z, Parak WJ, Lisdat F. 2010. Quantum dot-modified electrode for the detection of NAD-dependent dehydrogenase reactions. *Langmuir* 26:1395–400
134. Li Y, Srinivasan B, Jing Y, Yao X, Hugger MA, et al. 2010. Nanomagnetic competition assay for low abundance protein biomarker quantification in unprocessed human sera. *J. Am. Chem. Soc.* 132:4388–92
135. Mak AC, Osterfeld SJ, Yu H, Wang SX, Davis RW, et al. 2010. Sensitive giant magnetoresistive-based immunoassay for multiplex mycotoxin detection. *Biosens. Bioelectron.* 25:1635–39
136. Osterfeld SJ, Yu H, Gaster RS, Caramuta S, Xu L, et al. 2008. Multiplex protein assay based on real-time magnetic nanotag sensing. *Proc. Natl. Acad. Sci. USA* 105:20637–40
137. Deleted in proof
138. Hall DA, Gaster RS, Osterfeld SJ, Murmann B, Wang SX. 2011. GMR biosensor arrays: correction techniques for reproducibility and enhanced sensitivity. *Biosens. Bioelectron.* 25:2177–81
139. Zong C, Wu J, Wang C, Ju H, Yan F. 2012. Chemiluminescence imaging immunoassay of multiple tumor markers for cancer screening. *Anal. Chem.* 84:2410–15
140. Pei H, Li J, Lv M, Wang J, Gao J, et al. 2012. A graphene-based sensor array for high-precision and adaptive target identification with ensemble aptamers. *J. Am. Chem. Soc.* 134:13843–49
141. He X, Wang K, Cheng Z. 2010. In vivo near-infrared fluorescence imaging of cancer with nanoparticle based probes. *Wiley Interdiscip. Rev. Nanomed. Nanobiotechnol.* 2:349–66
142. Rivera-Gil P, Parak WJ. 2008. Composite nanoparticles take aim at cancer. *Am.Chem. Soc. Nano* 2:2200–5
143. Peteiro-Cartelle J, Rodríguez-Pedreira M, Zhang F, Rivera-Gil P, del Mercato LL, Parak WJ. 2009. One example on how colloidal nano- and microparticles could contribute to medicine. *Nanomedicine* 4:967–79
144. Weissleder R, Moore A, Mahmood U, Bhorade R, Benveniste H, et al. 2000. In vivo magnetic resonance imaging of transgene expression. *Nat. Med.* 6:351–55
145. Alexiou C, Arnold W, Hulin P, Klein RJ, Renz H, et al. 2001. Magnetic mitoxantrone nanoparticle detection by histology, X-ray and MRI after magnetic tumor targeting. *J. Magn.Magn.Mater.* 225:187–93

BLOQUE I. INTRODUCCIÓN

146. Morales MP, Bomati-Miguel O, de Alejo RP, Ruiz-Cabello J, Veintemillas-Verdaguer S, O'Grady K. 2003. Contrast agents for MRI based on iron oxide nanoparticles prepared by laser pyrolysis. *J. Magn. Magn. Mater.* 266:102–9
147. Harisinghani MG, Barentsz J, Hahn PF, Deserno WM, Tabatabaei S, et al. 2003. Noninvasive detection of clinically occult lymph-node metastases in prostate cancer. *N. Engl. J. Med.* 348:2491–99
148. Wang C, Gao X, Su XG. 2010. In vitro and in vivo imaging with quantum dots. *Anal. Bioanal. Chem.* 397:1397–415
149. Cheon J, Lee J-H. 2008. Synergistically integrated nanoparticles as multimodal probes for nanobiotechnology. *Acc. Chem. Res.* 41:1630–40
150. Liong M, Lu J, Kovichich M, Xia T, Ruehm SG, et al. 2008. Multifunctional inorganic nanoparticles for imaging, targeting, and drug delivery. *Am. Chem. Soc. Nano* 2:889–96
151. Nahrendorf M, Zhang HW, Hembrador S, Panizzi P, Sosnovik DE, et al. 2008. Nanoparticle PET-CT imaging of macrophages in inflammatory atherosclerosis. *Circulation* 117:379–87
152. Altinoğlu EI, Russin TJ, Kaiser JM, Barth BM, Eklund BC, et al. 2008. Near-infrared emitting fluorophore-doped calcium phosphate nanoparticles for in vivo imaging of human breast cancer. *Am. Chem. Soc. Nano* 2:2075–84
153. Kumar R, Roy I, Ohulchanskyy TY, Vathy LA, Bergey EJ, et al. 2010. In vivo biodistribution and clearance studies using multimodal organically modified silica nanoparticles. *Am. Chem. Soc. Nano* 4:699–708
154. Lipka M, Semmler-Behnke M, Sperling RA, Wenk A, Takenaka S, et al. 2010. Biodistribution of PEG modified gold nanoparticles following intratracheal instillation and intravenous injection. *Biomaterials* 31:6574–81
155. Ali Z, Abbasi AZ, Zhang F, Arosio P, Lascialfari A, et al. 2011. Multifunctional nanoparticles for dual imaging. *Anal. Chem.* 83:2877–82
156. Sperling RA, Pellegrino T, Li JK, Chang WH, Parak WJ. 2006. Electrophoretic separation of nanoparticles with a discrete number of functional groups. *Adv. Funct. Mater.* 16:943–48
157. Fernández-Argüelles MT, Yakovlev A, Sperling RA, Luccardini C, Gaillard S, et al. 2007. Synthesis and characterization of polymer-coated quantum dots with integrated acceptor dyes as FRET-based nanoprobe. *Nano Lett.* 7:2613–17
158. Corato RD, Quarta A, Piacenza P, Ragusa A, Figuerola A, et al. 2008. Water solubilization of hydrophobic nanocrystals by means of poly(maleic anhydride-*alt*-1-octadecene). *J. Mater. Chem.* 18:1991–96

I.2. Multiplexed sensing and imaging with nano- and microparticles

159. Sperling RA, Liedl T, Duhr S, Kudera S, Zanella M, et al. 2007. Size determination of (bio-)conjugated water-soluble colloidal nanoparticles—a comparison of different techniques. *J. Phys. Chem. C* 111:11552–59
160. Geidel C, Schmachtel S, Riedinger A, Pfeiffer C, Müllen K, et al. 2011. A general synthetic approach for obtaining cationic and anionic inorganic nanoparticles via encapsulation in amphiphilic copolymers. *Small* 7:2929–34
161. Lehmann AD, Parak WJ, Zhang F, Ali Z, Röcker C, et al. 2010. Fluorescent-magnetic hybrid nanoparticles induce a dose-dependent increase in proinflammatory response in lung cells in vitro correlated with intracellular localization. *Small* 6:753–62
162. Lin C-AJ, Sperling RA, Li JK, Yang T-Y, Li P-Y, et al. 2008. Design of an amphiphilic polymer for nanoparticle coating and functionalization. *Small* 4:334–41
163. Cui Y, Zheng XS, Ren B, Wang R, Zhang J, et al. 2011. Au@organosilica multifunctional nanoparticles for the multimodal imaging. *Chem. Sci.* 2:1463–69
164. McQueenie R, Stevenson R, Benson R, MacRitchie N, McInnes I, et al. 2012. Detection of inflammation in vivo by surface-enhanced Raman scattering provides higher sensitivity than conventional fluorescence imaging. *Anal. Chem.* 84:5968–75
165. Stone N, Kerssens M, Lloyd GR, Faulds K, Graham D, Matousek P. 2011. Surface enhanced spatially offset Raman spectroscopic (SESORS) imaging—the next dimension. *Chem. Sci.* 2:776–80
166. Guerrero-Martinez A, Pérez-Juste J, Liz-Marzán LM. 2012. Recent progress on silica coating of nanoparticles and related nanomaterials. *Adv. Mater.* 22:1182–95
167. Ma M, Chen H, Chen Y, Wang X, Chen F, et al. 2012. Au capped magnetic core/mesoporous silica shell nanoparticles for combined photothermo-/chemo-therapy and multimodal imaging. *Biomaterials* 33:989–98
168. Hwang DW, Ko HY, Lee JH, Kang H, Ryu SH, et al. 2012. A nucleolin-targeted multimodal nanoparticle imaging probe for tracking cancer cells using an aptamer. *J. Nucl. Med.* 51:98–105
169. Wang F, Deng R, Wang J, Wang Q, Han Y, et al. 2011. Tuning upconversion through energy migration in core-shell nanoparticles. *Nat. Mater.* 10:968–73
170. Xia A, Chen M, Gao Y, Wu D, Feng W, Li F. 2012. Gd³⁺ complex-modified NaLuF₄-based upconversion nanophosphors for trimodality imaging of NIR-to-NIR upconversion luminescence, X-ray computed tomography and magnetic resonance. *Biomaterials* 33:5394–405
171. Xing H, Bu W, Zhang S, Zheng X, Li M, et al. 2012. Multifunctional nanoprobes for upconversion fluorescence, MR and CT trimodal imaging. *Biomaterials* 33:1079–89

BLOQUE I. INTRODUCCIÓN

172. Jin Y, Jia C, Huang S-W, O'Donnell M, Gao X. 2010. Multifunctional nanoparticles as coupled contrast agents. *Nat. Commun.* 1:41
173. Abbasi AZ, Gutierrez L, del Mercato LL, Herranz F, Chubykalo-Fesenko O, et al. 2011. Magnetic capsules for NMR imaging: effect of magnetic nanoparticles spatial distribution and aggregation. *J. Phys. Chem. C* 115:6257–64
174. Johnston APR, Kamphuis MMJ, Such GK, Scott AM, Nice EC, et al. 2012. Targeting cancer cells: controlling the binding and internalization of antibody-functionalized capsules. *Am. Chem. Soc. Nano* 6:6667–74
175. Kondrashina AV, Dmitriev RI, Borisov SM, Klimant I, O'Brien I, et al. 2012. A phosphorescent nanoparticle-based probe for sensing and imaging of (intra)cellular oxygen in multiple detection modalities. *Adv. Func. Mater.* 22:4931–39
176. Fercher A, Borisov SM, Zhdanov AV, Klimant I, Papkovsky DB. 2011. Intracellular O₂ sensing probe based on cell-penetrating phosphorescent nanoparticles. *Am. Chem. Soc. Nano* 5:5499–508
177. Si D, Epstein T, Lee Y-EK, Kopelman R. 2012. Nanoparticle PEBBLE sensors for quantitative nanomolar imaging of intracellular free calcium ions. *Anal. Chem.* 84:978–86
178. Vetrone F, Naccache R, Zamarrón A, Juarranz de la Fuente A, Sanz-Rodríguez F, et al. 2010. Temperature sensing using fluorescent nanothermometers. *Am. Chem. Soc. Nano* 4:3254–58
179. Dong B, Cao B, He Y, Liu Z, Li Z, Feng Z. 2012. Temperature sensing and in vivo imaging by molybdenum sensitized visible upconversion luminescence of rare-earth oxides. *Adv. Mater.* 24:1987–93
180. Carregal-Romero S, Ochs M, Parak WJ. 2012. Nanoparticle-functionalized microcapsules for in vitro delivery and sensing. *Nanophotonics* 1:171–80
181. Rivera-Gil P, Nazareus M, Ashraf S, Parak WJ. 2012. pH sensitive capsules as intracellular optical reporters for monitoring lysosomal pH changes upon stimulation. *Small* 8:943–48
182. Yang KS, Budin G, Reiner T, Vinegoni C, Weissleder R. 2012. Bioorthogonal imaging of aurora kinase A in live cells. *Angew. Chem. Int. Ed.* 51:6598–603
183. Pelaz B, Jaber S, Jimenez de Aberasturi D, Wulf V, de la Fuente JM, et al. 2012. The state of nanoparticle based nanoscience and biotechnology: progress, promises, and challenges. *Am. Chem. Soc. Nano* 6:8468–83

I.3 Toxicidad asociada a las nanopartículas

El término *Nanotoxicología* apareció por primera vez en el año 2004 y se define como la rama de la Toxicología cuyo objetivo es reconocer y evaluar los riesgos y daños sobre la salud asociados a las nanopartículas (NPs) [1]. La Figura I.3.1 muestra la evolución en el número de artículos científicos publicados que contienen las palabras clave “Nanotoxicología”, “Nanotoxicidad” o “toxicidad de nanopartículas”, desde 1980 hasta la actualidad.

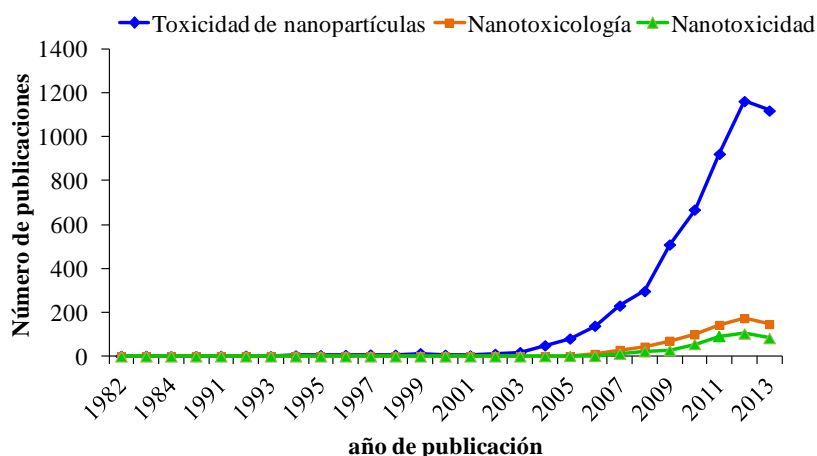


Figura I.3.1. Número de artículos científicos que contienen alguna de las siguientes palabras/frases clave: “Toxicidad de nanopartículas”, “Nanotoxicología” o “Nanotoxicidad” (Fuente bibliográfica: SCOPUS). La búsqueda consistió en identificar la presencia de estos términos en inglés en los artículos científicos publicados durante la ventana temporal que se especifica.

Como se observa en la gráfica, el número de publicaciones científicas relacionadas con la toxicidad de las NPs fue muy reducido entre 1980 y 2004, sin embargo a partir de este último año se produjo un crecimiento exponencial de la investigación enfocada a profundizar en este área de conocimiento.

La Figura I.3.2 esquematiza las temáticas que se abordarán a lo largo de esta sección y que pueden enmarcarse dentro del ámbito de la *Nanotoxicología*.

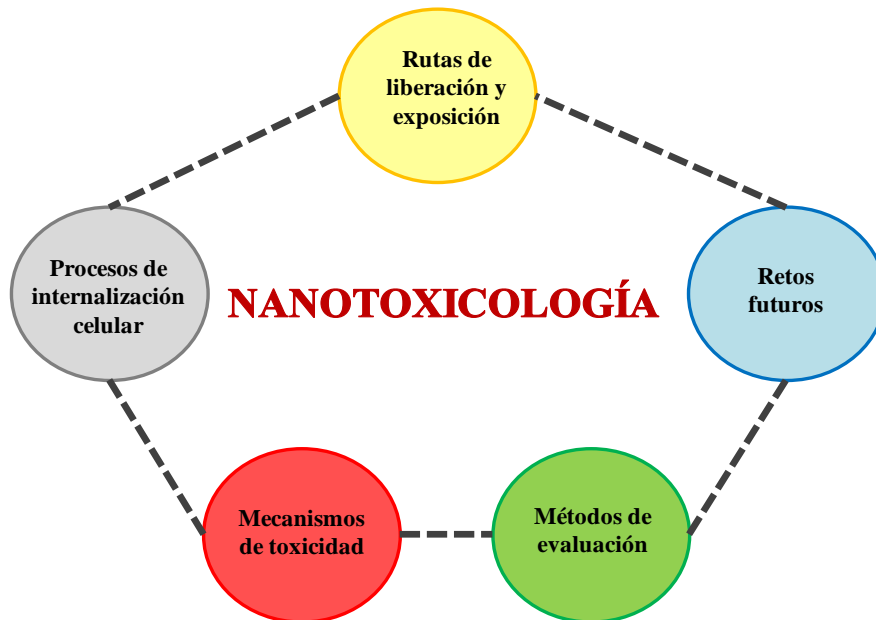


Figura 1.3.2. Temáticas que serán discutidas a lo largo de esta sección.

RUTAS DE LIBERACIÓN Y EXPOSICIÓN

Las NPs son liberadas al medio ambiente como consecuencia de diferentes actividades antropogénicas, tales como los procesos implicados en su fabricación, la eliminación de residuos del uso doméstico o de la actividad industrial que contengan NPs, o los vertidos accidentales.

Como consecuencia de su uso extendido, las NPs pueden entrar en contacto con los seres humanos a través de cuatro principales rutas de exposición incluyendo, el contacto directo con la piel, la inhalación, la ingestión, o la inyección intradérmica/intravenosa para aquellas NPs con futuras aplicaciones biomédicas [2].

PROCESOS DE INTERNALIZACIÓN CELULAR

Diferentes procesos de internalización celular permiten a las NPs atravesar las membranas celulares y penetrar en las células. Los mecanismos de internalización actualmente descritos en bibliografía se ilustran esquemáticamente en la Figura I.3.3. Conviene decir que según el tipo de línea celular y NP considerada, unos mecanismos tendrán mayor peso que otros.

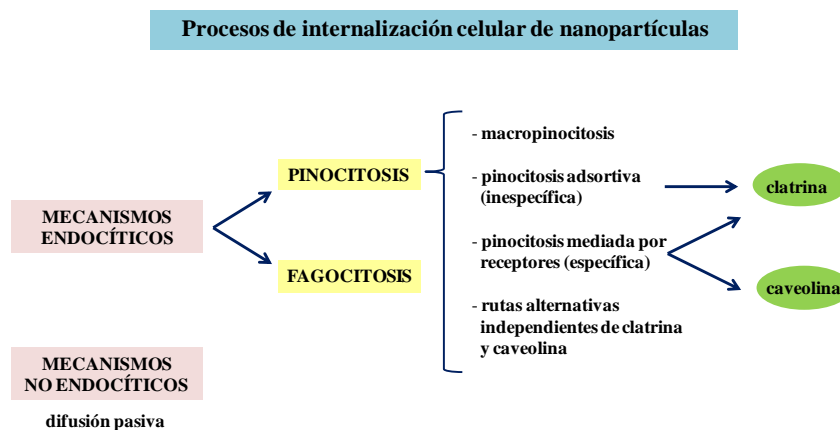


Figura I.3.3. Representación esquemática de los principales procesos que permiten a las NPs atravesar la membrana plasmática.

La endocitosis es el mecanismo general de transporte activo a través del cual la célula capta partículas o grandes moléculas del exterior formando vesículas o vacuolas que se segregan de la membrana celular. La mayoría de estudios científicos revelan que las NPs son internalizadas principalmente por mecanismos endocíticos como la fagocitosis o pinocitosis [3].

Fagocitosis

Este proceso es muy común en algunas células especializadas del sistema inmune (concretamente, monocitos y macrófagos) y permite engullir partículas

con diámetros superiores a 500 nm a través de mecanismos que suponen el reconocimiento por receptores [4]. Las proteínas que rodean superficialmente las NPs se unen de forma específica a los receptores presentes en la membrana plasmática. Estas interacciones *ligando-receptor* activan determinadas reacciones en cascada de señales intracelulares que resultan en la formación de protuberancias en la membrana, denominadas fagosomas, que engullen los complejos *nanopartícula-proteína* [3].

Pinocitosis

Este mecanismo es frecuente en todo tipo de células y permite la internalización de partículas con un tamaño que abarca de unos pocos a varios cientos de nanómetros. Existen distintos tipos de pinocitosis: macropinocitosis, pinocitosis adsortiva, pinocitosis mediada por receptores (clatrina y caveolina) y otras rutas alternativas independientes de clatrina y caveolina [3].

▪ *Macropinocitosis*

En términos generales, la macropinocitosis permite la internalización de fluidos externos dentro de la célula. La presencia de NPs en el medio extracelular pero muy próximas a la membrana plasmática hace que éstas puedan penetrar accidentalmente dentro de las células junto con los fluidos del exterior. La membrana forma entonces protuberancias con formas irregulares, denominadas macropinosomas, que envuelven e internalizan las NPs [3].

▪ *Pinocitosis adsortiva*

En este caso, las NPs con carga positiva pueden unirse de forma inespecífica a determinados sitios de unión de la superficie celular cargada negativamente, lo que permite su internalización dentro de la célula [3].

- *Pinocitosis mediada por receptores (clatrina y caveolina)*

A diferencia del mecanismo endocítico anterior, la pinocitosis mediada por receptores requiere un reconocimiento específico entre un ligando y su receptor complementario situado en la membrana plasmática. La internalización en este caso está mediada por las proteínas clatrina o caveolina [3].

La *endocitosis mediada por clatrina* es el proceso endocítico por excelencia para la internalización de NPs con un tamaño comprendido entre 100 y 150 nm. Las NPs penetran a través de invaginaciones que están recubiertas por las proteínas clatrina. A este mecanismo le sigue en importancia la *endocitosis mediada por caveolina* que es bastante común en células endoteliales. Las caveolinas son proteínas que integran la membrana celular y que están presentes en estructuras denominadas caveolas. Estas estructuras son invaginaciones con un tamaño entre 50 y 80 nm que se localizan en los dominios hidrofóbicos de la membrana plasmática que son ricos en colesterol. Las NPs pueden penetrar en la célula por su interacción con las caveolinas y posterior invaginación dentro de las caveolas que las transportan hasta otros compartimentos intracelulares [5].

- *Rutas alternativas independientes de clatrina y caveolina*

Hay otras rutas alternativas independientes de clatrina y caveolina que suponen la penetración de las NPs dentro de las células mediante mecanismos que están regulados por otras proteínas.

La Figura I.3.4 muestra los principales mecanismos endocíticos discutidos anteriormente.

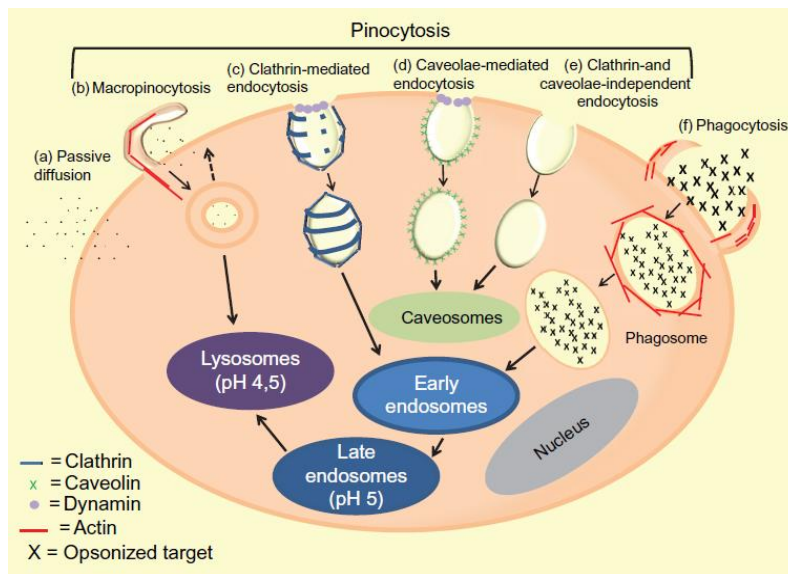


Figura I.3.4. Mecanismos de internalización celular de NPs. Figura perteneciente a [5].

Mecanismos no endocíticos

Además de las rutas endocíticas, también se han descrito algunos procesos de transporte en los que, concretamente los nanotubos de carbono (CNTs) funcionalizados, pueden difundir directamente a través de la membrana celular mediante un transporte pasivo y no selectivo. Los CNTs actúan como “*nanoagujas*” que pueden atravesar la bicapa lipídica de la membrana plasmática de forma espontánea.

La Figura I.3.5 muestra imágenes representativas de este mecanismo.

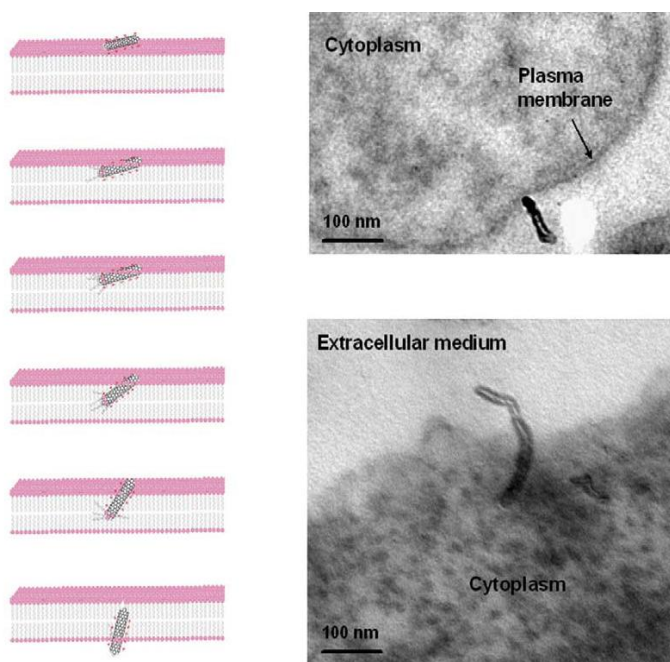


Figura I.3.5. Difusión pasiva de CNTs a través de la membrana plasmática. Imágenes TEM y figura pertenecientes a [6-8].

Factores influyentes en la internalización de las nanopartículas

La habilidad de las NPs para penetrar dentro de la célula depende en gran medida de sus propiedades fisicoquímicas, tales como su forma y tamaño. Algunos estudios científicos confirman que el grado de internalización de las NPs aumenta cuanto menor sea su tamaño y su forma más esférica. Cabe añadir que incluso habiendo caracterizado exhaustivamente las NPs antes de realizar los estudios de toxicidad, los cambios de estabilidad que sufren cuando entran en contacto con ambientes fisiológicos pueden resultar en la formación de agregados de NPs con tamaños y formas variables que dificultan enormemente la previsión de su grado de interacción con las células [9,10].

La presencia de grupos funcionales sobre la superficie de las NPs también condiciona su captación celular [10]. Un hecho ya demostrado es que las NPs

BLOQUE I. INTRODUCCIÓN

interaccionan con las proteínas del suero. En algunos casos esta unión favorece la internalización de los complejos *nanopartícula-proteína* a través de mecanismos endocíticos mediados por receptores. En otros, sin embargo, la interacción conlleva la pérdida de estructura de las proteínas lo que impide su reconocimiento por la célula y consecuentemente, la penetración de los complejos *nanopartícula-proteína*.

Con el propósito de evitar interacciones inespecíficas con determinados componentes celulares, las NPs se pueden recubrir superficialmente con ligandos tales como el polietilenglicol (PEG) que reduce considerablemente la adsorción de proteínas [10]. La funcionalización superficial de las NPs con grupos cargados negativamente reduce su afinidad por la membrana celular que presenta carga negativa. Sin embargo, incluso en esos casos, las NPs también pueden atravesar la membrana plasmática por uniones inespecíficas a los escasos sitios catiónicos presentes en la misma. Las NPs que son funcionalizadas con grupos cargados positivamente tienen obviamente una mayor afinidad por la membrana y son las más explotadas con fines biomédicos [10,11].

Sin embargo, aún considerando el mismo tipo de NP y con la misma carga superficial, ligeras variaciones en los grupos superficiales o incluso en su reordenamiento sobre la superficie condicionan un diferente grado de internalización celular para las NPs, lo que demuestra la enorme complejidad asociada a estos procesos [12,13].

Finalmente y una vez dentro del dominio intracelular, las NPs siguen determinadas rutas, destacando especialmente la ruta de los lisosomas, aunque también pueden acumularse en el interior de la mitocondria o incluso en el núcleo celular [14-16].

MECANISMOS QUE INDUCEN TOXICIDAD

Hasta la fecha se han descrito distintos mecanismos que explican la toxicidad asociada a las NPs y que se discutirán a continuación.

Generación de especies reactivas de oxígeno

Las especies reactivas de oxígeno (ROS) son generadas de forma natural como consecuencia del metabolismo celular del oxígeno. Sin embargo, cuando las células sufren un estrés ambiental, sus niveles de ROS incrementan considerablemente por encima de los niveles normales. La mayoría de células tienen mecanismos de defensa frente a este incremento de ROS, pero cuando los niveles son desmesurados, además de prolongados en el tiempo, se producen daños celulares inevitables. Las NPs activan la generación de ROS a través de los siguientes mecanismos:

1. Por reactividad directa, degradación de su superficie o liberación de iones (en NPs metálicas) cuando las NPs son expuestas al ambiente ácido del interior de los lisosomas/endosomas.
2. Por su interacción con orgánulos celulares como la mitocondria de forma que se altera la actividad funcional de ésta y también las cadenas intracelulares de transporte electrónico.
3. Por su interacción con proteínas redox como la NADPH oxidasa que estimulan la generación de ROS en las células del sistema inmune.
4. Por su interacción con receptores de la membrana que activan las cascadas de señales intracelulares y la expresión de genes relacionados con la respuesta al estrés [17,18].

Alteración de la morfología celular

Algunas NPs, como las NPs de oro, provocan cambios en la morfología de determinadas líneas celulares [19]. Estas deformaciones pueden ser temporales y parecen ser dependientes de la concentración intracelular de NPs [20].

Alteración de las cadenas de señales intracelulares y genotoxicidad

Las NPs también pueden ejercer efectos adversos sobre la homeostasis o equilibrio celular, que finalmente desembocan en daños sobre el material genético (genotoxicidad). Las NPs inducen genotoxicidad en las células a través de los siguientes mecanismos: *a)* por formación de ROS que dañan directamente el ADN; *b)* por localizarse en la zona perinuclear dificultando así la transcripción y traducción del material genético; *c)* por liberación de iones metálicos; *d)* por su interacción con receptores de la membrana de forma que se alteran las cascadas de señales intracelulares; *e)* por alterar la expresión de genes como respuesta al estrés causado por el incremento en ROS; y *f)* por interactuar directamente con el ADN del núcleo. La Figura I.3.6 muestra todos los mecanismos anteriormente citados.

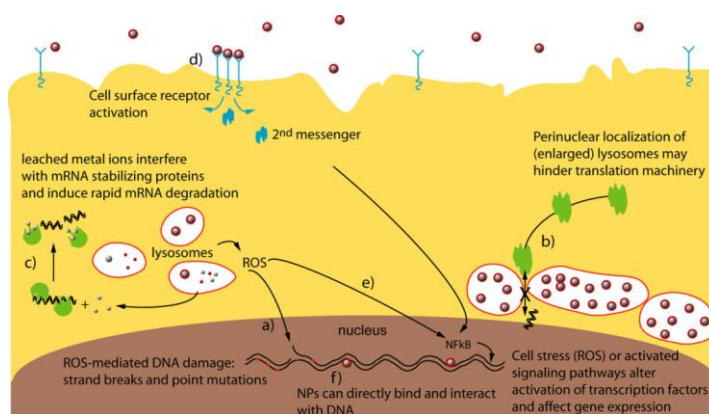


Figura I.3.6. Mecanismos que inducen genotoxicidad. Figura perteneciente a [17].

Liberación de iones al medio intracelular

Una vez internalizadas, las NPs se ven sometidas a fluctuaciones de pH y a la acción de enzimas proteolíticas como la catepsina L. El ambiente ácido del interior de los lisosomas y endosomas ($\text{pH} \approx 4.5$) puede degradar la superficie de la NP lo que sigue a la liberación de los iones presentes en su núcleo. Estos iones alteran la homeostasis celular y son en muchos casos la causa principal de toxicidad asociada a las NPs [17,21,22].

Interacción con biomoléculas

La elevada área superficial y densidad de carga de las NPs hacen que las proteínas las rodeen inmediatamente formando la estructura denominada como corona de proteínas (*protein corona*). Los efectos toxicológicos derivados de esta interacción podrían estar relacionados con los cambios conformacionales sufridos por las proteínas y sus pérdidas de funcionalidad [23,24]. Esto a su vez puede desembocar en otros efectos negativos en tanto en cuanto las proteínas alteradas son reconocidas por el sistema inmune como objetos extraños y como resultado pueden ser eliminadas [25]. Las NPs también pueden inducir defectos en la estructura de la bicapa lipídica como consecuencia de su interacción con los lípidos de la membrana. Esto puede promover la internalización directa de las NPs por mecanismos de difusión pasiva [26].

MÉTODOS DE EVALUACIÓN DE LA NANOTOXICIDAD

Evaluar la *Nanotoxicidad* resulta bastante complejo por la amplia variedad de factores que juegan un papel decisivo en la misma. Diferentes tipos de NPs, propiedades fisicoquímicas, condiciones de incubación (tiempo y concentración), líneas celulares, ensayos y posibles interferencias conforman

BLOQUE I. INTRODUCCIÓN

un marco de estudio muy amplio que dificulta enormemente el establecimiento de protocolos sistemáticos de evaluación así como la interpretación y extrapolación de los resultados [17]. A continuación se especifican los ensayos *in vitro* más utilizados actualmente para investigar la toxicidad de las NPs.

Ensayos de actividad metabólica

Una evidencia clara del daño celular ocasionado es la alteración de la actividad metabólica. Uno de los ensayos más populares en este campo, es el *ensayo del bromuro de 3-(4,5-dimetiltiazol-2-il)-2,5-difenil tetrazolio (MTT)*. Este ensayo se basa en la conversión de una sal de tetrazolio de color amarillo a un producto insoluble de color azul (formazán), bajo la acción de la succinato deshidrogenasa que es solo funcional en células vivas. El formazán generado se solubiliza con dimetilsulfóxido (DMSO) y se cuantifica finalmente con ayuda de un espectrofotómetro. Otras sales de tetrazolio como el 3-(4,5-dimetiltiazol-2-il)-5-(3-carboximetoxifenil)-2-(4-sulfofenil)-2H-tetrazolio y el 2,3-bis-(2-metoxi-4-nitro-5-sulfofenil)-2H-tetrazolio-5-carboxanilida también han sido empleadas con el mismo propósito. Dentro de este tipo de ensayos cabe mencionar también el *ensayo Azul Alamar o de la resazurina* en el que se mide el potencial redox de las células vivas para reducir el colorante resazurina a un producto fluorescente (resorufina) por la acción de sus enzimas mitocondriales [2,27].

Ensayos de proliferación celular

Las NPs pueden interferir en la tasa de proliferación celular y es por ello por lo que también existen ensayos que evalúan este parámetro en células que han sido expuestas a las NPs. En este sentido, los ensayos cologénicos investigan la *eficiencia de formación de colonias (CFE)* de las células incubadas con NPs y la comparan con aquella observada en células no expuestas

(controles). Asimismo, otro ensayo dentro de esta tipología evalúa la *incorporación de ³H-timidina en el ADN* de células vivas. La desventaja asociada a este último ensayo es la naturaleza radiactiva del isótopo tritio unido a la timidina, y los largos tiempos de incubación requeridos (24/48 horas) [2,28].

Ensayos de genotoxicidad

Las NPs con futuras aplicaciones biomédicas deben ser sometidas a una evaluación exhaustiva sobre sus posibles efectos adversos sobre el material genético. Los ensayos *in vitro* que permiten esta evaluación se basan principalmente en detectar la presencia de hebras de ADN fragmentadas, evidencia más que suficiente del daño genético causado. Los métodos más populares en este sentido son *el ensayo cometa* que permite detectar fragmentos de ADN por su diferente migración en electroforesis en gel, o bien los métodos que identifican la presencia de aberraciones cromosomales o miden la expresión de proteínas implicadas en la reparación del ADN. El *ensayo TUNEL* (Terminal deoxynucleotidyl transferase-mediated deoxyUridine triphosphate-Nick End Labeling) se basa en el marcaje de los extremos 3'OH de los fragmentos de ADN que se generan durante la apoptosis [2,27].

Ensayos de expresión génica alterada

La alteración de la expresión de determinados genes funcionales puede evaluarse cuantitativamente con el empleo de *(bio)chips de ADN (microarrays)* o mediante la técnica de *reacción en cadena de la polimerasa (PCR)* [2,29].

Ensayos de estrés oxidativo

El incremento desmesurado en la producción de ROS puede resultar por una respuesta inmune de la célula a la presencia de NPs, o bien como resultado

BLOQUE I. INTRODUCCIÓN

de la habilidad intrínseca de algunas NPs (tal es el caso de fullerenos u óxidos metálicos) para autocatalizar la formación de estas especies.

La presencia de ROS puede evaluarse directamente por cuantificar los niveles intracelulares de ROS o indirectamente, por monitorizar los efectos secundarios de sufrir un estrés oxidativo prolongado. Entre los métodos directos destaca la medida de los *niveles de glutatión (GSH)*, antioxidante que juega un papel clave en la defensa celular y cuya disminución es una prueba irrefutable del estrés oxidativo. No obstante, el método directo más extendido es el *ensayo del diacetato de diclorodihidrofluoresceína*, basado en un compuesto que penetra en las células y se hidroliza a un producto verde fluorescente solo en presencia de ROS. Los métodos indirectos estudian los eventos intracelulares originados por el incremento en la producción de ROS, como la peroxidación de lípidos. Tal es el caso del ensayo que cuantifica los *niveles de malondialdehído*, producto generado por la fragmentación de los ácidos grasos poliinsaturados [2,27].

Ensayos para evaluar la integridad de la membrana y la necrosis

La habilidad que presentan algunas NPs para destruir células (fenómeno conocido como necrosis) puede ser evaluada en base a los daños que ocasionan sobre la membrana celular. La integridad de la membrana puede ser investigada mediante el *ensayo del rojo neutro*, la determinación del *contenido de lactato deshidrogenasa (LDH)* en el medio extracelular, o el *ensayo de exclusión del azul de tripano*.

El *ensayo del rojo neutro* mide la capacidad de las células vivas para incorporar este colorante en los lisosomas, de forma que si la membrana está dañada, la internalización del compuesto disminuye. La citotoxicidad puede ser cuantificada entonces por medidas espectrofotométricas del colorante y

comparación con las células control. La *presencia de LDH* en el medio extracelular es un indicador de la presencia de células con membranas dañadas ya que en estos casos se promueve la excreción de esta enzima al medio extracelular. Finalmente, en el *ensayo de exclusión del azul de tripano*, este colorante solo es internalizado, y puede teñir los componentes intracelulares, de las células dañadas. El número de células sin teñir refleja por tanto el número de células vivas presentes en las muestras [2,27,30,31].

Ensayos de apoptosis

Varios ensayos *in vitro* en combinación con la técnica de citometría de flujo nos permiten evaluar la apoptosis o muerte celular programada en células que han sido expuestas a las NPs. En este sentido destacamos el *ensayo de las caspasas* y el *ensayo de la anexina V*. En el primero, se investiga la activación de las caspasas (enzimas con actividad proteolítica) que solo se produce durante las primeras fases de la apoptosis. En el *ensayo de la anexina V* esta proteína es marcada con un fluoróforo y se une fuertemente a la fosfatidilserina solo cuando ésta es translocada fuera de la membrana plasmática en las células que sufren apoptosis. La apoptosis también se identifica a través de la morfología del núcleo celular que es teñido con *4',6-diamidino-2-fenilindol (DAPI)* y se visualiza mediante microscopía de fluorescencia [27,28]. Asimismo, los ensayos de genotoxicidad anteriormente descritos pueden revelar indicios de apoptosis celular.

Ensayos de alteraciones morfológicas

Las NPs también pueden inducir cambios morfológicos en las células. Estas alteraciones pueden ser identificadas por microscopía, especialmente por análisis SEM o TEM. Asimismo, a diferencia de las técnicas anteriores, la microscopía de contraste de fases también permite examinar aquellas células

BLOQUE I. INTRODUCCIÓN

vivas en su estado natural sin necesidad de someterlas a ningún tipo de fijación o deshidratación [27].

Otros ensayos

Hay otro tipo de ensayos *in vitro* disponibles pero cuya aplicación está menos extendida. Tal es el caso de los *ensayos de exocitosis* que evalúan el efecto que tienen las NPs sobre la secreción celular de pequeñas moléculas electroactivas como la serotonina y la epinefrina. Este ensayo se lleva a cabo mediante amperometría con un microelectrodo de fibra de carbono [2]. Los *ensayos de hemolisis* son imprescindibles para aquellas NPs cuya aplicación futura en la diagnosis o el tratamiento de enfermedades suponga su introducción directa en el torrente sanguíneo. La lisis de los eritrocitos o glóbulos rojos es un claro indicador de la toxicidad celular extrema de las NPs. La evaluación en este caso se realiza por detección espectrofotométrica de la hemoglobina [2].

RETOS EN LA EVALUACIÓN DE LA NANOTOXICIDAD

Los ensayos *in vitro* anteriormente discutidos fueron en principio diseñados y establecidos para evaluar de forma sistemática la toxicidad asociada a los compuestos químicos. Sin embargo, estos mismos protocolos se están utilizando a día de hoy para evaluar la toxicidad asociada a las NPs, lo que ha supuesto la aparición de una serie de deficiencias en estas estrategias de evaluación. A continuación, se discuten las principales limitaciones encontradas en los métodos actuales de evaluación toxicológica cuando son aplicados al estudio de la *Nanotoxicidad*.

Interferencias en los ensayos

Las NPs pueden interferir en cierta medida con algunos ensayos de toxicidad *in vitro* lo que puede desembocar en la obtención de resultados no del todo fiables.

A modo de ejemplo, en el ensayo colorimétrico del MTT, los nanotubos de carbono multicapa (MWCNTs) son capaces de reducir el compuesto MTT al producto formazán en ausencia de células vivas, proporcionando así falsos positivos. Además, estas mismas NPs también pueden adsorber en superficie el formazán generado, estabilizando así su estructura e impidiendo su cuantificación. Esto genera falsos negativos y una subestimación en la viabilidad celular real de las muestras [32-34]. Por otro lado, también se han descrito interferencias de las NPs de dióxido de titanio con el ensayo de la lactato deshidrogenasa (LDH) [35].

Otro tipo de interferencias tienen su origen en el solapamiento espectral entre los espectros de absorción de las NPs y el producto a cuantificar en el ensayo. Esto indudablemente conlleva una sobreestimación de la viabilidad celular de las muestras (falsos positivos).

En cualquier caso, sería recomendable llevar a cabo estudios paralelos simultáneos con diferentes ensayos *in vitro*, así como controles internos específicos, con el propósito de incrementar la fiabilidad de los resultados obtenidos [2,31].

Caracterización de las nanopartículas

Un aspecto a tener en cuenta en cualquier estudio sobre *Nanotoxicidad* es la caracterización exhaustiva de las NPs implicadas. Conocer sus propiedades

BLOQUE I. INTRODUCCIÓN

fisicoquímicas incluyendo su composición química (impurezas, y composición del núcleo y del recubrimiento superficial), su distribución de tamaños y forma, su reactividad y área superficial, su estabilidad y estado de aglomeración, resulta extremadamente útil con vistas a definir sus efectos tóxicos asociados.

La interacción de las NPs con determinados componentes del medio biológico así como la presencia de sales o las fluctuaciones de pH pueden alterar la estabilidad de los nanomateriales y consecuentemente, su estado de aglomeración. Teniendo en cuenta los cambios a los que las NPs están sometidas en los medios fisiológicos, el escenario ideal sería realizar una caracterización de las mismas *ex ante*, *in itinere* y *ex post* de la evaluación de su toxicidad, con el objetivo de establecer una relación inequívoca y fiable entre NPs caracterizadas en matrices reales y su toxicidad inherente [2,31,36,37].

Estandarización de los protocolos de evaluación

Para obtener resultados de toxicidad que sean comparables y que permitan extraer conclusiones generalizadas, se deben introducir modificaciones en los protocolos de evaluación actuales.

Por lo general, los ensayos de citotoxicidad evalúan la toxicidad de un único tipo de NP y sobre una línea celular específica. Partiendo de la base de que la interacción entre las NPs y las células depende de la tipología celular seleccionada, resulta algo complejo extraer conclusiones generalizadas sobre los efectos tóxicos encontrados. Además cabe decir que no todas las líneas celulares son adecuadas para los ensayos de citotoxicidad, tal es el caso de las células cancerígenas, cuyas características las hacen ser menos propensas a mostrar determinados efectos citotóxicos [17].

I.3. Toxicidad asociada a las nanopartículas

Por otro lado, la estandarización de las condiciones de incubación estudiadas, incluyendo el rango de concentraciones de NPs o los tiempos de exposición, ayudaría significativamente a la interpretación global de los resultados obtenidos de diferentes protocolos de evaluación y de estudios interlaboratorio [17].

A esto hay que añadir el hecho de que existe una amplia variedad de ensayos de citotoxicidad disponibles cada uno de los cuales determina uno o más parámetros celulares, como la actividad mitocondrial o la integridad de la membrana. Esta variedad, si bien permite abarcar un marco de estudio más amplio, también impide la comparación directa de los resultados obtenidos a partir de ensayos diferentes. Es por ello por lo que deberían establecerse de forma sistemática varios parámetros celulares a evaluar de partida en todos los estudios de toxicidad que se lleven a cabo. La realización de múltiples ensayos en paralelo también enriquecería la información obtenida [17].

Concentraciones reales de nanopartículas que inducen toxicidad

Si bien es cierto que en la mayoría de estudios toxicológicos los efectos observados son dependientes de la concentración de NPs añadidas al medio de incubación, no siempre esas concentraciones se corresponden exactamente a aquellas que inducen los efectos citotóxicos. Es decir, la toxicidad depende de la habilidad de las NPs para ser internalizadas dentro de las células y no de la cantidad total de NPs presentes en el medio de incubación. Esto nos lleva a concluir que una misma concentración de NPs idénticas pero con diferente recubrimiento superficial pueden resultar en una toxicidad distinta como consecuencia de su diferente habilidad de penetración celular. Con lo cual, sería interesante correlacionar los resultados obtenidos con la concentración de NPs internalizadas y no con aquella añadida al medio de incubación [17].

Consideración de los efectos secundarios y a largo plazo

La citotoxicidad se evalúa generalmente por la exposición de las células a elevadas dosis de NPs durante cortos periodos de tiempo (citotoxicidad aguda). Sin embargo, una asignatura pendiente en la *Nanotoxicidad* es evaluar los efectos ocasionados por dosis más pequeñas de NPs durante exposiciones de mayor duración (citotoxicidad crónica). Esto es importante puesto que tanto la localización intracelular como la estabilidad de las NPs cambian con el tiempo. Las NPs pueden sufrir cambios estructurales o incluso ser degradadas por enzimas, con lo cual sus efectos sobre las células podrían ser solo temporales o en contraposición, agravarse con el tiempo. Se precisa por tanto, la aplicación de métodos que evalúen los efectos toxicológicos durante periodos de tiempo más largos (días e incluso semanas), y que monitoricen el estado y localización de las NPs en función del tiempo [17].

Referencias

- [1] K. Donaldson, V. Stone, C.L. Tran, W. Kreyling, P.J.A. Borm, *Nanotoxicology, Occup. Environ. Med.* 61 (2004) 727-728.
- [2] S.A. Love, M.A. Maurer-Jones, J.W. Thompson, Y.S. Lin, C.L. Haynes, Assessing nanoparticles toxicity, *Annu. Rev. Anal. Chem.* 5 (2012) 181-205.
- [3] H. Kettiger, A. Schipanski, P. Wick, J. Huwyler, Engineered nanomaterial uptake and tissue distribution: from cell to organism, *Int. J. Nanomed.* 8 (2013) 3255-3269.
- [4] F. Zhao, Y. Zhao, Y. Liu, X. Chang, C. Chen, Y. Zhao, Cellular uptake, intracellular trafficking and cytotoxicity of nanomaterials, *Small* 7 (2011) 1322-1337.
- [5] A. Panariti, G. Miserocchi, I. Rivolta, The effect of nanoparticle uptake on cellular behavior: disrupting or enabling functions?, *Nanotechnol. Sci. Appl.* 5 (2012) 87-100.
- [6] D. Pantarotto, R. Singh, D. McCarthy, M. Erhardt, J.-P. Briand, M. Prato, K. Kostarelos, A. Bianco, Functionalized carbon nanotubes for plasmid DNA gene delivery, *Angew. Chem. Int. Ed* 43 (2004) 5242-5246.
- [7] C.F. López, S.O. Nielsen, P.B. Moore, M.L. Klein, Understanding nature's design for a nanosyringe, *Proc. Natl. Acad. Sci. USA* 101 (2004) 4431-4434.
- [8] L. Lacerna, S. Raffa, M. Prato, A. Bianco, K. Kostarelos, Cell-penetrating CNTs for delivery of therapeutics, *Nanotoday* 2 (2007) 38-43.
- [9] Y. Qiu, Y. Liu, L. Wang, L. Xu, R. Bai, Y. Li, X. Wu, Y. Zhao, Y. Li, C. Chen, Surface chemistry and aspect ratio mediated cellular uptake of Au nanorods, *Biomaterials* 31 (2010) 7606-7619.
- [10] A. Verma, F. Stellacci, Effect of surface properties on nanoparticle-cell interactions, *Small* 6 (2010) 12-21.
- [11] O. Harush-Frenkel, N. Debotton, S. Benita, Y. Altschuler, Targeting of nanoparticles to the clathrin-mediated endocytic pathway, *Biochem. Biophys. Res. Commun.* 353 (2007) 26-32.
- [12] Z.J. Zhu, P.S. Ghosh, O.R. Miranda, R.W. Vachet, V.M. Rotello, Multiplexed screening of cellular uptake of gold nanoparticles using laser desorption/ionization mass spectrometry, *J. Am. Chem. Soc.* 130 (2008) 14139-14143.
- [13] A. Verma, O. Uzun, Y.H. Hu, Y. Hu, H.S. Han, N. Watson, S.L. Chen, D.J. Irvine, F. Stellacci, Surface-structure-regulated cell-membrane penetration by monolayer-protected nanoparticles, *Nat. Mater.* 7 (2008) 588-595.

BLOQUE I. INTRODUCCIÓN

[14] D. Pantarotto, J.P. Briand, M. Prato, A. Bianco, Translocation of bioactive peptides across cell membranes by carbon nanotubes, *Chem. Commun.* 1 (2004)16-17.

[15] L.W. Zhang, N.A. Monteiro-Riviere, Mechanisms of quantum dot nanoparticle cellular uptake, *Toxicol. Sci.* 110 (2009) 138-155.

[16] H.J. Johnston, M. Semmler-Behnke, D.M. Brown, W. Kreyling, L. Tran, V. Stone, Evaluating the uptake and intracellular fate of polystyrene nanoparticles by primary and hepatocyte cell lines in vitro, *Toxicol. Appl. Pharmacol.* 242 (2010) 66-78.

[17] S.J. Soenen, P. Rivera-Gil, J.M. Montenegro, W.J. Parak, S.C. De Smedt, K. Braeckmans, Cellular toxicity of inorganic nanoparticles: Common aspects and guidelines for improved nanotoxicity evaluation, *Nanotoday* 6 (2011) 446-465.

[18] L. Yan, Z. Gu, Y. Zhao, Chemical mechanisms of the toxicological properties of nanomaterials: generation of intracellular reactive oxygen species, *Chem. Asian. J.* (2013) DOI 10.1002/asia.201300542.

[19] H.K. Patra, S. Banerjee, U. Chaudhuri, P. Lahiri, A.K. Dasgupta, Cell selective response to gold nanoparticles, *Nanomed-Nanotechnol.* 3 (2007) 111-119.

[20] N. Pernodet, X. Fang, Y. Sun, A. Bakhtina, A. Ramakrishnan, J. Sokolov, A. Ulman, M. Rafailovich, Adverse effects of citrate/gold nanoparticles on human dermal fibroblasts, *Small* 2 (2006) 766-773.

[21] K.G. Li, J.T. Chen, S.S. Bai, X. Wen, S.Y. Song, Q. Yu, J. Li, Y.Q. Wang, Intracellular oxidative stress and cadmium ions release induce cytotoxicity of unmodified cadmium sulfide quantum dots, *Toxicol. In Vitro* 23 (2009) 1007-1013.

[22] K.M. Newton, H.L. Puppala, C.L. Kitchens, V.L. Colvin, S.J. Klaine, Silver nanoparticle toxicity to *Daphnia magna* is a function of dissolved silver concentration, *Environ. Toxicol. Chem.* 32 (2013) 2356-2364.

[23] P. Asuri, S.S. Bale, R.C. Pangule, D.A. Shah, R.S. Kane, J.S. Dordick, Structure, function, and stability of enzymes covalently attached to single-walled carbon nanotubes, *Langmuir* 23 (2007) 12318-12321.

[24] N. Wangoo, C.R. Suri, G. Shekhawat, Interaction of gold nanoparticles with protein: A spectroscopic study to monitor protein conformational changes, *Appl. Phys. Lett.* 92 (2008) 133104/1-133104/3.

[25] Z.J. Deng, M. Liang, M. Monteiro, I. Toth, R.F. Minchin, Nanoparticle-induced unfolding of fibrinogen promotes Mac-1 receptor activation and inflammation, *Nat. Nanotechnol.* 6 (2011) 39-44.

[26] J. Lin, H. Zhang, Z. Chen, Y. Zheng, Penetration of lipid membranes by gold nanoparticles: Insights into cellular uptake, cytotoxicity and their relationship, *ACS Nano* 4 (2010) 5421-5429.

• • •

I.3. Toxicidad asociada a las nanopartículas

- [27] J.L. Luque-Garcia, R. Sanchez-Díaz, I. Lopez-Heras, P. Martin, C. Camara, Bioanalytical strategies for in-vitro and in-vivo evaluation of the toxicity induced by metallic nanoparticles, *TrAC* 43 (2013) 254-268.
- [28] P. Takhar, S. Mahant, In vitro methods for Nanotoxicity assessment: advantages and applications, *Arch. Appl. Sci. Res.* 3 (2011) 389-403.
- [29] S.Y. Choi, S. Jeong, S.H. Jang, J. Park, J.H. Park, K.S. Ock, S.Y. Lee, S.W. Joo, In vitro toxicity of serum protein-adsorbed citrate-reduced gold nanoparticles in human lung adenocarcinoma cells, *Toxicol. In Vitro* 26 (2012) 229-237.
- [30] J.M. Hillegass, A. Shukla, S.A. Lathrop, M.B. MacPherson, N.K. Fukagawa, B.T. Mossman, Assessing nanotoxicity in cells in vitro, *Adv.Rev.* 2 (2010) 219-231.
- [31] L. Bregoli, S. Pozzi-Mucelli, L. Manodori, Molecular methods for Nanotoxicology, *Toxic Effects of Nanomaterials* Chapter 6 (2012) 97-120.
- [32] J.M. Wörle-Knirsch, K. Pulskamp, H.F. Krug, Oops they did it again! Carbon nanotubes hoax scientists in viability assays, *Nano Lett.* 6 (2006) 1261-1268.
- [33] R. Brayner, The toxicological impact of nanoparticles, *Nanotoday* 3 (2008) 48-55.
- [34] N.A. Monteiro-Riviere, A.O. Inman, L.W. Zhang, Limitations and relative utility of screening assays to assess engineered nanoparticle toxicity in a human cell line, *Toxicol. Appl. Pharmacol.* 234 (2009) 222-235.
- [35] X. Han, R. Gelein, N. Corson, P. Wade-Mercer, J. Jiang, P. Bismas, J.N. Finkelstein, A. Elder, G. Oberdörster, Validation of an LDH assay for assessing nanoparticle toxicity, *Toxicology* 287 (2011) 99-104.
- [36] B.D. Chithrani, A.A. Ghazani, W.C.W. Chan, Determining the size and shape dependence of gold nanoparticle uptake into mammalian cells. *Nano Lett.* 4 (2006) 662-668.
- [37] R.F. Hamilton, N.N. Wu, D. Porter, M. Buford, M. Wolfarth, A. Holian, Particle length-dependent titanium dioxide nanomaterials toxicity and bioactivity, *Part. Fibre Toxicol.* 6 (2009) 35-45.

J Nanopart Res (2013) 15:1534
DOI 10.1007/s11051-013-1534-4



REVIEW

**The social responsibility of Nanoscience and Nanotechnology:
an integral approach**

Encarnación Caballero-Díaz, Bartolomé M. Simonet, Miguel Valcárcel

Department of Analytical Chemistry, Marie Curie Building (Annex), Campus de Rabanales, University of Córdoba, 14071 Córdoba, Spain

ABSTRACT

The concept of social responsibility provides the ideal framework for raising awareness and arousing reflection on the social and environmental impact of nanoparticles in the range of 1-100 nm generated from research activities in Nanoscience and production-related activities in nanotechnology. The model proposed here relates the essential aspects of these concepts by connecting the classical sequence Research–Development–Innovation (R&D&I) to nanoscience and nanotechnology (N&N) and social responsibility (SR). This paper identifies the stakeholders of the process and provides an extensive definition of SR and related concepts. In addition, it describes the internal and external connotations of the implementation of SR at research centers and nanotechnological industries, and discusses the social implications of nanoscience and nanotechnology with provision for subjects such as

BLOQUE I. INTRODUCCIÓN

nanoethics, nanotoxicity and nanomedicine, which have emerged from the widespread use of nanomaterials by today's society.

1. INTRODUCTION

Nanotechnology has been deemed as a key emerging technology for fulfilling the “Grand Challenges of our Time” in areas such as health care, energy production, environmental protection (climate change and remediation) and potable water procurement (Lund Declaration 2009).

Like other highly promising technologies such as nuclear engineering and biotechnology, nanotechnology possesses two contradictory connotations, namely: the production of new materials with outstanding mechanical, optical, electric and magnetic properties for a wide variety of uses, which is highly positive; and its uncertain effects on human health and the environment, which is highly negative. Nanotechnology and its impacts have frequently been questioned in manners that have exposed the inability of national and international “regulatory” agencies to adapt themselves to the dramatic changes experienced in recent times. In fact, nanotechnology growth and impact (Groves et al. 2011) have been used as guidelines for allocating future responsibilities, managing risks and dealing with the growing significance of the mutual influence of technology and society. The ultimate aim here is to harmonize present and future opportunities in nanotechnology with its constraints in an integral management scheme.

Available literature on the general impacts of nanotechnology reflects two major deficiencies. One is that the risks and ethical implications of nanotechnology (Hunt and Mehta 2006) in the production and industrial domains have rarely been approached in a systematic manner at the first stage of basic research in this field, which is usually identified with “Nanoscience”, despite the recent dramatic growth of literature on the potential toxicity of nanoparticles (see Fig. 1). The other deficiency is that, although the potential hazards of nanotechnological products have been the subject of much literature

BLOQUE I. INTRODUCCIÓN

lately, their toxicity remains uncertain owing to the lack of scientific consensus in many cases. Also, properly dealing with this uncertainty in house remains an unresolved matter for many nanotechnological enterprises (Groves et al. 2011).

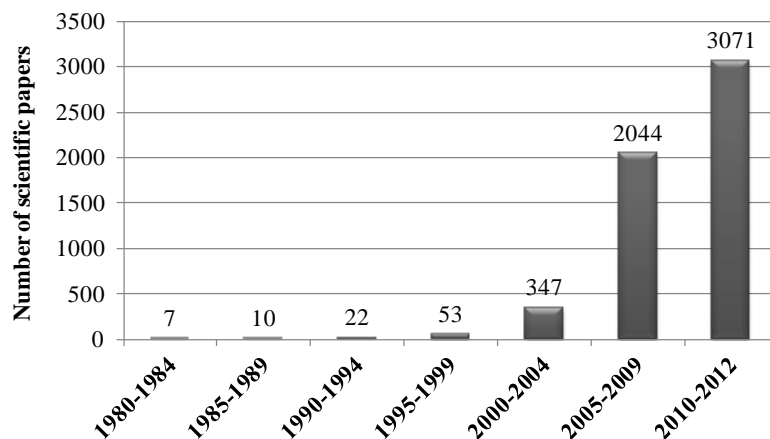


Figure 1. Number of papers on nanoparticles toxicity published in recent five-year periods and since 2010 (Source: SciFinder).

Responsibility, which is the ethical obligation to behave correctly (McCarty and Kelty 2010), and social responsibility (SR) in particular (see “The concept of social responsibility” section of this paper), provide the ideal framework for a systematic approach to these subjects and is thus used here to define SR in nanoscience and nanotechnology in a separate, but coherent manner, and also to distinguish corporate social responsibility (CSR), with its internal and external connotations (Fig. 5), from corporate social performance (CSP). Assimilating a R&D center to a corporation facilitates a unified treatment of the previous four concepts, which are obviously related to one another.

The developments and implications of SR in nanoscience and nanotechnology can be referred to previous advances, achievements, and failures in SR of Biotechnology (David and Thompson 2008), Genomics (Fisher 2005; Cassa et al. 2012), Proteomics (Liska 2004), Metabolomics (Manasco

I.4. Social responsibility of Nanoscience and Nanotechnology

2005), and Nuclear Engineering (Mizuo 2008). Also, SR is more apparent and important in some emerging sciences and technologies than in other more conventional technologies. Innovations in these sciences and technologies share many ethical, social, and environmental connotations. The scope and magnitude of the implications of emerging technologies require careful examination in not only scientific and technical, but also social, political, and ethical terms (Mcgregor and Wetmore 2009).

This paper proposes a SR framework that provides guidance for conducting socially responsible research (SR in nanoscience) with provision for the ethical and social implications of the transfer of nanomaterials from research centers to nanotechnological industries and, ultimately, to society and the environment (SR in nanotechnology). The proposed model integrates the SR concept into the well-known Research–Development–Innovation (R&D&I) sequence, whose stakeholders are identified and classified as internal, external, or mixed. The concept of SR is extensively dealt with, particularly in relation to its early implementation, existing regulation and stages. SR in nanoscience and nanotechnology are discussed separately, with special emphasis on its internal and external connotations— and their implications. Finally, selected issues in nanoethics, nanotoxicity, and nanomedicine are briefly commented on to illustrate the increasing usefulness of nanomaterials for today’s society.

2. GENERAL MODEL

Properly dealing with the subject matter of this paper entails previously developing a general model for the classical sequence Research–Development–Innovation (R&D&I). The proposed model is depicted in Fig. 2. As can be seen, nanoscience falls basically in the research domain and nanotechnology in the innovation domain. The development stage typically provides the interface for their harmonization and is the competence of and/or meeting point for both

BLOQUE I. INTRODUCCIÓN

research centers and technological industries, which are shown separately in the scheme. In addition, the development stage sets the above-described difference between CSR and CSP. Although the CSR concept is applicable to a nanotechnological research center, it may be more appropriate to exclude the corporate connotation and refer exclusively to SR of nanoscience if the center in question is mainly engaged in the development of basic nanoscience. In any case, the concepts illustrated in Fig. 2 have so far been approached in disparate manners. Thus, nanoscience has scarcely been addressed and rarely distinguished from nanotechnology. This paper is intended to alleviate the problems derived from the lack of a unified approach to this subject.

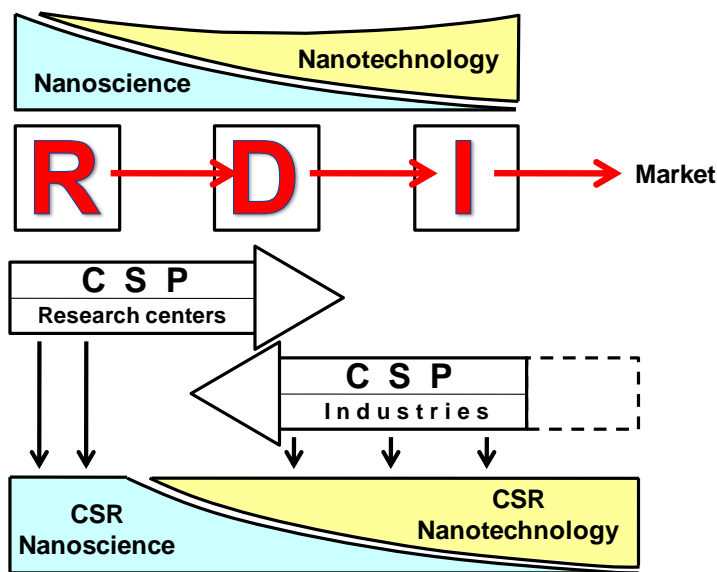


Figure 2. Social Responsibility in nanoscience and nanotechnology in the twofold domain of R&D&I and corporate social performance (CSP) in nanoscience research centers and nanotechnological enterprises.

3. THE STAKEHOLDERS

The word “stakeholders” has been extensively used in the ISO guides and standards issued in recent decades to designate the individuals or groups that

I.4. Social responsibility of Nanoscience and Nanotechnology

can not only be favorably or adversely affected by the activities of an organization or area, but also influence on their decisions. The dual (active and passive) nature of stakeholders here is crucial with a view to their integral definition and highlights their prominent role in SR.

Figure 3 shows the stakeholders of SR in N&N, and hence in nanoscience research centers and nanotechnological industries. The ultimate external stakeholders are society and the environment (specifically, people with unfulfilled basic needs who receive and enjoy nanotechnological innovations, others who are unintentionally exposed to nanomaterials, nanoscience research funding providers, and organizations such as NGOs concerned with environmental quality, climate change, or social welfare).

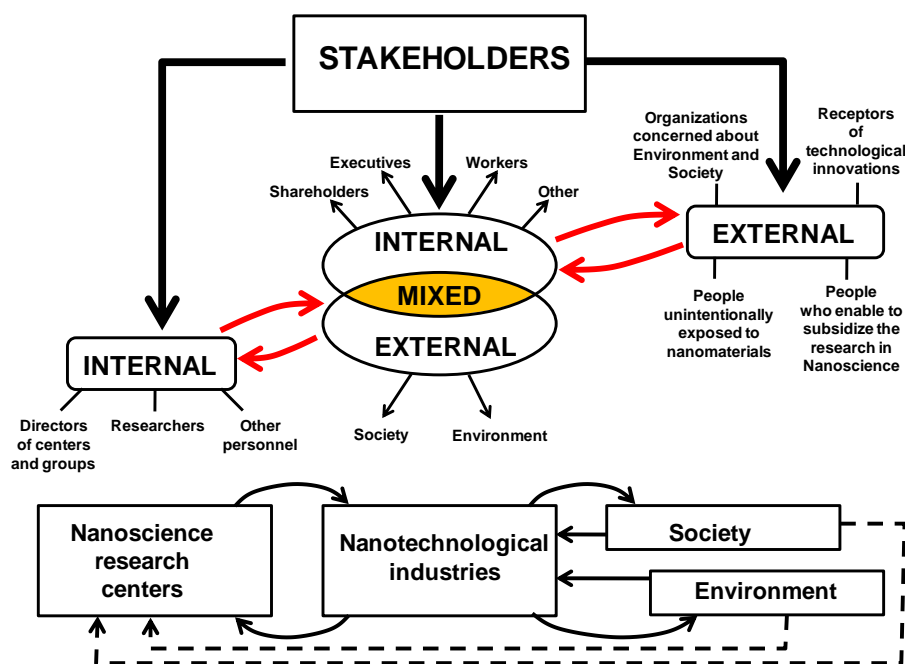


Figure 3. Types of stakeholders in N&N, and two-way relationships between them.

The stakeholders of nanotechnological industries are of *mixed* type since they possess the typical *external connotations* of corporations in relation to

society and the environment—both of which are ultimately affected by nanomaterials—, and also *internal connotations* as recipients of the “products” delivered by research centers. In addition, these stakeholders can be the recipients of social and environmental inputs or demands, and pose scientific and technical problems to be solved by research centers.

Finally, scientific and technical officials, and other staff of research centers, constitute *typically internal stakeholders* inasmuch as they deliver products and services required by industries or resulting from unguided basic research activities.

4. THE CONCEPT OF SOCIAL RESPONSIBILITY

Social Responsibility can be defined in simple terms as the combination of several key words including “responsibility”, “stakeholders”, “quality of life” (social welfare), and “sustainability”. More than 50 definitions of SR, each placing special emphasis on an individual aspect, have already been provided. One of the two most consequential definitions states that “The SR of human activities and organizations involves fully integrating into their activities social and environmental concerns leading to the development of good practices and the establishment of new internal and external relations among the stakeholders” (de la Cuesta 2005). The other, set in ISO 26000:2010 (ISO 26000:2010), defines SR as “The responsibility of an organization for the impacts of its decisions and activities on society and the environment through transparent and ethical behavior that contributes to sustainable development, including health and the welfare of society; takes into account the expectations of stakeholders; is in compliance with applicable law and consistent with international norms of behavior; and is integrated throughout the organization and practiced in its relationships.”

I.4. Social responsibility of Nanoscience and Nanotechnology

In summary, properly approaching SR in an organization or activity entails adopting a well-defined social and environmental commitment to bring about a major change in its internal management (CSP) and alliances facilitating the incorporation of social and environmental concerns. Becoming a socially responsible, sustainable organization, therefore, requires expanding the traditional body of stakeholders. Because social needs and expectations from nanotechnology have changed with time, so have the definitions of SR; this has led to a lack of general agreement on a standard definition for CSR in the industrial world (Kuzma and Kuzhabekova 2011).

The SR concept was born in the corporate domain; hence its initial designation “Corporate Social Responsibility” (CSR) (de la Cuesta 2005; Olcese 2007; AENOR 2008). In recent years, the concept has expanded to other areas of individual and collective human behavior. Thus, it is common to find explicit references to SR in Science & Technology (Larsen et al. 2011), among other general areas, and also in specific branches such as Chemistry (IUPAC 2006) or Analytical Chemistry (Valcárcel and Lucena 2012a, b).

The prior development and consolidation of SR in the corporate domain have led to the release of several widely acknowledged and accepted documents especially prominent among which are the following four:

- 1.** The UN Global Compact, which includes 10 basic principles of SR (United Nations Global Compact 1999).
- 2.** The OECD guidelines for SR (Organization for Economic Cooperation and Development Guidelines for Social Responsibility 2001).
- 3.** The ILO principles for SR (International Labour Organization principle for Social Responsibility 2006).

BLOQUE I. INTRODUCCIÓN

4. ISO (International Organization for Standardization) 26000:2010 on SR, which contains the principles and guidelines for implementing SR in a human organization or activity, as well as the requirements to be fulfilled by its stakeholders (ISO 26000:2010).

ISO 26000:2010 formulates the seven basic principles of SR depicted in Fig. 4. Three (accountability, transparency, and ethical behavior) are general in nature and the other four represent the consideration of and respect for references such as human rights, international norms of behavior and applicable law, as well as stakeholders' expectations—fulfillment of which is the ultimate target of SR and to which all other principles are thus subordinate.

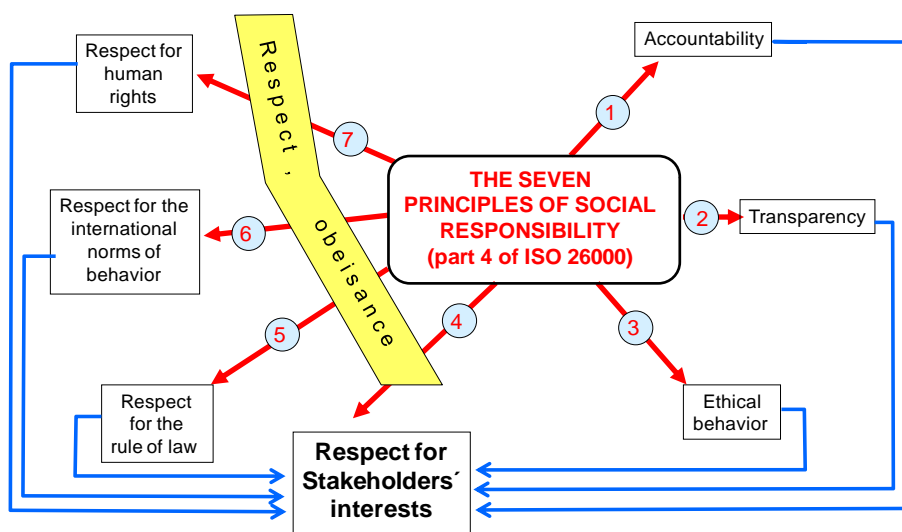


Figure 4. Principles of SR as per ISO 26000:2010 and significance of meeting stakeholders' expectations (ISO 26000:2010).

The *degree of commitment* in the implementation of SR can be modeled as a multiple pendulum oscillating between the extremes “causing no harm” (minimum) and “definitively improving” (maximum) in eight respects, namely:

I.4. Social responsibility of Nanoscience and Nanotechnology

1. The *natural environment*: from minimizing contamination to address sustainable innovation.
2. *Products*: from serving the client to develop “ethical” products.
3. *Staff*: from creating jobs and ensuring protection against labour risks to invest in continuing education, professional development, and diversity.
4. *The social environment*: from avoiding adverse impacts to contribute to social welfare.
5. *Governments*: from simply abiding by laws and regulations to go further in their fulfillment.
6. *Shareholders*: from maximizing short-term benefits to maximize long-term values.
7. *Clients*: from meeting the expectations of primary (direct) clients to also meet those of secondary (indirect) clients.
8. *Society*: from being a socially accepted member to become a socially respected member.

An organization’s bid to assume the principles and practices of CSR should start by internally incorporating CSP, which comprises internal policies, good practices, behavioral codes, regular reporting (Groves et al. 2011), and their associated resources (funding, staff, infrastructure and time) (McWilliams and Siegel 2000). As can be seen in Fig. 5, SR provides the general framework for placement of CSR and CSP. The figure exposes the main differences between CSR and CSP, which can be summarized as follows:

BLOQUE I. INTRODUCCIÓN

- 1) CSR has external connotations, whereas CSP has internal connotations;
- 2) CSR contains CSP; and
- 3) CSP can be viewed as the internal platform for developing an efficient, credible and reliable approach to CSR.

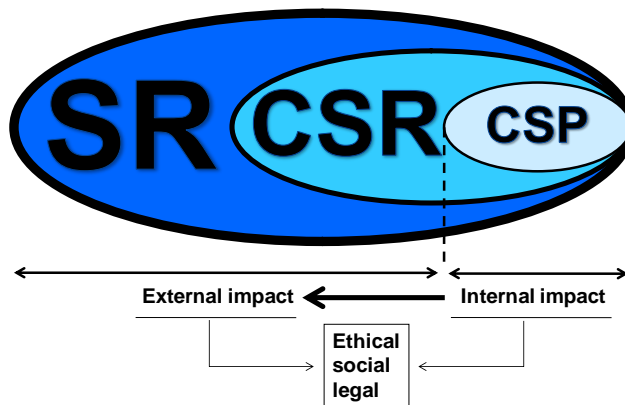


Figure 5. Differences between social responsibility (SR) domains: corporate social responsibility (CSR) and corporate social performance (CSP).

Despite their disagreement in other key subjects, experts in social and ethical issues almost unanimously agree that SR is very important and requires extensive implementation in emerging technologies (e.g., nanotechnology) in relation to conventional technologies. On the Clarkson scale (Clarkson 1995) of Fig. 6, nanotechnology requires a *proactive* rather than *accommodating*, *defensive* or *reactive* approach to CSR; one that lies at the positive extreme of the eight above-described respects.

Table 1 compares the “*reactive*” and “*proactive*” extremes of commitment to SR. As noted earlier, properly identifying and describing the different elements of SR in this context entails distinguishing between N&N, research centers, and nanotechnological industries, and also between their respective stakeholders (see Fig. 3).

I.4. Social responsibility of Nanoscience and Nanotechnology

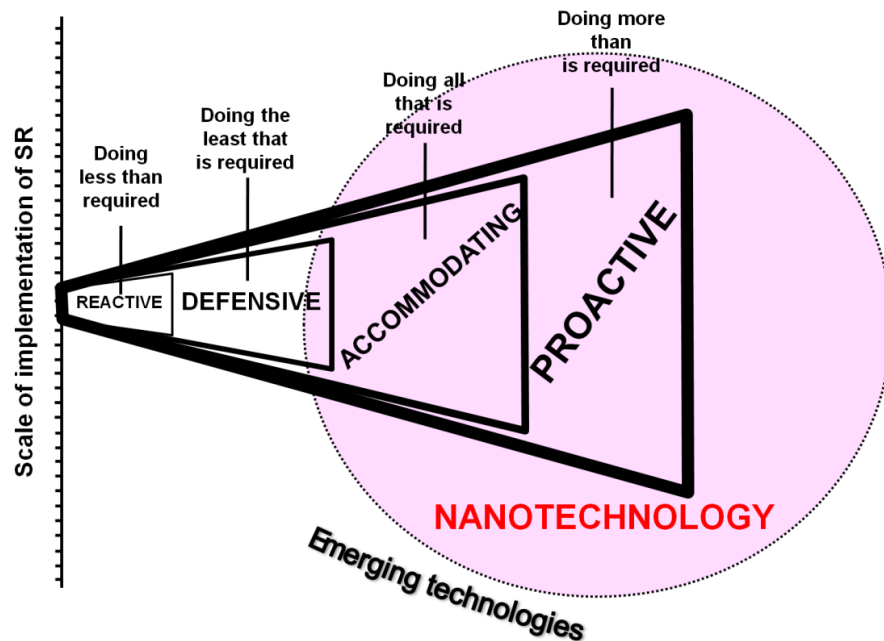


Figure 6. Clarkson scale of commitment to the implementation of social responsibility and position of RS in emerging technologies such as nanotechnology (Clarkson 1995).

Table 1. Differences between the reactive and proactive approaches to social responsibility (den Hond et al. 2007).

Reactive approach	Proactive approach
Comply with the minimum legislation	Expand the legislation to comply with
Maintain current reputation	Improve existing reputation
Maintain current staff	Recruit the best available employees
Maintain current morale and spirits	Improve current morale
Maintain current efficiency and benefits	Increase both
Maintain brand or style	Gradually improve them with added values
Adopt the "good business" notion	Adopt the "good business" notion

The acquisition of CSR by an enterprise requires adopting the CSP concept in its internal management, which involves the following five stages (Zadek 2004):

BLOQUE I. INTRODUCCIÓN

1. *Defensive stage*, where the enterprise meets with criticism from stakeholders—in the broad sense defined by ISO standards—and responds by mobilizing its legal department to dismiss all claims.
2. *Compliant stage*, where the enterprise adopts a corporate policy visible to all in order to maintain its reputation and reduce litigation expenses.
3. *Managerial stage*, where the enterprise includes social problems in its management policy in order to alleviate expenses in the mid term, and make profits in the long term, by incorporating responsible business practices into its daily practice.
4. *Strategic stage*, where the enterprise learns how to redirect its strategy to responsible business practices adapted to actual social problems and leading to increased competitiveness and success in the long term.
5. *Civil stage*, where the enterprise adopts a proactive attitude aimed at addressing social worries.

5. SOCIAL RESPONSIBILITY IN NANOSCIENCE

The general approach to SR in Science and Technology (Valcárcel and Lucena 2012) allows SR in nanoscience to be defined in two complementary ways, namely:

1. As the reflection on, and awareness of, the impact of the activities and outcomes of nanotechnological research on quality of life and the environment via their development and transfer by technological industries receiving, adapting, and marketing them.

I.4. Social responsibility of Nanoscience and Nanotechnology

2. As the honest, ethical behavior of researchers and officials at nanoscience research centers.

Social responsibility in nanoscience thus has a markedly indirect nature in its approach to society and the environment inasmuch as its influence is exerted via nanotechnological industries—where R&D&I departments are the most fluent in external communication. However, SR in nanoscience also has indirect connotations such as the protection and well-being of research laboratory staff (technicians included).

As shown below, SR has both internal and external connotations in relation to research centers conducting nanoscience activities.

5.1. Internal connotations

The internal connotations of SR in nanoscience involve its active stakeholders, namely: scientists, R&D agencies, and national and transnational governments. These connotations should materialize in the establishment of CSP in internal management (see Fig. 5) via a wide variety of action lines some of which are discussed below.

Research centers concerned with the development of nanoscience should be *permeable and sensitive to citizens' needs* in order to meet the “Grand Challenges of our Time” (Lund Declaration 2009). This entails switching from prioritizing the publication of papers in journals with a high impact factor to aiming at solving present and anticipated problems in providing nanotechnological industries with promising products or systems. Stakeholders should unanimously identify “grand challenges” and adopt appropriate research lines by fluent communication via the two-way connections of Fig. 3—these internal connotations are represented by the arrows pointing from right

to left in the figure. One key element of SR in nanoscience is an *appropriate selection of R&D projects and programs* to ensure the optimal use of available resources. This entails avoiding repetitive, “*sure-fire*” research with little added value, a mistake that is especially common among stakeholders concerned with emerging technologies, many of whom tend to believe that some vogue words and prefixes (e.g., “nano”) are the key to publish in many journals. History tells us that this is often the case when a new leading-edge technology is in its infancy.

Integral (ex ante, in itinere, and ex post) scientific and technical assessment is an essential element of CSP inasmuch as it is consistent with the accountability principle in ISO 26000:2010. In addition, experts in SR of Science (Larsen et al. 2011) advocate a *final systematic professional assessment* of the results of basic nanotechnological research with a view to facilitating the transfer of knowledge and technology in this area.

One strategic line for SR in nanoscience is the *systematic assessment of the potentially toxic effects of nanomaterials* by subjecting all new products to appropriate in vivo and in vitro tests as an essential element of their characterization—which currently relies virtually exclusively on their physical and chemical properties. The high complexity of nanoparticles and their properties require careful studies in order to anticipate potentially deleterious effects upon contact with the environment. Reliable information from regulatory agencies and scientific bodies can help people form their own, grounded opinion and reject the emerging alarmist literature on nanomaterials. Risk assessment in this field is confronted with two problems. One is the lack of adequate funding for health, safety, and environmental impact studies on nanotechnologies and the other is that of specific legislation on nanomaterials. Both deficiencies result in humans and the environment being exposed to nanomaterials with uncertain associated risks (Klaine et al. 2012). In vitro

I.4. Social responsibility of Nanoscience and Nanotechnology

assays are more expeditious, economical, and easily controlled than in vivo tests; also, the former are subject to lighter ethical constraints since they typically use no laboratory animals (Marquis et al. 2009). However, in vitro laboratory tests using cell cultures cannot exactly mimic environmental conditions; also, in vivo tests frequently involve nanoparticle concentrations and exposure times greatly exceeding those typically found in the environment. As a result, the latter are unable to detect nanoparticles at low concentrations and are only useful for assessing large-dose effects. One other major deficiency is that tests rarely monitor the pathways followed by nanoparticles after reaching the environment. This precludes distinguishing between their direct and indirect effects, and hence finding effective solutions to some environmental problems (Klaine et al. 2012).

At this point, one must concede that SR has not walked hand in hand with nanoscience since its birth, which is unjustifiable based on past experience with other emerging technologies (David and Thompson 2008; Fisher 2005; Cassa et al. 2012; Liska 2004; Manasco 2005; Mizuo 2008). However, market demands and the need for substantial investments to fulfill them have once again in the history of Science and Technology delayed the adoption of *proactive* SR, which should have started as early as the earliest research in nanoscience.

Corporate social responsibility in nanotechnological research centers should also include *appropriate management of labor and environmental resources and risks* as an essential ingredient of the protection of two prominent stakeholders: researchers and supporting staff.

One transversal aspect of the previous internal connotations of SR in nanoscience is *fostering education in the subject* from the earliest school levels. This is fully consistent with the internal connotations of nanotechnology discussed below. There are some especially useful dissemination textbooks on

Science in general (FECYT 2008) and nanotechnology in particular (FECYT 2009) to fulfill this objective, which is a key target according to experts (Larsen et al. 2011). Training activities are also viewed as especially effective tools for selecting scientists to be trained with a view to swelling the ranks of nanoscience research centers in the future. STEM programs, which are intended to attract an increasing number of students to the research field and change their views on nanotechnology, can be useful for this purpose. These programs (e.g., *the Nanotechnology Programs at the University of Illinois or the West Virginia University's WV Nano*, <http://www.stemedcoalition.org/>) typically include seminars, summer research opportunities for students and bridge programs for incoming graduate students.

5.2. External connotations

The external connotations of SR in nanoscience are largely of the passive type. Also, they supplement its internal connotations and pertain to the typical stakeholders of nanotechnological industries and, ultimately, to those concerned with society and the environment. These connotations are represented by the arrows joining the stakeholders in Fig. 3 from right to left.

First, external and mixed stakeholders should accurately identify social and environmental needs, and prioritize their fulfillment if needed. This requires establishing effective pathways for communication between all stakeholders and filtering it appropriately to ensure quality, consistence, and representativeness in the specific problems (challenges) addressed while discarding groundless, opportunistic, and demagogical attitudes. Direct communication and interaction between researchers and other experts in the social and ethical fields can dramatically help stakeholders approach and understand one another.

I.4. Social responsibility of Nanoscience and Nanotechnology

Second, promoting receptivity to scientific dissemination in nanoscience can help bridge the traditional gap between science and society. Ensuring truthful, easy, ethical, contextualized, efficient dissemination is a current bottleneck for SR in nanoscience. In addition to the indispensable accountability of public investments, citizens should be made fully aware not only of the potential of nanomaterials for improving their quality of life, but also of their potential hazards to humans and the environment. False expectations, groundless extrapolations, and unjustified alarms should be avoided at all costs.

Accordingly, one of the crucial missions of SR in nanoscience is to gain and increase citizens' trust in nanoscience, which can be accomplished by demonstrating that the applicable resource investments are efficiently used and the ensuing research outcomes are properly disseminated.

6. SOCIAL RESPONSIBILITY IN NANOTECHNOLOGY

In order to develop an effective CSR strategy, a nanotechnological enterprise must accurately define its own SR and the meaning of acting in a socially responsible manner.

Nanotechnological enterprises can adopt CSR for a variety of reasons including improving their social image, cutting expenses, or simply making the right choice of action. These reasons are of the internal or external type. *Internal reasons* are related to internal processes and stakeholders (staff and executives) and lead to the adoption of CSP, whereas *external reasons* are associated to external stakeholders and lead to the adoption of CSR in a more general context. The latter include the needs to comply with increasingly stringent legislation, compete with other enterprises, and fulfill clients' needs.

BLOQUE I. INTRODUCCIÓN

Improving their CSR can help enterprises to “soften” environmental and health protection legislation, and also to increase the trust of their clients and investors—who are increasingly concerned with the potential risks of nanotechnology—thereby boosting consumption of nanoproducts and raising corporate benefits.

A large fraction of CSR expenditure goes to documentation, administration, coverage, communication, training, and auditing. These expenses facilitate the use of improved techniques to assess the effects of new products on health; improvements in the systems required to integrate results and disseminate them in a transparent manner—with provision for intellectual property rights—; and the development of stakeholder training programs (Kuzma and Kuzhabekova 2011).

People at nanotechnological production enterprises (executives, employees, and shareholders) are mixed stakeholders as per the scheme of Fig. 3. Thus, they are external holders in relation to nanoscience (provided research in this area is not conducted in house) inasmuch as they receive research products, but internal stakeholders regarding society and the environment because they are the recipients of nanotechnological products.

The literature on SR in nanotechnology (Groves et al. 2011; Hunt and Mehta 2006; McCarty and Kelty 2010; David and Thompson 2008; Fisher 2005) is highly abundant relative to SR in nanoscience. In many cases, the distinction between both is artificial but necessary to avoid confusion. One should bear in mind that research centers and nanotechnological industries differ in their mission, vision, and strategic goals—and hence in their approach to SR.

The stakeholders of nanotechnological industries and enterprises are of mixed type and play a twofold (active and passive) role that should be in perfect

I.4. Social responsibility of Nanoscience and Nanotechnology

harmony rather than the isolated responsibility of tightly closed compartments; this requires efficient management of CSP in the industry or enterprise concerned.

Social responsibility in nanotechnology can also be assigned various internal and external connotations arising from the specificities of enterprises delivering nanotechnological products or services.

6.1. Internal connotations

Social responsibility in nanotechnological enterprises involves the active aspect of the activities of their whole staff and should materialize in the establishment of a CSP system for internal management with provision for the mixed stakeholder nature of such staff (see Fig. 3).

Social responsibility in nanotechnology should focus on establishing effective production lines to fulfill the “Grand Challenges of our Time” formulated in the Lund declaration (2009) by appropriate selection among the many available choices—some of which may be highly tempting on account of their easy implementation and economic benefits but should be given a lower priority if they are scarcely effective toward achieving the previous goal. This requires systematically assessing the results of internal and external research centers from a professional and technical rather than scientific perspective through permanent and fluent communication with other stakeholders. Some authors (Ebbesen 2008; Roco 2003) eagerly recommend the involvement of experts in the humanities and social sciences in the strategic decisions of nanotechnological enterprises in order to give some voice to external stakeholders. In fact, fruitful relations and communication of researchers in N&N with experts in ethics can have a significantly favorable social impact. Training researchers to discuss their work with other “experts” or even society

BLOQUE I. INTRODUCCIÓN

at large can help them realize the ethical and social implications of their actions (Mcgregor and Wetmore 2009).

Nanotechnological production should also be subjected to integral assessment with the aid of external agents. *Ex ante* assessment should focus on research outcomes on the one hand, and social and environmental demands on the other. *In itinere* assessment can be useful to certify that the health and safety conditions for the personnel involved in nanotechnological production processes are appropriate and whether optimal resources are being used to this end. Occupational safety and health can be assessed via an in-house survey of potential hazards and staff exposure which can be useful toward improving the working conditions. Finally, *ex post* assessment should focus on the degree of market acceptance of the nanotechnological products delivered and their potentially adverse effects. This requires transparent and fluent communication with the public to disseminate commercially available nanoproducts and the outcomes of their safety testing. Safety tests should be conducted by independent experts and made available for external assessment in order to increase credit of the originating enterprise (Kuzma and Kuzhabekova 2011).

As stated by Lee and Jose (2008), implementing CSR in nanotechnological industries involves facing unusual stress as a consequence of the conflict between self-interest in exploiting new technologies or developing innovative commercial products and self-restraint imposed by ethical rules such as maximizing the recipients' health and safety. This requires setting up an efficient CSP-based management system.

Also prominent among the strategic needs for CSP in nanotechnological industries is staff (engineer) qualification, not only of the scientific and technological types, but also in SR principles and practice (Zandvoort 2008).

6.2. External connotations

These are the SR aspects of an essentially passive nature in nanotechnological enterprises. In fact, they are not only active with respect to external stakeholders (society and the environment), which should not be mere recipients of nanotechnological innovations, but also convey their own needs and ambitions to enterprises and, ultimately, nanotechnological research centers. These actions are represented by the arrows pointing from right to left in Fig. 3.

External stakeholders should accurately communicate social and environmental needs—under a priority scheme, if needed. The Lund declaration (2009) can be used as a guideline here. It is essential to establish efficient communication pathways between all external and mixed stakeholders, and to filter it appropriately in order to both ensure quality, consistence, and representativeness in the problems (challenges) addressed and rule out groundless, opportunistic, or demagogical attitudes. These principles are shared by SR in Nanoscience.

Like SR in Nanoscience, SR in Nanotechnology requires an objective, truthful and reliable dissemination of the advantages and disadvantages of commercially available nanotechnological products. Dissemination here should include a clear explanation of the results of nanotoxicity studies. One of the most effective methods for this purpose is to encourage the participation of users or clients of nanotechnological innovations in the in-house management of CSP, which can no doubt have a favorable impact on CSR.

7. SOCIAL IMPLICATIONS OF NANOSCIENCE AND NANOTECHNOLOGY

Nanoethics, which is the term used to designate ethics in the development of nanosized objects, comprises three different fields of study the former two of which are closely related: *ecotoxicity*, *nanotoxicity*, and *violation of privacy*.

Ecotoxicity is concerned with the potential environmental damage of nanomaterials, whereas *Nanotoxicity* focuses on the effects of nanoparticles on health; however, both concepts are related to the risks of coming into contact with nanotechnological products. According to its advocates, Nanotechnology is useful toward facilitating efficient consumption of energy, having a cleaner environment and eradicating some health problems. However, its opponents criticize the lack of available knowledge about the actual impact of nanomaterials on the environment, the added stress they introduce, and their interactions with other natural components. Deeper investigations are, therefore, needed to balance the risks and benefits of using nanomaterials, and so is permanent, transparent communication in order to incorporate society's views into the decision-making process for the development of each new nanoproduct. Voluntarily adopting environmental risk assessment norms, taking part in national and transnational information exchange programs, and obtaining research-independent funding can help raise stakeholders' trust in the Nanoscience–Nanotechnology couple (Kuzma and Kuzhabekova 2011; Klaine et al. 2012). Assessing the risks of nanomaterials is especially important in the emerging field of *Nanomedicine*, where they are used to prevent, diagnose, and treat specific diseases by virtue, for example, of them possessing a high potential for improving the efficiency of existing technologies for tumor diagnosis and treatment (Mahmood et al. 2012; Nunes et al. 2012). In most cases, data protection interests prevail over information transparency (Kuzma and Kuzhabekova 2011), which is one of the principles of SR in ISO 26000:2010 (ISO 26000:2010) (see “The concept of social responsibility” section). Changes

I.4. Social responsibility of Nanoscience and Nanotechnology

in this respect are thus required to allow stakeholders (particularly nanodrug users) to acquire a clear, accurate knowledge about the risks and benefits of the new materials with a view to making grounded, informed decisions. These changes should start with the development of effective strategies to fund research into the potential hazards of the new materials on human health and facilitate open communication of the outcomes (Kuzma and Kuzhabekova 2011).

The *violation of privacy* field is associated with the production of nanosensors. The development of new communication technologies such as sensors or microphones in the twentieth century resulted in an increasing invasion of privacy and violation of personality rights. Although no causal relationship between the development of modern communication technologies and the threat on privacy and personal rights exists, these technologies provide ample opportunity for invading privacy (Ganascia 2011). To some, the privacy violation risks of nanotechnology are exactly the same as those previously posed by classical communication technologies; to others, the risk is even greater since nanotechnology has the power to produce invisible nanosensors.

The effects of nanotechnology on society can be viewed from a broader perspective. The contribution of new materials with improved properties to the advancement of other fields may increase their operational efficiency. Thus, creating more efficient energy sources may raise social demands and increase industrial and agricultural production, ultimately leading to the establishment of new, more competitive industries.

One key need here is for citizens to prioritize their needs and convey them in order to allow N&N to improve their lives with advances in foodstuff, renewable energy sources, new materials, healthcare products, or even environmental remediation (Roco and Baingridge 2005).

8. CONCLUSIONS

This paper deals for the first time with the concept of SR as applied to nanoscience in research centers and proposes an integral approach to SR in nanoscience and nanotechnology based on their mutual connections. The primary aim was to demonstrate that the principles and practices of SR fit perfectly well in nanoscience and nanotechnology, where CSP provides the most immediate, ideal platform for implementing CSR. The paper additionally helps identify the stakeholders of nanoscience centers and nanotechnology industries, which are depicted in Fig. 3.

The high impact and/or importance of emerging technologies such as biotechnology, information and communication technologies, and nanotechnology make the SR approach an undeniably useful tool for solving the “Grand Challenges of our Time” as stated in the Lund Declaration (2009). As noted earlier, the primary purpose of this paper was to establish a general framework for SR in an emerging scientific area (nanoscience) and an emerging technological area (nanotechnology). Both can be placed at the proactive level on the Clarkson commitment scale of Fig. 6 (Clarkson 1995).

Figure 7 summarizes the main internal and external connotations of SR in N&N. Note the coincidences in some subjects—with differences such as the mixed nature of nanotechnological industries as stakeholders—and the fact that the external nature of society and the environment as stakeholders is shared by the science and technology behind nanomaterials.

I.4. Social responsibility of Nanoscience and Nanotechnology

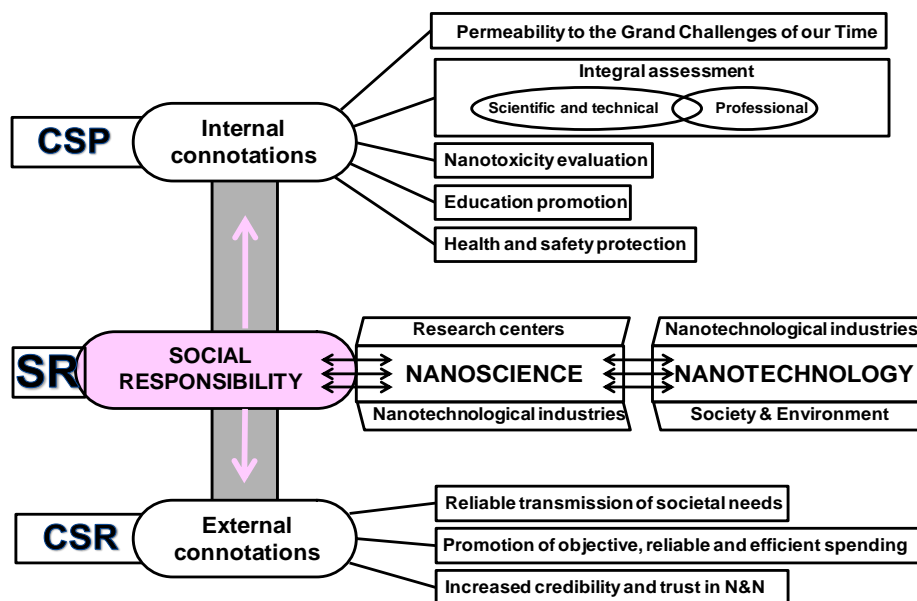


Figure 7. Internal and external connotations of social responsibility in N&N.

Finally, efficient implementation of SR in N&N will require dealing with previously established SR subjects contained in internationally circulated documents, albeit with provision for the specifications of the new science and technology. It is especially important in this respect to develop a series of interrelated indicators to assess the implementation and progress of SR with a view to demonstrate that nanotechnological research and production activities are conducted responsibly and sustainably.

Acknowledgments

This work was funded by Spain’s Ministry of Economy and Competitiveness within the framework of Project CTQ2011-23790. E. Caballero-Díaz wishes to thank the Ministry for the award of a Research Training Fellowship (Grant AP2008-02955).

BLOQUE I. INTRODUCCIÓN

References

Ciencias para el Mundo Contemporáneo. Aproximaciones didácticas (2008) Spanish Foundation for Science and Technology (FECYT), Madrid

Cassa CA, Savage SK, Taylor PL et al (2012) Disclosing pathogenic genetic variants to research participants: quantifying an emerging ethical responsibility. *Genome Res* 22:421–428

Clarkson ME (1995) A stakeholder framework for analyzing and evaluating corporate social performance. *AMR* 20:92–117

David K, Thompson PB (2008) What can nanotechnology learn from biotechnology? Academic Press, New York

de la Cuesta M (2005) Supportive and Alternative Economy Conferences. <http://www.hegoa.ehu.es/congreso/bilbo/doku/bat/responsabilidadsocialcorporativa.pdf>

den Hond F, de Bakker F, Neerdaard P (2007) Managing corporate social responsibility in action: talking, doing and measuring. Ashgate Publishing Ltd, Aldershot

Ebbesen M (2008) The role of the humanities and social sciences in Nanotechnology Research and Development. *Nanoethics* 2:1–13

Ética. Sistema de Gestión de la Responsabilidad de las Empresas (2008) Spanish Association for Standardisation and Certification (AENOR), Madrid

Fisher E (2005) Lessons learned from the Ethical, Legal and Social Implications program (ELSI): planning societal implications research for the National Nanotechnology Program. *Technol Soc* 27:321–328

Ganascia JG (2011) The new ethical trilemma: security, privacy and transparency. *C R Physique* 12:684–692

Groves C, Frater L, Lee R, Stokes E (2011) Is there room at the bottom for CSR? Corporate social responsibility and nanotechnology in the UK. *J Bus Ethics* 101:525–552

Hunt G, Mehta M (2006) Nanotechnology risks, ethics and laws. Routledge, Oxford. ILO principles of social responsibility (2006) <http://www.ilo.org>

ISO 26000:2010 Guidance on social responsibility (2010) International Organization for Standardization (ISO), Geneva

Klaine SJ, Koelmans AA, Horne N, Carley S, Handy RD, Kapustka L, Nowack B, von der Kammer R (2012) Paradigms to assess the environmental impact of manufactured nanomaterials. *Environ Toxicol Chem* 31:3–14

I.4. Social responsibility of Nanoscience and Nanotechnology

Kuzma J, Kuzhabekova A (2011) Corporate social responsibility for nanotechnology oversight. *Med Health Care Philos* 14:407–419

Larsen PK, Thostrup P, Besenbacher F (2011) Scientific social responsibility: a call to arms. *Angew Chem Int Ed* 50:10738–10740

Liska AJ (2004) The morality of problem selection in proteomics. *Proteomics* 4:1929–1931

Lund Declaration (2009) Europe must focus on the grand challenges of our time. http://www.se2009.eu/polopoly_fs/1.8460!menu/standard/file/lund_declaration_final_version_9_july.pdf

Mahmood M, Casciano D, Xu Y, Biris AS (2012) Engineered nanostructural materials for application in cancer biology and medicine. *J Appl Toxicol* 32:10–19

Manasco PK (2005) Ethical and legal aspects of applied genomic technologies: practical solutions. *Curr Med Chem* 5:23–28

Marquis BJ, Love SA, Braun KL, Haynes CL (2009) Analytical methods to assess nanoparticle toxicity. *Analyst* 134:425–439

McCarty E, Kelty C (2010) Responsibility and nanotechnology. *Soc Stud Sci* 40:405–432

Mcgregor J, Wetmore JM (2009) Researching and teaching the ethics and social implications of emerging technologies in the laboratory. *Nanoethics* 3:17–30

McWilliams A, Siegel D (2000) Corporate social responsibility and financial performance: correlation or misspecification? *Strateg Manag* 21:603–609

Mizuo J (2008) The social responsibility of nuclear energy. *Prog Nucl Energy* 50:694–699

Nunes A, Al-Jamal K, Nakajima T, Hariz M, Kostarelos K (2012) Application of carbon nanotubes in neurology: clinical perspectives and toxicological risks. *Arch Toxicol* 86(7):1009–1020

OECD Guidelines for social responsibility (2001) <http://www.oecd.org>

Olcese A (2007) *La Responsabilidad Social de la Empresa (RSE)*. Real Academia de Ciencias Económicas y Financieras, Madrid

Project 2006-043-3-050 The social responsibility of chemists: responsible stewardship (2006). IUPAC (International Union of Pure and Applied Chemistry), Livermore

RS10 Social Responsibility Management System. Requirements (2010) Spanish Association for Standardisation and Certification (AENOR), Madrid

BLOQUE I. INTRODUCCIÓN

Roco MC (2003) Broader societal issues of nanotechnology. *J Nanopart Res* 5:181–189

Roco MC, Baingridge WS (2005) Societal implications of nanoscience and nanotechnology: maximizing human benefit. *J Nanopart Res* 7:1–13

Unidad didáctica Nanociencia y Nanotecnología. Entre la ciencia ficción del presente y la tecnología del futuro (2009) Spanish Foundation for Science and Technology (FECYT), Madrid

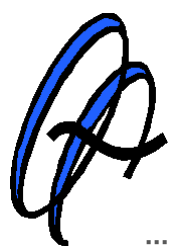
United Nations Global Compact (1999) <http://www.unglobalcompact.org>. See also World Compact Spanish Network <http://www.pactomundial.org>

Valcárcel M, Lucena R (2012a) La Responsabilidad Social de la Ciencia y Tecnología. *An Quim* 2:156–159

Valcárcel M, Lucena R (2012b) Social responsibility in analytical chemistry. *Trends Anal Chem* 31:1–7

Zadek S (2004) The path to corporate responsibility. *Harv Bus Rev* 82:125–132

Zandvoort H (2008) Preparing engineers for social responsibility. *Eur J Eng Educ* 2:133–140



BLOQUE II

Herramientas analíticas

II.1. Herramientas para los estudios de aplicaciones analíticas	149
- Analitos, reactivos y muestras	
- Nanopartículas	
- Síntesis de nanopartículas	
- Métodos de tratamiento de muestra	
- Instrumentación, aparatos y otros materiales	
II.2. Herramientas para los estudios de toxicidad	164
- Analitos y reactivos	
- Síntesis de nanopartículas de plata	
- Material biológico	
- Ensayos de viabilidad celular	
- Instrumentación	
II.3. Gestión de residuos generados	177

II.1. Herramientas para los estudios de aplicaciones analíticas

El desarrollo experimental de la investigación presentada en esta Memoria ha sido posible gracias al empleo de diferentes herramientas analíticas. A lo largo de este Bloque II se detallarán las herramientas empleadas tanto para los estudios de aplicabilidad analítica de las NPs (sección II.1) como para los estudios de toxicidad (sección II.2). En este sentido se hará referencia a los analitos, reactivos y muestras analizadas, así como a las NPs implicadas en los estudios. Asimismo se hará alusión a los métodos de tratamiento de muestra desarrollados o en su caso, ensayos de citotoxicidad realizados. Por último se comentarán los instrumentos, aparatos y otros materiales empleados.

II.1. Herramientas para los estudios de aplicaciones analíticas

ANALITOS, REACTIVOS Y MUESTRAS

Todos los analitos y reactivos empleados en este apartado fueron de pureza analítica o superior, y fueron adquiridos en su mayoría de la casa comercial Sigma-Aldrich.

Analitos

- *Hidrocarburos aromáticos policíclicos (PAHs): fluorantreno.*

Los PAHs son compuestos químicos que se generan de forma natural por la combustión incompleta de la materia orgánica, aunque también pueden tener un origen antropogénico. Su toxicidad junto con su ubicuidad y persistencia en el medio ambiente, los convierten en compuestos muy investigados en el medio ambiente.

BLOQUE II. HERRAMIENTAS ANALÍTICAS

- *Herbicidas: atrazina (2-cloro-4-etilamino-6-isopropilo-1,3,5-triazina).*

Atrazina es un herbicida perteneciente a la familia de las triazinas cuyo uso agrícola está muy extendido con el fin de controlar el crecimiento de las malas hierbas. Este herbicida se comporta como un disruptor endocrino, y como consecuencia de su aplicación directa al suelo y su posterior arrastre o lixiviación, puede contaminar tanto suelos como aguas superficiales y subterráneas.

- *Contaminantes emergentes: almizcle de cetona (3,5-dinitro-2,6-dimetil-4-terbutil-acetofenona) y ácido salicílico (ácido 2-hidroxibenzoico).*

El almizcle de cetona pertenece a la familia de los nitroalmizcles (*nitromusks*), que son compuestos sintéticos que se usan como sustitutos de las fragancias naturales en numerosos productos de consumo. El ácido salicílico es un metabolito del ácido acetilsalicílico perteneciente a la familia de los antiinflamatorios no esteroideos. Ambos compuestos son considerados contaminantes emergentes puesto que no se encuentran actualmente regulados por ninguna normativa y sus efectos sobre el medio ambiente y los seres vivos aún no están totalmente esclarecidos.

Disoluciones patrón de los analitos fueron preparadas en disolventes orgánicos y se almacenaron hasta su uso a 4 °C y en oscuridad. El periodo de almacenaje fue acorde a la estabilidad de los analitos en el disolvente seleccionado, descartando de esta forma cualquier tipo de degradación que pudiesen haber sufrido estos compuestos.

La Figura II.1.1 muestra las estructuras químicas de los analitos estudiados.

II.1. Herramientas para los estudios de aplicaciones analíticas

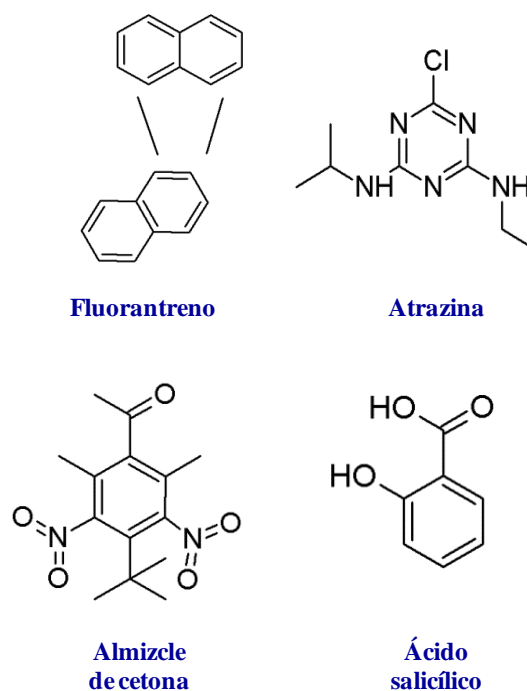


Figura II.1.1. Estructura química de los analitos seleccionados.

Reactivos

▪ *Ácidos y bases.* Se utilizaron ácido clorhídrico e hidróxido de sodio para el ajuste del pH de las muestras y los tampones electroforéticos en aquellos casos que lo precisaron. Asimismo, estos reactivos también se emplearon para preparar las disoluciones de acondicionamiento inicial de los capilares de CE. Los ácidos clorhídrico, nítrico y sulfúrico fueron utilizados para la oxidación de las NPs.

▪ *Disolventes orgánicos.* Metanol, acetonitrilo, acetona, etanol, y etilacetato se emplearon con diversos fines: *i)* para la preparación de disoluciones patrón de los analitos; *ii)* como eluyentes en los procesos de extracción; *iii)* para el acondicionamiento y limpieza de los sistemas de microextracción en fase sólida; *iv)* para la preparación de la interfase de CNPs

BLOQUE II. HERRAMIENTAS ANALÍTICAS

en la extracción líquido-líquido; v) para la purificación de los nanodiamantes; vi) como modificadores orgánicos de los tampones electroforéticos; y vii) como medio de inyección en CE.

- *Reactivos para la síntesis de nanopartículas híbridas (nanodiamantes—nanotubos de carbono).* 3-aminopropiltrimetoxisilano, tampón ácido acético/acetato, hidrocloreuro de *N*-(3-dimetilaminopropil)-*N'*-etilcarbodiimida y *N*-hidroxisuccinimida.

- *Reactivos para la síntesis de nanopartículas de plata.* Hidróxido de sodio, hidrocloreuro de hidroxilamina y nitrato de plata.

- *Sales.* Cloruro de sodio se empleó para alterar las condiciones experimentales iniciales en la técnica de extracción punto de nube.

- *Surfactantes.* Dodecil sulfato de sodio fue utilizado como tensioactivo en la extracción punto de nube, y como fase pseudoestacionaria en el tampón electroforético.

- *Disoluciones tamponadas electroforéticas.* Tetraborato de sodio decahidratado e hidrógeno fosfato disódico.

Muestras

Los procedimientos analíticos desarrollados en el transcurso de la Tesis Doctoral se aplicaron, en último término, a la determinación de los analitos que aparecen en la anterior Figura I.1.1, en las siguientes matrices ambientales:

- *Agua de río.* Los trabajos científicos recogidos en el Bloque III de esta Memoria, presentan métodos analíticos que fueron aplicados a la determinación

II.1. Herramientas para los estudios de aplicaciones analíticas

de contaminantes en aguas del río Guadalquivir o alguno de sus afluentes (Córdoba, España). Las muestras fueron recogidas y almacenadas, en frascos de vidrio color ámbar sin espacio de cabeza a 4 °C y en oscuridad, hasta su análisis. En algunos casos, las muestras fueron filtradas con filtros de nylon (0.45 µm de tamaño de poro) antes del tratamiento de muestra. Puesto que en ningún caso se hallaron los analitos de interés en las muestras recogidas, éstas fueron necesariamente fortificadas antes del análisis.

- *Suelo*. El procedimiento planteado en el trabajo de investigación que aparece en el apartado III.2 fue también aplicado a muestras de suelo agrícola proporcionadas por la Universidad Autónoma de Barcelona.

NANOPARTÍCULAS

Nanopartículas de carbono

- *Nanodiamantes (NDs)*. Estas NPs fueron adquiridas de la casa comercial NaBond Technologies (China) y se sintetizaron mediante procesos de detonación. Se emplearon dos tipos diferentes de NDs. Por un lado, aquellos con un diámetro de 3.2 nm y una pureza superior al 98%. Y por otro lado, NDs con carácter oleofílico, un tamaño medio de partícula entre 4 y 15 nm, y una pureza entre 55-75%.

- *Nanotubos de carbono de pared múltiple (MWCNTs)*. Tres tipos diferentes de MWCNTs fueron empleados en la fase experimental. Aquellos proporcionados por la casa comercial MER Corporation (Tucson, Arizona, EEUU) con un diámetro medio de 140 nm. Otros obtenidos de la casa comercial Nanocyl (Bélgica) con un diámetro de 9.5 nm y una longitud de 1.5 µm. Y por último, MWCNTs de la casa comercial Bayer (Alemania) con diámetros comprendidos entre 5-20 nm y longitudes entre 1-10 µm.

BLOQUE II. HERRAMIENTAS ANALÍTICAS

▪ *Nanotubos de carbono de pared simple (SWCNTs)*. Estas NPs fueron suministradas por la casa comercial Shenchen Nanotech Port Co., (Nanoport-NTP, China) y presentan diámetros inferiores a 2 nm y longitudes entre 5-15 μm .

SÍNTESIS DE NANOPARTÍCULAS

Nanopartículas de plata

Las NPs de plata (AgNPs) que se utilizaron para incrementar la sensibilidad de la técnica de detección por Espectroscopía Raman amplificada por superficie (SERS), fueron sintetizadas siguiendo el procedimiento experimental que se esquematiza en la Figura II.1.2.

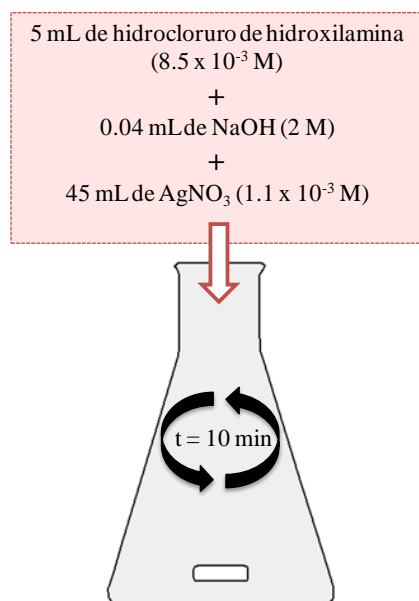


Figura II.1.2. Procedimiento de síntesis de coloides de plata [1].

[1] N. Leopold, B. Lendl, *J. Phys. Chem. B.* 107 (2003) 5723-5727.

II.1. Herramientas para los estudios de aplicaciones analíticas

Nanopartículas híbridas

Se sintetizaron NPs híbridas (NDs-MWCNTs) a partir de NDs comerciales obtenidos por procesos de detonación y MWCNTs adquiridos de la casa comercial MER Corporation. La Figura II.1.3 resume el procedimiento de síntesis llevado a cabo.

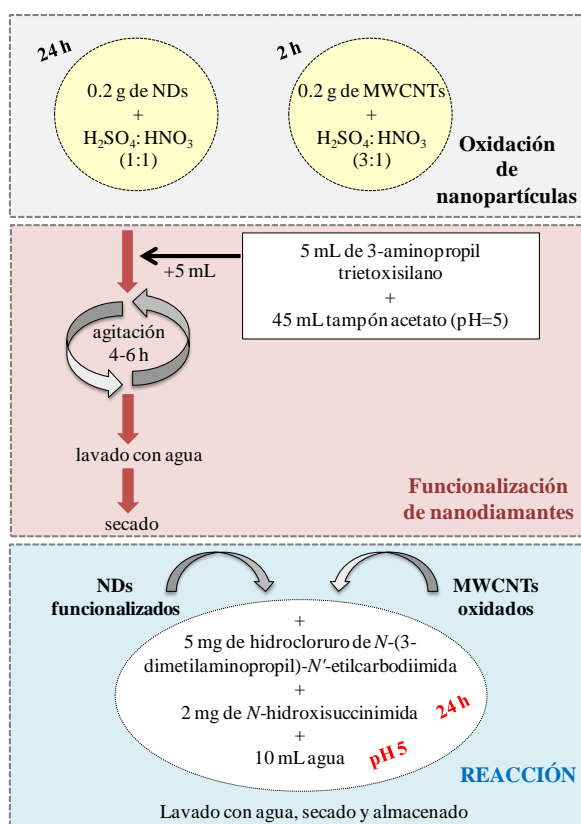


Figura II.1.3. Procedimiento de síntesis de NDs-MWCNTs.

MÉTODOS DE TRATAMIENTO DE MUESTRA

A continuación se exponen aquellos métodos de tratamiento de muestra que se desarrollaron en la Tesis Doctoral. Algunos de ellos corresponden a

técnicas de extracción convencionales que han sido modificadas con la inclusión de NPs en su esquema experimental. En otros casos, se han desarrollado unidades de extracción empleando nanotubos de carbono (CNTs) como adsorbentes de extracción en fase sólida (SPE) y por último, se han utilizado sistemas de extracción disponibles comercialmente, como es el caso de los MEPS (microextracción con adsorbentes empaquetados).

Extracción punto de nube con nanodiamantes (III.1)

La técnica de extracción punto de nube (CPE) se basa en la separación de una fase acuosa micelar homogénea en dos fases isotrópicas. Una fase de menor volumen y enriquecida en surfactante donde se encuentra el analito, y una fase acuosa de mayor volumen que contiene la matriz de la muestra y surfactante a una concentración inferior a su concentración micelar crítica (CMC). La separación en dos fases permite la extracción y preconcentración de los analitos por su interacción con el surfactante. Para que se produzca la separación deben cumplirse dos requisitos; *i)* que la concentración de surfactante en la fase acuosa inicial supere su CMC; y *ii)* que las condiciones experimentales tales como presión, temperatura o fuerza iónica, sean alteradas respecto al punto inicial.

En el trabajo recogido en el apartado III.1 de esta Memoria, se incluyeron NDs en la técnica de CPE con el propósito de evaluar su cometido en la extracción del analito. Nuestra hipótesis inicial se fundamentaba en el hecho de que estas NPs constituirían una fase adicional de interacción con el analito (aparte del surfactante) y por tanto, tendrían algún efecto sobre la eficiencia de extracción. El esquema experimental del procedimiento de CPE modificado se muestra en la Figura II.1.4.

II.1. Herramientas para los estudios de aplicaciones analíticas

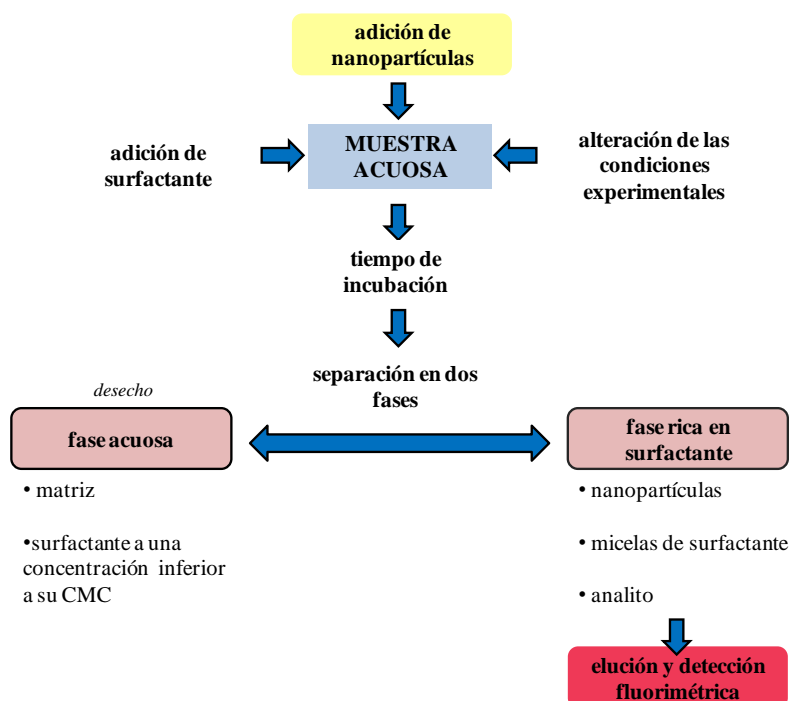


Figura II.1.4. Esquema general de la técnica de CPE modificada con NDs.

Extracción líquido-líquido asistida por nanotubos de carbono (III.2)

En este caso se llevó a cabo una extracción líquido-líquido (LLE) asistida por una interfase de CNPs estabilizadas en etilacetato que se localizó entre las fases acuosa y orgánica. El procedimiento fue optimizado para su aplicación principal en muestras de agua, aunque posteriormente se realizaron algunos ensayos en matrices de suelo.

Para muestras acuosas, la interfase fue preparada por mezclar en un mortero, 5 mg de MWCNTs con 1 mL de etilacetato hasta homogeneidad. Entonces, la interfase fue añadida a la matriz acuosa (20 mL) y posteriormente se adicionaron 3 mL de etilacetato. La mezcla se agitó y tras un tiempo de reposo se pudo apreciar claramente la formación de tres fases en el embudo de decantación donde tuvo lugar la extracción. Una fase acuosa inferior, una

interfase de CNPs y una fase orgánica superior. La Figura II.1.5 ilustra el procedimiento seguido para la formación de la interfase así como la formación de las tres fases dentro del embudo de decantación.

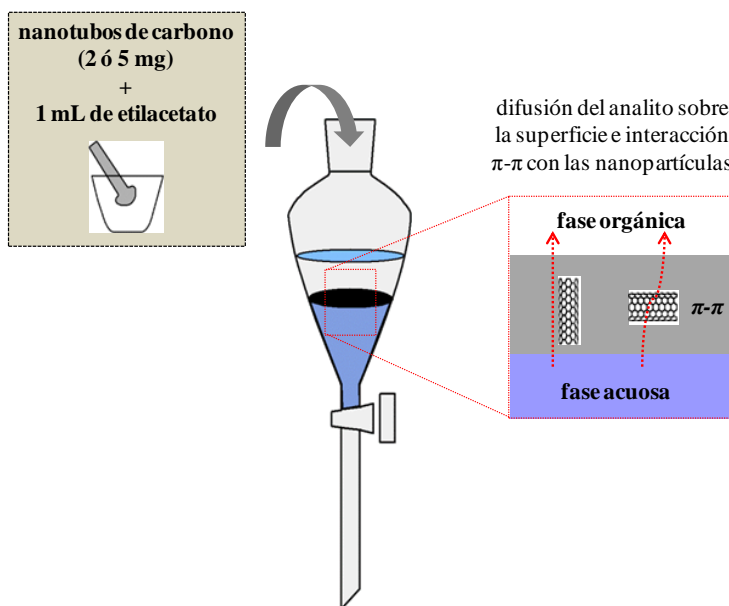


Figura II.1.5. Ilustración del procedimiento para formar la interfase de CNPs, así como de las tres fases implicadas en la extracción.

Extracción en fase sólida con nanotubos de carbono (III.3)

La extracción en fase sólida o SPE es la técnica de tratamiento de muestra más ampliamente utilizada en el análisis de muestras ambientales dado su mayor factor de preconcentración, y menor consumo de disolvente y tiempo de extracción en comparación con LLE.

La unidad de extracción desarrollada consistió en empaquetar 15 mg de MWCNTs en cartuchos de SPE de polipropileno de 6 mm de diámetro. Dos fritas de polipropileno fueron colocadas en la parte superior e inferior de los MWCNTs para evitar su pérdida durante la consecución del procedimiento de

II.1. Herramientas para los estudios de aplicaciones analíticas

extracción. Para la automatización de la etapa de carga de muestra acuosa, se hizo uso de una bomba peristáltica. La Figura II.1.6 muestra un esquema del empaquetamiento de los MWCNTs en los cartuchos así como de la automatización del paso de muestra.

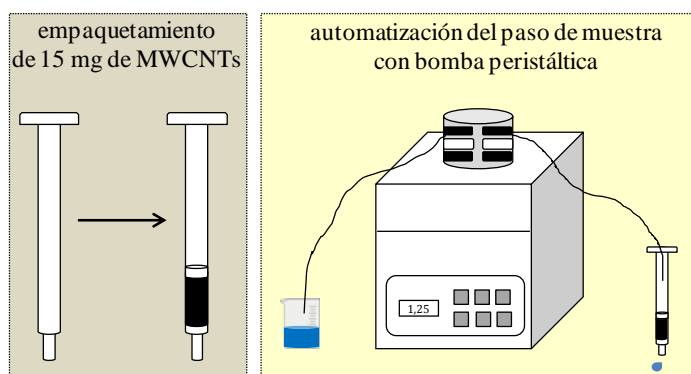


Figura II.1.6. Preparación de la unidad de SPE y automatización del paso de muestra.

Microextracción con adsorbentes empaquetados (MEPS) (III.4)

La microextracción con adsorbentes empaquetados (MEPS) es una modalidad de SPE en la que los volúmenes de muestra y de disolvente se reducen considerablemente. Los adsorbentes empleados son similares a aquellos usados en SPE, con la diferencia de que en este caso se integran en la aguja de una jeringa. La sencillez, junto con el bajo consumo de disolvente y la rapidez del proceso, hacen de ésta una técnica de extracción alternativa muy interesante para el tratamiento de muestra. La Figura II.1.7 representa las etapas generales que conforman el procedimiento de MEPS.

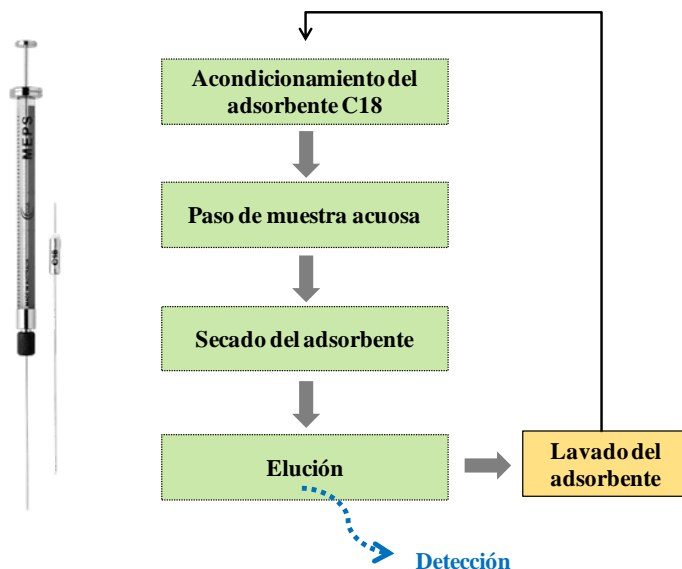


Figura II.1.7. Etapas del procedimiento de MEPS.

INSTRUMENTACIÓN, APARATOS Y OTROS MATERIALES

Una vez realizado el tratamiento de muestra, es necesario disponer de un sistema de detección adecuado. A continuación se describen aquellos instrumentos, aparatos y otros materiales que se emplearon en los trabajos enfocados en la aplicabilidad analítica de las NPs.

Instrumentación

▪ *Espectrofluorímetro.* Los espectros de fluorescencia fueron obtenidos usando un espectrofluorímetro PTI QuantaMaster™ (Photon Technology International) equipado con una lámpara de xenón de 75 W y un sistema de detección modelo 814 PTM. La obtención y el análisis de datos, así



II.1. Herramientas para los estudios de aplicaciones analíticas

como el control completo del instrumento se hicieron con el software Félix32. Todas las mediciones se realizaron en cubetas de cuarzo de 10 mm.

▪ *Electroforesis capilar.* Los análisis por CE fueron llevados a cabo con un instrumento P/ACE™ MDQ Beckman Coulter (Palo Alto, California, EEUU) equipado con un detector UV-Visible de diodos en fila (DAD). Los capilares de sílice fundida fueron de 75 μm de diámetro interno y tuvieron una longitud efectiva entre la muestra y el detector de 50 cm (longitud total del capilar de 60.2 cm). Todas las muestras fueron inyectadas en modo hidrodinámico y la separación se realizó por aplicación de voltaje en modo de polaridad positiva. Las condiciones de voltaje, presión, temperatura y longitud de onda de detección fueron diferentes según la aplicación. Tanto la adquisición y procesamiento de datos, como el control del instrumento fueron realizados con el software Karat32.



▪ *Espectrómetro Raman portátil.* Las medidas Raman se realizaron con un espectrómetro Raman portátil modelo innoRam-785S equipado con un láser de excitación de 785 nm y una sonda Raman con una potencia de láser máxima de 285 mW. Este instrumento consta de un detector CCD (12 μm x 12 μm tamaño de píxel, 2048 píxeles) enfriado por efecto Peltier. Los espectros Raman fueron medidos empleando un objetivo con una magnificación 50x y un rango de detección entre 368-3000 cm^{-1} . La adquisición y tratamiento de datos, así como el control del instrumento, se realizaron con el software BWSpec™.



BLOQUE II. HERRAMIENTAS ANALÍTICAS

▪ *Otros instrumentos*

- Balanza analítica de precisión OHAUS Explorer (Ohaus, Nänikon, Suiza).
- pH-metro modelo micropH 2000 (Crison, Barcelona, España).
- Microscopio electrónico de transmisión (TEM) de alta resolución JEOL JEM 1400 (SCAI, Córdoba). Este instrumento operaba con un voltaje de aceleración de 120 kV y una magnificación entre 50x-1000x.

Aparatos y otros materiales

- Agitador magnético (Velp Científica, Milán, Italia).
- Placa calefactora con agitación magnética Agimatic-N (J.P. Selecta, Barcelona, España).
- Baño de ultrasonidos Ultrasons de 50 W y 60 Hz de frecuencia (J.P. Selecta, Barcelona, España).
- Ultracentrífuga controlada por microprocesador Centronic BL-II (J.P. Selecta, Barcelona, España).
- Bomba peristáltica Minipuls 3 (Gilson, Inc. Middleton, EEUU).
- Cubetas macro de cuarzo con un paso óptico de 10 mm (Hellma, Barcelona, España).
- Cristales de fluoruro de calcio (CrystalTechno, Moscow, Russia).
- Rejillas Formvar Carbon Film (Electron Microscopy Sciences, EEUU).

II.1. Herramientas para los estudios de aplicaciones analíticas

- Jeringa MEPS de 250 μL con sorbente C18 para realizar microextracciones (SGE Analytical Science, Australia).
- Equipo de agua Milli-Q (Millipore, Bedford, MA, EEUU).
- Micropipetas.
- Material de vidrio de laboratorio clase A, para la preparación de estándares, medidas de volúmenes y otras tareas desempeñadas a lo largo de la fase experimental. El material siempre se lavó con jabón neutro, agua destilada, metanol y disolución o disolvente a emplear.
- Jeringas de plástico y filtros de nylon de 0.45 μm de tamaño de poro para la filtración de disoluciones acuosas y tampones electroforéticos. En algunos casos las muestras de agua de río fueron también filtradas antes de ser sometidas a la extracción correspondiente.
- Envases de vidrio para el correcto almacenamiento de los estándares, muestras y otras disoluciones.

II.2. Herramientas para los estudios de toxicidad

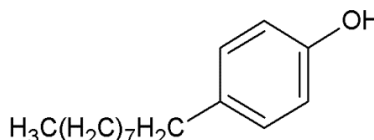
ANALITOS Y REACTIVOS

Todos los analitos y reactivos empleados en esta sección fueron de pureza analítica o en su caso, aptos para biología molecular. La mayoría de ellos fueron adquiridos de la casa comercial Sigma Aldrich.

Analitos

Los estudios realizados tuvieron como finalidad investigar la citotoxicidad de AgNPs con diferentes recubrimientos superficiales, o aquella asociada a nanotubos de carbono monocapa en presencia de un conocido contaminante ambiental (4-nonilfenol).

- *Nanopartículas de plata (AgNPs)*. Éstas fueron sintetizadas a partir del mismo núcleo de plata pero con diferentes recubrimientos superficiales: polímero anhídrido maleico de poliisobutileno modificado con dodecilamina (PMA), ácido 11-mercaptoundecanoico (MUA) y polietilenglicol de 10 kDa (PEG).
- *Nanotubos de carbono monocapa con polietilenglicol (SWCNTs-PEG)*. Estos CNTs presentan un diámetro entre 4-5 nm y una longitud entre 500-600 nm. Según la información proporcionada por el fabricante (Sigma Aldrich, St. Louis, MO, USA) su contenido en carbono supera el 80% y el contenido en trazas metálicas es inferior al 4%.
- *4-nonilfenol (NP)*. Este analito fue adquirido de la casa comercial Sigma Aldrich (Madrid, España).



Reactivos para la preparación de los medios de cultivo

Los medios de cultivo celulares fueron preparados a partir de los siguientes reactivos:

- *Medio de cultivo Eagle bajo en glucosa y modificado de Dulbecco (DMEM).*
- *Suero de ternero y suero fetal bovino (FBS).*
- *L-glutamina.*
- *Penicilina/estreptomicina (disolución antibiótica-antimicótica).*

Reactivos para los ensayos de citotoxicidad

En los ensayos de viabilidad celular se hizo uso de los siguientes reactivos obtenidos en su mayoría de la casa comercial Sigma-Aldrich:

- *Kit de ensayo de toxicología in vitro TOX8 basado en resazurina.*
- *Bromuro de 3-(4,5-dimetiltiazol-2-il)-2,5 difeniltetrazolio (MTT).*
- *Dimetilsulfóxido (DMSO).*
- *Disolución tampón fosfato salino (PBS).*

Reactivos para la síntesis de AgNPs

Para la síntesis de AgNPs se emplearon:

- *Reactivos de síntesis.* 1-bromodecano, tiosulfato de sodio pentahidratado, nitrato de plata, borohidruro de sodio, ácido ascórbico, y 1-etil-3-(3-dimetilaminopropil) carbodiimida (EDC).
- *Disoluciones tampón.* Tris-borato-EDTA, borato de sodio y fosfato salino.

BLOQUE II. HERRAMIENTAS ANALÍTICAS

- *Disolventes y estabilizantes.* Cloroformo, etanol, metanol y tetrahidrofurano.
- *Disolventes de lavado.* Agua desionizada, etanol y acetona.
- *Agentes de recubrimiento.* MUA, PMA y PEG.
- *Fluoróforos.* DY-636 modificado con grupos amino para los estudios de internalización celular de las AgNPs mediante microscopía confocal.

SÍNTESIS DE NANOPARTÍCULAS DE PLATA

Con el propósito de evaluar la influencia de la química superficial de las NPs sobre su citotoxicidad, se sintetizaron AgNPs a partir de un mismo núcleo de plata pero con diferentes agentes superficiales. AgNPs hidrofóbicas fueron sintetizadas en primer lugar, y a partir de éstas se obtuvieron AgNPs hidrofílicas mediante reacciones de intercambio de ligando o recubrimiento polimérico. A continuación se especifican todos los protocolos de síntesis seguidos.

Síntesis de AgNPs hidrofóbicas

Dos etapas conforman la síntesis de las AgNPs primarias hidrofóbicas a partir de las cuales se sintetizaron todas las demás de carácter hidrofílico. La primera etapa consistió en la síntesis del agente estabilizante de las AgNPs, es decir, dodeciltiosulfato sódico. La segunda y última etapa se basó en la síntesis propiamente dicha de las AgNPs en presencia del ligando sintetizado en el paso anterior.

II.2. Herramientas para los estudios de toxicidad

1) *Síntesis de dodeciltiosulfato sódico (estabilizante).* Aproximadamente 5 mL de 1-bromodecano se disolvieron en 50 mL de etanol a una temperatura de 50 °C. Por otro lado, 6 gramos de tiosulfato de sodio pentahidratado se disolvieron en agua y se añadieron a la disolución anterior. La mezcla se puso en reflujo durante 3 horas, y una vez enfriada a T^a ambiente se obtuvo un precipitado blanco que fue el ligando dodeciltiosulfato sódico.

2) *Síntesis de AgNPs hidrofóbicas en presencia del estabilizante.* Una vez sintetizado el dodeciltiosulfato sódico, una cantidad aproximada de 0.4 g de éste se disolvió en 90 mL de etanol a una temperatura de 50 °C. Entonces se añadieron 0.3 g de nitrato de plata (AgNO₃) y la disolución se agitó durante 10 minutos. Seguidamente, 0.3 g de borohidruro sódico se disolvieron en 15 mL de etanol y se añadieron a la mezcla. Tras 5 minutos de agitación, se añadieron 0.07 g de ácido ascórbico y la mezcla resultante se agitó durante tres horas. Pasado este tiempo se enfrió la mezcla y finalmente se obtuvo un precipitado (AgNPs) que fue lavado consecutivamente con agua, etanol y acetona en ciclos de centrifugación de 15 minutos a 3,000 rpm cada uno. Las AgNPs obtenidas se secaron por aplicación de vacío y por último, se redisolviéron en cloroformo.

Síntesis de AgNPs recubiertas con ácido 11-mercaptoundecanoico (AgNPs-MUA)

Las AgNPs-MUA fueron sintetizadas a partir de las AgNPs hidrofóbicas anteriores a través de una reacción de intercambio de ligando entre el dodeciltiol (estabilizante inicial) y el ácido 11-mercaptoundecanoico (recubrimiento final). El procedimiento de síntesis fue como sigue. Aproximadamente 10 mg de AgNPs hidrofóbicas se disolvieron en 20 mL de cloroformo. Por otro lado, 1.6 g de MUA se disolvieron en 130 mL de disolución

tampón tris-borato-EDTA por aplicación de ultrasonidos durante 45 minutos. A continuación, ambas disoluciones (AgNPs y MUA) se mezclaron y agitaron durante 5 minutos. En este tiempo, se produjo el intercambio de ligandos y las NPs, al adquirir carácter hidrofílico, pasaron a la fase acuosa. La mezcla se centrifugó entonces (2,000 rpm durante 20 minutos) para separar las AgNPs-MUA. La disolución de NPs obtenida se concentró usando filtros de centrifuga con un tamaño de poro de 100 kDa. Las AgNPs-MUA fueron purificadas en último término mediante electroforesis en gel y cromatografía líquida de alta resolución (HPLC).

Síntesis de AgNPs recubiertas con polímero anfílico (AgNPs-PMA)

Para obtener estas NPs, se sintetizó en primer lugar el polímero anfílico de recubrimiento (PMA) y en último lugar, las NPs en presencia de este polímero.

1) *Síntesis del PMA.* El polímero (con un peso molecular de $\approx 6000 \text{ g mol}^{-1}$) se agitó con dodecilamina en 100 mL de tetrahidrofurano. Tras varias horas de agitación a 60 °C, se evaporó el disolvente por aplicación de vacío, y el polímero resultante se redisolvió en cloroformo anhidro hasta obtener una concentración de 50 mM. El protocolo de síntesis del PMA ha sido detallado específicamente en bibliografía ya publicada².

2) *Síntesis de AgNPs-PMA.* Las disoluciones de PMA y AgNPs hidrofóbicas preparadas en cloroformo se mezclaron durante 30 minutos. Después de la evaporación del disolvente, las AgNPs-PMA obtenidas se redisolviéron en disolución tampón borato sódico (50 mM, pH 12). La disolución de AgNPs-PMA se concentró con el empleo de filtros de centrifuga (100 kDa) y finalmente se purificó mediante electroforesis en gel y HPLC.

² C.A.J. Lin, R.A. Sperling, J.K. Li, T.Y. Yang, P.Y. Li, M. Zanella, W.H. Chang, W.J. Parak, *Small* 4 (2008) 334-341.

Síntesis de AgNPs recubiertas con polietilenglicol (AgNPs-PEG)

En este procedimiento de síntesis se empleó EDC para poder unir los extremos $-NH_2$ del polímero PEG a la superficie de las AgNPs-PMA rica en grupos $-COOH$. Para ello se prepararon disoluciones separadas de AgNPs-PMA, PEG y EDC en borato de sodio (50 mM, pH 9) a diferentes concentraciones.

- *Síntesis de AgNPs-PMA-satPEG.* Brevemente, se mezclaron las disoluciones preparadas de AgNPs-PMA y PEG, de forma que el número de moléculas PEG excediera considerablemente al de NPs. Posteriormente, se tomaron alícuotas de 20 μ L de esta mezcla y a cada una se le añadieron 10 μ L de la disolución de EDC. El tiempo de reacción fue de 90 minutos.
- *Síntesis de AgNPs-PMA-1PEG.* En este caso, se mezclaron alícuotas de 1 mL de cada una de las disoluciones de AgNPs-PMA, PEG, y EDC. La reacción se dejó en reposo durante 90 minutos, tiempo tras el cual se hizo una purificación progresiva con electroforesis en gel con el propósito de obtener NPs con una única molécula PEG en superficie.

El protocolo experimental detallado del recubrimiento de las AgNPs con PEG está recogido en bibliografía³.

Síntesis de AgNPs marcadas con fluoróforo

Los estudios de internalización celular fueron realizados con AgNPs marcadas con un fluoróforo y microscopía de láser confocal. Para ello, el polímero de recubrimiento PMA fue modificado con el fluoróforo DY-636 de la siguiente manera. Aproximadamente 2 mg de DY-636 se disolvieron en 10 mL

³ R.A. Sperling, T. Pellegrino, J.K. Li, W.H. Chang, W.J. Parak, *Adv. Funct. Mater.* 16 (2006) 943-948.

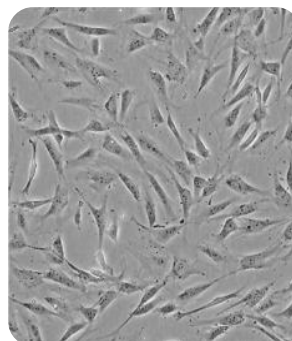
BLOQUE II. HERRAMIENTAS ANALÍTICAS

de metanol y la disolución se transfirió a un matraz en el que se aplicó vacío con objeto de evaporar el disolvente. A continuación, se añadieron 1.3 mL de una disolución de PMA en cloroformo (50 mM) y 4 mL de tetrahidrofurano. La mezcla se agitó durante 24 h a ≈ 60 °C. Posteriormente, el disolvente se evaporó a vacío y el PMA modificado se redisolvió en 1.3 mL de cloroformo. Finalmente las NPs fueron sintetizadas con el polímero modificado siguiendo el protocolo anteriormente descrito para AgNPs-PMA y AgNPs-PMA-satPEG⁴.

MATERIAL BIOLÓGICO

Las líneas celulares utilizadas en la evaluación de los efectos citotóxicos de las NPs fueron:

- *Fibroblastos embrionicos de ratón NIH/3T3* obtenidos de la casa comercial LGC Promochem (Teddington, Reino Unido).
- *Fibroblastos embrionicos de ratón 3T3-L1* proporcionados por la casa comercial American Type Culture Collection (Virginia, EEUU).



En ambos casos se trata de fibroblastos de ratón, pero las células 3T3-L1 presentan la característica distintiva de poder diferenciarse a adipocitos.

ENSAYOS DE VIABILIDAD CELULAR

En este apartado se detallan los ensayos de citotoxicidad realizados durante la fase experimental de la Tesis Doctoral. Estos ensayos miden la

⁴ C.A.J. Lin, R.A. Sperling, J.K. Li, T.Y. Yang, P.Y. Li, M. Zanella, W.H. Chang, W.J. Parak, *Small* 4 (2008) 334-341.

actividad metabólica de las células una vez que han sido expuestas a las NPs. La reducción de su actividad metabólica (por comparación con la actividad observada en las células no expuestas o células control) es una prueba irrefutable del daño celular ocasionado y por tanto, está directamente relacionada con la toxicidad de las NPs.

Ensayo de citotoxicidad del MTT

El ensayo colorimétrico del bromuro de 3-(4,5-dimetiltiazol-2-il)-2,5 difeniltetrazolio o MTT, se basa en la capacidad de las células vivas para reducir el compuesto MTT de color amarillo a formazán de color azul por acción de sus enzimas mitocondriales (en concreto, la succinato deshidrogenasa).

Siguiendo nuestro protocolo específico, células 3T3-L1 fueron sembradas en placas de cultivo celular de 12 pocillos durante 3-4 días a 37 °C y 5% de CO₂. Seguidamente fueron tratadas durante 24/48 horas con SWCNTs-PEG, 4-nonilfenol y mezclas de ambos. Las células que no fueron tratadas fueron consideradas controles negativos. Se estudió la presencia de suero (10% de FBS) en el medio de incubación ya que éste tiene un efecto directo sobre la estabilidad de las NPs y consecuentemente, sobre su toxicidad. Transcurrido el tiempo de tratamiento, se retiró el medio de cultivo y las células fueron incubadas con una disolución de MTT (0.1 mg mL⁻¹) durante 5 horas. Posteriormente, se retiró la disolución de MTT, se hizo un lavado con disolución tampón fosfato salino (PBS) y los cristales de formazán generados se disolvieron con 1 mL de DMSO bajo agitación durante 15 minutos. Las medidas de absorbancia se realizaron en un espectrofotómetro a una longitud de onda de 570 nm. Los valores de absorbancia obtenidos se relacionan directamente con el porcentaje de viabilidad celular de las muestras, de forma que una mayor absorbancia es consecuencia de una mayor generación de formazán por un mayor número de células vivas presentes. La Figura II.2.1 representa la

BLOQUE II. HERRAMIENTAS ANALÍTICAS

conversión del compuesto MTT a formazán y la Figura II.2.2 muestra las etapas seguidas en la consecución del ensayo.

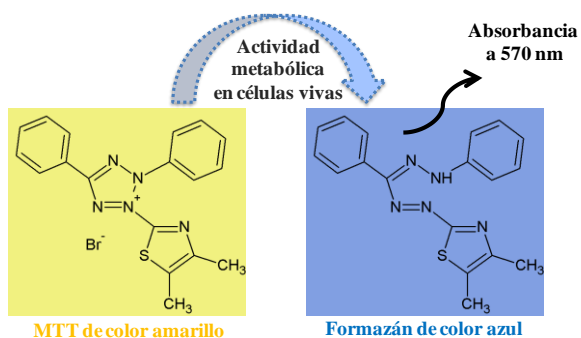


Figura II.2.1. Conversión del MTT a formazán en células vivas.

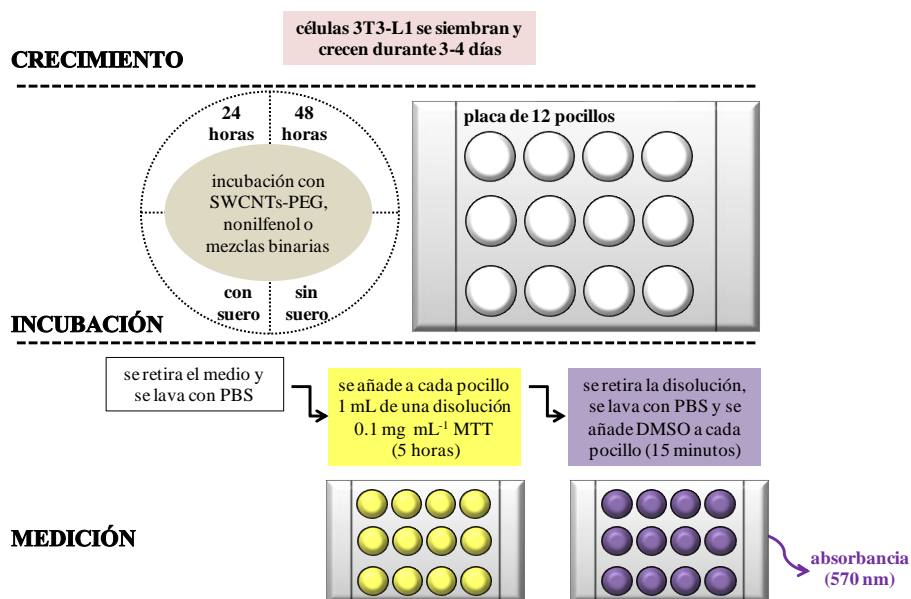


Figura II.2.2. Protocolo adaptado para el ensayo MTT.

Ensayo de citotoxicidad del Azul Alamar o de la resazurina

Este ensayo colorimétrico mide la actividad metabólica de las células vivas a través de su potencial para reducir la resazurina (sal sódica azul no fluorescente) a resorufina (sal sódica rosa fluorescente). La señal de fluorescencia emitida se relaciona con la conversión de resazurina a resorufina y por tanto, con la viabilidad celular de las muestras. No obstante, el máximo valor de fluorescencia no siempre se asocia a aquellas células sin tratar (controles) ya que la resorufina se puede reducir en mayor grado a la especie hidrorresorufina (transparente y no fluorescente).

A continuación se detalla el protocolo específico seguido en nuestro caso. Células NIH/3T3 fueron sembradas en placas de cultivo celular de 96 pocillos durante 24 horas a 37 °C y 5% de CO₂. Posteriormente, se trataron durante 24 horas con AgNPs con distintos recubrimientos superficiales. Células incubadas con AgNO₃ fueron los controles positivos y aquellas sin tratar los controles negativos. Transcurridas 24 horas, se lavó con PBS y entonces se añadió una disolución de resazurina preparada al 10% en medio de cultivo. Tras 3 horas de incubación, se midió la fluorescencia de las muestras en un espectrofluorímetro empleando una longitud de onda de excitación de 560 nm y un rango de emisión entre 572-650 nm. Las curvas dosis-respuesta se construyeron con los valores de fluorescencia normalizados (con respecto al valor máximo) y el logaritmo de las concentraciones de AgNPs estudiadas.

La Figura II.2.3 muestra la conversión de la resazurina en las distintas especies reducidas. La Figura II.2.4 ilustra el protocolo seguido para el desempeño de este ensayo colorimétrico.

BLOQUE II. HERRAMIENTAS ANALÍTICAS

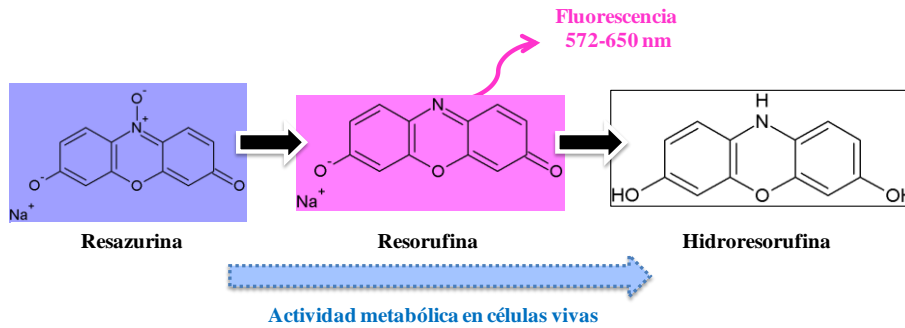


Figura II.2.3. Conversión de resazurina a resorufina e hidroresorufina.

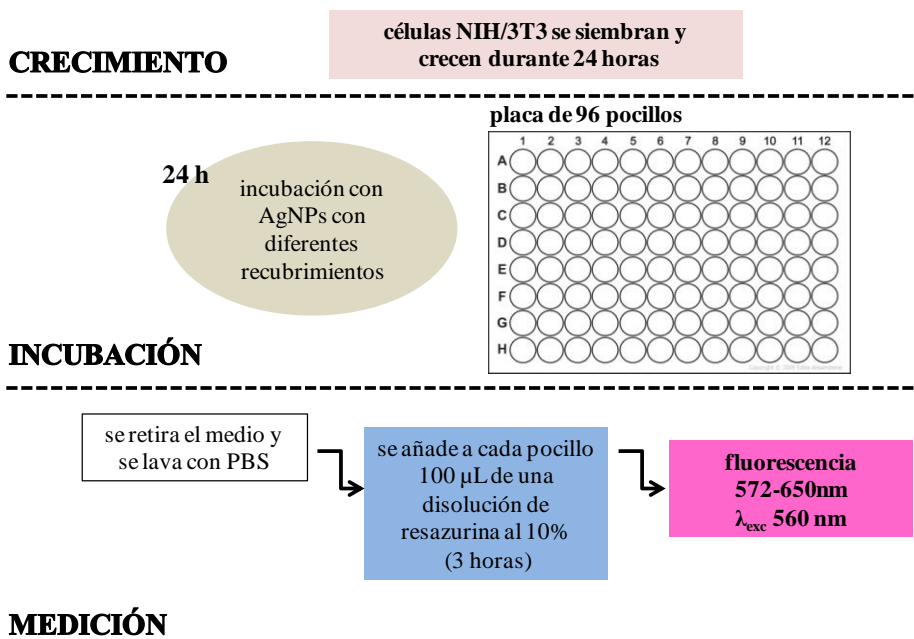


Figura II.2.4. Protocolo adaptado para el ensayo de resazurina.

INSTRUMENTACIÓN

Los instrumentos que se detallan a continuación fueron los que se emplearon en los estudios de toxicidad.

- *Microscopio electrónico de transmisión (TEM) JEOL JEM modelo 3010.* Las imágenes TEM obtenidas para caracterizar las NPs fueron realizadas con este microscopio.
- *Malvern Zetasizer.* El diámetro hidrodinámico (d_h) así como el potencial zeta de todas las AgNPs sintetizadas experimentalmente fueron proporcionados por este instrumento.
- *Espectrofotómetro Agilent 8453.* Los espectros de absorción de las AgNPs fueron medidos con este equipo instrumental.
- *Espectrómetro de masas con plasma de acoplamiento inductivo (ICP-MS) PerkinElmer Sciex modelo ELAN DRC-e.* Este instrumento está equipado con un nebulizador concéntrico y una cámara de spray ciclónica. Se utilizó para analizar la concentración de iones plata en las suspensiones preparadas así como para los estudios de oxidación de las AgNPs.
- *Electroforesis en gel BIO-RAD PowerPack Basic.* La purificación de las AgNPs con diferente grado de recubrimiento se llevó a cabo mediante electroforesis en gel. Las NPs migraron a través de gel de agarosa (2%) aplicando un campo eléctrico de $10 \text{ V}\cdot\text{cm}^{-1}$ durante 1 hora.
- *Cromatógrafo de líquidos de alta presión (HPLC) Agilent serie 1100.* Provisto de una columna de Sepharcyl S300-HR fue empleado para la

BLOQUE II. HERRAMIENTAS ANALÍTICAS

purificación y separación de AgNPs con diferente grado de recubrimiento superficial.

- *Espectrofluorímetro Horiba FluoroLog*. Fue empleado para obtener los espectros de fluorescencia de las AgNPs marcadas con el fluoróforo DY-636 y asimismo, para realizar las medidas de fluorescencia derivadas de los ensayos de citotoxicidad basados en resazurina.

- *Espectrofotómetro Beckman DU-70*. Fue utilizado para las medidas de absorbancia derivadas de los ensayos *in vitro* con MTT.

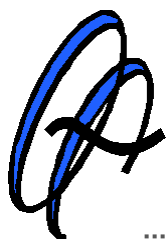
II.3. Gestión de residuos generados

La concienciación ambiental es una materia todavía pendiente en la sociedad actual. Dentro del ámbito de la investigación, el empleo de reactivos potencialmente tóxicos conlleva una responsabilidad ambiental adicional que implica tanto su manipulación como su disposición final.

Como consecuencia del desarrollo de la fase experimental de la Tesis Doctoral, se emplearon y desecharon reactivos químicos tóxicos, residuos biológicos y materiales de laboratorio impregnados de los mismos. Es por ello por lo que se hizo una cuidadosa gestión de los mismos que consistió en almacenarlos correctamente en los recipientes apropiados, y gestionar su recogida a través de un servicio externo.

El Servicio de Protección Ambiental (SEPA) es el órgano encargado de la gestión ambiental en la Universidad de Córdoba y pertenece a la Dirección General de Prevención y Protección Ambiental. Entre los principales cometidos del SEPA destaca el desarrollo de acciones que incrementen la concienciación ambiental en la gestión de la Universidad (actividades de asesoramiento y formación), así como la prevención de la contaminación y el cumplimiento de todos los requisitos legales existentes. Previa solicitud, el SEPA se encarga de la recogida selectiva y gestión de todos los residuos peligrosos generados en la Universidad. Es por tanto, el servicio que complementa a la perfección la labor investigadora desarrollada en nuestros laboratorios.

BLOQUE III



Nanopartículas como herramientas analíticas

Introducción	181
III.1. Nanodiamonds assisted-cloud point extraction for the determination of fluoranthene in river water	185
III.2. Liquid-liquid extraction assisted by a carbon nanoparticles interface. Electrophoretic determination of atrazine in environmental samples	209
III.3. Carbon nanotubes as SPE sorbents for extraction of salicylic acid from river water	231
III.4. Microextraction by packed sorbents combined with Surface-enhanced Raman spectroscopy for determination of musk ketone in river water	249

INTRODUCCIÓN

Debido a sus extraordinarias propiedades fisicoquímicas, las NPs han sido muy utilizadas en el ámbito analítico, destacando su aportación a las técnicas de extracción convencionales enmarcadas dentro del tratamiento de muestra del procedimiento analítico [1].

La mayoría de aplicaciones analíticas descritas en este sentido emplean las NPs como sólidos sorbentes en las técnicas de (micro)extracción en fase sólida, ya sea de forma aislada [2], o formando híbridos con otros materiales convencionales [3]. Las NPs pueden utilizarse en distintas modalidades; empaquetadas [4], dispersas [5] o en forma de recubrimientos [6], para extraer y preconcentrar analitos de diferente naturaleza. Sin embargo, los nanomateriales no han tenido mucha acogida en las técnicas de (micro)extracción líquido-líquido a excepción de las NPs magnéticas que sí se han empleado en este ámbito pero únicamente para facilitar la retirada de la fase orgánica del medio [7,8]. No obstante, hasta la fecha no se ha considerado la posibilidad de combinar la fase orgánica con las NPs como fases extractantes simultáneas del analito.

Las técnicas de extracción basadas en el empleo de surfactantes, como la extracción punto de nube, se han propuesto para la extracción de algunas NPs metálicas de matrices acuosas, si bien en esos casos las NPs constituyen los analitos objeto de determinación y no las fases extractantes. Actualmente, un único trabajo de investigación describe el empleo de NPs de alúmina en combinación con el surfactante Tritón X-114 como fases extractantes para la separación y preconcentración de determinados iones metálicos [9]. El empleo de las NPs en este ámbito como agentes de extracción y no como analitos *per se*, es por tanto un área de investigación poco explotada a día de hoy.

BLOQUE III. NANOPARTÍCULAS COMO HERRAMIENTAS ANALÍTICAS

Además del tratamiento de muestra, la separación instrumental y la detección son las otras dos etapas del procedimiento analítico que pueden beneficiarse con el empleo de NPs. En este sentido, conviene destacar el enorme potencial de las NPs metálicas para incrementar la sensibilidad de la detección por Espectroscopía Raman gracias a su utilización como superficies o plataformas SERS.

En resumen, este Bloque III pretende indagar en la aplicabilidad analítica de las NPs a través de tres diferentes técnicas de extracción enfocadas en la determinación de varios analitos de interés ambiental. Se intenta profundizar por lo tanto en la aplicación de las partículas nanométricas en esquemas de extracción en los que no han sido tan investigadas hasta la fecha, como son la extracción mediada por surfactantes y la extracción líquido-líquido. Asimismo se confirma el potencial de las NPs como sólidos sorbentes en un área más que consolidada como es la extracción en fase sólida. Por último, este Bloque III también quiere extender el estudio de las NPs como herramientas en la etapa de detección Raman demostrando nuevamente su versatilidad de aplicación dentro del procedimiento analítico.

References

- [1] K. Pyrzynska, Use of nanomaterials in sample preparation, *TrAC* 43 (2013) 100-108.
- [2] Q. Liu, J. Shi, L. Zeng, T. Wang, Y. Cai, G. Jiang, Evaluation of graphene as an advantageous adsorbent for solid-phase extraction with chlorophenols as model analytes, *J. Chromatogr. A* 1218 (2011) 197-204.
- [3] M.L. Polo-Luque, B.M. Simonet, M. Valcárcel, Solid phase extraction-capillary electrophoresis determination of sulphonamide residues in milk samples by use of C18-carbon nanotubes as hybrid sorbent materials, *Analyst* 138 (2013) 3786-3791.
- [4] I. Marquez-Sillero, E. Aguilera-Herrador, S. Cárdenas, M. Valcárcel, Determination of parabens in cosmetic products using multi-walled carbon nanotubes as solid phase extraction sorbent and corona-charged aerosol detection system, *J. Chromatogr. A* 1217 (2010) 1-6.
- [5] M.C. Alcudia-Leon, R. Lucena, S. Cárdenas, M. Valcárcel, Magnetically confined hydrophobic nanoparticles for the microextraction of endocrine-disrupting phenols from environmental waters, *Anal. Bioanal. Chem.* 405 (2013) 2729-2734.
- [6] A. Mehdinia, M.O. Aziz-Zanjani, Recent advances in nanomaterials utilized in fiber coatings for solid-phase microextraction, *TrAC* 42 (2013) 205-215.
- [7] K.M. Giannoulis, L.D. Giokas, Q. Zhu, G.Z. Tsogas, A.G. Vlessidis, Q. Pan, Surfactant-enhanced liquid-liquid microextraction coupled to micro-solid phase extraction into highly hydrophobic magnetic nanoparticles, *Microchim. Acta* 180 (2013) 775-782.
- [8] K.S. Tay, N.A. Rahman, M.R.B. Abas, Magnetic nanoparticle assisted dispersive liquid-liquid microextraction for the determination of 4-n-nonylphenol in water, *Anal. Methods* 5 (2013) 2933-2938.
- [9] S. Dadfarnia, F. Shakerian, A. Mohammad, H. Shabani, Suspended nanoparticles in surfactant media as a microextraction technique for simultaneous separation and preconcentration of cobalt, nickel and copper ions for electrothermal atomic absorption spectrometry determination, *Talanta* 106 (2013) 150-154.

Analytical
Methods

PAPER

RSC | Advancing the
Chemical Sciences |

Anal. Methods, 2013, 5, 3864



Nanodiamonds assisted-cloud point extraction for the determination of fluoranthene in river water

Encarnación Caballero-Díaz, Bartolomé M. Simonet, Miguel Valcárcel

Department of Analytical Chemistry, Marie Curie Building (Annex), Campus de Rabanales, University of Córdoba, 14071 Córdoba, Spain

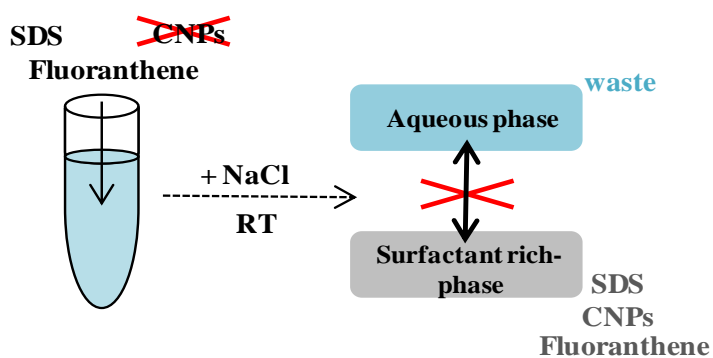
ABSTRACT

The classic cloud point extraction has been modified by the inclusion of nanodiamonds and applied to the extraction-preconcentration of fluoranthene from river water. The effects of ionic strength and surfactant concentration, process temperature, incubation time, nanoparticle type and concentration, and elution conditions were investigated in depth. The effect of the carbon nanoparticles (CNPs) on the performance of the conventional cloud point scheme enabled the formation of two phases in a relatively short time and without temperature requirements. Experiments carried out under optimized conditions but in absence of nanoparticles were unsuccessful in terms of phase separation and consequently, the nanoparticles are indispensable to the analytical performance. The work developed here, confirms the versatility of the CNPs to be introduced in diverse sample treatment processes, resulting very interesting to investigate in each case their impact on the performance of the process.

BLOQUE III. NANOPARTÍCULAS COMO HERRAMIENTAS ANALÍTICAS

The application of the proposed method followed by fluorimetric detection enabled the determination of fluoranthene in spiked river water providing a good relative standard deviation (RSD) (6.6%, n=3) and acceptable recovery values (>65%).

GRAPHICAL ABSTRACT



1. INTRODUCTION

Analytical methods with high sensitivity, selectivity and resolution are required in order to determine analytes at trace concentration levels in complex matrices. Extraction–separation techniques overcome this problem since they isolate analytes from the matrix, thereby reducing, controlling or eliminating the interferences originally present, and additionally, preconcentrate and determine the analytes at very low concentrations.¹ Conventional extraction techniques such as liquid–liquid or solid-phase extraction (LLE, SPE), and liquid-phase or solid-phase microextraction (LPME, SPME), are relatively expensive, tedious and consume large amounts of organic solvents.²

Cloud point extraction (CPE) has become one of the most outstanding extraction techniques. This technique is based on the separation of a homogeneous micellar aqueous solution into two isotropic liquid phases. One of them, the smaller-volume surfactant-rich phase, contains the surfactant interacting with the analyte molecules at a concentration above its critical micellar concentration (CMC), that is the surfactant concentration above which the surfactant molecules aggregate to form micelles. The other larger-volume aqueous phase is only composed of surfactant molecules at a concentration close to the CMC. In comparison to the above mentioned extraction techniques, CPE shows remarkable advantages such as versatility for extracting and preconcentrating analytes of different nature, variable preconcentration factors depending on the amount of surfactant added, lower loss of analyte since it is not necessary to evaporate the solvent, low cost, and no toxicological effects thanks to the use of biodegradable surfactants. The limitations are mainly related to the high background absorbance of the surfactants in the UV region and to the handling of the surfactant-rich phase since this is too viscous to be directly injected into conventional analytical instruments and therefore, a previous dilution or clean up step is usually necessary before detection.¹⁻³ In

order to ensure that separation into two phases occurs, two conditions are required. The first is that the surfactant concentration must exceed their CMC for the formation of micelles. The second is that the experimental conditions such as temperature, pressure or ionic strength must be altered. When separation into two phases takes place, the solution becomes turbid due to the diminished solubility of the surfactant in water. However, this phenomenon is reversible when the experimental conditions return to their initial point. The cloud point temperature (CPT), temperature at which the solution becomes turbid, plays an important role in the formation of the two phases when nonionic or zwitterionic surfactants are used. The mechanism by which two phases are formed is still subject of controversy. However, it may be attributed to the competition between the entropy (which promotes the solubility of the micelles in water) and enthalpy (which promotes the separation of the micelles from water) when the temperature of the system increases.⁴ The water molecules lattices surrounding the surfactant molecules are destroyed with the rise in temperature causing the dehydration, and consequently, the van der Waals interactions among the surfactant molecules prevail. As a result, agglomeration of the surfactant micelles takes place in the surfactant-rich phase and thus, the volume of this phase decreases.³⁻⁵ On the other hand, it has been shown that micellar solutions of anionic surfactants such as sodium dodecyl sulfate (SDS) may also form two isotropic phases at room temperature under highly acidic conditions.⁶

Carbon nanoparticles (CNPs) have been extensively used as sorbents in solid phase extraction techniques since they may adsorb different pollutants on their surface.⁷⁻⁹ This is a consequence of the different interactions that can occur between the nanoparticles and pollutants, such as hydrophobic, π - π and electrostatic interactions, or hydrogen bonds.¹⁰ Among CNPs, nanodiamonds have become extensively investigated due to their high adsorption capacity and specific surface area, simple surface functionalization, chemically inert cores

III.1. Nanodiamonds assisted-cloud point extraction

which are combined with a hydrophobic surface, and ability to be incorporated in the design of new sensors.¹¹ Nanodiamonds are CNPs with a truncated octahedral architecture and are about 2 to 8 nm in diameter.¹² Among their applications one must highlight their use in electrochemical coatings,¹³ polymer compositions,¹⁴ anticorrosion coatings¹⁵ and lubricants,¹⁶ although their most widely described applications are in the biology field, where they are used as, nanobioprobes to visualize protein–bacteria interactions,¹⁷ carriers of biomolecules in column chromatography,¹⁸ drug carriers,¹⁹ or platforms to extract and elute peptides, proteins, DNA, glycans and other molecules.²⁰ To date, few analytical applications of nanodiamonds in the sample treatment field have been described.

Nanoparticle–surfactant interactions *via* electrostatic or hydrophobic attractions have been widely studied and are the basis of those works where CPE is applied to the extraction–preconcentration of nanoparticles from environmental samples.^{21,22} Therefore, from our knowledge, nanoparticles could interact with micelles forming micellar complexes that may extract the analyte from an aqueous matrix. The extraction would be assisted by the given interactions between the analytes and micelles, and reinforced by the interactions between the stabilized-nanoparticles and the analyte. However, the effect of including nanoparticles in the cloud point scheme for the extraction of a pollutant has not been studied until now.

Here, we evaluated the impact of the inclusion of different CNPs, such as nanodiamonds, multi-walled carbon nanotubes and hybrid nanoparticles, on the conventional CPE. Our experimental study consisted of optimizing a CPE procedure at room temperature assisted by SDS, an electrolyte and nanoparticles. Also, the optimum experimental procedure was tested for the extraction of fluoranthene from river water samples followed by fluorimetric detection. Fluoranthene was taken as model analyte since its aromatic structure

was expected to favor interactions with the CNPs. Since previously published papers about CPE and fluoranthene led to good recoveries and low limits of detection,²³⁻²⁶ our purpose here lay in studying the role of the CNPs in this conventional extraction technique.

2. EXPERIMENTAL

2.1. Instrumentation

Fluorescence spectra were obtained using a PTI QuantaMaster™ Spectrofluorometer (Photon Technology International) equipped with a 75 W xenon short arc lamp and a model 814 PTM detection system. FeliX32 software was used for fluorescence data collection and analysis, and it also controlled the whole instrument. All the fluorescence measurements were made using 10 mm quartz cells from Hellma Analytics. The instrument excitation and emission slits both were adjusted to 7 nm.

Micellar aqueous solutions containing nanoparticles were sonicated in an ultrasound bath without heating (Ultrason model, Selecta, 50 W, 60 Hz).

2.2. Reagents

All reagents were of analytical grade and were used without any further purification except for the nanodiamonds. The model analyte chosen was fluoranthene (99%) and it was purchased from Sigma Aldrich (St. Louis, MO, USA). Acetonitrile for luminescence ($\geq 99.5\%$, GC) was used for fluorescence measurements and was also obtained from Sigma Aldrich (St. Louis, MO, USA). The chemical and spectral properties of fluoranthene are summarized in Table 1. Sodium dodecyl sulfate (SDS) ($\geq 98.5\%$) was selected as the surfactant for carrying out the cloud point procedure and was purchased from Sigma Aldrich

III.1. Nanodiamonds assisted-cloud point extraction

(St. Louis, MO, USA). Sodium chloride (NaCl) ($\geq 99\%$) from Sigma Aldrich (St. Louis, MO, USA) was selected as the electrolyte to induce the separation of the homogeneous aqueous phase into two isotropic phases. Acetonitrile (99.9%) and acetone (99.9%) were used to purify the commercial nanodiamonds before the extraction. Hydrochloric (37%), nitric (69%) and sulfuric (95–98%) acids were used in order to oxidize the nanoparticles by introducing carboxylic and hydroxylic superficial groups. These last chemical reagents were all purchased from Panreac (Barcelona, Spain).

Table 1. Chemical and spectral properties of the model analyte.

Analyte	Formula	$\log(K_{ow})^a$	Water solubility ($\text{mg}\cdot\text{mL}^{-1}$)	λ_{ex}^b (nm)	λ_{em}^c (nm)
Fluoranthene	$\text{C}_{16}\text{H}_{10}$	5.08	0.26	350	460

^a K_{ow} : octanol-water partition coefficient. ^b λ_{ex} : maximum excitation wavelength.

^c λ_{em} : maximum emission wavelength.

2.3. Synthesis of hybrid nanoparticles

The chemical reagents used to synthesize the hybrid nanoparticles were 3-aminopropyltrimethoxysilane ($\geq 98\%$), acetic acid ($\geq 99.85\%$), *N*-(3-dimethylaminopropyl)-*N'*-ethylcarbodiimide hydrochloride (commercial grade) and *N*-hydroxysuccinimide ($\geq 97\%$). All these reagents were acquired from Sigma Aldrich (St. Louis, MO, USA).

Nanodiamonds (NDs) obtained by detonation processes with a mean diameter of 3.2 nm and a purity $>98\%$ were provided by NaBond Technologies. Multi-walled carbon nanotubes (MWCNTs) with a mean diameter of 140 nm were provided by MER Corporation. 0.2 g of each type of nanoparticle were separately oxidized, as previous step to the synthesis of the hybrid nanoparticles, in a mixture of sulfuric and nitric acids, being the oxidation

conditions different for the NDs (ratio 1:1 for 24 hours) compared to the MWCNTs (ratio 3:1 for 2 hours).

The synthesis of hybrid nanoparticles (NDs–MWCNTs) was as follows. Firstly, the previously oxidized NDs (about 0.2 g) were shaken for 4–6 hours in 5 mL of a solution that was previously prepared by mixing 5 mL of 3-aminopropyltriethoxysilane with 45 mL of a 0.05 M acetate–acetic acid buffer solution at pH 5. The resulting NDs were centrifuged three times at 13000 rpm with Milli-Q water (in order to remove superficial residues) and then air-dried. Next, around 0.2 g of oxidized multi-walled carbon nanotubes (MWCNTs_{ox}) were mixed with the previously obtained NDs in a 10 mL aqueous solution containing 2 mg of *N*-hydroxysuccinimide and 5 mg of *N*-(3-dimethylaminopropyl)-*N*'-ethyl-carbodiimide hydrochloride. The final pH was adjusted to 5 and the reaction time was 24 hours. The resulting hybrid nanoparticles were centrifuged three times at 13000 rpm with Milli-Q water, then air-dried and finally stored for their future use.

2.4. Purification procedure of nanodiamonds

In order to ensure the absence of impurities derived from their synthesis, the commercial NDs were subjected to a purification procedure before being used in the extraction procedure. This purification consisted of two consecutive centrifugations in presence of 2 mL of acetone and 2 mL of acetonitrile. In both cases, the centrifugation conditions were 10000 rpm for 5 minutes. The supernatant was removed after each washing and finally the purified NDs were air-dried and stored.

2.5. Nanodiamonds assisted-cloud point extraction

The experimental procedure scheme is depicted in Fig. 1 and was as follows. 36 mg of the NDs (previously purified) were added to a 6 mL aqueous solution containing 0.1 mol L⁻¹ SDS, and then this was sonicated in an ultrasonic bath for 30 minutes. Afterwards, the samples were spiked at different concentrations and 10 min was selected as the optimum incubation time. Fluoranthene was selected as model polycyclic aromatic hydrocarbon to perform the extraction as its fluorescence emission maximum (460 nm) is rather distant of that from the NDs (327 nm) and as a consequence, the fluorescence interference on the analytical signal was negligible. Additionally, fluoranthene has an aromatic structure that promotes the interplay with the CNPs through π - π interactions. Following the experimental procedure, 90 mg of NaCl was added to the micellar solution (0.25 mol L⁻¹ of NaCl in total) and the mixture was allowed to rest for 60 min in order to enable the formation of two phases at room temperature. Centrifugation at 3500 rpm for 10 min was used to enhance phase separation. Subsequently, the aqueous phase was withdrawn by simple decantation and 1.5 mL of acetonitrile was added to the surfactant-rich phase (that contained the NDs), mixed, and allowed to sit for 5 min. Then, the upper phase (approximately 1.5 mL of acetonitrile containing the analyte) was carefully transferred to a glass tube with a Pasteur pipette, and a centrifugation step at 3500 rpm for 5 min was necessary to remove the NDs that had been transferred into the acetonitrile. For the fluorescence measurements, a volume of 1 mL of acetonitrile was used rather than the full 1.5 mL obtained and this was transferred into the quartz cell. The fluorescence signal of fluoranthene was measured according to the excitation and fluorescence wavelengths provided in Table 1.

BLOQUE III. NANOPARTÍCULAS COMO HERRAMIENTAS ANALÍTICAS

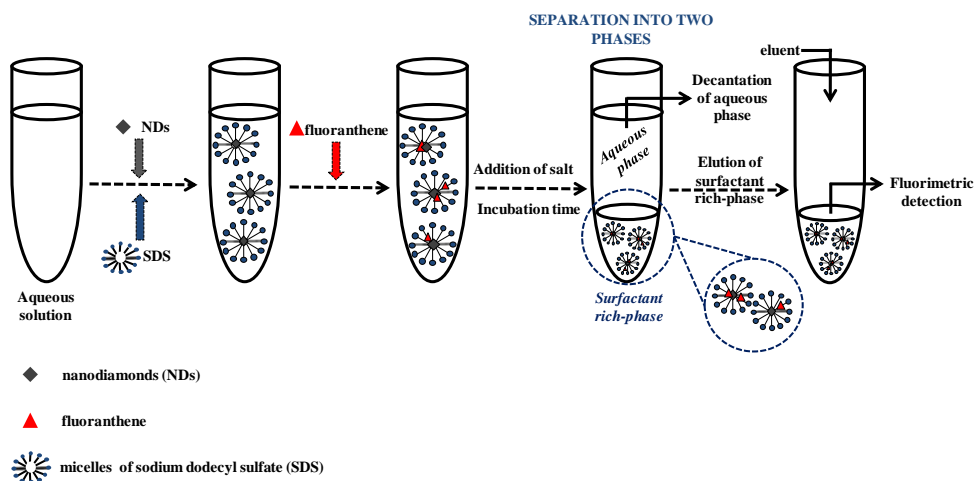


Figure 1. A scheme showing the nanodiamonds assisted-cloud point extraction.

2.6. River water samples

River water samples were collected from the Guadalquivir River (Córdoba, Spain). Since there were no real positive samples, the samples were necessarily spiked with fluoranthene at a concentration of 0.060 mg L^{-1} . 6 mL of water sample were subjected to the previously described experimental procedure (see section 2.5).

3. RESULTS AND DISCUSSION

CPE needs to be carried out under optimum conditions so that the preconcentration factor and extraction efficiency can be maximized in each case. Several experimental factors must be taken into account to achieve this objective such as type and concentration of surfactant and additive, process temperature, pH and incubation times. With this same purpose, the optimization of diverse experimental factors has been investigated here. Firstly, the experimental conditions related to the conventional cloud point system were studied, including ionic strength, surfactant concentration, process

III.1. Nanodiamonds assisted-cloud point extraction

temperature and incubation times. Once these variables were set, the optimization of the CNP type and concentration and the elution conditions were subject of study. SDS was initially used as the surfactant, taking as reference a published work on the extraction of polycyclic aromatic hydrocarbons (PAHs) by cloud point extraction with SDS followed by fluorimetric detection.⁶ The pH effect was not considered here because it has been described that its influence on the extraction efficiency and recovery is not crucial for neutral or non-ionized compounds such as PAHs.^{3,27}

It should be noted that the role of the nanoparticles in assisting the classic cloud point technique is still unknown and several theories are possible. One hypothesis is that the inclusion of nanomaterials in the system could reinforce the micellar extraction of the analyte from the aqueous matrix by establishing supplementary interactions with it, such as hydrophobic and π - π attractions, which are due to the fact that both CNPs and fluoranthene have hydrophobic nature and contain aromatic rings. The extraction would be, therefore, carried out by the interplay between the analyte molecules with both the hydrophobic chains inside the micelles and the surfactant stabilized-nanoparticles. Other hypothesis would be that the presence of the nanoparticles was found to be significant or, on the other hand, negligible, to the performance of the cloud point extraction. This work was mainly focused on the development of an experimental approach different to the conventional one by optimizing several key parameters. This allowed us to finally demonstrate the applicability of the optimized method to the fluoranthene extraction from river water samples. Needless to say, additional studies must be conducted with a view to further analytical applications.

3.1. The effect of ionic strength

The addition of salt to a micellar aqueous solution can modulate the extraction efficiency of the CPE process inasmuch the water molecules surrounding the surfactant micelles are preferably attracted by the salt ions and tend to solvate them, and as a consequence, the number of water molecules that interact with the micelles in the surfactant-rich phase decreases (this is the sorting out phenomenon that also applies to other extraction techniques). This effect leads to a decrease in the volume of the enriched phase and consequently, an increase in the preconcentration factor.^{1,27} Additionally, the inorganic salts promote the hydrophobic interactions among the surfactant aggregates and analytes, favoring their extraction from the matrix.⁵ The effects of salt addition on the CPT were not taken into account in this work since SDS is neither a nonionic nor zwitterionic surfactant and thus, a variation in temperature above/below the CPT is not indispensable for the formation of the two phases. It is important to point out that previous experiments carried out with hydrochloric acid as electrolyte were unsuccessful in terms of phase separation. The influence of ionic strength on the performance of the CPE was then investigated at different concentrations of NaCl (0.05–0.4 mol L⁻¹) while other experimental conditions were kept constant. Fig. 2 shows the variation in the fluorescence signal of fluoranthene depending on the amount of electrolyte added to the solution. A higher analytical signal corresponding to fluoranthene was observed as the concentration of NaCl in the solution increased, which may be explained by the previously mentioned phenomenon. However, the fluorescence signal of fluoranthene remained practically constant above 0.25 mol L⁻¹ of NaCl. Thus, this value of concentration was selected as the optimum.

III.1. Nanodiamonds assisted-cloud point extraction

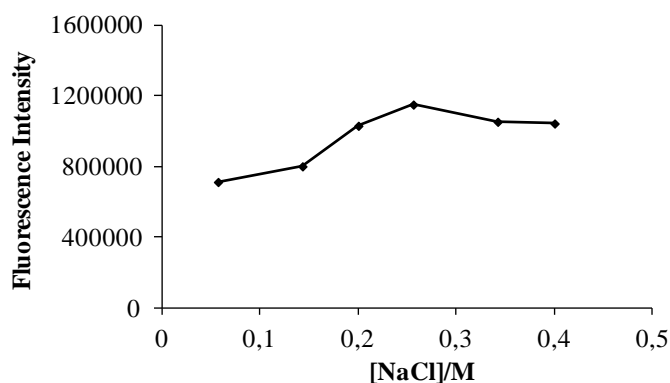


Figure 2. The effect of the sodium chloride (NaCl) concentration on the fluorescence intensity of fluoranthene after carrying out the cloud point procedure under the following conditions: $90 \mu\text{g L}^{-1}$ of fluoranthene, 3 mg mL^{-1} of nanodiamonds, 0.6 mol L^{-1} of SDS, room temperature.

3.2. The effect of SDS concentration

The presence of surfactant is an indispensable factor in any cloud point extraction in order to form two isotropic phases from one aqueous solution. Additionally, in our case, the surfactant also enabled the stabilization of the CNPs in the aqueous solution. In this work, SDS was chosen as surfactant taking as reference existing literature.⁶ Furthermore, SDS does not significantly interfere with the fluoranthene fluorescence signal due to the absence of an aromatic moiety in its structure. The most likely interactions between the surfactant molecules containing aromatic rings and the CNPs are preferably of the π - π stacking type. In our study, on the other hand, the interactions between the SDS molecules and CNPs are expected to be hydrophobic since the graphitic unit cells adjust well to the methylene units of the SDS hydrocarbon chains.²⁸ However, it has been suggested that the SDS molecules are adsorbed on the carbon nanotubes in a random way without any preferential arrangement of the head and tail groups.²⁹

BLOQUE III. NANOPARTÍCULAS COMO HERRAMIENTAS ANALÍTICAS

The SDS concentration was studied over a much greater range than its critical micellar concentration (8 mmol L^{-1}) to ensure the presence of micelles in the solution. Furthermore, the concentration range under investigation was in accordance with the literature.⁶ Fig. 3 depicts the variation in the fluorescence signal of fluoranthene within the SDS concentration range of $0.1\text{--}0.6 \text{ mol L}^{-1}$. An increase in the extraction with the surfactant concentration would be the expected trend. However, high SDS concentrations (for a constant concentration of nanoparticles) led to the formation of progressive multilayers on the nanoparticles surface. Consequently, the excess of surfactant molecules present in the solution start interacting (by hydrophobic interactions) with those linked to the nanoparticles surface. The given interactions favor the association of the surfactant coated-nanoparticles and as a result, the CNPs tend to agglomerate reducing, in that way, their contact surface with the analyte molecules.²⁸ This mechanism could explain the decrease in fluoranthene extraction above 0.1 mol L^{-1} of SDS, and therefore, this was finally chosen as optimum surfactant concentration in order to maximize the extraction of analyte.

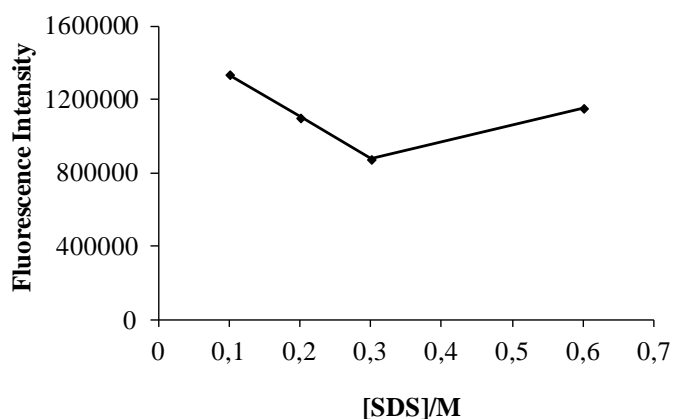


Figure 3. The effect of the sodium dodecyl sulfate (SDS) concentration on the fluorescence intensity of fluoranthene after carrying out the cloud point procedure under the following experimental conditions: $90 \mu\text{g L}^{-1}$ of fluoranthene, 3 mg mL^{-1} of nanodiamonds, 0.25 mol L^{-1} of NaCl, room temperature.

3.3. The effect of incubation temperature

The cloud point temperature (CPT) is a key factor in the formation of two phases when nonionic or zwitterionic surfactants are used, as in these cases, it is necessary to heat or cool the micellar aqueous solution above or below the CPT respectively, to achieve the phase separation. In spite of the fact that an anionic surfactant was used in this work, the effect of the temperature of the process on the fluoranthene extraction was studied in the range of 10–60 °C. The results showed that the analytical signal obtained at room temperature was quite similar to that obtained at higher temperatures and consequently, all the experiments were carried out at room temperature. This is a remarkable advantage for the extraction procedure, since it prevents from the decomposition and loss of low molecular weight PAHs due to high temperatures.³⁰

3.4. The effect of incubation times

CPE has been traditionally treated in terms of a two-phase process in which analytes present in an aqueous solution are solubilized by surfactant micelles that are concentrated in a smaller volume phase (enriched phase) after the alteration of the experimental conditions. In this work, the inclusion of the CNPs as third phase in the cloud point system requires new experimental variables to be considered. The incubation times were studied at three different stages of the process. Firstly, the time of interaction between the CNPs and the surfactant in solution was considered. The purpose of this study was to optimize the time required to obtain a stable suspension of surfactant stabilized-nanoparticles. The presence of aggregates leads to a reduced surface interplay between the nanoparticles and the compounds in solution, and an increased irreproducibility. Sonication times between 30 and 90 min were studied. 30 min was finally selected as optimum sonication time since it allowed

us to obtain surfactant stabilized-nanoparticles, thus maximizing their contact surface area with the analyte. In a second study, the interplay between the surfactant micelles, nanoparticles and fluoranthene was investigated in the range of 10–80 min, although no sonication was used in this stage. 10 min was enough to carry on with the cloud point procedure. Ultimately, the experimental conditions must be altered by the addition of a salt (NaCl) in order to induce the phase separation. Different incubation times after the addition of NaCl were studied in the range of 60–500 min. The reaction was stopped at 60 min since a longer reaction time did not increase considerably the quantitative extraction of fluoranthene.

3.5. The effect of the nanoparticles type and concentration

Different types of CNPs were investigated in order to select the best conditions for the previously set cloud point extraction. We focused on CNPs because they have been widely described as sorbents in sample treatment processes.³¹ NDs, MWCNTs, MWCNTs_{ox} and NDs–MWCNTs were tested as third phase in the cloud point extraction. The results are depicted in Fig. 4 and concluded that the NDs were the most effective CNPs in the process. For the same concentration of CNPs, the number of NDs present in solution is higher than for the rest of the studied CNPs due to their extremely reduced diameter (3.2 nm). Consequently, the overall surface area of these nanoparticles available for interaction with the analyte is greater, and this explains the better extraction results. Moreover, larger nanoparticles have a greater tendency to agglomerate in solution, which reduces considerably their ability to interact with other compounds. The use of NDs also led to the formation of two clearly defined phases (an aqueous phase, and an enriched phase containing the micellar aggregates, NDs and analyte) unlike those observed with other CNPs, thus facilitating the subsequent handling of the surfactant-rich phase previous to the fluorimetric detection.

III.1. Nanodiamonds assisted-cloud point extraction

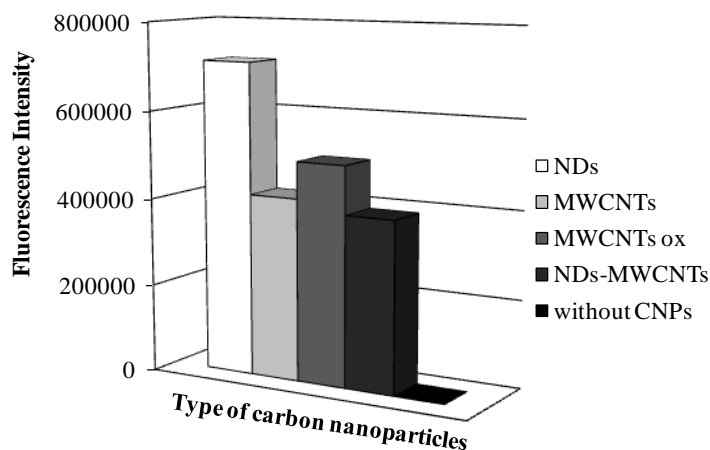


Figure 4. The effect of the type of carbon nanoparticles (CNPs) on the fluorescence intensity of fluoranthene after carrying out the cloud point procedure under the following experimental conditions: $90 \mu\text{g L}^{-1}$ of fluoranthene, 0.1 mol L^{-1} of SDS, 0.25 mol L^{-1} of NaCl, room temperature and 0.33 mg mL^{-1} of different types of carbon nanoparticles (NDs: nanodiamonds, MWCNTs: multi-walled carbon nanotubes, MWCNTs_{ox}: oxidized multi-walled carbon nanotubes, NDs-MWCNTs: hybrid nanoparticles).

With regard to the effect of the nanoparticles concentration, it should be pointed out that previous experiments under optimum conditions but in absence of NDs resulted failed in the separation into two phases, and consequently, in the fluoranthene extraction. Therefore these nanoparticles have become essential for conducting the described extraction procedure. On the whole, several experiments were conducted using different concentrations of NDs. Increasing the concentration of nanoparticles in the solution can have two effects on the analyte extraction from an aqueous matrix. On the one hand, it increases the surface area available to interact with the analyte but on the other hand, the agglomeration of the nanoparticles is more likely to occur at high concentrations, which reduces the availability of interaction places for the analyte and as a consequence, the extraction is affected adversely. The effect of the ND concentration on the fluoranthene extraction by the described procedure was evaluated in the range of $0.5\text{--}6 \text{ mg mL}^{-1}$. The results are shown in Fig. 5 where it can be observed that when the concentration of the NDs

increases, the fluoranthene extraction also increases and consequently, the effect of a larger available sorption surface prevails over the problems that arise from agglomeration. The optimum ND concentration was set at 6 mg mL⁻¹ since this value led to the greatest fluoranthene extraction. Further experiments carried out at higher concentrations were unsuccessful in the quantitative extraction of analyte due to problems of agglomeration of nanoparticles.

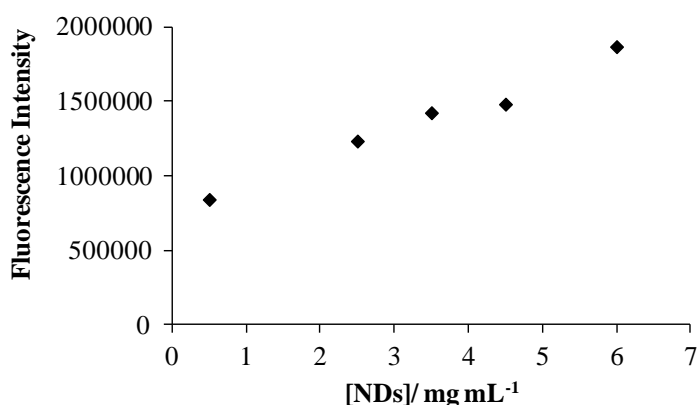


Figure 5. The effect of the nanodiamonds (NDs) concentration on the fluorescence intensity of fluoranthene after carrying out the cloud point procedure under the following conditions: 90 $\mu\text{g L}^{-1}$ of fluoranthene, different concentrations of nanodiamonds, 0.1 mol L⁻¹ of SDS, 0.25 mol L⁻¹ of NaCl, room temperature.

3.6. Elution

Acetonitrile, hexane and octane were tested as eluents in order to extract the analyte from the surfactant-rich phase in which it remains interacting with both NDs and micellar aggregates. Acetonitrile led to a higher extraction of analyte from the enriched phase and it was chosen as optimum for all experiments. Once the eluent was chosen, three different elution volumes (1, 1.5 and 2 mL) were studied. 1.5 mL of acetonitrile provided the best results. In all cases, 5 min were enough to achieve the elution of fluoranthene from the enriched phase. A 5 min centrifugation step prior to the fluorescence

III.1. Nanodiamonds assisted-cloud point extraction

measurements was necessary to remove the nanoparticles that had been transferred from the surfactant-rich phase into the solvent.

3.7. Analytical performances and applicability to real samples

Under optimum experimental conditions (see Table 2), the relationship between the response (fluorescence) and the initial analyte concentration was investigated by determining the amount of fluoranthene at different concentrations.

Table 2. Optimum experimental conditions for the nanodiamonds assisted-cloud point extraction.

Variables	Optimized value
Ionic strength	0.25 mol L ⁻¹ of sodium chloride
Concentration of surfactant	0.1 mol L ⁻¹ of sodium dodecyl sulfate
Concentration and type of nanoparticle	6 mg mL ⁻¹ of nanodiamonds
Temperature	Room temperature
Sonication time nanoparticles-surfactant (min)	30
Incubation time nanoparticles-surfactant-analyte (min)	10
Incubation time with the electrolyte (min)	60
Elution	1.5 mL of acetonitrile

The calibration graph using the developed method was linear in the range of 0.05–0.3 mg L⁻¹ of fluoranthene, but it became asymptotic at higher concentrations. The obtained equation in the lineal range was $Y=1.926 \times 10^7 X + 138710$; $R^2= 0.9938$, where Y is the fluorescence value obtained after the complete experimental procedure and X is the initial fluoranthene concentration present in the water samples in mg L⁻¹. For a constant ND concentration (also supposing a constant SDS concentration), an increase in the analyte concentration in solution above the lineal range of the calibration graph implies a progressive reduction of the availability of the sorption places until

BLOQUE III. NANOPARTÍCULAS COMO HERRAMIENTAS ANALÍTICAS

reaching the total saturation of these places. This mechanism would explain the change of the linear response into an asymptotic curve above 0.3 mg L^{-1} of analyte in solution. The limit of detection (LOD) was 0.017 mg L^{-1} while the limit of quantitation (LOQ) was 0.05 mg L^{-1} . The reproducibility of the complete experimental procedure was calculated as % relative standard deviation for 4 replicates containing 0.160 mg L^{-1} of fluoranthene and was found to be 4.8 %.

The proposed method was applied to the determination of fluoranthene in river water samples from the Guadalquivir River (Córdoba, Spain). Since there were no real positive samples, it was necessary to spike the samples with fluoranthene at a concentration of 0.060 mg L^{-1} . Samples were filtered previous to the extraction. Acceptable results for the RSD (6.6%) and recoveries above 65% were finally obtained by the optimized procedure.

Although it is true that previously published works on the determination of fluoranthene by cloud point extraction have reported much better LOD values than those presented here, the experimental procedures in most of these cases entailed an incubation time of at least 60 min with the application of heat to observe phase separation. In these studies, incubation times of up to 48 h have also been described. The obtained RSD values were found to be quite satisfactory and the recoveries were acceptable. The most remarkable contribution of the work presented here was that, under the experimental conditions set (0.1 M SDS, 0.25 M NaCl and room temperature), the presence of the NDs allowed the formation of two clearly defined phases and therefore the NDs were found to be essential for the analytical performance. This was demonstrated when experiments conducted in the absence of these nanoparticles failed in terms of phase separation. As far as the drawbacks of the proposed method are concerned, it should be noted that the sensitivity is limited in comparison to that found for other already described methods^{6,23-25,32} and therefore, this experimental approach would not be recommendable

III.1. Nanodiamonds assisted-cloud point extraction

for those cases in which severe sensitivity restrictions are required. On the other hand, no special temperature requirements or excessively long incubation times are needed what simplify considerably the procedure in comparison to other described experimental approaches.^{23,25,26} Going back to the previously mentioned subject concerning the role of the carbon nanoparticles in assisting the conventional cloud point technique, this work confirmed finally that the NDs are essential for the formation of two phases, although no enhanced extraction efficiencies were observed with respect to the related literature.^{6, 23-25,32}

4. CONCLUSION

Nanodiamonds assisted-cloud point extraction followed by a fluorimetric detection has been applied to the determination of fluoranthene in river water. The effect of the introduction of nanoparticles as a third phase in the conventional cloud point scheme applied to the determination of an organic contaminant has been studied for the first time. In an experimental procedure carried out at room temperature with SDS as surfactant and NaCl as electrolyte, it was demonstrated that the presence of the NDs was essential for phase separation. In comparison to the related literature, the developed method was less time consuming^{23,26} and without temperature requirements²³⁻²⁵ what enables its application to cases in which a high sensitivity is not required. The determination of fluoranthene by the optimized method led to acceptable recovery values (>65%) and a good RSD (6.6%) for the spiked river water samples, demonstrating thereby the versatile application of CNPs in sample treatment processes.

Acknowledgments

The authors would like to express their gratitude to the Spanish Ministry of Economy and Competitiveness for project CTQ2011-23790 and to Junta de Andalucía for the project FQM-4801. E. Caballero-Díaz also wishes to thank the Ministry for the award of a Research Training Fellowship (Grant AP2008-02955).

References

- 1 E. K. Paleologos, D. L. Giokas and M. I. Karayannis, *TrAC*, 2005, **24**, 426.
- 2 T. Tang, K. Qian, T. Shi, F. Wang, J. Li and Y. Cao, *Anal. Chim. Acta*, 2010, **680**, 26.
- 3 Z. S. Ferrera, C. P. Sanz, C. M. Santana and J. J. S. Rodríguez, *TrAC*, 2004, **23**, 469.
- 4 R. Kjellander and E. Florin, *J. Chem. Soc., Faraday Trans.*, 1981, **177**, 2053.
- 5 M. F. Silva, E. S. Cerutti and L. D. Martinez, *Microchim. Acta*, 2006, **155**, 349.
- 6 I. Y. Goryacheva, S. N. Shtykov, A. S. Loginov and I. V. Panteleeva, *Anal. Bioanal. Chem.*, 2005, **382**, 1413.
- 7 K. Yang and B. Xing, Abstracts of Papers, 240th *ACS National Meeting*, Boston, MA, United States, 2010.
- 8 R. Skorek, E. Turek, B. Zawisza, E. Margui, I. Queralt, M. Stempin, P. Kucharski and R. Sitko, *J. Anal. At. Spectrom.*, 2012, **27**, 1688.
- 9 J. M. Jiménez Soto, S. Cárdenas and M. Valcárcel, *J. Chromatogr. A*, 2012, **1245**, 17.
- 10 A. El-Sheikh, M. Al-Jafari and J. Sweileh, *Int. J. Environ. Anal. Chem.*, 2011, **92**, 1.
- 11 A. S. Barnard, *Analyst*, 2009, **134**, 1751.
- 12 R. A. Shimkunas, E. Robinson, R. Lam, S. Lu, X. Xu, X.-Q. Zhang, H. Huang, E. Osawa and D. Ho, *Biomaterials*, 2009, **30**, 5720.
- 13 V. P. Isakov, A. I. Lyamkin, D. N. Nikitin, A. S. Shalimova and A. V. Solntsev, *Prot. Met. Phys. Chem. Surf.*, 2010, **46**, 578.
- 14 R. Zhang, Z. Shi, Y. Liu and J. Yin, *J. Appl. Polym. Sci.*, 2012, **125**, 3191.
- 15 H. Gomez, M. K. Ram, F. Alvi, E. Stefanakos and A. Kumar, *J. Phys. Chem. C*, 2010, **114**, 18797.
- 16 M. G. Ivanov, S. V. Pavlyshko, D. M. Ivanov, I. Petrov, G. McGuire and O. Shenderova, *Mater. Res. Soc. Symp. Proc.*, 2010, **1203**, 89.
- 17 J.-I. Chao, E. Perevedentseva, P.-H. Chung, K.-K. Liu, C.-Y. Cheng, C.-C. Chang and C.-L. Cheng, *Biophys. J.*, 2007, **93**, 2199.
- 18 K. V. Purtov, A. P. Puzyr and V. S. Bondar, *J. Biochem. Mol. Biol.*, 2008, **419**, 72.
- 19 Y. Zhu, J. Li, W. Li, Y. Zhang, X. Yang, N. Chen, Y. Sun, Y. Zhao, C. Fan and Q. Huang, *Theranostics*, 2012, **2**, 302.

BLOQUE III. NANOPARTÍCULAS COMO HERRAMIENTAS ANALÍTICAS

- 20 X. Kong and P. Cheng, *Materials*, 2010, **3**, 1845.
- 21 J.-F. Liu, J.-B. Chao, R. Liu, Z.-Q. Tan, Y.-G. Yin, Y. Wu and G.-B. Jiang, *Anal. Chem.*, 2009, **81**, 6496.
- 22 M. F. Nazar, S. S. Shah, J. Eastoe, A. M. Khan and A. Shah, *J. Colloid Interface Sci.*, 2011, **363**, 490.
- 23 C. F. Li, J. W. C. Wong, C. W. Huie and M. M. F. Choi, *J. Chromatogr. A*, 2008, **1214**, 11.
- 24 B. Delgado, V. Pino, J. H. Ayala, V. González and A. M. Afonso, *Analyst*, 2005, **130**, 571.
- 25 B. Delgado, V. Pino, J. H. Ayala, V. González and A. M. Afonso, *Anal. Chim. Acta*, 2004, **518**, 165.
- 26 K.-C. Hung, B.-H. Chen and L. E. Yu, *Sep. Purif. Technol.*, 2007, **57**, 1.
- 27 S. Xie, M. C. Paau, C. F. Li, D. Xiao and M. M. F. Choi, *J. Chromatogr. A*, 2010, **1217**, 2306.
- 28 R. Rastogi, R. Kaushal, S. K. Tripathi, A. L. Sharma, I. Kaur and L. M. Bharadwaj, *J. Colloid Interface Sci.*, 2008, **328**, 421.
- 29 L. Vaisman, H. D. Wagner and G. Marom, *Adv. Colloid Interface Sci.*, 2006, **128-130**, 37.
- 30 V. Pino, J. H. Ayala, A. M. Afonso and V. González, *J. Chromatogr. A*, 2002, **949**, 291.
- 31 M. Valcárcel, S. Cárdenas, B. M. Simonet, Y. Moliner-Martínez and R. Lucena, *TrAC*, 2008, **27**, 34.
- 32 D. Sicilia, S. Rubio, D. Pérez-Bendito, N. Maniasso and E. A. G. Zagatto, *Anal. Chim. Acta*, 1999, **392**, 29.

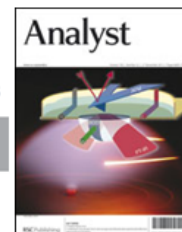
III.2. Liquid-liquid extraction assisted by a carbon nanoparticles interface

Analyst

RSC | Advancing the
Chemical Sciences

PAPER

Analyst, 2013, **138**, 5913



Liquid-liquid extraction assisted by a carbon nanoparticles interface. Electrophoretic determination of atrazine in environmental samples

Encarnación Caballero-Díaz, Bartolomé M. Simonet, Miguel Valcárcel

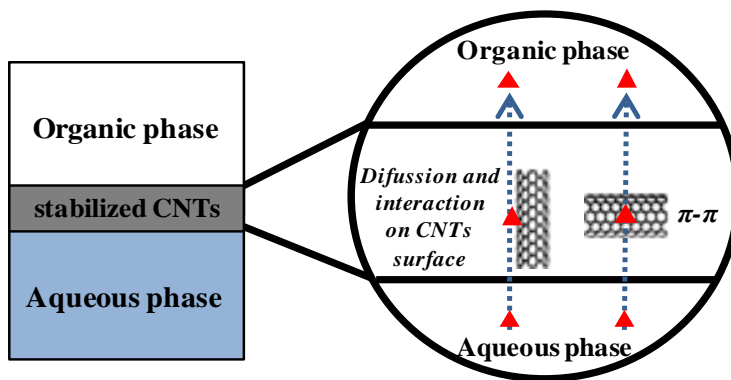
Department of Analytical Chemistry, Marie Curie Building (Annex), Campus de Rabanales, University of Córdoba, 14071 Córdoba, Spain

ABSTRACT

A novel method for the determination of atrazine, using liquid-liquid extraction assisted by a nanoparticles film formed *in situ* and composed of organic solvent stabilized-carbon nanoparticles, is described. The presence of nanoparticles located at the liquid-liquid interface reinforced the extraction of analyte from matrix prior to capillary electrophoresis (CE) analysis. Some influential experimental variables were optimized in order to enhance the extraction efficiency. The developed procedure confirmed that carbon nanoparticles, especially multi-walled carbon nanotubes, are suitable to be used in sample treatment processes introducing new mechanisms of interaction with the analyte. The application of the proposed preconcentration method followed by CE detection enabled the determination of atrazine in spiked river water providing acceptable RSD values (11.6%) and good recoveries

(about 87.0–92.0%). Additionally, a similar extraction scheme was tested in soil matrices with a view to further applications in real soil samples.

GRAPHICAL ABSTRACT



1. INTRODUCTION

The excessive and uncontrolled use of herbicides in agriculture crops causes the contamination of soils, and due to their persistence and mobility, the surface and ground waters are also affected by mechanisms such as the leaching or runoff of these compounds.

Atrazine (2-chloro-4-ethylamino-6-isopropylamino-1,3,5-triazine) is a herbicide belonging to the triazines family and it is widely used for broadleaf and grassy weed control. Among its known toxic effects, its estrogenic activity should be pointed out since this herbicide acts as environmental endocrine disruptor resulting in high toxicity.¹ As a consequence, atrazine has been already determined in different kinds of environmental matrices such as soils,² groundwater,³ surface waters⁴ and atmosphere.⁵ The analytical techniques frequently reported in the detection of this herbicide focus on liquid or gas chromatography optionally coupled with mass spectrometry,^{6,7} although to a lesser extent, capillary electrophoresis,⁸ immunoassay,⁹ voltammetry¹⁰ and spectrophotometry¹¹ among others techniques, have been also used with this same purpose. In most cases, a preconcentration step prior to analytical detection is necessary since herbicides are usually found at low concentrations in waters. Liquid-liquid extraction (LLE),¹² solid-phase extraction (SPE),¹³ solid phase microextraction (SPME),¹⁴ and liquid phase microextraction (LPME)⁷ have been reported as sample treatment techniques in order to extract atrazine from different matrices, SPE being the most widely described technique to date.

The use of nanoparticles as components of the extracting phase in liquid extraction procedures has gained importance. Carbon nanotubes (CNTs) are considered as excellent sorbents for organic compounds due to their large adsorption surface and high affinity for these compounds.¹⁵ Nanodiamonds (NDs), carbon nanoparticles with a truncated octahedral architecture, have also

been extensively investigated because of their high adsorption capacity and specific surface area, however their applications in sample treatment processes are still reduced. Their sorption properties make carbon nanoparticles potentially useful in membrane extraction processes. The limitations of conventional polymeric membranes used for water purification¹⁶ and gas separation¹⁷ lie in their low selectivity, permeability, susceptibility to the obstruction or fouling (what results in a reduced diffusion flux), as well as low chemical and thermal resistance. The use of CNT-based membranes has considerably increased in these application fields and offers possibilities to improve the extraction efficiency by adding new channels to mass transfer. These membranes consist of CNTs embedded in a polymer matrix, so that the selectivity and permeability of analytes are improved in comparison to those for non-modified membranes.¹⁸ These membranes have been fabricated using different polymeric matrices such as polyethersulfone (PES),¹⁹ poly(bisphenol A-co-4-nitrophthalic anhydride-co-1,3-phenylenediamine) (PBNPI),²⁰ polysulfone (PSF)²¹ or polyamide.²² This modality of CNT modified-membranes has already been used to extract toluene and naphthalene from aqueous matrices,²³ or caffeic acid from herbal extracts.²⁴ In a typical CNT mediated-membrane extraction, when the two phases come into contact at the pores, the interactions can take place *via* rapid solute exchange on the CNTs, thus accelerating the effective rate of mass transfer and flux.²⁵

We propose here to eliminate the polymeric support of the extraction membrane and to replace it by a carbon nanoparticles film or interface through which the analyte molecules diffuse from aqueous phase to organic phase. Consequently, it was not necessary to fabricate a nanocomposite (nanoparticles and polymeric matrix) to conduct the extraction procedure. In this study the potential of different carbon nanoparticles as additional phase in the liquid-liquid extraction of atrazine was therefore evaluated by the formation *in situ* of a film of nanoparticles located at the interface between both donor (aqueous)

III.2. Liquid-liquid extraction assisted by a carbon nanoparticles interface

and acceptor (organic) phases. The developed extraction method was applied to the determination of atrazine in spiked river water samples followed by CE analysis. Additionally, a similar extraction procedure was proposed and successfully tested in soil matrices.

2. MATERIALS AND METHODS

2.1. Instrumentation

Capillary electrophoresis was performed on a Beckman Coulter (Palo Alto, CA, USA) MDQ instrument equipped with an on-column UV detector and a diode array detector (DAD). The instrumental setup was governed, and data were acquired and processed by using the software 32 Karat.

2.2. Reagents

Multi-walled carbon nanotubes (MWCNTs) with diameters between 110–170 nm and 2 μm long were obtained from Mer (Tucson, AZ, USA). Single-walled carbon nanotubes (SWCNTs) with diameters lower than 2 nm and lengths between 5 and 15 μm were provided by Shenzhen Nanotech Port Co. Ltd (NTP) (China). Nanodiamonds with appearance of grey powder (ND_s) (>98%; 3.2 nm average particle size) and oleophilic nanodiamonds (ND_o) (>55–75%; 4–15 nm average particle size) were all supplied by NaBond (China).

Sodium hydrogen phosphate, acetonitrile and ethanol were supplied by Panreac (Barcelona, Spain). Sodium dodecyl sulfate (SDS) and ethylacetate anhydrous (99.8%) were obtained from Sigma-Aldrich (Madrid, Spain). Atrazine (2-chloro-4-ethylamine-6-isopropylamino-s-triazine) was selected as target analyte and was purchased from Sigma-Aldrich (Madrid, Spain).

Stock standard solutions (1000 mg L⁻¹ and 100 mg L⁻¹) were prepared in methanol and stored at 4 °C.

2.3. Electrophoretic conditions

CE separations were accomplished by using an uncoated fused-silica capillary of 75 µm ID with effective length between the inlet and detector being 50 cm (total length of 60.2 cm). The electrophoretic buffer was composed of 10 mM sodium hydrogen phosphate, 20 mM SDS and 4% acetonitrile at pH 9.0. The capillary cartridge and samples were kept at 20 °C throughout the process. Samples were injected in the hydrodynamic mode at 0.5 psi for 10 s. Tests were carried out in the positive polarity mode, using a detection wavelength of 222 nm and a constant voltage of 15 kV. For the initial conditioning of the capillary, this was sequentially rinsed with 1M HCl, purified water, 0.1 M NaOH and purified water for 5 min each, and finally with running buffer for 15 min. Between runs, the capillary was flushed sequentially at 20 psi with 0.1 M NaOH (2 min), purified water (2 min) and electrophoretic buffer (2 min). All electrophoretic conditions were taken from the existing literature.²⁶

2.4. Extraction procedure for water samples

Fig. 1 summarizes the experimental scheme carried out for water samples. The carbon nanoparticles interface was first prepared by mixing in a mortar 5 mg of carbon nanoparticles with 1 mL of ethylacetate up to homogeneity. 20 mL of spiked river water were placed in a 50 mL separatory funnel and then, the carbon nanoparticles phase was added. Subsequently, another 3 mL of ethylacetate were added to the funnel, and this was manually shaken for one minute. A 15 min rest time was enough to clearly distinguish the two immiscible phases: an upper organic phase and a lower aqueous phase, separated from each other by an ethylacetate stabilized-carbon nanoparticles

III.2. Liquid-liquid extraction assisted by a carbon nanoparticles interface

film. Later, the upper organic phase was transferred with a Pasteur pipette into a glass tube and centrifuged at 4000 rpm for 5 min in order to remove those nanoparticles that could have been taken together with the upper phase. Subsequently, 1.4 mL of ethylacetate was transferred into a 4 mL glass vial and dried under a flow of nitrogen at room temperature. The transferred ethylacetate volume remained constant in all experiments. This was finally reconstituted in 100 μ L of 2:8 v/v ethanol:Milli-Q water (Millipore, Bedford, MA, USA) prior to CE analysis.

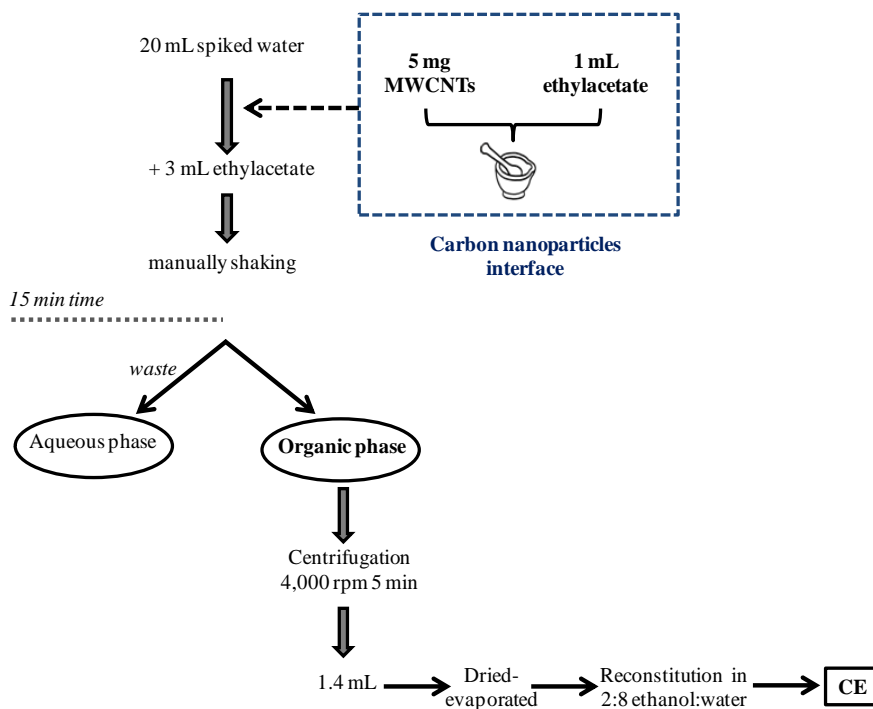


Figure 1. Schematic of the experimental procedure developed for aqueous matrices.

2.5. Extraction procedure for soil matrices

Fig. 2 shows the experimental procedure followed for soil matrices. 200 mg of soil sample were placed in a centrifuge tube, and then, 3 mL of water was added. The sample was necessarily spiked, because of the lack of positive

BLOQUE III. NANOPARTÍCULAS COMO HERRAMIENTAS ANALÍTICAS

samples, by the addition of a standard of atrazine in methanol. This type of spiking was taken from existing literature.^{27,28} The mixture was manually shaken and left in contact for 20 min to favor the interaction between analyte and matrix. Meanwhile, the carbon nanoparticles interface was prepared by mixing in a mortar 2 mg of nanoparticles with 1 mL of ethylacetate up to homogeneity. Subsequently, the interface was added to the centrifuge tube (that contains soil suspension) and then the mixture was manually shaken for one minute. The carbon nanoparticles interface was left in contact with the soil suspension for 60 min before transferring the supernatant into a clean glass vial. Then, another 1 mL of ethylacetate was added to the suspension and this was again manually shaken for one minute. After 15 min, the supernatants were combined. Finally, the resulting supernatant was dried under a flow of nitrogen at room temperature into a 4 mL glass vial, and then reconstituted in 100 μ L of 2:8 v/v ethanol:Milli-Q water (Millipore, Bedford, MA, USA) prior to CE analysis.

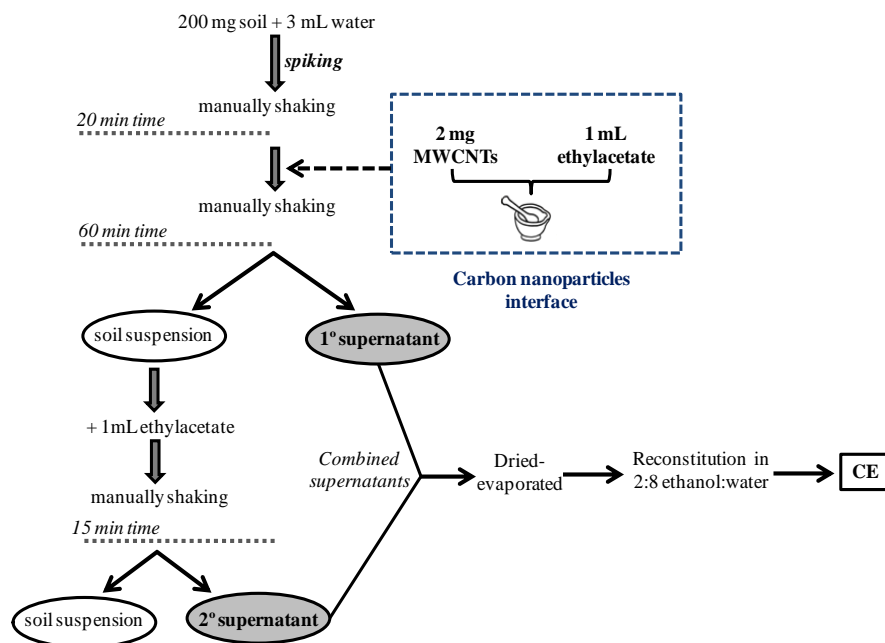


Figure 2. Schematic of the experimental procedure developed for soil matrices.

III.2. Liquid-liquid extraction assisted by a carbon nanoparticles interface

2.6. Determination in environmental samples

River water samples were collected from the Guadalquivir River (Córdoba, Spain). Because there were no real positive samples, these were necessarily spiked with a standard of atrazine in methanol, and carefully homogenized before extraction. A 20 mL aliquot was subjected to the previously described experimental procedure. Some preliminary studies were carried out in agricultural soil reference materials (Barcelona University) with a view of future applications in real samples.

3. RESULTS AND DISCUSSION

In this paper, the potential of different carbon nanoparticles (CNPs) as additional extracting phase for assisting the classic liquid–liquid extraction was studied. A CNPs interface was formed *in situ* and located between the aqueous and organic phases in such a way that both immiscible phases come into contact at the CNP film. The basis is similar to the CNPs mediated-membrane extraction, but with the difference that here any polymeric matrix is used to support nanoparticles, and consequently, these do not need to be functionalized to improve their adhesion to the membrane. It is described²³ that the inclusion of CNPs in the liquid–liquid system modifies the analyte transport from the aqueous phase to organic phase accelerating the flux rate. A higher flux of analyte can be achieved by increasing the effective surface area and partition coefficients, and also by reducing the membrane thickness. These conditions may be achieved by the inclusion of a thin nanoparticles film in the liquid–liquid interface.

Nanoparticles act as nano-scale carriers and solid-phase extractants that interact with analyte molecules and transfer them from donor to acceptor phases by consecutive adsorption–desorption mechanisms. The sorption sites

on CNPs are easily accessible since these nanoparticles are not embedded into a membrane, so that more specific surface area is available to interact with the analyte. In general, the mechanism of solute transfer involves both liquid- and solid-phase extractions since there are two extractants in the system, the organic phase and CNPs. The global effect is to increase the solute partition coefficient and its permeability.²³

In order to obtain high extraction efficiency, parameters such as the evaporation method, the organic phase volume, and the type and concentration of CNPs, were optimized using aqueous standards spiked at a concentration of 5 mg L⁻¹. Peak area at 222 nm was selected for the quantification in all cases.

3.1. Effect of the evaporation method on the analytical performance

Once the organic phase is separated by centrifugation, 1.4 mL of this is transferred into a vial for its evaporation and posterior reconstitution in 100 µL of 2:8 v/v ethanol:Milli-Q water prior to CE analysis. The evaporation procedure was studied by two different approaches in order to achieve a greater process efficiency. The results of analysis of atrazine standards prepared in ethylacetate (at 20 mg L⁻¹), evaporated and reconstituted in 100 µL of 2:8 ethanol:Milli-Q water, were compared to those obtained from directly measuring atrazine standards prepared in 2:8 ethanol:Milli-Q water at the same concentration. On the first approach, standards were evaporated into a 4 mL vial until about a 0.2 mL volume left, and then this was transferred into a CE minivial and evaporated to dryness. The reconstitution in 100 µL of 2:8 v/v ethanol:Milli-Q water and the posterior injection in CE was carried out in that same minivial. In a second approach, standards were evaporated to dryness in a 4 mL vial and then reconstituted and transferred into a minivial prior to CE analysis. The performance of evaporation and reconstitution steps was calculated by the ratio between, the analytical signal obtained in procedures in which standards were

III.2. Liquid-liquid extraction assisted by a carbon nanoparticles interface

evaporated, and that obtained for standards measured directly. The second approach allowed us to obtain a higher analytical signal reducing the loss of analyte in the evaporation and reconstitution stages. And it is that when evaporation occurs, a portion of the analyte can remain on the walls of the vial, what consequently leads to the loss of analyte whether an ideal reconstitution is not achieved later. If one takes into account that for the first approach the complete evaporation stage took place in two different vials, and for the second approach it occurred in only one vial, it is logical to conclude that the loss of analyte during the complete evaporation process was lower for the second approach. Additionally, the reproducibility of this evaporation method was calculated and it resulted to be 3.6% (n=4). Consequently, this second approach was selected as optimum to conduct the rest of experiments.

3.2. Extraction time

The extraction time is a key parameter because it influences the partition of the analyte between the donor and acceptor phases. The interface consisted of a porous layer through which the analyte was transported by diffusion through pores and the surface of CNPs. Therefore, the porosity of these nanoparticles should strongly affect the extraction dynamics. Nanometer-sized pores might lead to a longer equilibrium time for the extraction of atrazine, compared to the conventional liquid-liquid membrane extraction. Although a maximum sensitivity is achieved under equilibrium conditions, it is not necessary for routine analyses to reach equilibrium as long as the extraction time is kept constant.²⁴ Taking into account these considerations, 15 min was chosen as extraction time for all experiments based on a balance between a good sensitivity and analysis speed.

3.3. Optimization of the type of CNPs

Different types of CNPs were investigated in order to select the most appropriate for the proposed extraction method. We focused on CNPs because they have been widely described as sorbents of organic compounds such as triazines.^{29,30} Single- (SWCNTs) and multi-walled carbon nanotubes (MWCNTs), and two different kinds of nanodiamonds (ND_s and ND_{ol}), were tested as components of the film or interface to perform the extraction. Control experiments without CNPs were taken as reference. The results are shown in Fig. 3, and concluded that MWCNTs were optimum in order to achieve a higher extraction of atrazine. The procedure carried out in the presence of nanodiamonds (both studied types) resulted longer and tedious because these nanoparticles remained in suspension and did not form a clear film at the liquid-liquid interface, what dragged out the extraction until the two immiscible phases were clearly distinguished. In this case, no additional centrifugation step was included in order not to alter the experimental conditions with respect to those used in the procedures for the rest of the studied nanoparticles. In the absence of nanoparticles, the extraction efficiency was inferior to that found for the experiments with nanoparticles, which confirms that CNPs provide additional avenues for solute transport from donor to acceptor phases, and reinforce the extraction by a combination of liquid- and solid-phase extractions. Higher analytical signals were obtained for MWCNTs and SWCNTs, being slightly superior for MWCNTs, so that this type of CNPs was finally chosen as optimum to perform the experimental procedure.

III.2. Liquid-liquid extraction assisted by a carbon nanoparticles interface

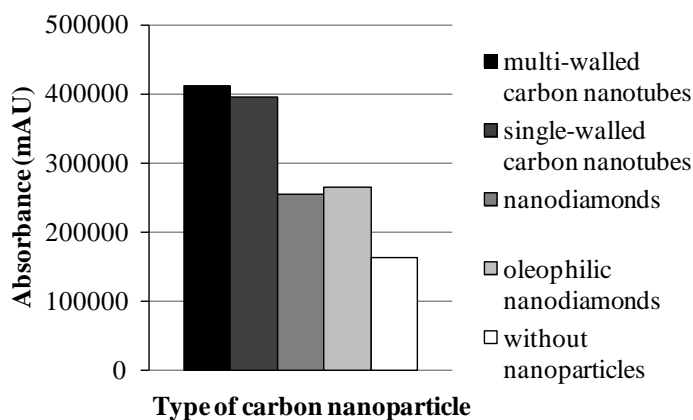


Figure 3. Effect of type of CNPs on the method performance. Conditions: analyte concentration, 5 mg L^{-1} ; film, 2 mg of different CNPs and 1 mL of ethylacetate; aqueous phase volume, 20 mL; total organic phase volume, 4 mL; extraction time, 15 min.

3.4. Optimization of MWCNTs concentration

The influence of concentration of CNPs on the extraction capacity of atrazine was studied by experiments in which the film was prepared by mixing different amounts of MWCNTs with 1 mL of ethylacetate. The rest of experimental conditions such as volume of aqueous phase (20 mL), total volume of ethylacetate (4 mL), and type of CNPs (MWCNTs), remained always constant. Fig. 4 shows that the analytical signal varies depending on the amount of MWCNTs used to prepare the film. This amount is expressed as the concentration of MWCNTs in aqueous phase volume (mg MWCNTs per mL of water). An increase in the extraction up to 0.25 mg mL^{-1} can be observed. Higher concentrations resulted in worse extraction efficiencies since CNPs tended to form a denser layer, decreasing pore size and, therefore, reducing the permeability of analyte. Consequently, 0.25 mg mL^{-1} was the selected MWCNTs concentration.

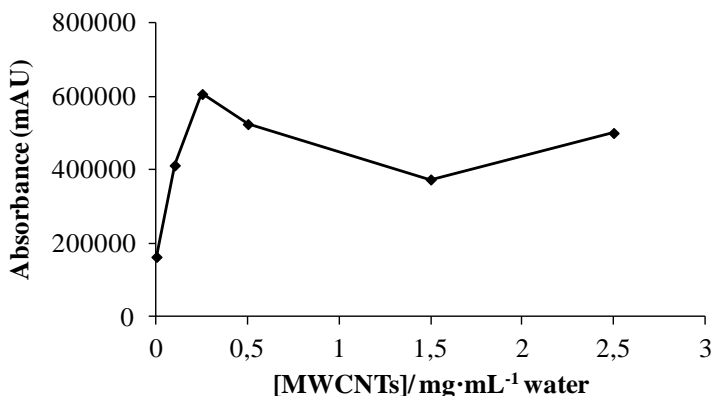


Figure 4. Effect of MWCNTs concentration on the method performance. Conditions: analyte concentration, 5 mg L⁻¹; film, different amounts of MWCNTs and 1 mL of ethylacetate; aqueous phase volume, 20 mL; total organic phase volume, 4 mL; extraction time, 15 min.

3.5. Optimization of organic phase volume

Ethylacetate was chosen as extracting organic phase taking as reference the existing literature about adsorption of atrazine on CNPs.²⁹ In this study, the optimum volume of the organic solvent was also investigated. To this end, atrazine was extracted with different volumes of ethylacetate (2, 4, 6, and 10 mL) for a constant volume of aqueous phase. In all cases, the added MWCNTs interface was composed of 1 mL of ethylacetate which was also taken into account in the total volume of ethylacetate used. Fig. 5 represents the variation of the analytical signal depending on the organic phase volume as well as the enrichment factors calculated for each one of the conditions. It is clear that by increasing the volume of the extraction solvent, recovery also increases, and this is what occurs from 2 to 4 mL of ethylacetate. However, at higher organic phase volumes the enrichment factor (EF) decreases and as a consequence, the analytical signal. For this reason, 4 mL of ethylacetate, from which 1 mL was used to prepare the CNPs film, was selected as optimum organic phase volume.

III.2. Liquid-liquid extraction assisted by a carbon nanoparticles interface

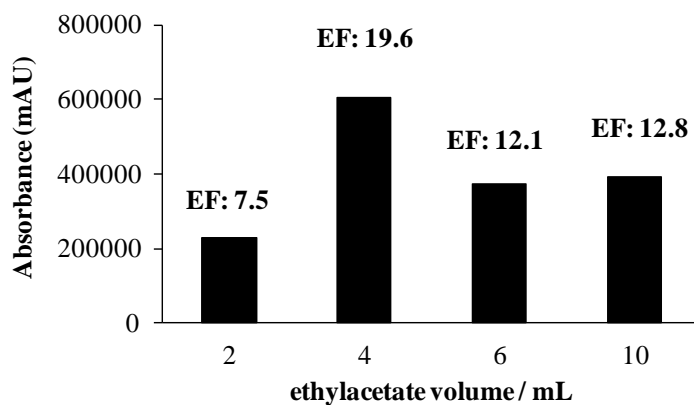


Figure 5. Effect of ethylacetate volume on the method performance. Conditions: analyte concentration, $5 \text{ mg}\cdot\text{L}^{-1}$; film, 5 mg of MWCNTs and 1 mL of ethylacetate; aqueous phase volume, 20 mL; extraction time, 15 min. EF: enhancement factors obtained for each volume studied.

3.6. Applicability in environmental samples

Most studies were developed in water samples although some proofs were additionally carried out in soil matrices with the objective of testing the versatility of the MWCNTs interface for other environmental matrices.

3.6.1. Study of interferences in river water

The interferences of river water with the analytical signal were considered in this work. To this end, 1 mL of both river water sample and ethylacetate were manually shaken for 1 min. Once two immiscible phases were clearly distinguished, the organic phase was transferred into a 4 mL glass vial, evaporated to dryness, and reconstituted in 100 μL of 20 mg L^{-1} atrazine standard in 2:8 ethanol:water prior to CE analysis. In this case, the added atrazine interacts with the possible interferences from the matrix that have been previously extracted with ethylacetate. The results were compared to those obtained when standards of atrazine in ethylacetate (at the same

BLOQUE III. NANOPARTÍCULAS COMO HERRAMIENTAS ANALÍTICAS

concentration) were evaporated to dryness and reconstituted in 100 μL of 2:8 ethanol:water. For this last case, no river water matrix interferences were present. Neither the atrazine quantitative extraction nor the baseline noise of electropherograms was negatively affected by the interferences present in river water, and consequently, no river water sample pretreatment was required before the extraction procedure for removing the interferences present.

3.6.2. Analytical performances of proposed methods for water and soil.

Table 1 summarizes the analytical figures of merit of the proposed methods applied to both aqueous and soil matrices. Under optimum experimental conditions, the relationship between the analytical signal (absorbance) and initial concentration of analyte in aqueous standards was investigated by determining atrazine at different concentrations (1–50 mg L^{-1}). The reproducibility of the complete experimental procedure was calculated as the percentage of relative standard deviation for 3 replicates containing 5 mg L^{-1} of atrazine, and it resulted to be 9.0%.

Table 1. Analytical performances of the proposed methods in different environmental matrices.

CNP ^a involved	Matrix	Linear equation	R ² ^b	LOD ^c	LOQ ^d
MWCNTs	water	Y= 42401X + 434751	0.9813	0.5	1
MWCNTs	soil	Y= 35913X + 33460	0.9686	0.2	0.5

^a CNP: Carbon nanoparticle; MWCNTs: multi-walled carbon nanotubes. ^b R²: correlation coefficient for five (aqueous samples) or six (soil samples) standards. ^c LOD: Limit of detection in mg L^{-1} , which is the analyte concentration which produces a signal that can be statistically distinguished from the blank signal. ^d LOQ: Limit of quantification in mg L^{-1} , which is the analyte concentration which produces a signal than can be considered the lower limit of the linear range of the calibration curve.

III.2. Liquid-liquid extraction assisted by a carbon nanoparticles interface

The proposed method was applied to the determination of atrazine in river water samples from the Guadalquivir River (Córdoba, Spain). Since there were no positive real samples, these were spiked at 5 mg L⁻¹. Water samples were not subjected to a filtration stage prior to the extraction method. The recoveries were calculated by the ratio between the analytical signals obtained carrying out the procedure in aqueous standards, and those obtained by the procedure applied to river water samples, both spiked at the same concentration. Acceptable results of RSD (11.6%, n=3) and relative recoveries about 87.0–92.0% were finally obtained. Fig. 6 shows the electropherograms obtained for a blank and a river water sample spiked at 5 mg L⁻¹ both subjected to the experimental procedure proposed for water samples.

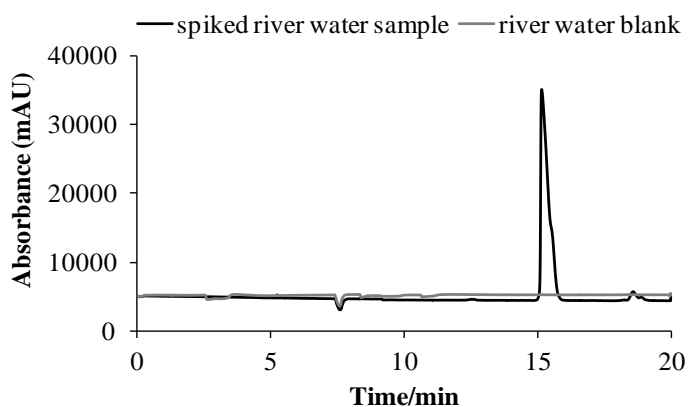


Figure 6. Electropherograms obtained for a river water blank and sample spiked at 5 mg L⁻¹ both subjected to the experimental method described for water samples.

Preliminary studies using a MWCNT interface were conducted on agricultural soil reference materials spiked at different concentrations of atrazine (0.5–19.6 mg L⁻¹), and they led to acceptable results of extraction taking into account the presence of matrix interferences. Fig. 7 shows the electropherograms obtained for a blank and a sample spiked at 1 mg L⁻¹, both subjected to the experimental procedure proposed for soil samples. The

BLOQUE III. NANOPARTÍCULAS COMO HERRAMIENTAS ANALÍTICAS

complete experimental procedure was carried out without eliminating the soil matrix, although posterior studies about matrix interferences revealed that these were significant. However, good analytical signals were achieved under these conditions. The main aim of this last study was to confirm the versatility of the proposed MWCNTs interface for the extraction of atrazine from different environmental matrices. Obviously, it would be undeniable that, for future applications in real soil samples, the extraction efficiency was maximized by including a prior matrix separation stage and the optimization of all influential variables.

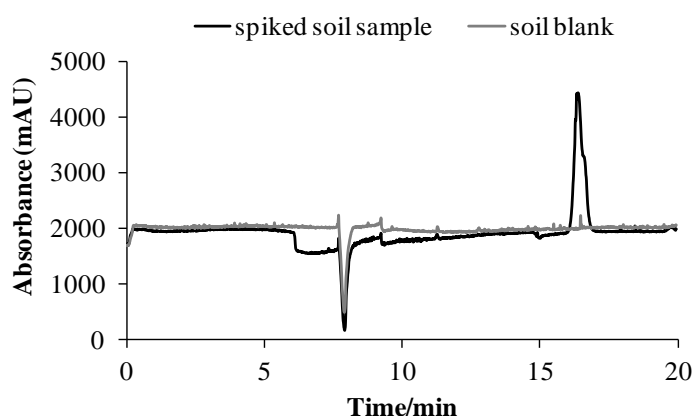


Figure 7. Electropherograms obtained for a soil blank and soil sample spiked at 1 mg L^{-1} both subjected to the experimental method described for soil matrices.

Most published research studies on extraction and determination of atrazine from environmental samples use chromatography as instrumental technique,^{14,31-33} although to a lesser extent capillary electrophoresis has also been used with this same purpose.^{34,35} While the results presented here show a limit of detection superior to those found in related literature,^{34,35} and low enhancement factors, the recovery values are completely in accordance with those reported in other studies.³⁵ Regarding the extraction time, this is relatively short for water samples (being inferior to 30 minutes), but longer for

III.2. Liquid-liquid extraction assisted by a carbon nanoparticles interface

soil samples, nevertheless, in most cases our extraction times are comparable or inferior to others already described.^{31,36} The novelty of the proposed method is not therefore an enhanced sensitivity with respect to the published literature but the use of a CNPs interface to reinforce the extraction in a conventional liquid–liquid system.

4. CONCLUSION

The use of CNPs as third solid phase in the classic liquid–liquid extraction opens up new possibilities to increase the efficiency of matter transfer between the two immiscible phases. The nanoparticles formed *in situ* a film at the interface, and acted as carriers of the analyte from one phase to another. Their peculiar chemical and physical properties increased the extraction on one hand, and added solid-phase extraction mechanisms on the other. Among the CNPs studied, MWCNTs were the most adequate to perform the proposed extraction procedure. In order to demonstrate the usefulness of the experimental approach, atrazine was selected as target analyte, and river water and agricultural soil were tested as environmental matrices. The obtained results using the proposed interface were quite satisfactory. No doubt this is a promising avenue to improve the conventional liquid–liquid extraction although, needless to say that complementary studies should be made with a view to future applications.

Acknowledgements

The authors would like to express their gratitude to the Spanish Ministry of Economy and Competitiveness for project CTQ2011-23790 and to Junta de Andalucía for the project FQM-4801. E. Caballero-Díaz also wishes to thank the Ministry for the award of a Research Training Fellowship (Grant AP2008-02955).

References

- 1 I. De La Casa-Resino, A. Valdehita, F. Soler, J.M. Navas and M. Pérez-López, *Comp. Biochem. Physiol., Part C: Toxicol. Pharmacol.*, 2012, **156**, 159–165.
- 2 C. Wang, S. Ji, Q. Wu, C. Wu and Z. Wang, *J. Chromatogr. Sci.*, 2011, **49**, 689–694.
- 3 N. Dujakovic, S. Grujic, M. Radisic, T. Vasiljevic and M. Lausevic, *Anal. Chim. Acta*, 2010, **678**, 63–72.
- 4 H. Bagheri, N. Alipour and Z. Ayazi, *Anal. Chim. Acta*, 2012, **740**, 43–49.
- 5 O. Briand, M. Millet, F. Bertrand, M. Clément and R. Seux, *Anal. Bioanal. Chem.*, 2002, **374**, 848–857.
- 6 A. Penetra, V. Vale Cardoso, E. Ferreira and M. J. Benoliel, *Water Sci. Technol.*, 2010, **62**, 667–675.
- 7 M. Shamsipur, N. Fattahi, M. Pirsahab and K. Sharafi, *J. Sep. Sci.*, 2012, **35**, 2718–2724.
- 8 R. Carabias-Martínez, E. Rodríguez-Gonzalo, E. Miranda-Cruz, J. Domínguez-Álvarez and J. Hernández-Méndez, *J. Chromatogr. A*, 2006, **1122**, 194–201.
- 9 Y. Na, W. Sheng, M. Yuan, L. Li, B. Liu, Y. Zhang and S. Wang, *Microchim. Acta*, 2012, **177**, 177–184.
- 10 L.C.S. Figueiredo-Filho, D.C. Azzi, B.C. Janegitz and O. Fatibello-Filho, *Electroanalysis*, 2012, **24**, 303–308.
- 11 U. Tamrakar, S.B. Mathew, V.K. Gupta and A.K. Pillai, *J. Anal. Chem.*, 2009, **64**, 386–389.
- 12 A.T.K. Tran, R.V. Hyne and P. Doble, *Chemosphere*, 2007, **67**, 944–953.
- 13 L.T.D. Cappelini, D. Cordeiro, S.H.G. Brondi, K.R. Prieto and E.M. Vieira, *Environ. Technol.*, 2012, **33**, 2299–2304.
- 14 R.I. Bonansea, M.V. Amé and D.A. Wunderlin, *Chemosphere*, 2013, **90**, 1860–1869.
- 15 R. Lucena, B. M. Simonet, S. Cárdenas and M. Valcárcel, *J. Chromatogr. A*, 2011, **1218**, 620–637.
- 16 G. A. Manella, V. La Carrubba and V. Brucato, *J. Appl. Polym. Sci.*, 2011, **122**, 3557–3563.
- 17 E. Favre, *Compr. Membr. Sci. Eng.*, 2010, **2**, 155–212.

III.2. Liquid-liquid extraction assisted by a carbon nanoparticles interface

- 18 A.V. Herrera-Herrera, M.A. González-Curbelo, J. Hernández-Borges and M.A. Rodríguez Delgado, *Anal. Chim. Acta*, 2012, **734**, 1–30.
- 19 E. Celik, L. Liu and H. Choi, *Water Res.*, 2011, **45**, 5287–5294.
- 20 T. H. Weng, H. H. Tseng and M. Y. Wey, *Int. J. Hydrogen Energy*, 2009, **34**, 8707–8715.
- 21 S. Qiu, L. Wu, X. Pan, L. Zhang, H. Chen and C. Gao, *J. Membr. Sci.*, 2009, **342**, 165–172.
- 22 A.V. Penkova, G.A. Polotskaya, V.A. Gavrilova, A.M. Toikka, J.-C. Liu, M. Trchová, M. Slouf and Z. Pientka, *Sep. Sci. Technol.*, 2009, **45**, 35–41.
- 23 K. Hylton, Y. Chen and S. Mitra, *J. Chromatogr. A*, 2008, **1211**, 43–48.
- 24 Z. Es'haghi, M. Ahmadi, A. Saify, A. Akbar, Z. Rezaeifar and Z. Alian-Nezhadi, *J. Chromatogr. A*, 2010, **1217**, 2768–2775.
- 25 M. Bhadra and S. Mitra, *TrAC*, 2013, **45**, 248–263.
- 26 Y. Moliner-Martínez, M. Barrios, S. Cárdenas and M. Valcárcel, *J. Chromatogr. A*, 2008, **1194**, 128–133.
- 27 G. Shen and H.K. Lee, *J. Chromatogr. A*, 2003, **985**, 167–174.
- 28 T. Dagnac, S. Bristeau, R. Jeannot, C. Mouvet and N. Baran, *J. Chromatogr. A*, 2005, **1067**, 225–233.
- 29 G. Min, S. Wang, H. Zhu, G. Fang and Y. Zhang, *Sci. Total Environ.*, 2008, **396**, 79–85.
- 30 J.M. Jiménez-Soto, S. Cárdenas and M. Valcárcel, *J. Chromatogr. A*, 2012, **1245**, 17–23.
- 31 C. Wang, S. Ji, Q. Wu, C. Wu and Z. Wang, *J. Chromatogr. Sci.*, 2011, **49**, 689–694.
- 32 M. Shamsipur, N. Fattahi, M. Pirsahab and K. Sharafi, *J. Sep. Sci.*, 2012, **35**, 2718–2724.
- 33 M. Pirsahab, N. Fattahl, M. Shamsipur and T. Khodadadi, *J. Sep. Sci.*, 2013, **36**, 684–689.
- 34 C.L. da Silva, E.C. de Lima and M.F.M. Tavares, *J. Chromatogr. A*, 2003, **1014**, 109–116.
- 35 A. Sánchez Arribas, M. Moreno, E. Bermejo, A. Zapardiel and M. Chicharro, *Electrophoresis*, 2011, **32**, 275–283.
- 36 M.F. Amadori, G.A. Cordeiro, C.C. Reboucas, P.G. Peralta-Zamora, M.T. Grassi and G. Abate, *J. Braz. Chem. Soc.*, 2013, **24**, 483–491.

Accepted in Journal of Separation Science DOI 10.1002/jssc.201301204



Carbon nanotubes as SPE sorbents for extraction of salicylic acid from river water

Encarnación Caballero-Díaz, Miguel Valcárcel

Department of Analytical Chemistry, Marie Curie Building (Annex), Campus de Rabanales, University of Córdoba, 14071 Córdoba, Spain

ABSTRACT

This paper deals the ability of different types of carbon nanotubes to adsorb salicylic acid in river water samples. The use of these nanoparticles as sorbent in a SPE procedure prior to CE analysis is essential for improving the enrichment factor and the recovery values. Several experimental variables were optimized in order to maximize the extraction efficiency. The proposed analytical method is simple, short time-consuming, and entails low solvent consumption. Furthermore, salicylic acid could be extracted from river water providing good recovery values in the range from 76.2% to 102.0% (RSD<8.2%). The combination of, the specific chemical properties of analyte, and the unique physicochemical features of carbon nanotubes, sheds new light on the use of these nanoparticles as excellent sorbent materials of pharmaceutical compounds in environmental matrices.

1. INTRODUCTION

Pharmaceutical compounds are a class of emerging pollutants widely used throughout the world and as a consequence, are being continually released into the environment through excreta, or disposal of unused or expired products [1]. Most of them are not entirely eliminated from wastewater treatment plants due to their polarity and high stability [2]. This involves that both parent compounds and their metabolites may finally come into contact with surface waters and therefore, their environmental monitoring has aroused much attention. For this purpose, chromatographic separation followed by mass spectrometric detection seems to be the most popular choice [3-7]. Nevertheless, this instrumentation is very expensive, requires trained personnel, and is not available in all laboratories. Besides, while GC has drawbacks related to the analyte loss during the derivatization process and the background noise, LC presents problems due to the occurrence of matrix effects [6]. On the other hand, there are many compounds that can potentially be assayed by CE, being this a less complex and expensive alternative to chromatographic techniques, but also appropriate for analysis of pharmaceuticals in water samples when no severe sensitivity restrictions are required [8-11].

Nonsteroidal anti-inflammatory drugs are some of the most commonly detected pharmaceuticals [9,12]. Salicylic acid (SA) belongs to this family of compounds and is produced by degradation of acetylsalicylic acid [11]. Several analytical methodologies based on GC or LC coupled to MS have been reported for determining SA in different samples [3,5,13,14], however CE has been also used for this same purpose taking advantage of the ionic nature of this compound [8-10,15,16].

III.3. Carbon nanotubes as SPE sorbents for extraction of salicylic acid

Pharmaceutical residues are usually present at low concentrations in the environment and consequently, their determination requires an enrichment step prior to detection. To this end, different commercial SPE sorbents have been employed including Strata-X, C8, C18, Oasis HLB or Lichrolut EN [1,3,5,17]. The unusual physicochemical properties of carbon nanotubes (CNTs) make them to be promising materials in many analytical applications [13]. In this regard, CNTs have been extensively employed as SPE sorbents thanks to their high specific surface area and excellent ability for sorption of organic compounds [13,18-21]. However, despite their extraordinary features, nanoparticles has been scarcely exploited for extracting pharmaceutical compounds from environmental samples [22,23].

In this work, a simple and low-cost analytical method for determining SA in river water by using CNTs as SPE sorbent is proposed. Three types of CNTs were compared in terms of their ability for sorption of SA in samples. SA was selected as target analyte since it is considered as an emerging pollutant and one of the most studied pharmaceutical compounds in the aquatic environment according to related literature [3,5,6,17]. The proposed analytical method involved an initial preconcentration step using CNTs as sorbent material prior to CE-UV analysis. Several experimental variables were optimized and lastly, the developed analytical procedure was applied to the determination of SA in river water.

2. MATERIALS AND METHODS

2.1. Chemicals and reagents

All chemicals were of analytical reagent-grade. Sodium tetraborate decahydrate (99.5-105.0%) was used to prepare the electrophoretic buffer and was purchased from Sigma-Aldrich (Madrid, Spain). SA (2-hydroxybenzoic acid)

BLOQUE III. NANOPARTÍCULAS COMO HERRAMIENTAS ANALÍTICAS

was selected as target analyte and was also obtained from Sigma-Aldrich (Madrid, Spain). Sodium hydroxide pellets (98.0%; PA-ACS-ISO) and hydrochloric acid (37.0%; HPLC-grade) were supplied by Panreac (Barcelona, Spain), and were employed for adjusting the pH of electrophoretic buffer and samples, respectively. Methanol ($\geq 99.9\%$; HPLC-PLUS gradient) and acetone (99.9%; PAI-ACS) solvents were provided by Carlo Erba reagents (Barcelona, Spain) and Panreac, respectively.

Different types of commercially available CNTs were evaluated as sorbents in this work. Multi-walled CNTs (MWCNTs) of 9.5 nm diameter and 1.5 μm length were obtained from Nanocyl (Belgium) (MWCNTs-nanocyl). MWCNTs with diameters between 5 and 20 nm and lengths between 1 and 10 μm were provided by Bayer (Germany) (MWCNTs-bayer). Single-walled CNTs (SWCNTs) with lower diameters than 2 nm and lengths between 5 and 15 μm were purchased from Shenzhen Nanotech Port (China).

Stock solutions of SA (1000 mg/L) were prepared in solvent and preserved at 4 °C. Working solutions were made by diluting the stock solution in deionized water (18 M Ω) from a Milli-Q water purified system (Millipore, Bedford, MA, USA).

River water samples were collected from the Guadalquivir River (Córdoba, Spain), filtered through 0.45 μm nylon filters, and adjusted to pH 2.0 prior to extraction.

2.2. Instrumentation

CE analysis was performed on a Beckman Coulter (Palo Alto, CA, USA) MDQ instrument equipped with an on-column UV detector and diode array

III.3. Carbon nanotubes as SPE sorbents for extraction of salicylic acid

detector. The instrumental setup was governed, and data acquired and processed by using the software 32 Karat.

2.3. Preparation of CNTs cartridges and SPE procedure

Fifteen milligrams of CNTs were packed inside 1 mL empty polypropylene SPE cartridges (Supelco, Madrid, Spain). Polypropylene upper and lower frits were retained at each end of the column to hold the nanoparticles packing in place. The cartridge was not conditioned prior to extraction. Then, the sample solution containing SA (10 mL at pH 2.0) was passed through the cartridge at a flow rate of 0.19 mL/min. All samples were previously adjusted at pH 2.0 with 0.1 M HCl. After loading the sample, the cartridge was dried by passing air through it, and the analyte retained was finally eluted with 1 mL of acetone (at a flow rate around 0.12 mL/min). The extract obtained was directly injected into CE system.

2.4. CE operation conditions

CE separations were accomplished by using an uncoated fused-silica capillary 75 μm id from Beckman (Fullerton, CA, USA) with an effective length between inlet and detector of 50 cm (60.2 cm total length). The electrophoretic buffer was composed of 13 mM sodium tetraborate adjusted at pH 9.6 with 1 M NaOH [9]. The capillary cartridge and samples were kept at 22 °C throughout. Samples were injected in hydrodynamic mode under a pressure of 0.5 psi for 10 s. Tests were carried out in the positive polarity mode, using a detection wavelength of 200 nm, a constant voltage of 20 kV, and over imposed pressure of 50 psi in both vials in order to prevent the current from being interrupted due to the evaporation of the organic solvent in samples. The current was around 40 μA in all analyses. For the initial conditioning of the capillary, it was rinsed with 0.1 M NaOH (5 min), deionized water (5 min) and running buffer (5

min). For conditioning between analyses, flushing with running buffer for 5 min was sufficient. All conditioning steps were performed at 20 psi.

3. RESULTS AND DISCUSSION

The steps involved in the optimization of SPE procedure are presented in Fig. 1. All optimization experiments were conducted using aliquots of deionized water spiked with 5 mg/L of SA. Sample volume and pH, type and amount of CNTs, sample flow rate, and elution conditions, were investigated in this work. The analytical signal taken for quantifying was peak area at 200 nm. All experiments were performed in triplicate, and average analytical signals as well as standard deviations were used to plot the graphs.

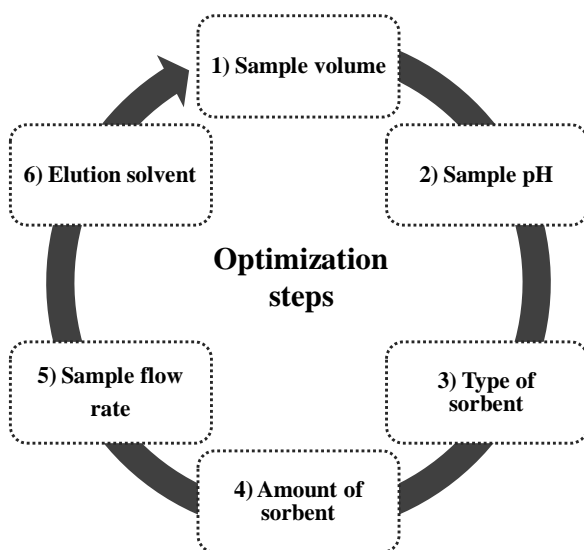


Figure 1. Diagram illustrating the steps of optimization of the SPE procedure.

3.1. Optimization of sample volume

The optimum sample loading volume was investigated by extracting SA from aqueous solutions with different volumes ranging from 5 to 20 mL. All

III.3. Carbon nanotubes as SPE sorbents for extraction of salicylic acid

samples were spiked with SA at a concentration of 5 mg L⁻¹, and then subjected to the extraction procedure involving the use of 5 mg of CNTs as sorbent. As can be seen in Fig. 2, the analytical signal remained practically constant between 5-10 mL. Larger volumes (15 mL and 20 mL) led to moderately greater analytical signals but entailing a worse reproducibility and longer extraction times. Similar results were obtained from 15 mL on, suggesting that the sorbent reached its maximum loading capacity then. This term could be defined as the maximum amount of SA (mg) that can be adsorbed per mg of CNTs. The maximum loading capacity was 0.015 mg SA/mg of CNTs, calculated by the ratio between the amount of SA present in 15 mL samples and the amount of sorbent used for extraction (5 mg). Under the studied conditions, the breakthrough volume was not achieved since no decreases in the extraction efficiency of SA were observed for increasing sample volumes. Ultimately, 10 mL was chosen for all subsequent analyses as a compromise to achieve a high sensitivity, good reproducibility and short time of analysis.

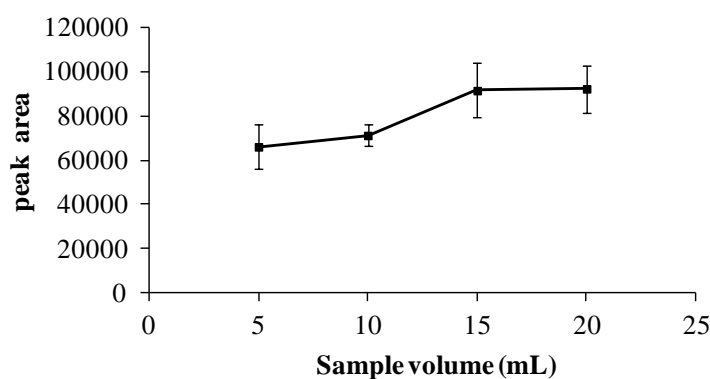


Figure 2. Effect of sample volume on the analytical signal. Concentration of SA, 5 mg/L; different sample volumes; sample pH, 2.0; sample flow rate, 0.19 mL/min; sorbent, 5 mg of CNTs; elution conditions, 1 mL of methanol.

3.2. Optimization of sample pH

Sample pH plays an important role in the SPE procedure given that it determines the state of the analyte as ionic or molecular form and consequently, affects its different degree of interaction with CNTs and the extraction efficiency. Assuming a pK_a value of 3 for SA [14], the studied pH values were: 2.0, 3.7 and 9.9, in order to cover the mostly protonated or partially/completely deprotonated species of this analyte. Neutral pH was not considered in this study since some available literature reported low recoveries of SA upon those extraction conditions [4,5,24-26]. Results revealed a notable decrease in analytical signal when the solution pH was increased from 2.0 to 3.7. Similar results were obtained at pH 3.7 and 9.9. Data confirmed that the mostly protonated specie (at pH 2.0) interacts with CNTs to a greater extent than the partially (pH 3.7) or completely (pH 9.9) deprotonated species of SA. The results suggest thereby that the interplay between SA and CNTs is mostly governed by π - π stacking interactions between aromatic structures and not by electrostatic forces. Finally, pH 2.0 was selected as optimum sample pH for conducting the extraction.

3.3. Optimization of type of CNTs

Different types of commercial CNTs were tested in order to select the most suitable for the extraction. We focused on CNTs because of these nanoparticles have been widely described as sorbents in sample treatment processes [13]. SWCNTs, MWCNTs-nanocyl and MWCNTs-bayer were tested as sorbents packed in SPE cartridges. The results are presented in Fig. 3.

III.3. Carbon nanotubes as SPE sorbents for extraction of salicylic acid

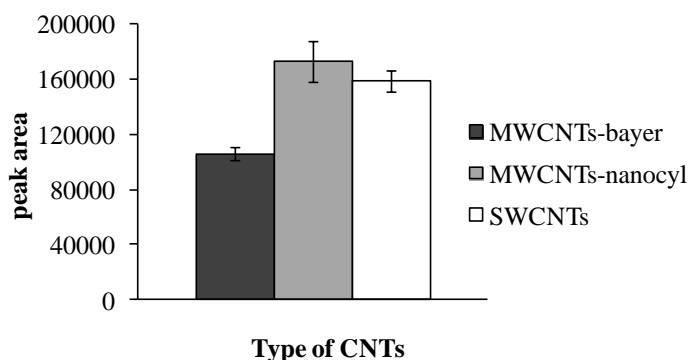


Figure 3. Effect of the type of CNTs on the analytical signal. Concentration of SA, 5 mg/L; sample volume, 10 mL; sample pH, 2.0; sample flow rate, 0.19 mL/min; sorbent, 15 mg of different CNTs; Elution conditions, 1 mL of methanol.

As can be observed, higher extraction efficiencies were achieved using MWCNTs-nanocyl for favoring an enhanced interaction with SA. Consequently, these nanoparticles were selected as optimum.

Only slight differences in extraction efficiencies between MWCNTs-nanocyl and SWCNTs were found. This fact confirms that, despite that the interactions between analyte and sorbent were mainly governed by π - π stacking, not always the higher number of graphene layers determines a greater sorbent capacity for MWCNTs respects to SWCNTs. Furthermore, due to their less size, the number of SWCNTs present in the cartridge in comparison to MWCNTs will be higher considering a fixed mass of sorbent. The higher number of nanometer-sized particles into the cartridge entails that a greater density of interstitial pores is available for the flow of aqueous sample and as a consequence, the potential interaction of SA with the surface of CNTs is promoted. Moreover, the surface area to volume ratio of nanoparticles is increased with the number of particles present, and this provides a larger surface area of nanoparticles available for adsorbing the analyte molecules. The

combination of both determining factors (number of graphene layers and number of particles in cartridge) defined finally a similar extraction behavior for SWCNTs and MWCNTs-nanocyl.

On the other hand, meaningful differences were reported using two different types of MWCNTs. This could be warranted given their different specific surface area that is defined by their diameter and number of graphene layers. Nanoparticles with a larger specific surface area would exhibit a greater potential for interacting with SA and therefore, a greater extraction efficiency. Additionally, different residual groups on surface of MWCNTs arising from the synthesis process may affect their degree of interaction with SA and thus, their different extraction behavior.

3.4. Optimization of amount of CNTs

The influence of amount of MWCNTs-nanocyl on the extraction efficiency of SA was evaluated by performing experiments with different amounts of MWCNTs-nanocyl packed in cartridge (2-25 mg). As can be observed in Fig. 4, the analytical signal was strongly dependent on the amount of MWCNTs-nanocyl packed in SPE cartridge. Peak areas were decreased for MWCNTs-nanocyl less than 10 mg due to a lower adsorption of SA, and were also decreased above 15 mg of MWCNTs-nanocyl, which seems to be as a result of incomplete desorption of analyte from surface of nanoparticles. Amounts of 10 and 15 mg led to very similar responses although 15 mg provided more reproducible results. Finally, 15 mg of MWCNTs-nanocyl was selected as optimum sorbent amount for experiments.

III.3. Carbon nanotubes as SPE sorbents for extraction of salicylic acid

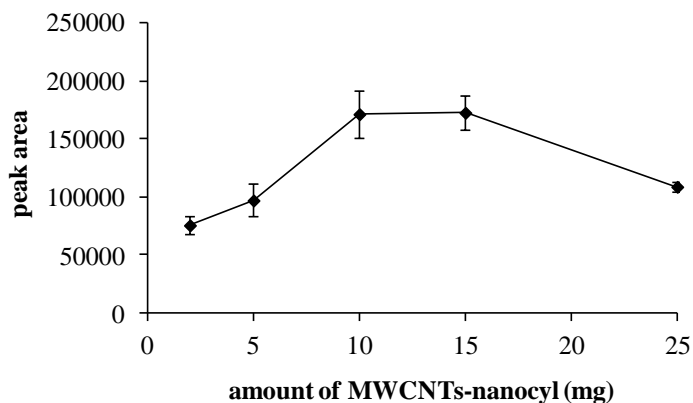


Figure 4. Effect of the amount of MWCNTs-nanocyl on the analytical signal. Concentration of SA, 5 mg/L; sample volume, 10 mL; sample pH, 2.0; sample flow rate, 0.19 mL/min; sorbent, different amounts of MWCNTs-nanocyl; elution conditions, 1 mL of methanol.

3.5. Optimization of sample flow rate

The sample loading onto SPE cartridge was automated using a peristaltic pump. With the purpose of optimizing this variable, samples were passed through prepared SPE cartridges at different flow rates: 0.19, 0.41 and 0.73 mL/min. The results demonstrated that the lower flow rate resulted in the greatest analytical signal by favouring a longer contact time between analyte and sorbent. Higher flow rates did not provide improved analytical signals, thus, 0.19 mL/min was chosen as optimum sample flow rate.

3.6. Optimization of elution conditions

An important aspect of SPE optimization is the choice of a suitable solvent for analyte elution; in this work, methanol, acetone and pH 10.0 deionized water were tested for this purpose taking as reference published research [1,5,9,17]. In all cases, 1 mL of solvent was passed through the cartridge by gravity (flow rate around 0.12 mL/min). As in scientific literature related [17],

acetone proved to be the best solvent for eluting the analyte from sorbent. Further experiments passing consecutive acetone volumes (in 1 mL-steps) through cartridge revealed that around 85% of SA was eluted with the first milliliter of acetone, indicating an almost complete elution and consequently, no higher solvent volumes were employed here. Finally, the elution step was carried out with 1 mL of acetone.

3.7. Matrix effect and Analytical figures of merit

The matrix effect, expressed as the ratio of the analyte signal in matrix to the analyte signal in solvent, was tested at a concentration of 5 mg/L. The analytical signal was not significantly affected by the presence of matrix constituents, as the signal change, in our case enhancement, was less than 11%. Consequently, it was not necessary to use matrix-matched standards to construct the calibration curve. Besides, no interfering components were observed in electropherograms at the same migration time of SA and thereby, the analytical signal measured was not influenced by other substances.

The linearity of the method was then studied using deionized water standards, spiked at increasing concentrations of SA (1-15 mg/L), and subjected to the optimized extraction method (Table 1). A linear response ($Y = 51,394 X + 18293$; $R^2 = 0.9959$) was obtained in the range 2-10 mg/L by plotting the peak area (absorbance at 200 nm) *versus* spiked analyte concentration. The enrichment factors calculated as the ratio between the analyte concentration found in the solvent extract and the initial concentration in aqueous standards were between 10 and 12. The LOD was 0.5 mg/L while the LOQ was 1.7 mg/L (calculated as three and ten times, respectively, the S_a value between the scope).

III.3. Carbon nanotubes as SPE sorbents for extraction of salicylic acid

Table 1. Experimental conditions of the proposed SPE-CE method.

Variable	Studied values	Optimum value
Sample volume (mL)	5, 10, 15, 20	10
Sample pH	2.0, 3.7, 9.9	2.0
Type of sorbent	MWCNTs-nanocyl, MWCNTs-bayer, SWCNTs	MWCNTs-nanocyl
Amount of sorbent (mg)	2, 5, 10, 15, 25	15
Sample flow rate (mL/min)	0.19, 0.41, 0.73	0.19
Elution solvent	Methanol, acetone, deionized water at pH 10.0	acetone

The optimized method was lastly applied to the determination of SA in river water samples collected from the Guadalquivir River (Córdoba, Spain). Blank analyses (unspiked samples) were performed and the content of SA found resulted to be below the LOD. As a consequence, samples were necessarily spiked at three different concentrations (4, 6, and 8 mg/L) before performing the recovery studies. Relative recovery values were calculated as the percentage of the ratio between the concentration of SA found in spiked samples after performing the complete extraction procedure, and the initially spiked analyte concentration. Table 2 summarizes the results arising from this study. As can be seen, good recoveries were obtained within the range of 76.2%-102.0% with SDs not higher than 8.2%.

Table 2. Recoveries study in spiked river water samples.

Added concentration (mg/L)	Found concentration (mg/L)	Relative Recovery ^a (%)	RSD ^a (%)
4	3.51 ± 0.19	81.65-92.06	5.33
6	5.14 ± 0.41	76.17-93.73	8.03
8	7.50 ± 0.62	86.71-101.99	8.20

^a Calculated from four independent spiked samples

BLOQUE III. NANOPARTÍCULAS COMO HERRAMIENTAS ANALÍTICAS

Fig. 5 shows the electropherograms of the acetone solvent and those obtained from a blank and a spiked sample, both subjected to the developed procedure. As can be observed, the analysis time was quite short (less than 12 minutes) and the electropherograms showed greatly stable baselines.

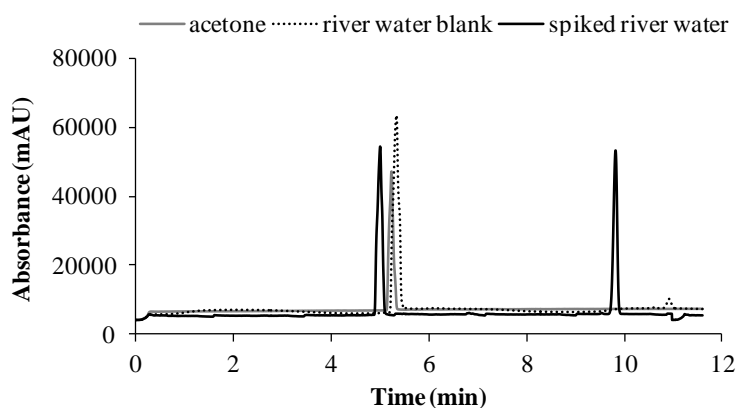


Figure 5. Electropherograms obtained from a blank and a river water sample spiked with 6 mg/L of SA, both subjected to the complete analytical procedure. Electropherogram of acetone solvent is also presented.

4. CONCLUDING REMARKS

As noted earlier, most published research on extraction and determination of pharmaceuticals in water samples use chromatography coupled to mass spectrometry as instrumental technique. Obviously, the LOD provided by those techniques is lower compared to that for CE and hence, a suitable and efficient sample treatment process is mandatory to maximize the preconcentration factor prior to CE detection. In this work, an alternative method, that combines a SPE procedure involving CNTs as sorbent with CE analysis, is proposed for determining SA in those scenarios where no severe restrictions of sensitivity are imperative. It is worth noting that this method is low cost and extremely simple given that it only involves packing CNTs into a

III.3. Carbon nanotubes as SPE sorbents for extraction of salicylic acid

cartridge and loading the aqueous sample, with the added advantage that this last step is entirely automated. Furthermore, the total solvent consumption is only 1 mL, and the method provides good recovery values. Besides, CE analysis time is shorter (less than 12 minutes), and the baseline of the electropherograms is remarkably more stable, in comparison to previous research works [8,9]. Taking all into consideration, this analytical method could be applied to routine analyses laboratories. Undoubtedly, the outstanding properties of CNTs open new avenues for promoting their use in the analysis of pharmaceuticals in environmental matrices.

Acknowledgements

The authors would like to express their gratitude to the Spanish Ministry of Economy and Competitiveness for Project CTQ2011-23790 and to Junta de Andalucía for the Project FQM-4801. E. Caballero-Díaz also wishes to thank the Ministry for the award of a Research Training Fellowship (Grant AP2008-02955).

The authors have declared no conflict of interest.

References

- [1] Gracia-Lor, E., Sancho J.V., Hernández, F., *J. Chromatogr. A.* 2010, *1217*, 622–632.
- [2] Shaaban, H., Górecki, T., *Talanta* 2012, *100*, 80–89.
- [3] Lacey, C., McMahon, G., Bones, J., Barron, L., Morrissey, A., Tobin, J.M., *Talanta* 2008, *75*, 1089–1097.
- [4] Grujic, S., Vasiljevic, T., Lausevic, M., *J. Chromatogr. A.* 2009, *1216*, 4989–5000.
- [5] Migowska, N., Caban, M., Stepnowski, P., Kumirska, J., *Sci. Total. Environ.* 2012, *441*, 77–88.
- [6] Wille, K., De Brabander, H.F., De Wulf, E., Van Caeter, P., Janssen, C.R., Vanhaecke, L., *TrAC* 2012, *35*, 87–108.
- [7] Parrilla-Vázquez, M.M., Parrilla Vázquez, P., Martínez Galera, M., Gil García, M.D., Uclés, A., *J. Chromatogr. A.* 2013, *1291*, 19–26.
- [8] Deng, Y., Fan, X., Delgado, A., Nolan, C., Furton, K., Zuo, Y., Jones, R.D., *J. Chromatogr. A.* 1998, *817*, 145–152.
- [9] Villar Navarro, M., Ramos Payán, M., Fernández-Torres, R., Bello-López, M.A., M. Callejón Mochón, M.A., Guiráum Pérez, A., *Electrophoresis* 2011, *32*, 2107–2113.
- [10] Wang, J., Guo, Y., Yuan, R., Liu, D., Bao, J.J., *J. Chromatogr. Sci.* 2011, *49*, 51–56.
- [11] Fatta-Kassinos, D., Meric, S., Nikolaou, A., *Anal. Bioanal. Chem.* 2011, *399*, 251–275.
- [12] Sarafray-Yazdi, A., Assadi, H., Es’Haghi, Z., Danesh, N.M., *J. Sep. Sci.* 2012, *35*, 2476–2483.
- [13] Valcárcel M., Cárdenas, S., Simonet, B.M., Moliner-Martínez, Y., Lucena, R., *TrAC* 2008, *27*, 34–43.
- [14] Gilart, N., Marcé, R.M., Borrull, F., Fontanals, N., *J. Sep. Sci.* 2012, *35*, 875–882.
- [15] Capka, L., Lacina, P., Vavrova, M., *Fresen. Environ. Bull.* 2012, *21*, 3312–3317.
- [16] Chen, H.L., Fan, L.Y., Chen, X.G., Hu, Z.D., Zhao, Z.F., Hooper, M., *J. Sep. Sci.* 2003, *26*, 863–868.
- [17] Camacho-Muñoz, D., Marín, J., Santos, J.L., Aparicio, I., Alonso, E., *J. Sep. Sci.* 2009, *32*, 3064–3073.
- [18] Fang, G., Wang, X., Wang, S., *Chromatographia* 2010, *72*, 403–409.

III.3. Carbon nanotubes as SPE sorbents for extraction of salicylic acid

- [19] Hussain, C.M., Mitra, S., *Anal. Bioanal. Chem.* 2011, 399, 75–89.
- [20] Pyrzynska, K., *Chemosphere* 2011, 83, 1407–1413.
- [21] Dahanem, S., Gil García, M.D., Martínez Bueno, M.J., Moreno Uclés, A., Martínez Galera, M., Derdour, A., *J. Chromatogr. A* 2013, 1297, 17–28.
- [22] Moliner-Martínez, Y., Ribera, A., Coronado, E., Campíns-Falcó, P., *J. Chromatogr. A* 2011, 1218, 2276–2283.
- [23] Miah, M., Iqbal, Z., Lai, E.P.C., *Anal. Methods* 2012, 4, 2866–2878.
- [24] Farré, M., Ferrer, I., Ginebreda, A., Figueras, M., Olivella, L., Tirapu, L., Vilanova, M., Barceló, D., *J. Chromatogr. A* 2001, 938, 187–197.
- [25] Yu, Z., Peldszus, S., Huck, P.M., *J. Chromatogr. A* 2007, 1148, 65–77.
- [26] Irakli, M.N., Samanidou, V.F., Biliaderis, C.G., Papadoyannis, I.N., *Food Chem.* 2012, 134, 1624–1632.



Anal Bioanal Chem (2013) 405:7251–7257
DOI 10.1007/s00216-013-7185-6

RESEARCH PAPER



Microextraction by packed sorbents combined with surface-enhanced Raman spectroscopy for determination of musk ketone in river water

Encarnación Caballero-Díaz, Bartolomé M. Simonet, Miguel Valcárcel

Department of Analytical Chemistry, Marie Curie Building (Annex), Campus de Rabanales, University of Córdoba, 14071 Córdoba, Spain

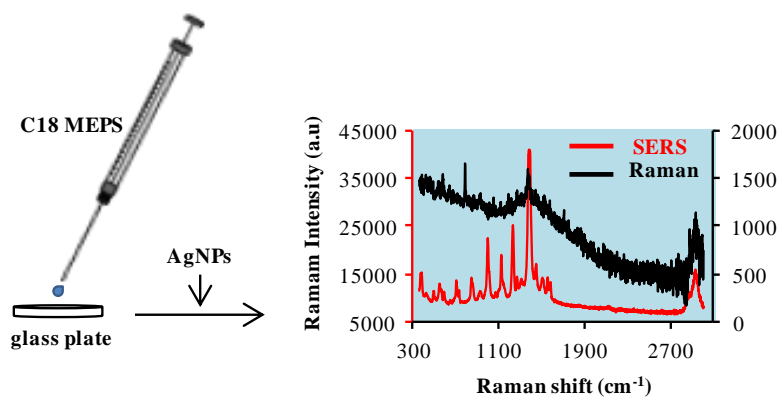
ABSTRACT

Microextraction by packed sorbents (MEPS) combined with Surface-enhanced Raman spectroscopy (SERS) was investigated, and applied to the determination of musk ketone (MK) in river water samples. The full MEPS-SERS method includes analyte enrichment by MEPS preconcentration with C18 sorbent followed by SERS detection supported by silver nanoparticles. An eluent drop containing the analyte is deposited directly from the MEPS syringe on a CaF₂ glass plate. When the drop has dried, a specific volume of silver nanoparticles solution is added on it before each SERS measurement. Several experimental variables were studied in depth; under the optimum experimental conditions, MK can be extracted from a 500 μ L sample with recoveries in the range 47–63%. The limit of detection was 0.02 mg L⁻¹ and the relative standard deviation 15.2% ($n=4$). Although not investigated in this work, the proposed method

BLOQUE III. NANOPARTÍCULAS COMO HERRAMIENTAS ANALÍTICAS

might be suitable for *in situ* monitoring, because of the portability of the Raman spectrometer used.

GRAPHICAL ABSTRACT



1. INTRODUCTION

Currently, there is an increasing attention on musk compounds because they are common additives in numerous consumer products, for example detergents, cosmetics, and other personal care products [1]. Because of their widespread use, musk products have become ubiquitous emerging contaminants that can be found in different environmental matrices near wastewater discharge urban areas [1]. Synthetic musks can be classified into three families: polycyclic musks, nitromusks, and macrocyclic musks, being the first of them the most commonly used. The nitromusks family includes five compounds: musk ambrette, musk moskene, musk tibetene, musk xylene (MX), and musk ketone (MK); although only the last two are permitted [2]. Permitted maximum concentrations (w/v, %) for MX and MK are, respectively, 1.0% and 1.4% in fine fragrances, 0.4% and 0.5% in eau de toilette, and 0.03% and 0.04% in other products [3,4].

The effect of musk compounds on biota and ecosystems has become an emerging research area. Polycyclic musks and nitromusks are lipophilic in nature; this results in a slow biodegradation and a tendency to bioaccumulate in different environmental compartments, for example sediments [5, 6], sludge [7, 8], and biota [9, 10]. Although MK is suspected of increasing the carcinogenic effects of other substances, few related toxicological studies have been conducted. Comutagenic effects between benzo[*a*]pyrene and MK have been described in human derived hepatoma cell lines, because MK amplifies the genotoxicity of that carcinogen [11]. Furthermore, recent *in vitro* studies have confirmed that some polycyclic musks bind weakly to estrogen, androgen, or progesterin receptors, and thus have endocrine-disrupting properties [12].

Determination of musk compounds in environmental samples has already been performed by different analytical techniques. A preconcentration step is

usually required because of the low concentrations at which these compounds are found. Solid-phase microextraction (SPME) is a solventless preconcentration technique that consists of extracting the analytes from a sample into a sorbent phase. It is a simple, reproducible and sensitive alternative, faster and with lower reagent consumption in comparison to conventional liquid-liquid (LLE) and solid-phase extractions (SPE) [13]. Microextraction by packed sorbents (MEPS) is a type of SPME in which the sorbent is directly inserted into a syringe barrel and the sample solution is pushed through it several times. Any sorbent material can be used, including silica-based materials (C2, C8, C18), strong cation exchangers (SCX), and carbon [14]. The extracted analytes can be eluted by using a small volume of solvent, which makes it an especially attractive preconcentration method. In comparison with SPME, MEPS needs less handling time, the number of possible extractions before changing the cartridge is higher, and final recoveries and sensitivity are improved [14, 15]. To date, only a few works on extraction of musk compounds from water samples using MEPS has been reported in the literature [16, 17].

With regard to the instrumental analysis that follows preconcentration, determination of musks by gas chromatography with tandem mass spectrometry has been widely described, being this the most used technique up to now [1, 2, 5, 6, 18]. Other techniques used for this purpose, although to a lesser extent, are capillary electrophoresis (CE) [19] and Surface-enhanced Raman spectroscopy (SERS) [20]. SERS is a Raman spectroscopy technique in which a greatly enhanced Raman signal is obtained from Raman-active analyte molecules adsorbed on prepared metal surfaces. Increases in the Raman intensity of the order of 10^4 – 10^6 have been regularly observed, and can be as high as 10^8 and 10^{14} for some systems [21].

III.4. MEPS-SERS method for determination of musk ketone

In brief, the main objective of this work was to develop an analytical method for determination of MK in river water by using MEPS preconcentration followed by SERS detection. The eluent from the MEPS system was deposited directly on a CaF₂ glass plate, forming a drop above which colloidal silver was added before each SERS measurement. Some experimental conditions, for example the order of deposition of compounds on the measurement plate, volume of silver nanoparticles solution, solvent type, and sample and cleaning volumes, were studied in order to find the optimum working conditions.

2. EXPERIMENTAL

2.1. Reagents and materials

All chemical reagents were of analytical grade and were not subjected to any additional purification. Hydroxylamine hydrochloride (98%) and silver nitrate ($\geq 99\%$) were purchased from Sigma-Aldrich (Madrid, Spain). Acetonitrile (HPLC Chromasolv) was purchased from Sigma-Aldrich (Steinheim, Germany). Sodium hydroxide (NaOH) pellets (PA-ACS-ISO) and methanol (HPLC PAI-ACS) were obtained from Panreac (EU). 4-*tert*-Butyl-2,6-dimethyl-3,5-dinitroacetophenone ketone moschus (musk ketone, MK), purity $\geq 98\%$, was obtained from Sigma-Aldrich (Madrid, Spain). The chemical structure of MK is depicted in Fig. 1. To perform the experiments, stock solutions of MK were prepared in methanol. MEPS syringes and the barrel inserts and needles were obtained from SGE Analytical Science (UK). River water samples were collected from the Guadalquivir River (Córdoba, Spain) and were not subjected to any pretreatment.

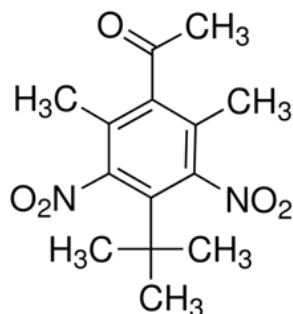


Figure 1. Chemical structure of musk ketone.

2.2. Equipment

Raman measurements were acquired with a portable Raman spectrometer system known as innoRam with a wavelength of 785 nm, and a maximum laser output power of 348 mW and 285 mW at the system's excitation port and in the probe, respectively. Both Raman spectrometer and probe (model BAC-150) were provided by B&W TEK (USA).

UV-visible measurements were performed by using a halogen lamp for excitation and the monochromator and photonic detector of a PTI QuantaMaster spectrofluorimeter (Photon Technology International) system as detector, with Felix32 software.

Transmission electron microscopy images were recorded by using a Jeol JEM 1400 microscope operating at an accelerating voltage of 120 kV (S.C.A.I. Córdoba).

2.3. Synthesis of silver nanoparticles

With the objective of synthesizing silver nanoparticles, several aqueous solutions were initially prepared: 8.5×10^{-3} mol L⁻¹ hydroxylamine, 2 mol L⁻¹

III.4. MEPS-SERS method for determination of musk ketone

NaOH, and 1.1×10^{-3} mol L⁻¹ silver nitrate. The hydroxylamine (5 mL), NaOH (0.04 mL), and silver nitrate (45 mL) solutions were then added in that same order into an Erlenmeyer flask, and the mixture was stirred vigorously at 500 rpm for 10 min [22], by using a magnetic stirrer from J.P. Selecta (Barcelona, Spain). The synthesis solution was freshly prepared each week to prevent from degradation of silver nanoparticles. The reproducibility of the synthesis was demonstrated because the same experiments performed with silver nanoparticles from different batches led to similar results. Colloidal silver synthesis solution was analyzed by UV-visible spectroscopy, which showed the absorbance maximum was at 444 nm. TEM images were also acquired (Fig. 2).

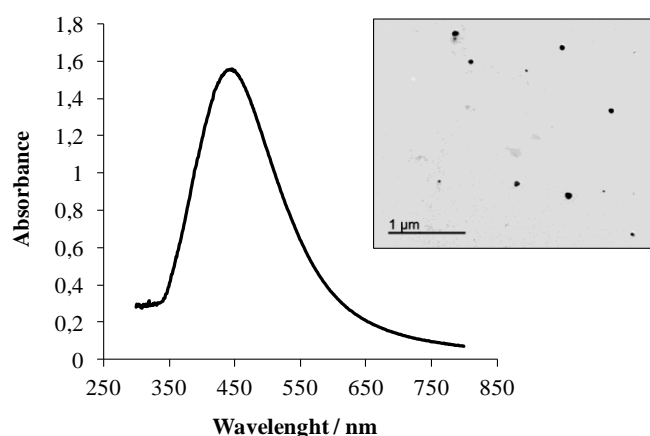


Figure 2. Absorbance spectrum and TEM image of colloidal silver synthesis solution.

2.4. Measurement of Raman and SERS spectra

Measurements were conducted on 32 mm x 3 mm calcium fluoride (CaF₂) glass plates obtained from CrystalTechno (Moscow, Russia). Spectra were collected by using a 50× microscope objective, with 1 s data acquisition time, one only acquisition, and a detection range from 368 to 3000 cm⁻¹. These measurement conditions enabled us to achieve a high signal-to-noise ratio.

BLOQUE III. NANOPARTÍCULAS COMO HERRAMIENTAS ANALÍTICAS

The software of the detection system allowed us to set a percentage of the laser power to be applied to each sample. This value was always adjusted to 10%; as a result, the laser power on the sample was 28.5 mW.

Raman and SERS measurements were always conducted in the same way. First, the Raman spectrum of MK was recorded from the dried drop on the CaF₂ glass by manual focalization of the microscope on it. The volume of MK solution deposited on the plate for all measurements was always 10 µL. To obtain the SERS spectrum, 6 µL of the silver nanoparticles solution was placed on the dried analyte drop with a micropipette. Blank analyses only with silver nanoparticles were performed before each SERS measurement to check the suitability of the silver nanoparticles solution for the detection, and it is that the silver tends to degrade over time by mechanisms such as oxidation, resulting in interferences on the SERS signal.

2.5. MEPS-SERS procedure

The sample treatment procedure was performed by using MEPS. Each 8 µL cartridge contained ~4 mg of C18 packing; the particle size was 45 µm and the pore size 60 Å.

Before extraction, the MEPS system was conditioned with two portions of methanol and ultrapure water (200 µL each). The aqueous sample containing MK (500 µL) was passed through the MEPS cartridge in 2 x 250 µL steps at an aspiration speed of 5 µL s⁻¹. To remove traces of water, the solid phase was then dried by passing air through the sorbent at a flow rate of 20 µL s⁻¹. Subsequently, 10 µL of methanol was drawn through the MEPS in order to elute the analyte. The eluent containing MK was deposited directly on a CaF₂ glass plate and quickly dried by heat application what contributed to a more reproducible evaporation. The silver solution (6 µL) was then added on the

III.4. MEPS-SERS method for determination of musk ketone

dried drop using a micropipette. The colloidal silver solution was completely dried before each SERS measurement. Between analyses, the MEPS cartridge was washed with 200 μL of methanol. The analytical procedure is depicted schematically in Fig. 3.

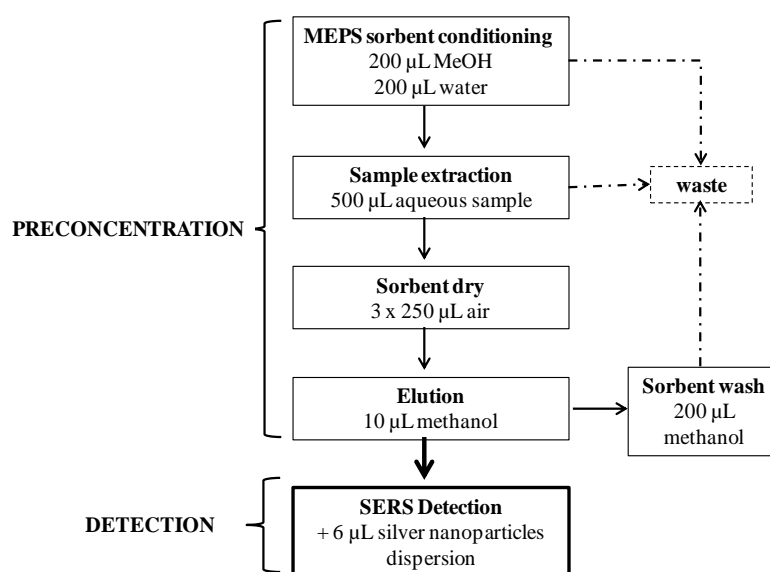


Figure 3. Schematic diagram of the optimized MEPS-SERS method for determination of MK in 500 μL aqueous samples. The syringe used for the MEPS step has a volume of 250 μL .

3. RESULTS AND DISCUSSION

3.1. Optimization of SERS detection

To optimize SERS detection, a series of experiments were conducted by depositing analyte and colloidal silver solution on a CaF_2 glass plate. The Raman spectra were recorded from each deposited spot once dried, and then SERS spectra were recorded after addition of silver solution to each spot.

BLOQUE III. NANOPARTÍCULAS COMO HERRAMIENTAS ANALÍTICAS

First, the order of deposition of the silver solution and MK was studied by using stock solutions of MK in methanol ($100 \mu\text{g L}^{-1}$). In a first approach, the silver solution was first deposited on the CaF_2 glass and the droplet containing the analyte was placed on it afterwards. Poor results were obtained because the silver nanoparticles were not firmly immobilized on the plate and might have been removed when the methanolic solution of MK was added on top. In a second study, the analyte was deposited on the glass first and the colloidal silver solution was added on top of the analyte drop once dried. By this last experimental approach, there was no loss of silver solution by drag and thus, this solution covered a larger area on the analyte drop, generating a higher density of hot spots. This scheme led to a greater SERS enhancement factor and reproducible results, and finally it was selected as optimum.

Raman and SERS spectra of MK at concentrations of 1000 mg L^{-1} and $100 \mu\text{g L}^{-1}$ are shown in Fig. 4. Some prominent peaks can be distinguished in the SERS spectrum. The NO_2 symmetric stretching vibration is located at 1390 cm^{-1} . The nitro-group scissoring mode is cautiously assigned to the peak at 713 cm^{-1} [20]. The bands at 1004 cm^{-1} and 1276 cm^{-1} are tentatively associated to the aromatic ring chain vibration and to aliphatic chain vibration (*t*-butyl group), respectively.

The difference between the Raman intensities at 1390 cm^{-1} and at 1299 cm^{-1} in the spectrum of MK was adopted as analytical signal in all experiments.

III.4. MEPS-SERS method for determination of musk ketone

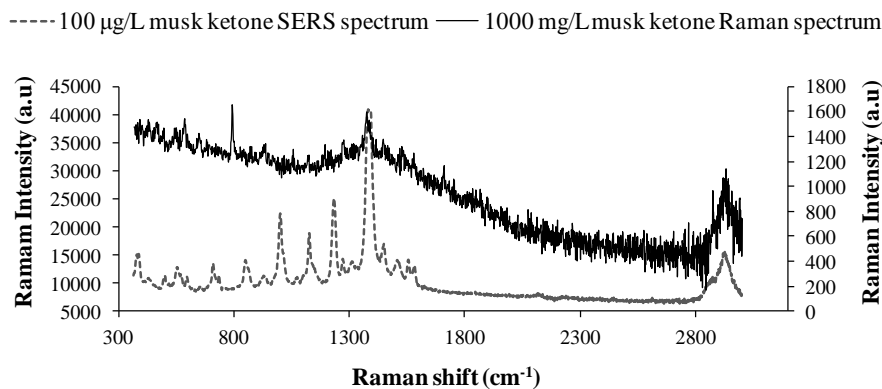


Figure 4. Raman and SERS spectra obtained from 1000 mg L⁻¹ and 100 µg L⁻¹ MK respectively.

As is apparent from Fig. 4, the Raman intensity increased substantially, i.e. by a factor of 9.3×10^5 after deposition of colloidal silver solution. The enhancement factor, EF, was calculated using the following equation [22]:

$$EF \text{ (enhancement factor)} = \left(\frac{N_{\text{Raman}}}{N_{\text{SERS}}} \right) \cdot \left(\frac{I_{\text{SERS}}}{I_{\text{Raman}}} \right)$$

where I_{SERS} and I_{Raman} are, respectively, the SERS intensity and the normal Raman scattering intensity of MK at 1390 cm⁻¹, and N_{SERS} and N_{Raman} represent the number of molecules of MK deposited onto the substrate in each case.

The effect of the volume of colloidal silver solution added to the analyte drop was then studied by first depositing methanolic solution of MK (100 µg L⁻¹, 10 µL) and then adding different volumes (2, 6, 20, 40, or 70 µL) of the synthesized silver solution. The SERS enhancement increased when the volume of silver nanoparticles solution was increased from 2 to 6 µL; above this volume however, the signal decreased progressively (being very similar for 20 µL and 40 µL) until reaching a minimum at 70 µL of silver solution. The explanation of these results is that for greater volumes of silver solution the resulting drop size

becomes larger and spreads over a larger plate area. As a result, the silver colloids tend to accumulate at the limits of the drop, which has a double effect: it complicates the interaction between analyte and silver, reducing the SERS enhancement factor, and also reduces the reproducibility of the method. Therefore, 6 μL was set as optimum volume since it provides a greater SERS enhancement factor. The SERS spectra and the Raman intensities are shown in Fig. 5.

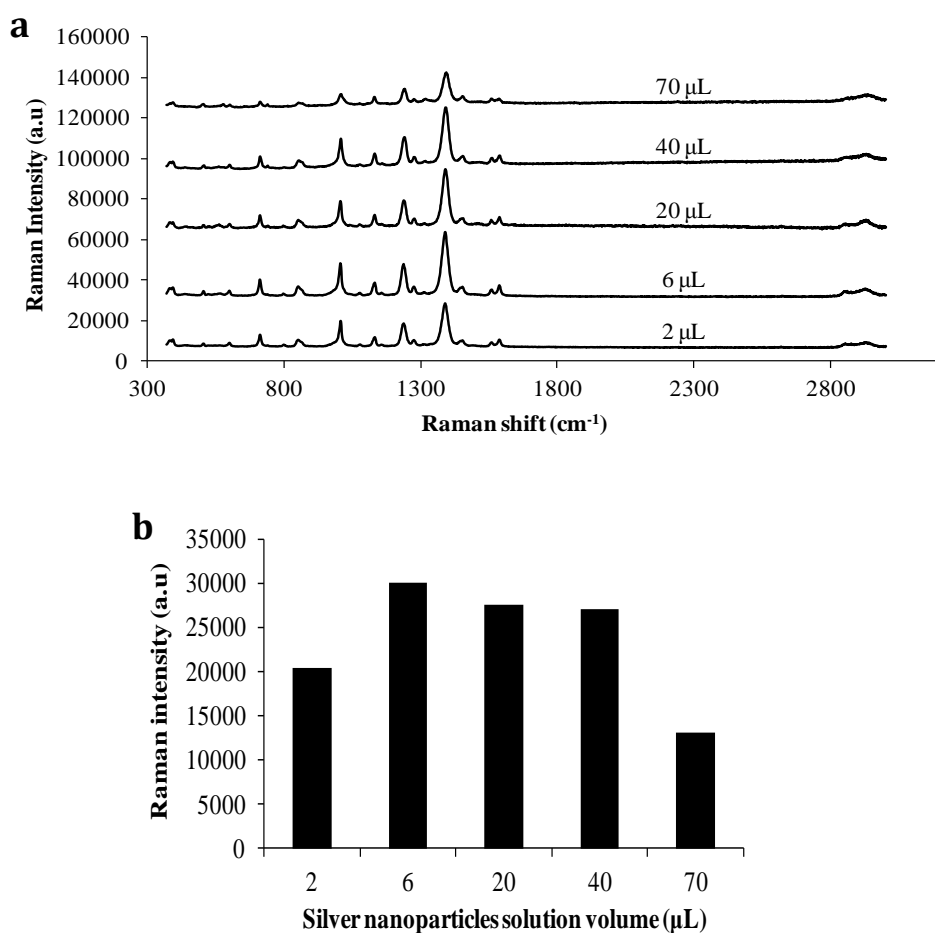


Figure 5. *a* SERS spectra for $100 \mu\text{g}\cdot\text{L}^{-1}$ of MK adding different volumes of silver nanoparticles solution. *b* SERS intensities calculated by subtracting the intensities at 1299 cm^{-1} to those obtained at 1390 cm^{-1} .

III.4. MEPS-SERS method for determination of musk ketone

The optimum order of deposition of compounds on the glass was again studied using the silver solution volume previously optimized (6 μL). For this purpose, the same procedure was followed—using 10 μL of methanolic solution of MK and 6 μL of silver solution, and the order of deposition was changed in parallel experiments. Again, it was confirmed that stronger SERS intensities were obtained when the analyte was deposited first and the silver solution was added later.

The optimized detection procedure thus entailed depositing 10 μL of methanolic solution of MK on the CaF_2 glass, and then adding 6 μL of the synthesized silver nanoparticles solution to the dried analyte drop. The Raman and SERS measurements were performed after the evaporation of the liquids on the glass plate.

In further studies, the reproducibility of the proposed detection method and the homogeneity of deposition scheme on the plate were investigated. With this objective, the optimized detection method was repeated using different 1 mg L^{-1} MK standards. The RSD found resulted to be 9.9% for three replicates. The homogeneity of deposition scheme was assessed by measuring a same sample (1 mg L^{-1} MK standard) at different randomly selected locations inside the dried drop. This procedure was repeated for several samples. Reproducibility was in the range 6.2–8.4% depending on the sample analyzed.

3.2. Optimization of MEPS preconcentration step

The variables optimized were solvent type, and sample and cleaning volumes. The optimization experiments were performed by using water standards spiked with MK at a concentration of 1 mg L^{-1} .

BLOQUE III. NANOPARTÍCULAS COMO HERRAMIENTAS ANALÍTICAS

The elution solvent volume was set at 10 μL to match the resulting drop size to the measurement plate size, and also to preserve the analyte-to-silver volume ratio used in the previous optimization experiments (discussed in the section “Optimization of SERS detection”). Moreover, larger elution volumes resulted in a loss of sensitivity and reproducibility of the method because larger drops were formed on the glass plate and the analyte was distributed by a larger surface, complicating in this way the interplay between MK and silver nanoparticles.

Two different organic solvents were evaluated as eluents, methanol and acetonitrile. Methanol enabled a greater extraction yield and was finally chosen as optimum solvent.

To determine the cleaning volume of the MEPS cartridge required after each preconcentration stage, consecutive elutions with 10 μL methanol in each step were performed until MK was not detected in the elution fraction. The volume of methanol used for cleaning was 200 μL , because no interferences on the analytical signal were detected after that volume passed through the MEPS cartridge.

The effect of the aqueous sample volume was also investigated. Aqueous samples of 50, 200, 500, and 1000 μL were spiked at concentrations such that the final concentration in the volume of eluent was identical in all cases, assuming the same extraction yield for all the samples. In other words, the sample volume was different in each case although the total amount of analyte in the sample always remained constant. Taking into account that the starting MK concentration was different for each volume of sample studied, one might believe that the critical condition in this study was the concentration of MK and not the volume of sample. However, when a sample is passed through a MEPS cartridge, the volume becomes a significant parameter because larger samples

III.4. MEPS-SERS method for determination of musk ketone

(passed through MEPS cartridge in different loading cycles) could lead to a better and longer interaction between analyte and sorbent, resulting in a increased extraction efficiency [14]. Sample volumes of 500 and 1000 μL provided similar SERS enhancement factors, because both enabled greater interaction between MK and sorbent. Nevertheless, a compromise must be reached between analysis time and the obtained SERS response; consequently, 500 μL was eventually selected as optimum sample volume.

The effect of ion strength on extraction efficiency was not considered because previous investigations showed no effects of salt addition on extraction yield of musk compounds [21].

3.3. Analytical features of the MEPS-SERS method

The sensitivity, limits of detection (LOD) and quantification (LOQ), and precision of the MEPS-SERS method were also evaluated. The analytical signal was quantified by the difference between the Raman intensities obtained at 1390 cm^{-1} and 1299 cm^{-1} in the spectrum of MK. However, other Raman bands at 713 cm^{-1} , 1004 cm^{-1} , and 1276 cm^{-1} could also be used to identify this analyte. To determine the detection limit of the proposed MEPS-SERS method, ultrapure water standards spiked at different concentrations of MK were subjected to the previously optimized experimental method. A calibration graph was constructed by plotting the analytical signals obtained after performance of the MEPS-SERS method against the initial MK concentrations in the ultrapure water standards. The data were fitted to a Langmuir isotherm, $Y = (a \times b \times X^{(1-c)}) / (1 + b \times X^{(1-c)})$; $a=22448$, $b=29$, $c=-0.23$, and the fit was acceptable in the range 0.05–1 mg L^{-1} of MK ($R^2=0.9772$). The LOD was estimated to be 0.02 mg L^{-1} and the LOQ was 0.05 mg L^{-1} . Fitting of the calibration graph to a Langmuir isotherm has previously been described in other works on SERS detection of other compounds, for example malathion and melanine [23].

It should be emphasized that several measurements were taken at different spots of each sample to calculate statistically an average intensity value. Reproducibility was between 4 and 6.9%. To study the reproducibility of the full MEPS-SERS method, four independent samples spiked with 1 mg L^{-1} MK were analyzed. The RSD obtained for the full procedure was 15.2%, which is in accordance with values found in the literature [24, 25]. Taking into account SERS limitations related to the irreproducibility of deposition of the SERS-active substrate, it is apparent that the sensitivity and RSD of our experimental method are acceptable.

3.4. Application to river water samples

Water samples were collected from the Guadalquivir River (Córdoba, Spain). The samples were analyzed by the proposed method using an extraction volume of $500 \mu\text{L}$, and a preconcentration step with C18-MEPS followed by SERS detection with silver nanoparticles. A typical SERS spectrum obtained from a spiked real sample subjected to the complete experimental procedure is shown in Fig. 6.

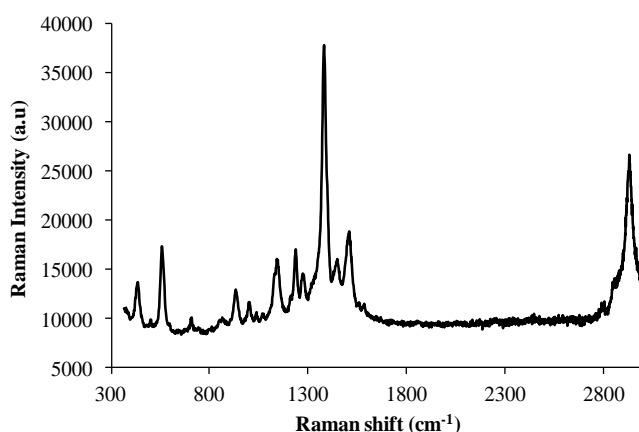


Figure 6. Example of a SERS spectrum obtained from a river water sample (spiked at $0.2 \text{ mg}\cdot\text{L}^{-1}$) subjected to the developed MEPS-SERS method.

III.4. MEPS-SERS method for determination of musk ketone

Recovery for triplicate analysis was calculated by comparison of, the SERS intensity obtained by use of the MEPS-SERS method for 500 μL river water spiked with 0.2 mg L^{-1} MK, with the SERS intensity obtained by use of the MEPS-SERS method for 500 μL ultrapure water spiked at the same concentration. Results ranged from 46.6 to 62.6% depending on the sample analyzed. These recoveries are in accordance with results reported in the literature [16]. The presence of interferences in the river water samples might explain why higher recoveries were not obtained. In this regard, two different hypotheses are important. On the one hand, natural components present in river water could interact with the analyte reducing its extraction from the matrix, and on the other hand, these same components could occupy the hot spots on the SERS substrates, thus further reducing the analytical signal.

4. CONCLUSIONS

SERS is an emerging novel analytical technique with a satisfactory performance in detection of trace amounts of analytes. In this study a MEPS-SERS method was developed by combining an initial MEPS preconcentration step followed by SERS detection with silver nanoparticles. Different experimental conditions were optimized for both detection and preconcentration steps, including the deposition order of compounds on the plate and the volume of silver nanoparticles solution for detection, and solvent type, and sample and cleaning volumes for preconcentration. The experimental conditions finally selected were: 500 μL of sample volume, 10 μL of methanol for elution, and 6 μL of silver nanoparticles solution to be added to the dried analyte drop on the CaF_2 glass before each measurement. The LOD of the optimized method for ultrapure water was 0.02 mg L^{-1} , and its final application to river water samples led to recoveries in the range 46.6–62.6%, confirming the suitability of this experimental approach for determination of MK in real water samples. Although previously published works on analysis of musk

BLOQUE III. NANOPARTÍCULAS COMO HERRAMIENTAS ANALÍTICAS

compounds by other techniques led to lower detection limits [1, 2, 16, 18], here we present a combination of MEPS with SERS detection for determination of musk ketone in water samples for those scenarios in which no severe sensitivity restrictions are required. The most remarkable advantages of this method are:

1. the portability of both the extraction scheme and detection system, which could lead to *in situ* studies;
2. the simplicity of the proposed analytical method; and
3. reduced analysis time.

The features and advantages of this method would enable its future application to other types of sample (e.g. cosmetics).

Acknowledgements

E. Caballero-Díaz would like to thank the Ministry of Education for the award of a FPU fellowship (grant AP2008-02955) and Junta de Andalusia for their project FQM4801.

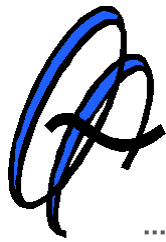
References

1. Ramírez N, Marcé R, Borrull F (2011) *J Chromatogr A* 1218:156-161.
2. Polo M, García-Jares C, Llompart M, Cela R (2007) *Anal Bioanal Chem* 388:1789-1798.
3. Sánchez-Prado L, Llompart M, Lamas JP, García-Jares C, Lores M (2011) *Talanta* 85:370-379.
4. Regulation (EC) N^o 1223/2009 of the European Parliament and of the Council of 30 November 2009 on cosmetic products (2009) 59-209.
5. Rubinfeld S, Luthy RG (2008) *Chemosphere* 73:873-879.
6. Hu X, Zhou Q (2011) *Chromatographia* 74:489-495.
7. Guo R, Lee I-S, Kim U-J, Oh J-E (2010) *Sci Total Environ* 408:1634-1639.
8. Smyth SA, Lishman L, Alaee M, Kleywegt S, Svoboda L, Yang J-J, Lee H-B, Seto P (2007) *Chemosphere* 67:267-275.
9. Leonards P, Boer J (2004) *Handb Environ Chem* 3:49-84.
10. Moon HB, An YR, Choi SG, Choi M, Choi HG (2012) *Environ Toxicol Chem* 31:477-485.
11. Mersch-Sundermann V, Schneider H, Freywald C, Jenter C, Parzefall W, Knasmüller S (2001) *Mutat Res* 495:89-96.
12. Witorsch RJ, Thomas JA (2010) *Crit Rev Toxicol* 40:1-30.
13. Silva AR, Nogueira JM (2010) *Anal Bioanal Chem* 396:1853-1862.
14. Abdel-Rehim M (2011) *Anal Chim Acta* 701:119-228.
15. Duan C, Shen Z, Wu D, Guan Y (2011) *Trends Anal Chem* 30:1568-1574.
16. Moeder M, Schrader S, Winkler U, Rodil R (2010) *J Chromatogr A* 1217:2925-2932.
17. Vallecillos L, Pocurull E, Borrull F (2012) *J Chromatogr A* 1264:87-94.
18. Posada-Ureta O, Olivares M, Navarro P, Vallejo A, Zuloaga O, Etxebarria N (2012) *J Chromatogr A* 1227:38-47.
19. Martínez-Girón AB, Crego AL, González MJ, Marina ML (2010) *J Chromatogr A* 1217:1157-1165.

BLOQUE III. NANOPARTÍCULAS COMO HERRAMIENTAS ANALÍTICAS

20. Wackerbarth H, Gundrum, L, Salb, C, Christou K, Viol W (2010) *Appl Opt* 49:4367-4371.
21. SERS Surface Enhanced Raman Spectroscopy (2001) Michigan State University, USA <http://www.cem.msu.edu/~cem924sg/ChristineHicks.pdf>.
22. Carrillo-Carrión C, Simonet BM, Valcárcel M, Lendl B (2012) *J Chromatogr A* 1225:55-61.
23. Yu WW, White IM (2012) *Analyst* 137:1168-1173.
24. Jiang L, Yin P, You T, Wang H, Lang X, Guo L, Yang S (2012) *ChemPhysChem* 13:3932-3936.
25. Prochazka M, Simakova P, Hajdukova-Smidova N (2012) *Colloids Surf A Physicochem Eng Aspects* 402:24-28.

BLOQUE IV



Estudios toxicológicos de nanopartículas

Introducción	271
IV.1. The toxicity of silver nanoparticles depends on their uptake by cells and thus on their surface chemistry	273
IV.2. Effects of the interaction of single-walled carbon nanotubes with 4-nonylphenol on their <i>in vitro</i> toxicity	315

INTRODUCCIÓN

A lo largo del Bloque III de esta Memoria se expusieron detalladamente las aplicaciones analíticas desarrolladas durante el transcurso de la Tesis Doctoral basadas en el empleo de las NPs como herramientas en el ámbito de la Química Analítica. Sin embargo, otra faceta no menos importante es la consideración de los posibles efectos tóxicos que conlleva el empleo de estos nanomateriales y que se tratará a lo largo del presente Bloque IV.

La investigación de nuevas aplicaciones para las NPs debe ir acompañada de la evaluación de sus potenciales efectos tóxicos. No obstante, alcanzar un desarrollo equilibrado entre estos dos ámbitos de estudio no siempre se consigue y constituye un reto a alcanzar. Por ello, esta Tesis Doctoral pretende abarcar dos vertientes claramente definidas. Por un lado, desarrollar nuevos procedimientos analíticos con el empleo de NPs y por otro, profundizar en el estudio de la toxicidad asociada a estos nanomateriales.

En este Bloque IV se encuadran dos aportaciones científicas al ámbito de la *Nanotoxicología* en cuestión. En primer lugar se abordará un trabajo enfocado a realizar un estudio comparativo entre NPs de plata sintetizadas con diferentes recubrimientos superficiales, en términos de su estabilidad coloidal, su grado de oxidación, su internalización celular y su citotoxicidad. La importancia de este trabajo radica en evaluar cómo y en qué grado el recubrimiento superficial de las NPs puede modular su toxicidad por condicionar diferentes propiedades fisicoquímicas de las mismas o definir su diferente interacción con las células. La segunda aportación científica tiene su origen en la hipótesis de que los contaminantes no se encuentran aislados en el medio ambiente sino que pueden entrar en contacto e interactuar de alguna manera con otras especies. Esta hipótesis gana aún más peso si tenemos en cuenta la capacidad de adsorción de las NPs hacia determinados compuestos

Introducción

orgánicos, capacidad que ha sido y sigue siendo explotada a día de hoy en multitud de métodos de extracción en fase sólida. Esto nos lleva a plantear un estudio en el que se evalúa cuál es el efecto de la coexistencia de los nanotubos de carbono con un contaminante ambiental común sobre su toxicidad *in vitro*, teniendo en cuenta que ambas especies presentan un uso extendido en la sociedad actual y pueden interaccionar como consecuencia de su estructura aromática.

IV.1. Toxicity of silver nanoparticles depends on their surface chemistry



Part. Part. Syst. Charact. 2013, 30, 1079–1085



The toxicity of silver nanoparticles depends on their uptake by cells and thus on their surface chemistry

Encarnación Caballero-Díaz^{1,2}, Christian Pfeiffer¹, Lena Kastl¹, Pilar Rivera-Gil¹, Bartolome Simonet², Miguel Valcárcel², Javier Jiménez-Lamana³, Francisco Laborda³, and Wolfgang J. Parak^{1,4}

¹Fachbereich Physik, Philipps Universität Marburg, Marburg, Germany.

²Department of Analytical Chemistry, Campus de Rabanales, University of Córdoba, Córdoba, Spain.

³Group of Analytical Spectroscopy and Sensors (GEAS), Institute of Environmental Sciences (IUCA), University of Zaragoza, Zaragoza, Spain.

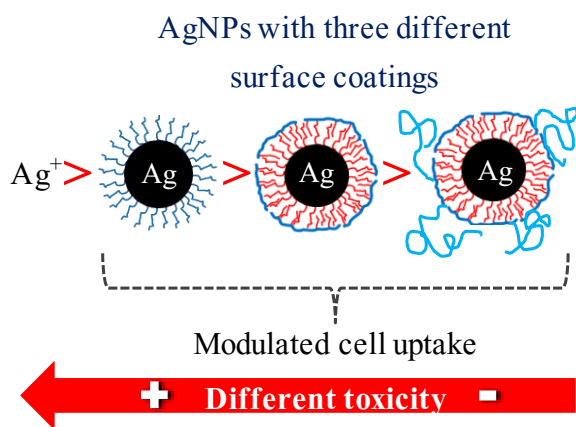
⁴CIC Biomagune, San Sebastián, Spain.

ABSTRACT

A set of three types of silver nanoparticles (Ag NPs) are prepared, which have the same Ag cores, but different surface chemistry. Ag cores are stabilized with mercaptoundecanoic acid (MUA) or with a polymer shell [poly(isobutylene-alt-maleic anhydride) (PMA)]. In order to reduce cellular uptake, the polymer-coated Ag NPs are additionally modified with polyethylene glycol (PEG). Corrosion (oxidation) of the NPs is quantified and their colloidal stability is investigated. MUA-coated NPs have a much

lower colloidal stability than PMA-coated NPs and are largely agglomerated. All Ag NPs corrode faster in an acidic environment and thus more Ag(I) ions are released inside endosomal/lysosomal compartments. PMA coating does not reduce leaching of Ag(I) ions compared with MUA coating. PEGylation reduces NP cellular uptake and also the toxicity. PMA-coated NPs have reduced toxicity compared with MUA-coated NPs. All studied Ag NPs were less toxic than free Ag(I) ions. All in all, the cytotoxicity of Ag NPs is correlated on their uptake by cells and agglomeration behavior.

GRAPHICAL ABSTRACT



IV.1. Toxicity of silver nanoparticles depends on their surface chemistry

1. INTRODUCTION

Silver nanoparticles (Ag NPs) are frequently used in industry, mainly because of their antimicrobial properties,^[1] with applications in an increasing number of medical and consumer products. However, their antibacterial features and extremely small size, which makes them to have a high surface area and to be more reactive, also suggest a toxicological risk when these NPs come into contact with biological systems.^[2] Countless toxicological studies involving Ag NPs have already been carried out in different organisms ranging from bacteria to humans.^[3-5] Although it is generally known that corrosion (oxidation) and subsequent release of Ag(I) ions is a major source of toxicity,^[6,7] there is still a lack of detailed general knowledge concerning the origin of the Ag NPs' toxicity. Most important shortcomings are that individual studies are often based on different NPs, and also on different types of cells, which complicate the comparison and extrapolation of results. In some studies, the final toxicity resulted to be an unclear combination of effects among the Ag NPs and their released Ag(I) ions, whereas in other works the Ag(I) ions showed a greater (or even the only) contribution to the toxicity than the Ag NPs *per se*.^[3,7-9] Several studies describe the release of Ag(I) ions upon NP oxidation and subsequent partial dissolution of the Ag NPs over time as amplification of the toxicity of the (undissolved) Ag NPs, which can cause intracellular reactions, as, for example, in the mitochondria.^[5] Other studies even claim that the only effect originates from Ag ions, which acts on the cell membrane, whereas under the same conditions Ag NPs had no effect.^[9] Studies indicate that toxicity depends on size,^[10] shape,^[11] charge,^[12] and colloidal stability^[13] of the Ag NPs.

Although correlation of the physicochemical properties of NPs to their interaction with cells is attempted by a large-body research studies, a comprehensive picture is still missing (not only for Ag NPs but in general) albeit many effects are well established. This is partly due to the fact that not all

physicochemical properties are easy to be determined experimentally, and most of them are entangled (e.g., loss in colloidal stability/reduced dispersion also increases the effective hydrodynamic diameter of the NPs).^[14] The interaction of NPs with cells is not only governed directly, but also it is strongly influenced by interplay with the medium. Salt can reduce colloidal stability, and the NP surface will be covered with a corona of proteins, which provides signature to the NP surface.^[15] This interaction is not static, but rather dynamic and may change with time.^[16] Although this already gives a complex scenario for the NP–medium interaction, modern techniques such as fluorescence correlation spectroscopy (FCS) allow for detailed investigation of the physicochemical properties of NPs in many protein-containing media^[17] (but not in all, for instance, not in blood). Characterization is, however, complicated as soon as NPs enter cells. Going back to the dynamic picture of the protein corona,^[15] its composition certainly will change inside cells. Enzymes in endo/lysosomal compartments can, for example, digest part of the protein corona.^[18] Also the pH in these compartments, in which NPs are typically residing, is highly acidic. In particular in the case of Ag NPs, this may enhance oxidation of the inorganic NP core by release of Ag(I) ions, which in turn would affect toxicity. In order to single out such effects, highly defined NPs, in which parameters are varied in a controlled way, and appropriate test media, are warranted.

In the present study, we wanted to investigate two hypotheses. The first one is that toxicity of Ag NPs is correlated with their uptake by cells, i.e., the more internalized Ag NPs, the greater their toxicity. This was motivated by previous studies based on different types of NPs.^[19] In order to test this hypothesis, cells need to be exposed to the same amounts of Ag NPs, but different amounts are internalized. One possibility to enhance uptake of Ag NPs is coupling them to magnetic NPs. Enhanced internalization of Ag NPs via magnetofection has been demonstrated to increase cytotoxicity.^[20] In our study,

IV.1. Toxicity of silver nanoparticles depends on their surface chemistry

we wanted to attempt an alternative strategy. Ag NPs are internalized via endocytotic pathways,^[21] whereby uptake can be controlled by the surface chemistry of the NPs. Polyethylene glycol (PEG) of 10 kDa molecular weight is commonly used to reduce NP uptake by cells *in vitro*^[22] and also to increase *in vivo* retention times.^[23] Thus, in this study, we modulate uptake of Ag NPs by PEGylation and compare toxic effects obtained for Ag NPs with PEG to those obtained for the same Ag NPs but without PEG. The second hypothesis is that toxicity of Ag NPs is correlated to how fast they corrode, i.e., how fast they dissolve under physiological conditions. Also this hypothesis has been motivated by previous reports.^[7] As pointed out above, one hereby needs to consider that NPs internalized in endo/lysosomal structures are exposed to highly acidic pH, which enhanced NP dissolution, in contrast to the neutral pH in extracellular media. In our study, we attempt to modulate oxidation of Ag NPs by different protective surface coatings. Often Ag NPs are capped by a monolayer of surfactant, and thus have been also termed previously as monolayer-protected clusters.^[24] Additionally, we protected and stabilized the NP surface by wrapping a polymer around the original surfactant shell.^[25] Altogether the key point of our study is that all experiments are based on the same Ag cores. By modification of the surface chemistry, both uptake by cells and oxidation are controlled. As the actual Ag cores of the different Ag NPs are identical, and also the final Ag NPs are well defined and characterized, comparative studies can be performed.

2. MATERIALS AND METHODS

2.1. Synthesis of hydrophobic Ag NPs ^[26]

Ag NPs capped with dodecylthiol were synthesized following the protocol of Mari et al.^[27] These hydrophobic NPs were dispersed in chloroform and had a core diameter (i.e., the diameter of the inorganic Ag NP, excluding the organic

capping^[14], of $d_c = 4.2 \pm 0.4$ nm and an experimentally determined molecular extinction coefficient of $\epsilon = 16.9 \times 10^6 \text{ M}^{-1} \text{ cm}^{-1}$ at the surface plasmon peak at 430 nm. Based on this, we calculated that each Ag NP in average contains $N_{\text{Ag}} \approx 2200$ Ag atoms in total, whereby $\approx 30\%$ ($N_{\text{Ag,surf}} \approx 650$) Ag atoms are located on the surface of each NP. For a detailed description of the synthesis protocol and the calculations, we refer to the Supporting Information. In the following section, different strategies on how these NPs were transferred to aqueous phase will be described.

2.2. Synthesis of hydrophilic Ag NPs

The hydrophobic Ag NPs were transferred *via* two strategies to aqueous phase. First, the hydrophobic dodecylthiol ligands were replaced with hydrophilic mercaptoundecanoic acid (MUA) ligands by a ligand-exchange procedure, resulting in water-soluble Ag-MUA NPs. Second, an amphiphilic polymer [dodecylamine-modified poly(isobutylene-alt-maleic anhydride) PMA] was wrapped around the original ligand shell, leading to water-soluble Ag-PMA NPs. Advantages and disadvantages of both procedures have been compared in previous works.^[28] The resulting Ag NPs were stringently purified by gel electrophoresis and size exclusion chromatography, which allows for sufficient removal of excess of reactants and polymeric micelles^[29] (for the case of polymer-coating). Using EDC (1-ethyl-3-(3-dimethylaminopropyl)carbodiimide) chemistry, 10 kDa amino-modified polyethylene glycol $\text{NH}_2\text{-PEG-CH}_3$ (Rapp Polymere) was linked *via* the amino group to the carboxyl groups on the surface of Ag-PMA NPs. NPs saturated with PEG (Ag-PMA-satPEG NPs) and with exactly one PEG per NP (Ag-PMA-1PEG NPs) were obtained and fractionated *via* gel electrophoresis. Thus, four different surface modifications based on the same original hydrophobic NPs were obtained: Ag-MUA, Ag-PMA, Ag-PMA-1PEG, Ag-PMA-satPEG (Figure 1). Details of the surface modification protocols are reported in detail in the Supporting Information.

IV.1. Toxicity of silver nanoparticles depends on their surface chemistry

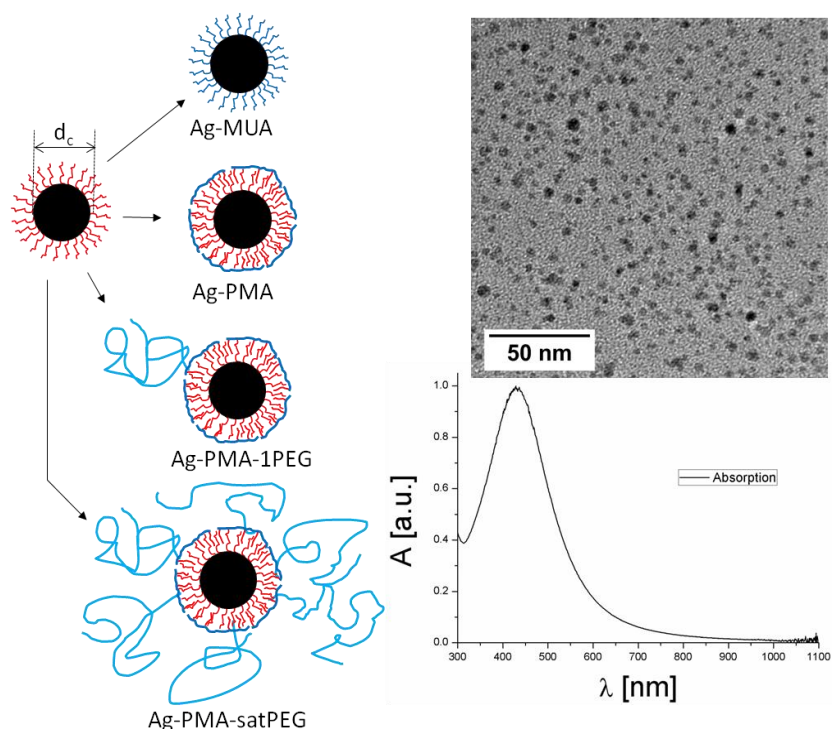


Figure 1. Sketch of the four types of surface modifications, which were applied to the same hydrophobically capped Ag NPs. The Ag cores (with core diameter d_c) are depicted in black, and the original hydrophobic ligand shell is depicted in red. The following surface modifications have been applied to obtain water-soluble NPs. a) Ligand exchange to mercaptoundecanoic acid (Ag-MUA NPs; the hydrophilic ligands are depicted in blue). b) Overcoating with an amphiphilic polymer (Ag-PMA NPs). c) Overcoating with an amphiphilic polymer and conjugation with one PEG molecule per NP (Ag-PMA-1PEG NPs). d) Overcoating with an amphiphilic polymer and subsequent saturation of the surface with polyethyleneglycol (Ag-PMA-satPEG NPs).

2.3. Characterization of colloidal properties

The colloidal properties of the Ag NPs were characterized according to our standard protocols,^[30] including determination of the hydrodynamic diameter (d_h) by dynamic light scattering (DLS), the zeta-potential (ζ)^[31] by laser Doppler anemometry (LDA), and stability in salt-containing solutions (Table 1). For the stability assays, changes in the d_h upon the presence of NaCl were recorded (Figure 2).

2.4. Characterization of NP oxidation

Despite stringent purification after synthesis, the Ag cores of the Ag NPs corrode over time, leading to the release of Ag(I) ions.^[7] Release of Ag(I) was quantified both, at neutral (pH=7) and acidic (pH=3) conditions, using ultrafiltration and inductively coupled plasma mass spectrometry (ICP-MS).

2.5. Analysis of NP uptake by cells

The cellular uptake of Ag NPs was analyzed by confocal laser scanning microscopy (CLSM). NIH/3T3 embryonic fibroblasts were seeded on Ibidi-Plates at cell densities of 2×10^4 cells/well in 300 μ L growth medium (DMEM-F12 Ham's basal medium supplemented with 10% calf serum, 1% L-glutamine, and 1% penicillin/streptomycin). The next day, the cells were rinsed with phosphate-buffered saline (PBS) and incubated with DY-636-modified fluorescent Ag NPs (Supporting Information) at a concentration of $c(\text{Ag NP}) = 10 \times 10^{-9}$ M ($\lambda_{\text{excitation}}$ 645 nm and $\lambda_{\text{emission}}$ 671 nm) for 15 h at 37 °C and 5% CO₂. The cells were then analyzed with a CLSM (Zeiss LSM Meta; Figure 3).

2.6. Analysis of cell viability

Viability of NIH/3T3 embryonic fibroblasts upon incubation with Ag NPs was probed with a standard resazurin assay.^[32] Silver nitrate was used as positive control. Resazurin is a blue, non-fluorescent sodium salt, which is converted to resorufin by metabolically active cells. Resorufin is a pink, fluorescent sodium salt that accumulates outside the cells. This reduction process requires functional mitochondrial activity, which is inactivated immediately after cell death. Thus, cell viability was assessed by the increase in the fluorescence signal and is given as mean of normalized intensities against the concentration of Ag. The response curves were fitted with a sigmoidally

IV.1. Toxicity of silver nanoparticles depends on their surface chemistry

shaped curve, of which the point of inflection was taken as LD_{50} value, i.e., the concentration when cell viability was reduced by half (Figure 4).

3. RESULTS AND DISCUSSION

3.1. Colloidal properties

Four different surface modifications applied to the same Ag cores were compared. All NP samples have comparable hydrodynamic diameters (Table 1) in PBS. PEGylation increases the diameter, which is indicated in gel electrophoresis and size exclusion chromatography experiments (Supporting Information). Surprisingly, we were reproducibly not able to observe this also with DLS, which is however within the error bars. In the DLS data, MUA and PMA provide negative charge to the NPs, and thus colloidal stability *via* electrostatic repulsions (the zeta-potential data in Table 1). Saturation of the NPs surface with PEG (Ag-PMA-satPEG NPs) reduces the negative charge, but the colloidal stability is conducted by steric repulsions.

Table 1. Colloidal (hydrodynamic diameter d_h and zeta-potential ζ) and toxic properties (concentration of half viability, LD_{50}) of Ag NPs with different surface coating, with a core diameter of $d_c = 4.2$ nm. The concentrations refer to the number of Ag atoms in solution ($c(\text{Ag})$). The LD_{50} value for AgNO_3 was determined as $0.022 \pm 1.24 \times 10^{-5} \times 10^{-3}$ M.

Sample	d_h [nm]	ζ [mV]	LD_{50} [$\times 10^{-3}$ M]
Ag-MUA	11 ± 4	-24.9 ± 1.7	$0.04 \pm 2.83 \cdot 10^{-4}$
Ag-PMA	12 ± 3	-31.0 ± 1.3	$0.65 \pm 8.66 \cdot 10^{-3}$
Ag-PMA-1PEG	13 ± 4	-41.1 ± 1.5	$0.73 \pm 6.48 \cdot 10^{-3}$
Ag-PMA-satPEG	12 ± 3	-10.9 ± 0.4	$1.34 \pm 2.49 \cdot 10^{-2}$

However, as soon as NaCl is added to PBS, dramatic differences in colloidal stability of the NPs are visible. While for Ag-PMA NPs, the hydrodynamic diameter upon the presence of NaCl (up to 2.5 M) remains relatively unaffected, Ag-MUA NPs completely agglomerate, which is visible by

their huge hydrodynamic diameters (Figure 2). Please note that colloidal characterization was performed in neutral PBS buffer containing different amounts of NaCl, not in the actual cell media. The presence of NaCl can provoke electrostatic screening and thus induces agglomeration. The presence of proteins (in serum-containing cell media) also could act on colloidal stability. However, as proteins and the NPs in this study have hydrodynamic radii on the same order of magnitude, DLS is hard to perform.^[33] Data with similar NPs (the same polymeric surface coating but Au instead of Ag cores) demonstrate that the presence of proteins can under our experimental conditions further reduce colloidal stability.^[33] Thus, we can conclude that Ag-MUA NPs are highly agglomerated even at neutral pH and without the presence of proteins, whereas Ag-PMA NPs (with/without PEGylation) are much better dispersed. This is due to the more negative zeta-potential of PMA versus MUA coatings, which leads to stronger electrostatic repulsions for Ag-PMA NPs than for Ag-MUA NPs. For PEGylated NPs, the loss of colloidal stability due to electrostatic screening by NaCl is compensated by steric repulsions.

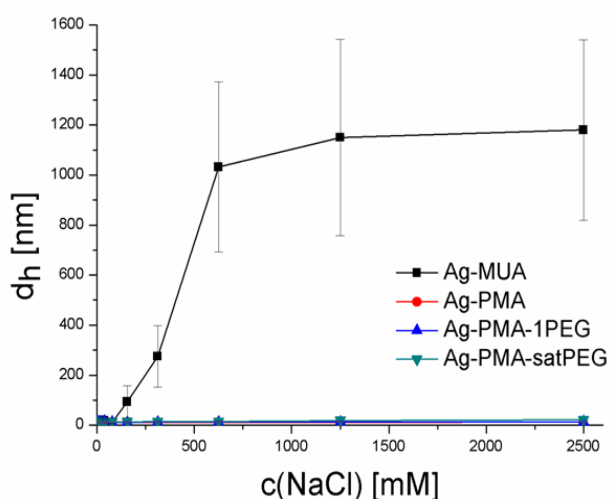


Figure 2. Change of the hydrodynamic diameter (d_h) of the Ag NPs upon presence of NaCl (d_h was detected directly after exposure of the Ag NPs to AgCl). The error bars belong to the width of the peak.

IV.1. Toxicity of silver nanoparticles depends on their surface chemistry

3.2. NP oxidation

The Ag NPs were stringently cleaned after synthesis, leading to the removal of excess Ag(I) ions in solution. Kittler et al.^[7] demonstrated release of Ag(I) from the Ag NPs due to oxidation. In order to study the release of Ag(I), NP samples incubated in water were analyzed by ultrafiltration followed by ICP-MS. At pH 7, even after 7 days of incubation, the amount of Ag(I) released from the Ag NPs was below the detection limit (<0.0015%; Supporting Information for details). On the other hand, after 7 days of incubation at pH 3 solution, around 1% of the Ag from the Ag NPs was detected as Ag(I) in solution. This suggests that Ag NPs inside acidic endo/lysosomal compartments release more Ag(I) than NPs in the extracellular neutral medium. No significant differences among the four different NP samples were observed. This can be explained by the fact that all are capped by thiolated hydrocarbon chains of comparable length (mercaptoundecanoic acid for Ag-MUA NPs and dodecylthiol for Ag-PMA NPs, respectively). Thus, changes in the outer surface cappings as PEGylation did not have significant effects on NPs oxidation. We also found in agreement with Kittler et al.^[7] that Ag NPs are not completely dissolved and only a certain amount of Ag(I) is released. Analyses were performed in water at different pH, and not in the cell medium. To the best of our knowledge, proteins as particular enzymes in the cell medium can partly disintegrate the organic shell around,^[18] but not extensively dissolve inorganic (e.g., Ag) cores.

3.3. NP internalization

As can be clearly seen in Figure 3, the uptake of Ag-PMA NPs was strongly reduced when the surface of the NPs was saturated with PEG molecules of 10 kDa size (Ag-PMA-satPEG NPs vs Ag-PMA NPs). We did not quantify uptake as this has been already previously done with similar NPs,^[22,33] and the qualitative

results are sufficiently indicative. Data also clearly demonstrate that Ag-PMA NPs are internalized to a much higher extent than Ag-PMA-satPEG NPs. Unfortunately, we were not able to quantitatively compare the uptake of Ag-MUA NPs and Ag-PMA NPs. This is due to the fact that on the basis of different surface chemistry, the DY636 fluorescence labels were attached differently to the NPs. Besides different amount of fluorophore per NP, they also will have different distance to the Ag cores and thus different quenching effects. The main statement of the uptake experiments thus is that PEGylation drastically reduces the uptake of NPs by cells, in accordance with previous works.

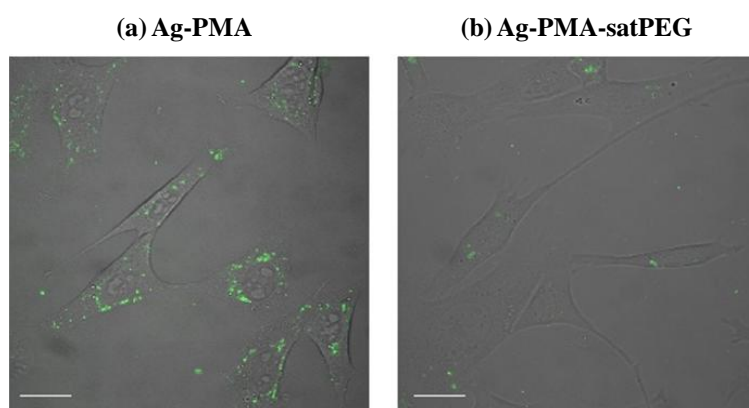


Figure 3. Fluorescence images of 3T3 fibroblasts which had been exposed for 15 hours to fluorescence (DY636) labeled a) polymer-coated Ag NPs or b) polymer-coated Ag NPs whose surface has been saturated with 10 kDa PEG molecules. The images correspond to the overly images of the transmission and fluorescence channel. Scale bars correspond to 20 μm .

3.4. Cell viability

As expected, free Ag(I) ions (AgNO_3 solution as positive control) significantly reduce the viability of NIH/3T3 cells, as quantitatively demonstrated in dose-response curves (one time point, one type of assay, and one cell type; Figure 4). Also in case Ag(I) is introduced in the cells *via* Ag NPs, the cell viability is reduced. In comparison to the MUA coating, the PMA coating

IV.1. Toxicity of silver nanoparticles depends on their surface chemistry

was effective in reducing the toxicity of the Ag NPs. The surface modification of PMA-coated Ag NPs with one single PEG molecule (10 kDa) per NP (Ag-PMA-1PEG NPs) exhibited a similar dose-response curve (with similar LD₅₀ values) to Ag-PMA NPs. In contrast, dose-response curve for Ag-PMA-satPEG NPs was strongly shifted to higher concentrations values. This indicates that much lower concentrations of nonPEGylated Ag NPs than of PEGylated NPs are necessary to induce cell death.

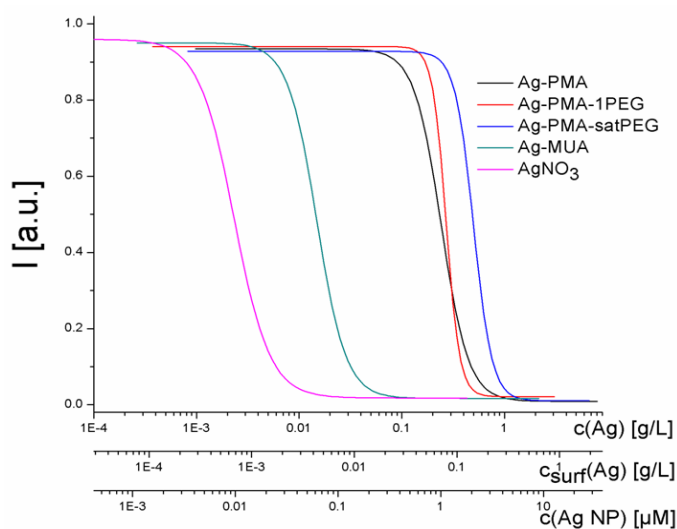


Figure 4. Resazurin-based viability test of 3T3 fibroblasts, which had been incubated for 24 hours with Ag NPs. Onset of fluorescence (as quantified by the measured intensity I) is an indicator for viability of cells. The amount of Ag is quantified in a) the total amount of Ag ($c(\text{Ag})$), b) the amount of Ag atoms which are present on the NP surface ($c_{\text{surf}}(\text{Ag})$), and c) the amount of Ag NPs ($c(\text{Ag NP})$). The following scaling factors were used (Supporting Information): $c_{\text{surf}}(\text{Ag}) = 0.29 c(\text{Ag})$ and $c(\text{Ag NP}) = 4.2 \cdot 10^{-9} \text{ mol mg}^{-1} c(\text{Ag})$. In case of AgNO_3 as silver source, only the $c(\text{Ag})$ concentration scale is valid; in case of all the NPs, all three concentration scales are valid.

4. CONCLUSIONS

Correlation of the interaction of the NPs with cells and their physicochemical properties allows for a set of conclusions: i) Toxicity of Ag NPs

was lower in comparison to Ag(I) ions, in case of normalization of the absolute amount of Ag. In Figure 4, NP concentration is given in terms of $c(\text{Ag})$ gram per liter, which allows for direct comparison. Even if one assumed that in the case of Ag-MUA NPs all Ag atoms on the NP surface went into solution, there is still a lower toxic effect in comparison to the same amount of free Ag(I) ions (from AgNO₃). Even in the worst case (Ag-MUA NPs), the toxicity from all Ag atoms on the surface still is lower than the one for free Ag(I), in case the $c_{\text{surf}}(\text{Ag})$ scale for Ag NPs is compared with the $c(\text{Ag})$ scale for AgNO₃. In addition, while $\approx 30\%$ of the Ag within Ag NPs is bound on surface, our ICP-MS data indicated that even at pH 3, only $\approx 1\%$ of Ag is released from the Ag NPs into solution. Thus, under our experimental conditions, Ag NPs are less toxic compared to Ag(I) ions in terms of absolute amounts of Ag, as most of the Ag in NPs is bound to the NPs and not available as Ag(I). Please note that this is the opposite as reported by Cronholm et al.,^[9] who, however, worked under different experimental conditions (other NPs and cells). In our case, even if one assumed the outer capping of Ag NPs to be oxidized, there is still lower toxicity compared to AgNO₃. Additionally, PMA coating did not reduced the release of Ag(I) *versus* MUA coating, but reduced cytotoxicity; *ii*) Toxicity of Ag NPs depends on their uptake by cells. One may argue that the 1% of released Ag(I) ions from internalized Ag NPs has a more cytotoxic effect than assuming a scenario in which all Ag atoms situated at the Ag NP surface ($\approx 30\%$) would be released extracellularly. Ag(I) as free ion is not membrane permeable (although it can be complexed by serum proteins) and thus Ag NPs are an efficient carrier to transport Ag(I) ions inside cells. The difference between intracellular and extracellular Ag is demonstrated upon comparison of Ag-PMA and Ag-PMA-satPEG NPs. PEGylation reduces cellular uptake, which goes hand in hand with a lower cytotoxicity; *iii*) Agglomeration is a key parameter in Ag NPs toxicity. Comparing the cytotoxic effects between Ag-MUA NPs and Ag-PMA NPs, different agglomeration behavior is the most likely reason. Ag-MUA NPs showed a greater tendency to agglomerate what finally resulted in an increased

IV.1. Toxicity of silver nanoparticles depends on their surface chemistry

cytotoxicity. Toxic effects may be explained by clouding the cell membrane, as has been speculated previously.^[34] Although our data clearly demonstrate that toxicity due to intracellular Ag is higher than that due to extracellular Ag (note that in contrast, in the report by Cronholm et al.,^[9] toxicity was generated by the extracellular interaction of Ag(I) to the cell membrane, unfortunately we could not quantify this in terms of the contribution of Ag from Ag(I) or Ag NPs. Characterization of physicochemical properties of internalized NPs still remains a future challenge, which, however, is strongly needed for further unraveling pathways of cytotoxic effects and their attribution to distinct physicochemical properties.

Acknowledgements

E.C.-D. and C.P. contributed equally to this work. This work was supported by the BMBF Germany (project UMSICHT to WJP). E.C.-D. also would like to thank the Spanish Ministry of Education for the award of a FPU fellowship (Grant AP2008-02955).

References

- [1] a) C. Marambio-Jones, E. M. V. Hoek, *J. Nanopart. Res.* **2010**, *12*, 1531; b) M. J. Hajipour, K. M. Fromm, A. A. Ashkarran, D. J. d. Aberasturi, I. R. d. Larramendi, T. Rojo, V. Serpooshan, W. J. Parak, M. Mahmoudi, *Trends Biotechnol.* **2012**, *30*, 499; c) S. Chernousova, M. Epple, *Angew. Chem Int. Ed.* **2013**, *52*, 1636.
- [2] S. W. P. Wijnhoven, W. J. G. M. Peijnenburg, C. A. Herberts, W. I. Hagens, A. G. Oomen, E. H. W. Heugens, B. Roszek, J. Bisschops, I. Gosens, D. Van de Meent, S. Dekkers, W. H. De Jong, M. Van Zijverden, A. J. A. M. Sips, R. E. Geertsma, *Nanotoxicology* **2009**, *3*, 109.
- [3] C. Beer, R. Foldbjerg, Y. Hayashi, D. S. Sutherland, H. Autrup, *Toxicol. Lett.* **2012**, *208*, 286.
- [4] a) J. S. Teodoro, A. M. Simoes, F. V. Duarte, A. P. Rolo, R. C. Murdoch, S. M. Hussain, C. M. Palmeira, *Toxicol. In Vitro* **2011**, *25*, 664; b) R. Liu, S. J. Lin, R. Rallo, Y. Zhao, R. Damoiseaux, T. Xia, S. Lin, A. Nel, Y. Cohen, *Plos One* **2012**, *7*, e35014; c) E. Demir, G. Vales, B. Kaya, A. Creus, R. Marcos, *Nanotoxicology* **2011**, *5*, 417; d) C. Greulich, J. Diendorf, J. Gessmann, T. Simon, T. Habijan, G. Eggeler, T. A. Schildhauer, M. Epple, M. Koller, *Acta Biomater.* **2011**, *7*, 3505; e) S. Shrivastava, T. Bera, S. K. Singh, G. Singh, P. Ramachandrarao, D. Dash, *ACS Nano* **2009**, *3*, 1357.
- [5] P. V. AshaRani, G. Low Kah Mun, M. P. Hande, S. Valiyaveetil, *ACS Nano* **2009**, *3*, 279.
- [6] a) J. Liu, D. A. Sonshine, S. Shervani, R. H. Hurt, *ACS Nano* **2010**, *4*, 6903; b) J. Liu, R. H. Hurt, *Environ. Sci. Technol.* **2010**, *44*, 2169.
- [7] S. Kittler, C. Greulich, J. Diendorf, M. Koller, M. Epple, *Chem. Mater.* **2010**, *22*, 4548.
- [8] R. Foldbjerg, P. Olesen, M. Hougaard, D. A. Dang, H. J. Hoffmann, H. Autrup, *Toxicol. Lett.* **2009**, *190*, 156.
- [9] P. Cronholm, H. L. Karlsson, J. Hedberg, T. A. Lowe, L. Winnberg, K. Elihn, I. O. Wallinder, L. Moller, *Small* **2013**, *9*, 970.
- [10] a) M. V. Park, A. M. Neigh, J. P. Vermeulen, L. J. de la Fonteyne, H. W. Verharen, J. J. Briede, H. van Loveren, W. H. de Jong, *Biomaterials* **2011**, *32*, 9810; b) H.-J. Yen, S.-H. Hsu, C.-L. Tsai, *Small* **2009**, *5*, 1553; c) C. Carlson, S. M. Hussain, A. M. Schrand, L. K. Braydich-Stolle, K. L. Hess, R. L. Jones, J. J. Schlager, *J. Phys. Chem. B* **2008**, *112*, 13608.
- [11] L. C. Stoehr, E. Gonzalez, A. Stampfl, E. Casals, A. Duschl, V. Puentes, G. J. Oostingh, *Part. Fibre Toxicol.* **2011**, *8*, 36.
- [12] A. M. El Badawy, R. G. Silva, B. Morris, K. G. Scheckel, M. T. Suidan, T. M. Tolaymat, *Environ. Sci. Technol.* **2010**, *45*, 283.

IV.1. Toxicity of silver nanoparticles depends on their surface chemistry

- [13] I. Romer, T. A. White, M. Baalousha, K. Chipman, M. R. Viant, J. R. Lead, *J. Chromatogr. A* **2011**, *1218*, 4226.
- [14] P. Rivera-Gil, D. Jimenez de Aberasturi, V. Wulf, B. Pelaz, P. del Pino, Y. Zhao, J. de la Fuente, I. Ruiz de Larramendi, T. Rojo, X.-J. Liang, W. J. Parak, *Acc. Chem. Res.* **2013**, *46*, 743.
- [15] M. P. Monopoli, C. Aberg, A. Salvati, K. A. Dawson, *Nat. Nanotechnol.* **2012**, *7*, 779 .
- [16] S. Milani, F. B. Bombelli, A. S. Pitek, K. A. Dawson, J. Radler, *ACS Nano* **2012**, *6*, 2532.
- [17] a) C. Röcker, M. Pötzl, F. Zhang, W. J. Parak, G. U. Nienhaus, *Nat. Nanotechnol.* **2009**, *4*, 577; b) X. Jiang, S. Weise, M. Hafner, C. Röcker, F. Zhang, W. J. Parak, G. U. Nienhaus, *J. R. Soc. Interface* **2010**, *7*, S5.
- [18] M. Chanana, P. Rivera-Gil, M. A. Correa-Duarte, W. J. Parak, L. M. Liz-Marzán, *Angew. Chem Int. Ed.* **2013**, *52*, 4179.
- [19] N. Lewinski, V. Colvin, R. Drezek, *Small* **2008**, *4*, 26.
- [20] R. Di Corato, D. Palumberi, R. Marotta, M. Scotto, S. Carregal-Romero, P. Rivera-Gil, W. J. Parak, T. Pellegrino, *Small* **2012**, *8*, 2731.
- [21] C. Greulich, J. Diendorf, T. Simon, G. Eggeler, M. Epple, M. Koller, *Acta Biomater.* **2011**, *7*, 347.
- [22] C. Brandenberger, C. Mühlfeld, Z. Ali, A.-G. Lenz, O. Schmid, W. J. Parak, P. Gehr, B. Rothen-Rutishauser, *Small* **2010**, *6*, 1669.
- [23] M. Lipka, M. Semmler-Behnke, R. A. Sperling, A. Wenk, S. Takenaka, C. Schleh, T. Kissel, W. J. Parak, W. G. Kreyling, *Biomaterials* **2010**, *31*, 6574.
- [24] D. E. Cliffler, F. P. Zamborini, S. M. Gross, R. W. Murray, *Langmuir* **2000**, *16*, 9699.
- [25] C.-A. J. Lin, R. A. Sperling, J. K. Li, T.-Y. Yang, P.-Y. Li, M. Zanella, W. H. Chang, W. J. Parak, *Small* **2008**, *4*, 334.
- [26] Y. Sun, *Chem. Soc. Rev.* **2013**, *42*, 2497.
- [27] A. Mari, P. Imperatori, G. Marchegiani, L. Pilloni, A. Mezzi, S. Kaciulis, C. Cannas, C. Meneghini, S. Mobilio, L. Suber, *Langmuir* **2010**, *26*, 15561.
- [28] T. Pellegrino, S. Kudera, T. Liedl, A. M. Javier, L. Manna, W. J. Parak, *Small* **2005**, *1*, 48.
- [29] M. T. Fernández-Argüelles, A. Yakovlev, R. A. Sperling, C. Luccardini, S. Gaillard, A. S. Medel, J.-M. Mallet, J.-C. Brochon, A. Feltz, M. Oheim, W. J. Parak, *Nano Lett.* **2007**, *7*, 2613.

BLOQUE IV. ESTUDIOS TOXICOLÓGICOS DE NANOPARTÍCULAS

[30] C. Geidel, S. Schmachtel, A. Riedinger, C. Pfeiffer, K. Müllen, M. Klapper, W. J. Parak, *Small* **2011**, *7*, 2929.

[31] T. L. Doane, C. H. Chuang, R. J. Hill, C. Burda, *Acc. Chem. Res.* **2012**, *45*, 317.

[32] J. O'Brien, I. Wilson, T. Ortaon, F. Pognan, *Toxicology* **2001**, *164*, 132.

[33] D. Hühn, K. Kantner, C. Geidel, K. Chiad, S. Brandholt, S. Soenen, U. Linne, P. Rivera-Gil, J. M. Montenegro, K. Braeckmans, K. Müllen, U. G. Nienhaus, M. Klapper, W. J. Parak, *ACS Nano* **2013**, *7*, 3253.

[34] C. Kirchner, T. Liedl, S. Kudera, T. Pellegrino, A. Muñoz Javier, H. E. Gaub, S. Stölzle, N. Fertig, W. J. Parak, *Nano Lett.* **2005**, *5*, 331.

IV.1. Toxicity of silver nanoparticles depends on their surface chemistry

SUPPORTING INFORMATION

I) Synthesis of hydrophobic Ag nanoparticles.

II) Ligand exchange for obtaining hydrophilic Ag NPs (Ag-MUA NPs).

III) Polymer coating for obtaining hydrophilic Ag NPs (Ag-PMA NPs).

IV) PEGylation of polymer coated Ag NPs (Ag-PMA-1PEG, Ag-PMA-satPEG NPs).

V) Characterization of NP size and colloidal stability with gel electrophoresis.

VI) Characterization of NP size and colloidal stability with HPLC.

VII) Characterization of NP size and colloidal stability with dynamic light scattering.

VIII) Characterization of NP corrosion with ICP-MS.

IX) Viability tests.

I) Synthesis of hydrophobic Ag nanoparticles

The synthesis of the silver nanoparticles (Ag NPs) was done following the synthesis route reported by Mari *et al.*^[1]. First the ligand which is needed for the stabilization of the NPs (Sodium S-dodecylthiosulfate) was prepared. Then, the Ag NPs were synthesized in ethanol under presence of the ligand.

First, 1-bromodecane (25 mmol; 5.187 mL) was dissolved at 50 °C in 50 mL ethanol; sodium thiosulfate pentahydrate (25 mmol; 6.21 g) was dissolved in water and added. The mixture was refluxed for 3 h and after cooling down to room temperature the obtained white precipitate (sodium S-dodecylthiosulfate, *cf.* Figure SI-1) was filtered and again crystallized from ethanol.

For the synthesis of the Ag NPs, the ligand sodium S-dodecylthiosulfate (1.26 mmol; 390 mg) was dissolved in 90 mL ethanol at 50 °C. AgNO₃ (1.68 mmol; 282 mg) was added to the solution and stirred for 10 min. The mixture was white at the beginning and turned brown after a few minutes. After 10 min, sodium borohydride (8.4 mmol; 318 mg) in 15 mL ethanol was added and the mixture turned dark brown almost black immediately. After another 5 min of stirring, ascorbic acid (0.42 mmol; 74 mg) was added and the reaction was stirred for 3 h. Afterwards the reaction was cooled down to RT by removing the heat source. The precipitated Ag NPs were separated by centrifugation at 3000 rpm for 15 min, washed with water, ethanol and acetone, and finally dried in vacuum. The Ag NPs were then finally dissolved in chloroform. For a general review about Ag NPs synthesis in organic solvents *cf.* Sun *et al.* ^[2].

IV.1. Toxicity of silver nanoparticles depends on their surface chemistry

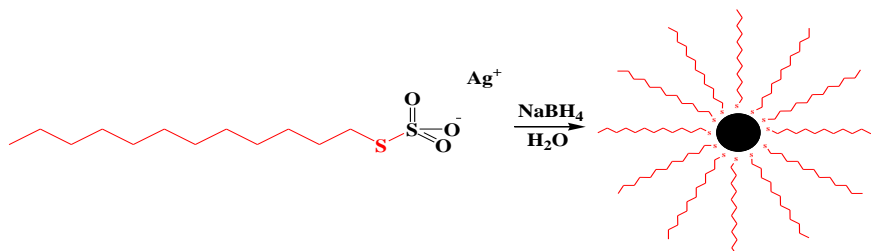


Figure SI-1. Reduction of Ag⁺ ions with NaBH₄ under the presence of S-dodecylsodium-sulfate, leading to the formation of Ag NPs. During this reaction the S-S bond cleaves, so that the final NP is coated with dodecylthiol [1].

The resulting Ag NPs were characterized by transmission electron microscopy (TEM). For this purpose, a Jeol JEM3010 was used. An image of the Ag NPs assembled on a TEM grid and the corresponding histogram of the distribution of the core diameters d_c is given in Figure SI-2. Note that the organic ligands (dodecylthiol) which are present of the Ag core do not provide contrast in TEM [3].

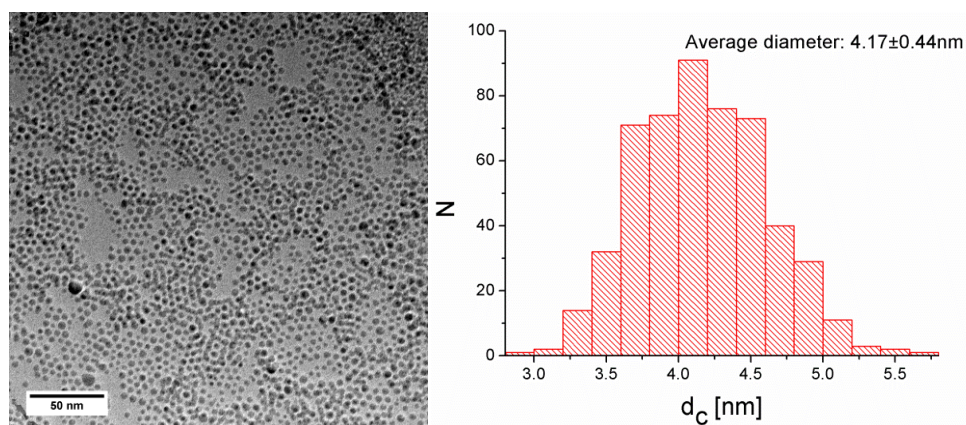


Figure SI-2. TEM image and a size distribution of dodecylthiol-capped Ag NPs. The scale bar corresponds to 50 nm. N denotes the number of counts as determined in the histogram. The average core diameter d_c was found to be 4.2 ± 0.4 nm.

BLOQUE IV. ESTUDIOS TOXICOLÓGICOS DE NANOPARTÍCULAS

The concentration of Ag NPs was determined *via* UV/Vis spectroscopy (Agilent 8453 spectrometer) assuming a molecular extinction coefficient of $\epsilon = 16,857,700 \text{ M}^{-1}\cdot\text{cm}^{-1} \approx 16.9\cdot 10^6 \text{ M}^{-1}\cdot\text{cm}^{-1}$ at the surface plasmon peak at 430 nm, *cf.* Figure SI-3.

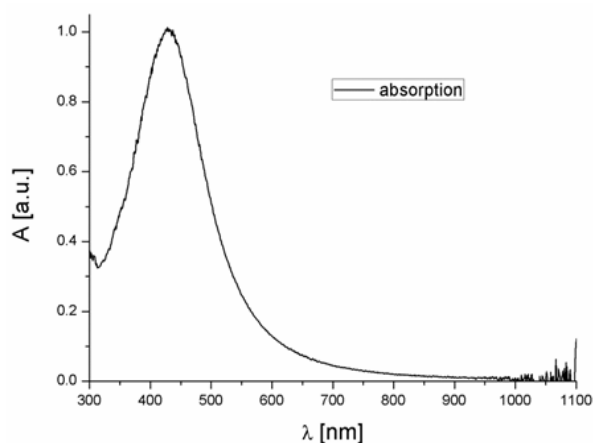


Figure SI-3. Absorption spectrum of Ag-PMA NPs in water. The plasmon peak at 430 nm is clearly visible.

The molecular extinction coefficient was experimentally derived with the following procedure. At first the amount of silver $c(\text{Ag})$ [$\text{kg}\cdot\text{L}^{-1}$] of a suspension of Ag-PMA NPs (*cf.* Chapter III) was measured with inductively coupled plasma mass spectrometry (ICP-MS) and the absorption spectra of a dilution series of this sample was measured. The mass of the inorganic core of one single Ag NP was calculated to be $m(\text{Ag NP}) = \rho_{\text{Ag}}\cdot V(\text{Ag NP}) = \rho_{\text{Ag}}\cdot(4\pi/3)\cdot(d_c/2)^3 = 3.99\cdot 10^{-22} \text{ kg} = 3.99\cdot 10^{-16} \text{ mg}$, based on the experimentally determined core diameter $d_c = 4.17 \text{ nm}$ (*cf.* Figure SI-2) and the density of bulk silver $\rho_{\text{Ag}} = 10.49 \text{ g/cm}^3$. The volume of one Ag core is $V(\text{Ag NP}) = 38 \text{ nm}^3$. The concentration for all the NP samples $c(\text{Ag NP})$ [$\text{mol}\cdot\text{L}^{-1}$] of the dilution series was then calculated as $c(\text{Ag NP})$ [$\text{mol}\cdot\text{L}^{-1}$] = $c(\text{Ag})$ [$\text{kg}\cdot\text{L}^{-1}$] / $\{m(\text{Ag NP})$ [kg] $\cdot N_A$ [mol^{-1}]\}. Where $N_A = 6.02\cdot 10^{23} \text{ mol}^{-1}$ is the Avogadro constant and $c(\text{Ag})$ is the concentration value of Ag atoms obtained by ICP-MS. Finally these concentrations were plotted against the

IV.1. Toxicity of silver nanoparticles depends on their surface chemistry

respective absorption values as recorded at 430 nm (with a cuvette of 1 cm pathlength). The slope of the linear fit of the data yields the extinction coefficient ϵ (cf. Figure SI-4). A UV/Vis spectra of the Ag NPs dissolved in water is shown in Figure SI-3. The NPs show the typical surface plasmon band for Ag NPs at 430 nm. Note that literature values for the extinction coefficient of silver NPs of sizes between 20 nm and 300 nm in gelatin sols [4] vary from $4.16 \cdot 10^9 \text{ M}^{-1} \cdot \text{cm}^{-1}$ (20 nm) up to $8 \cdot 10^{11} \text{ M}^{-1} \cdot \text{cm}^{-1}$ (300 nm), and are thus at least two orders of magnitude higher than the here calculated value.

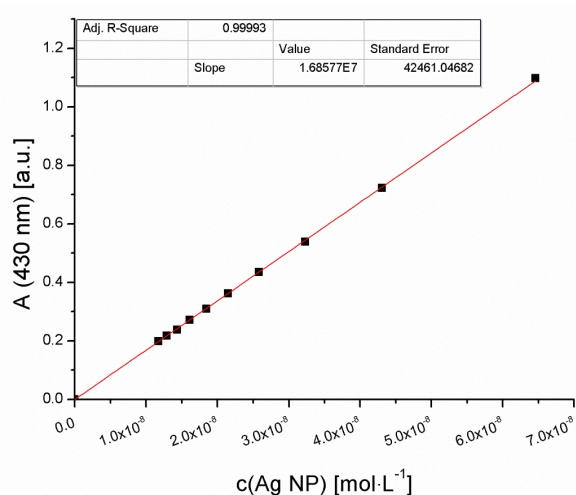


Figure SI-4. Absorption spectrum of Ag-PMA NPs plotted versus the concentration of Ag NPs $c(\text{Ag NP})$, which has been determined by ICP-MS.

The molar volume ($V_{\text{mol,Ag}}$) of silver is known to be $10.27 \text{ cm}^3 \cdot \text{mol}^{-1}$. The number of Ag atoms per Ag NP (N_{Ag}) thus is $N_{\text{Ag}} = N_{\text{A}} \cdot V(\text{Ag NP}) / V_{\text{mol, Ag}} = 2228 \approx 2200$. The number of surface atoms ($N_{\text{Ag,surf}}$) of one NP was estimated as following: the surface of one silver nanoparticle ($A_{\text{Ag,NP}}$) is defined by $A_{\text{Ag,NP}} = 4 \cdot \pi \cdot (d_c/2)^2$, with $d_c/2$ being the radius of the NP. If each silver atom is assumed to be a sphere with a covalent radius $r_{\text{Ag}} = 0.145 \text{ nm}$, this sphere has a cross-sectional area of $A_{\text{cross,Ag}} = \pi \cdot r_{\text{Ag}}^2$. The number of surface atoms can be estimated by $N_{\text{Ag,surf}} = A_{\text{Ag,NP}} / A_{\text{cross,Ag}} = 4 \cdot (d_c/2)^2 / r_{\text{Ag}}^2$ without considering the gaps between

the atoms. In case of the highest density packing only 90% of the surface area is covered by atoms, accordingly $N_{Ag,surf} = 0.9 \cdot A_{Ag,NP} / A_{cross,Ag} = 0.9 \cdot 4 \cdot (d_c/2)^2 / r_{Ag}^2$. Finally, the radius $(d_c/2 - r_{Ag})$ was taken for each NP instead of $d_c/2$, in order to consider the curvature of the surface. This leads to the resulting formula $N_{Ag,surf} = 0.9 \cdot 4 \cdot (d_c/2 - r_{Ag})^2 / r_{Ag}^2$ with $d_c/2 = 2.084$ nm. The number of surface atoms per NP was thus estimated to be $N_{Ag,surf} = 0.9 \cdot 4 \cdot (2.084 \text{ nm} - 0.145 \text{ nm})^2 / (0.145 \text{ nm})^2 = 643 \approx 650$ ($\Rightarrow N_{Ag,surf} / N_{Ag} = 29\% \approx 30\%$).

Thus concentrations of Ag can be given in three different ways:

- $c(Ag)$ [mg/L] = concentration of Ag atoms in the solution (from the whole Ag NPs).

- $c_{surf}(Ag)$ [mg/L] = concentration of Ag atoms in the solution which are situated on the surface of the Ag NPs.

$$c_{surf}(Ag) = c(Ag) \cdot N_{Ag,surf} / N_{Ag} = 0.29 \cdot c(Ag) \quad (Eq. 1)$$

- $c(Ag \text{ NP})$ [mol/L] = concentration of Ag NPs in the solution.

$$c(Ag \text{ NP}) = c(Ag) / (m(Ag \text{ NP}) \cdot N_A) = 4.2 \cdot 10^{-9} \text{ mol/mg} \cdot c(Ag) \quad (Eq. 2)$$

II) Ligand exchange for obtaining hydrophilic Ag NPs (Ag-MUA NPs)

In order to substitute the hydrophobic ligands to hydrophilic ones dodecylthiol was exchanged with 11-mercaptoundecanoic acid (MUA). The exchange was done using the following procedure. Hydrophobic Ag NPs as synthesized above (10 mg NP powder) were dissolved in 20 mL chloroform. MUA (7.3 mmol; 1.6 g) was dissolved in 130 mL Tris-borate-EDTA buffer (TBE 0.5x) for 45 min in an ultrasonic bath. The Ag NPs solution was added and the mixture was shaken for 5 min. During this procedure the Ag NPs underwent an exchange of the ligands and related to this a phase transfer from the chloroform

IV.1. Toxicity of silver nanoparticles depends on their surface chemistry

to the aqueous phase. To separate the Ag NPs from the organic phase and the excess ligand, the mixture was centrifuged (2,000 rpm; 20 min). The aqueous phase with the Ag NPs was then situated on top of the chloroform phase and a white solid phase which contained the excess ligands. The Ag NP solution was extracted with a pipette. As further purification step, the Ag NP solution was concentrated by using a centrifuge filter (100 kDa MWCO). During this concentration step the Ag NPs were washed with water. This procedure yielded hydrophilic Ag NPs in which the Ag cores are capped with a monolayer of MUA (Ag-MUA NPs). After the concentration, the NPs were first purified by gel electrophoresis. For this purpose a BIO-RAD Power Pack Basic and a BIO-RAD electrophoresis chamber were used. Tris-borate EDTA buffer (TBE 0.5x) was used as buffer solution. The NPs were run through a 2% Agarose gel for 1 h at $10 \text{ V}\cdot\text{cm}^{-1}$. The resulting band, which consists of the purified NPs, was cut out of the gel and placed into a dialysis membrane tube (50 kDa MWCO). The tube was filled with fresh TBE, locked at both ends that no buffer could leak out and placed back into the electrophoresis chamber. By running the chamber for another 20 min the NPs moved out of the gel but stayed inside the dialysis tube. The now empty piece of Agarose gel was discarded and the purified NPs were collected and again concentrated by using a centrifuge filter (100 kDa MWCO). For further purification, the NPs were run through a high pressure liquid chromatography (HPLC) set-up. Here an Agilent 1100 Series HPLC machine and a self packed column filled with Sepharcyl S300-HR were used. The system was run for 2 hours at a flow rate of $1 \text{ mL}\cdot\text{min}^{-1}$ and the NPs were collected at their respective elution peaks (*cf.* Chapter VI). The last step of the purification was again the concentration of the Ag NPs by using a centrifuge filter (100 kDa MWCO).

In order to fluorescence label the Ag-MUA NPs, they were labeled with the amino-modified fluorophore DY-636 (dyomics). This was done by using EDC (1-ethyl-3-(3-dimethylaminopropyl) carbodiimide) chemistry [5]. The same

method to couple amino-modified PEG to NPs which has been reported in our previous studies [6,7] was used to couple the fluorophore to the Ag-MUA NPs. Hereby the NH_2 groups of the fluorophore were coupled with EDC to the COOH groups of the MUA at the surface of the NPs. The amount of EDC which was needed varied from batch to batch and had to be tested before.

III) Polymer coating for obtaining hydrophilic Ag NPs (Ag-PMA NPs)

Alternatively the hydrophobic NPs were transferred to aqueous phase by coating them with an amphiphilic polymer. We followed hereby our own previous protocols [6]. For this purpose, first the amphiphilic polymer (dodecylamine modified poly(isobutylene-alt-maleic anhydride), (PMA) was synthesized according to Lin *et al.* [6]. Hereby 75% of the anhydride rings were reacted with dodecylamine. PMA was dissolved in chloroform as stock solution of 50 mM, whereby the concentration refers to the number of monomer units. This stock solution was added to the hydrophobic Ag NPs dispersed in chloroform. The amount of polymer was adjusted in a way that $R_{p/\text{area}} = 100 \text{ nm}^{-2}$ (monomer units per nm^2) of effective surface area of the Ag NPs was added. The effective surface area is the sum of the effective surface areas of all NPs in solution, whereby the surface area $A_{\text{eff, NP}} = 120 \text{ nm}^2$ of one Ag NP was calculated as surface of a sphere with an effective diameter $d_{\text{eff}} = 6.2 \text{ nm}$. The effective diameter comprises the core diameter $d_c = 4.2 \text{ nm}$ and 2 times the thickness of the ligand shell [6]. In contrast to our initial protocol, [8] no crosslinker was added. The chloroform was removed under reduced pressure and the NPs were dissolved in basic aqueous buffer (50 mM sodium borate buffer; pH 12) and concentrated by using a centrifuge filter (100 kDa MWCO). Further purification was carried out in the same way as has been described for the Ag-MUA NPs (*cf.* Chapter II).

IV.1. Toxicity of silver nanoparticles depends on their surface chemistry

In order to obtain fluorescence labeled Ag-PMA NPs, a PMA modified with the amino-modified dye DY-636 (Dyomics) was used. Attachment of the fluorophore to the polymer was carried out according to our standard procedures [6]. The plain PMA stock polymer solution (50 mM) as described above still comprises 25% of closed anhydride rings. 2% of these rings were used for the modification with the dye. A typical batch was prepared in the following way. First, 2 mg of the dye were dissolved in methanol and transferred to a 10 mL round flask. The methanol was completely removed under reduced pressure to prevent any side reactions. Then, 1.3 mL of the plain polymer (50 mM monomer concentration) and 4 mL THF were added to the flask. This mixture was stirred and heated up to 58 °C for at least 24 hours. Afterwards the solvents were removed under reduced pressure and the dry modified polymer was again dissolved in 1.3 mL of chloroform to a final concentration of 50 mM monomer units. The polymer coating procedure with the dye modified polymer was identical to the one with the plain polymer, as were the purification steps. The UV/Vis absorption and fluorescence spectra of dye-modified Ag-PMA NPs are shown in Figure SI-5.

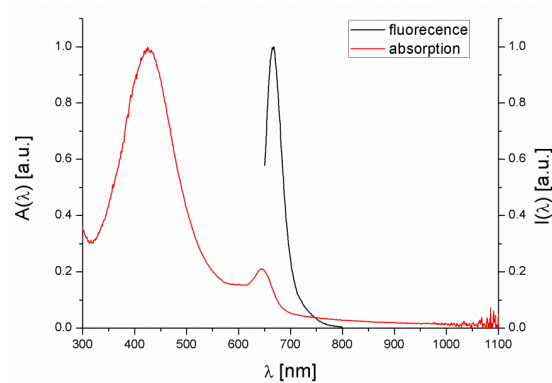


Figure SI-5. Normalized absorbance $A(\lambda)$ and fluorescence spectra $I(\lambda)$ of DY-636 labeled Ag-PMA NPs. The absorbance spectrum shows the typical surface plasmon band at 430 nm originating from the Ag NPs, and the absorption peak of DY-636 at 645 nm. For the fluorescence spectrum (recorded with a Horiba FluoroLog) the NPs were excited at 645 nm and the emission was recorded from 650 nm to 800 nm. The fluorescence emission maximum is located at 668 nm.

IV) PEGylation of polymer coated Ag NPs (Ag-PMA-1PEG, Ag-PMA-satPEG NPs)

The surface of the Ag-PMA NPs is rich in carboxylic groups [7,9] and thus can be easily modified *via* EDC (1-ethyl-3-(3-methylaminopropyl)carbodiimide) chemistry [5] afterwards. We followed here our previously published protocol [7] for linkage of 10 kDa NH₂-PEG-CH₃ (Rapp Polymere) *via* the NH₂ terminal with EDC to the COOH groups present on the polymer surface. Two samples were produced. First, by binding only few polyethylene glycol (PEG) molecules per NP, and by subsequent fractionation *via* gel electrophoresis [7], Ag NPs with exactly one PEG attached per NP were obtained (Ag-PMA-1PEG). For the second modification the ratio of EDC to polymer was set to a value at which the whole NP surface is saturated with PEG molecules (Ag-PMA-satPEG).

V) Characterization of NP size and colloidal stability with gel electrophoresis

The different Ag NP samples were run in a 2% Agarose gel at 10 V·cm⁻¹ for 1 h in tris-borate-EDTA buffer (TBE 0.5x). The fact that all Ag NP samples run on the gel without precipitation demonstrates that the organic surface coating must be at least decently stable and provides colloidal stability. Dependent on the hydrodynamic diameter d_h and the charge of the NPs, each sample runs with a different speed, although all the NPs have the same Ag core [3,10]. As reference 10 nm phosphine coated Au NPs were run on the same gel [11]. Assuming similar surface charge due to -COO⁻ groups for all samples besides the Ag-PMA-satPEG NPs [7] NPs are fractionated on the gel by size, with the smallest sample running fastest [3]. The Ag-MUA NPs run fastest. Also the Ag-PMA NPs run faster than the phosphine coated 10 nm Au NPs (British biocell international; phosphine modification according to Pellegrino et al. [11]). As expected the NPs, which carry one 10 kDa PEG in addition to the PMA coating (Ag-PMA-1PEG) run slower, and

IV.1. Toxicity of silver nanoparticles depends on their surface chemistry

the NPs saturated with 10 kDa PEG (Ag-PMA-satPEG) show almost no movement because of their big size and low charge [7]. A gel with all NP samples is shown in Figure SI-6. Qualitative statements about the relative hydrodynamic diameters are in correspondence with the data obtained with HPLC.

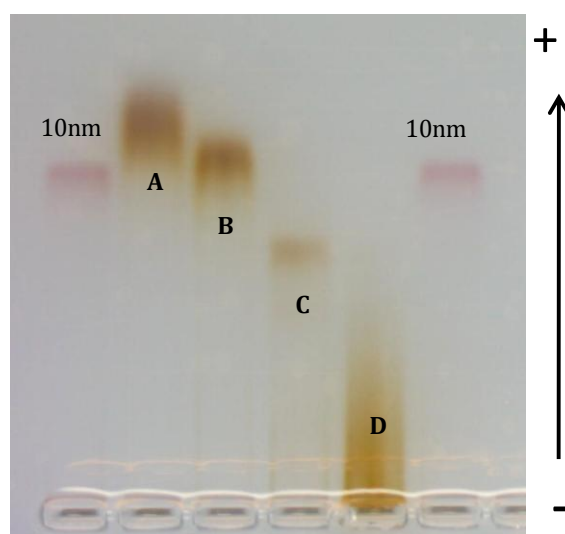


Figure SI-6. Comparison of the four different NP samples in a 2% Agarose gel to which an electric field of $10 \text{ V} \cdot \text{cm}^{-1}$ had been applied for 1 h. The NPs run from the wells (at the bottom of the image) towards the positive electrode. **A:** Ag-MUA NPs; **B:** Ag-PMA NPs; **C:** Ag-PMA-1PEG NPs; **D:** Ag-PMA-satPEG NPs. 10 nm phosphine stabilized Au NPs were run as reference [11].

VI) Characterization of NP size and colloidal stability with HPLC

Ag NPs were analyzed with size exclusion chromatography (SEC). For this purpose, high performance liquid chromatography (HPLC; Agilent 1100 Series) with a column filled with Sephacryl S300HR and a flow rate of $1 \text{ mL} \cdot \text{min}^{-1}$ using phosphate buffered saline (PBS) was used. The fact that all Ag NP samples run through the column without precipitation demonstrates that the organic surface coating must be at least decently stable and provides colloidal stability. The resulting chromatogram is shown in Figure SI-7. The chromatogram shows

the expected result, in which biggest NPs elute first. For a detailed explanation we refer to our previous report Sperling *et al.* [3]. As biggest NPs the Ag-PMA-satPEG NPs elute first (maximum after 56 min). The Ag-PMA-1PEG NPs elute second with the maximum after 68 min. The Ag-PMA NPs and the Ag-MUA NPs elute at almost the same time [maximum at 73 min (Ag-PMA NPs) and 75 min (Ag-MUA-NPs)].

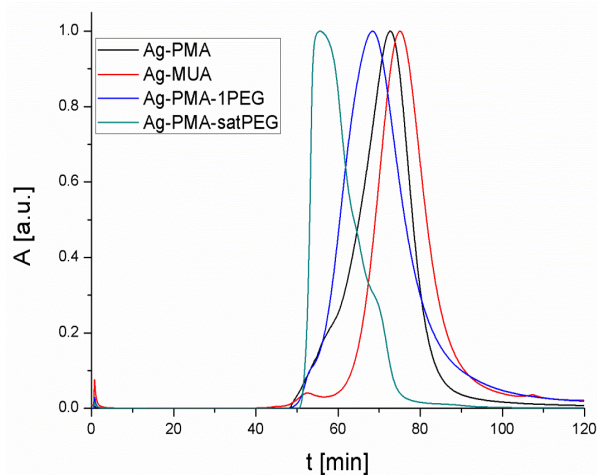


Figure SI-7. Size exclusion chromatography of Ag NPs with different surface chemistry. The absorption A at 430 nm of the eluate is shown.

VII) Characterization of NP size and colloidal stability with dynamic light scattering

To measure the hydrodynamic diameter d_h (with dynamic light scattering, DLS) and the zeta potential (with laser Doppler anemometry, LDA) of the four different types of Ag NPs a Malvern Zetasizer was used. All the samples were equilibrated for 15 min at 25 °C to be sure that the measured movements only belong to the Brownian motion and not to any thermal conversion. The NP samples were measured at 173° backscatter settings. The hydrodynamic diameter d_h is a good indicator for the colloidal stability of the NPs. If d_h

IV.1. Toxicity of silver nanoparticles depends on their surface chemistry

increases with time or changed conditions, this is a sign for NP agglomeration. To probe the colloidal stability of the different NPs the hydrodynamic diameter of the NP samples under different sodium chloride concentrations and at two different exposure times were measured. The results are shown in Figures SI-8 to SI-11. The results obtained with the Ag-MUA NPs are clearly different from the other three NP samples, which involve the polymer coating. The hydrodynamic diameter of the Ag-MUA NPs increased strongly with an increasing concentration of sodium chloride. The hydrodynamic diameters of the other three NP samples stayed more or less constant with increasing concentration of sodium chloride up to 2.5 M. After 24 h exposure to NaCl, all the samples were measured again to probe for colloidal stability. The hydrodynamic diameters of the three polymer coated Ag NP samples stayed constant in respect to the values determined directly after exposure. Also the Ag-MUA NPs kept constant hydrodynamic diameter (as compared to the one determined directly after addition of NaCl) up to a sodium chloride concentration of 160 mM. The Ag-MUA NPs exposed to higher NaCl concentration were completely agglomerated, precipitated, and thus could not be measured any more. It has to be pointed out that the measurements here involving NaCl exposure are much more sensitive to colloidal instability than simple analysis that NPs are running in HPLC columns / Agarose gels upon gel electrophoresis. Thus these data clearly indicate that Ag-MUA NPs have a clearly reduced colloidal stability compared to the samples involving Ag-PMA NPs. The hydrodynamic diameters are summarized in Table SI-1. Please note that we would have expected a higher hydrodynamic diameter of Ag-PMA-satPEG NPs, in accordance with HPLC data.

BLOQUE IV. ESTUDIOS TOXICOLÓGICOS DE NANOPARTÍCULAS

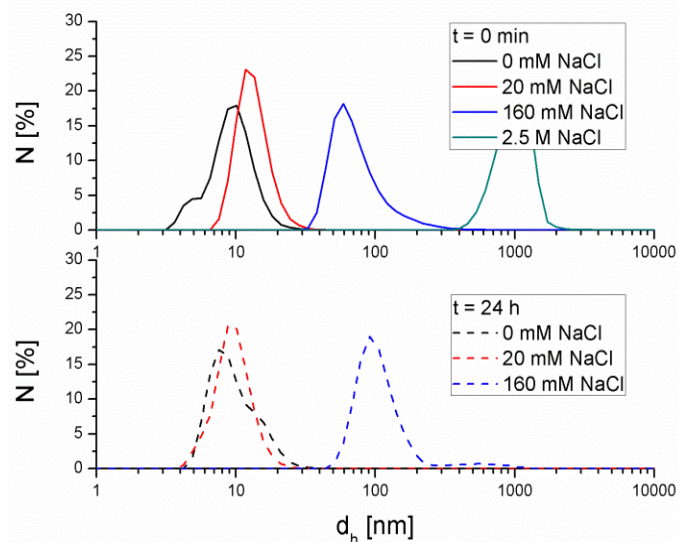


Figure SI-8. Probing of the colloidal stability of Ag-MUA NPs in solutions with different NaCl concentration via DLS. The number distribution N of the hydrodynamic diameter d_h is plotted after 1 h and 24 h exposure time. After 24 h the NPs which had been mixed with 2.5 M NaCl were completely agglomerated and precipitated.

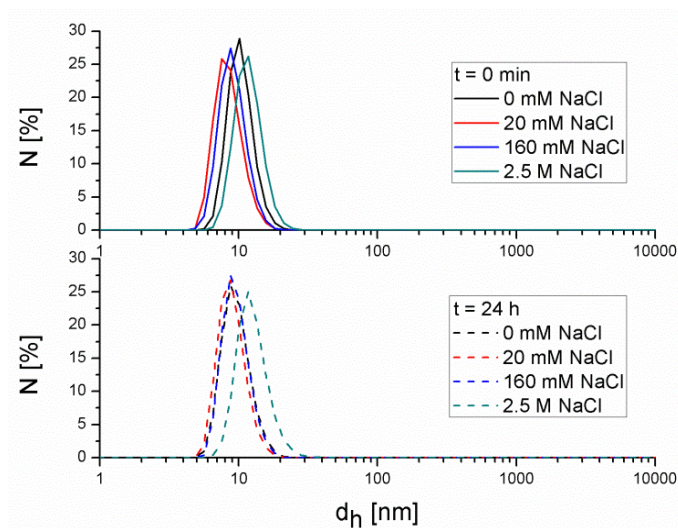


Figure SI-9. Probing of the colloidal stability of Ag-PMA NPs in solutions with different NaCl concentration via DLS. The number distribution N of the hydrodynamic diameter d_h is plotted after 1 h and 24 h exposure time.

IV.1. Toxicity of silver nanoparticles depends on their surface chemistry

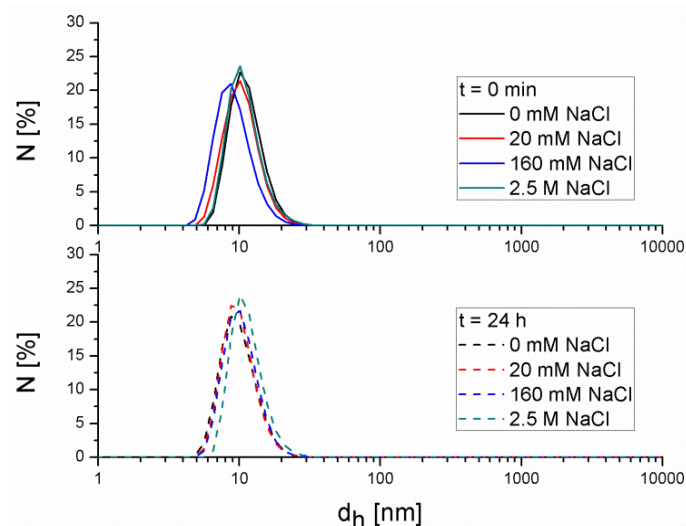


Figure SI-10. Probing of the colloidal stability of Ag-PMA-1PEG NPs in solutions with different NaCl concentration via DLS. The number distribution N of the hydrodynamic diameter d_h is plotted after 1 h and 24 h exposure time.

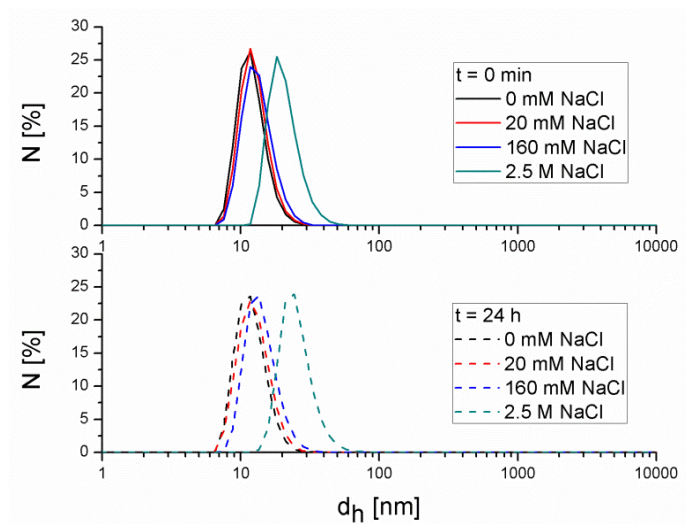


Figure SI-11. Probing of the colloidal stability of Ag-PMA-satPEG NPs in solutions with different NaCl concentration via DLS. The number distribution N of the hydrodynamic diameter d_h is plotted after 1 h and 24 h exposure time.

BLOQUE IV. ESTUDIOS TOXICOLÓGICOS DE NANOPARTÍCULAS

Table SI-1. Summary of mean hydrodynamic diameters d_h (nm) and their corresponding standard deviation, as derived from the data presented in Figures SI-8 to SI-11.

<i>t=0 h</i>				
c(NaCl)	0 mM	20 mM	160 mM	2.5 M
Ag-MUA	11.23 ± 4.4	13.54 ± 4.2	93.48 ± 63.9	1180 ± 361
Ag-PMA	12.04 ± 2.7	9.97 ± 2.4	10.60 ± 2.4	13.77 ± 3.3
Ag-PMA-1PEG	13.22 ± 3.8	12.36 ± 3.8	10.87 ± 3.5	12.88 ± 3.9
Ag-PMA-satPEG	12.16 ± 3.0	12.68 ± 3.2	13.49 ± 3.6	20.84 ± 5.9
<i>t=24 h</i>				
c(NaCl)	0 mM	20 mM	160 mM	2.5 M
Ag-MUA	11.91 ± 5.2	11.46 ± 3.9	122.3 ± 42.1	→∞
Ag-PMA	11.27 ± 2.8	10.52 ± 2.5	11.19 ± 2.6	14.82 ± 4.1
Ag-PMA-1PEG	11.87 ± 3.7	11.87 ± 3.5	12.19 ± 3.6	13.43 ± 3.9
Ag-PMA-satPEG	12.09 ± 3.2	12.67 ± 3.4	14.26 ± 3.9	25.64 ± 7.6

Another parameter for the colloidal stability of the NPs is their zeta potential. In combination with the hydrodynamic diameter it is possible to conclude if the colloidal stability of a NP sample is derived *via* electrostatic interaction or steric hindrance [12]. In Table SI-2 the values of the zeta potential of the different NP samples are shown. It is known from literature that particles with a zeta potential of ±30 mV to ±40 mV show a moderate colloidal stability [13]. For the Ag-MUA, Ag-PMA, Ag-PMA-1PEG NPs the zeta potentials are above 20 mV, which indicates that the colloidal stability of these samples originates from electrostatic repulsion. Within these three samples the Ag-MUA NPs show the smallest zeta potential (-24.9 mV). This might be the reason why these NPs start to agglomerate easier than the others upon presence of salt. On the other hand, the Ag-PMA-satPEG NPs have a zeta potential of *ca.* -11 mV. This value is a sign that their colloidal stability is caused by the steric hindrance of the PEG molecules on their surface.

IV.1. Toxicity of silver nanoparticles depends on their surface chemistry

Table SI-2. Zeta potential values of the four different Ag NP samples.

Sample	Zeta potential [mV]
Ag-MUA	-24.9 ± 1.7
Ag-PMA	-31.0 ± 1.3
Ag-PMA-1PEG	-41.1 ± 1.5
Ag-PMA-satPEG	-10.9 ± 0.4

VIII) Characterization of NP corrosion with ICP-MS

In order to quantify the amount of Ag^+ ions which have been released from the Ag NPs, the dissolved silver was separated by ultracentrifugation and ultrafiltrates were analyzed by ICP-MS. Corrosion was either probed in water or under acidic (pH 3) conditions. Samples for the pH 3 release experiment were prepared from the original NP samples dissolved in water by addition of HNO_3 .

The concentration of total silver in the Ag NP suspensions $c_{\text{tot}}(\text{Ag})$ (= released Ag^+ ions and Ag in undissolved Ag NPs) was determined by ICP-MS. Note that in Chapter I we assumed that all Ag was associated with the Ag NPs and that there is negligible corrosion (*i.e.* $c(\text{Ag})=c_{\text{tot}}(\text{Ag})$). For this, a Perkin-Elmer Sciex model ELAN DRC-e ICP mass spectrometer equipped with a concentric nebulizer and a cyclonic spray chamber was used. Ag NP suspension were diluted with ultrapure water and analyzed directly. Both dissolved silver and silver NPs behave in the ICP-MS in a similar way [14]. In our series solutions containing 15-30 $\text{mg}\cdot\text{L}^{-1}$ Ag were analyzed ($c_{\text{tot}}(\text{Ag})=28.06\pm 0.23$ $\text{mg}\cdot\text{L}^{-1}$ for Ag-MUA NPs; $c_{\text{tot}}(\text{Ag})=15.33\pm 0.02$ $\text{mg}\cdot\text{L}^{-1}$ for Ag-PMA NPs; and $c_{\text{tot}}(\text{Ag})=22.76\pm 0.12$ $\text{mg}\cdot\text{L}^{-1}$ for Ag-PMA-satPEG NPs).

In a next step, the dissolved Ag^+ ions $c(\text{Ag}^+)$ were isolated by removing the undissolved Ag NPs $c_{\text{NP}}(\text{Ag})$ using Nanosep Pall centrifugal ultrafilter devices with polyethersulfone membrane with 3 kDa MW cut-off. The nominal pore size of the 3 kDa membranes is not available, but the manufacturer quotes a pore

BLOQUE IV. ESTUDIOS TOXICOLÓGICOS DE NANOPARTÍCULAS

size diameter of 5 nm for 50 kDa cut-off membranes. Ultrafilter devices were washed by centrifugation with 500 μL of ultrapure water twice. The second washing was kept to check for any potential contamination. Ag NP suspensions were sonicated for two minutes, 300 μL of the suspension were subjected to centrifugation for 15 min at 9000 rpm at 20 $^{\circ}\text{C}$. The ultrafiltrate (ca. 275 μL , which contains the Ag^+ ions; the Ag NPs are too big to pass the membrane) was diluted up to 10 mL with ultrapure water prior the ICP-MS analysis. ICP-MS determination of Ag^+ in the flow through $c(\text{Ag}^+)$ was correlated to the total amount of Ag $c_{\text{tot}}(\text{Ag})$ and thus the fraction of Ag^+ released from the Ag NPs was determined: $c(\text{Ag}^+)/c_{\text{tot}}(\text{Ag})$. This was applied to the silver NP suspensions and the released Ag^+ was measured weekly. After 14 days, silver was just detected in the ultrafiltrate of the sample Ag-PMA NPs. The same was done for Ag NP suspension at pH 3. Results are summarized in Table SI-3.

Table SI-3. The amount of released Ag^+ ions $c(\text{Ag}^+)/c_{\text{tot}}(\text{Ag})$, in dependence on their exposure to water or acidic solution. At day 0 all residual Ag^+ had been removed by ultrafiltration.

Sample	released Ag (water): $c(\text{Ag}^+)/c_{\text{tot}}(\text{Ag})$ [%]		
	day 0	day 7	day 14
Ag-MUA	<0.0015	<0.0015	<0.0015
Ag-PMA	<0.0015	<0.0015	0.146 \pm 0.001
Ag-PMA-satPEG	<0.0015	<0.0015	<0.0015

Sample	released Ag (pH 3): $c(\text{Ag}^+)/c_{\text{tot}}(\text{Ag})$ [%]	
	day 1	day 7
Ag-MUA	0.781 \pm 0.002	1.316 \pm 0.002
Ag-PMA	1.120 \pm 0.004	1.390 \pm 0.003
Ag-PMA-satPEG	0.701 \pm 0.001	0.735 \pm 0.001

The following controls and characterizations were performed. In case no Ag is lost during the separation of Ag^+ from Ag NPs, $c_{\text{tot}}(\text{Ag})=c(\text{Ag}^+)+c_{\text{NP}}(\text{Ag})$. However, Ag^+ might be lost by adsorption to the filter membrane. Thus the behavior of the polyethersulfone membranes with respect to the adsorption of

IV.1. Toxicity of silver nanoparticles depends on their surface chemistry

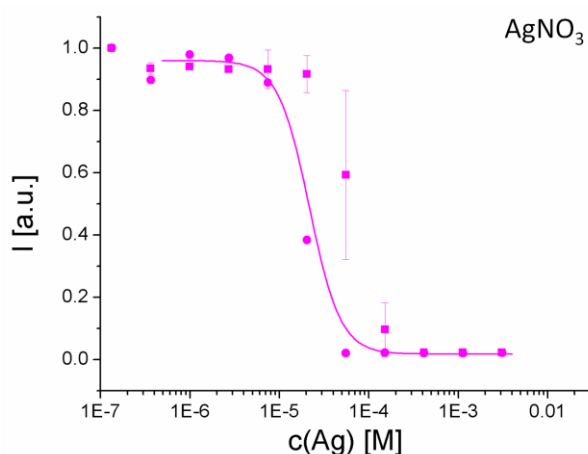
Ag⁺ was studied by ultrafiltration of Ag⁺ solutions in ultrapure water at two concentration levels (0.2 and 20 mg·L⁻¹). 99.70%±1.32 and 102.81%±2.00 of the Ag⁺ was recovered upon filtering 20 mg·L⁻¹ and 0.2 mg·L⁻¹ of Ag⁺ solutions, respectively. This demonstrates that retention of the ionic silver subjected to ultrafiltration can be considered negligible. Also the detection limit of Ag with the used ICP-MS set-up was determined. For this purpose, silver in the ultrafiltrates was determined by using the ¹⁰⁷Ag isotope. Attainable limits of quantification (10 times the standard deviation of the blank criterion) were 10 ng L⁻¹. Taking into account the dilution of the ultrafiltrates, the limits of quantification referred to the suspensions were 333 ng L⁻¹. Thus for a suspension with a total silver content of 20 mg L⁻¹, the procedure followed was able to detect the release of a 0.0015% of silver from the NPs.

IX) Viability tests

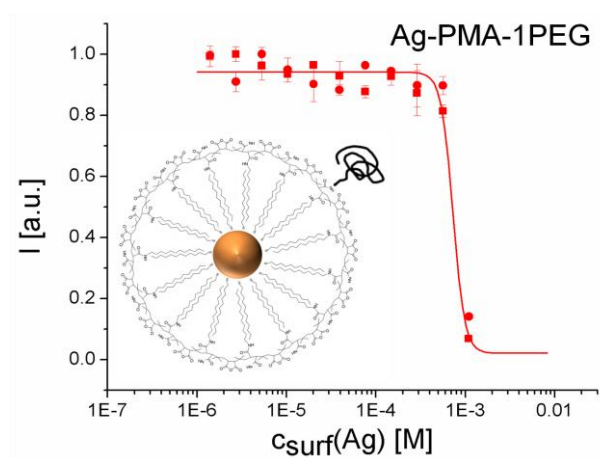
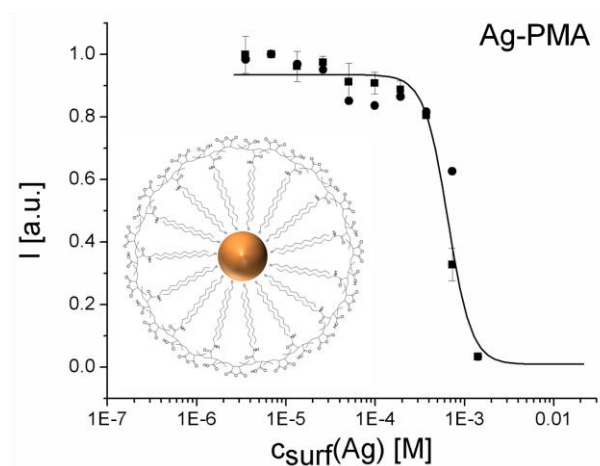
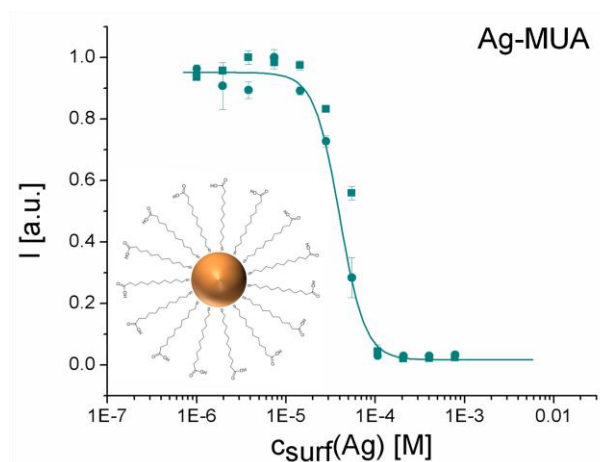
NIH/3T3 embryonic fibroblasts were seeded in a 96-well-plate at a cell density of 3·10⁴ cells/well in 100 µL growth medium (DMEM-F12 Ham's basal medium supplemented with 10% calf serum, 1% L-glutamine and 1% penicillin/streptomycin). The next day, the cells were incubated with the different NPs and with the AgNO₃ solution (which acted as positive control) for 24 h. All concentrations were done in duplicate and each experiment was performed at least 3 times. Cells that were not treated with Ag served as a negative control for viability. After 24 h, the cells were washed once with PBS and 100 µL of a 10% resazurin solution (in growth medium) were added to each well and incubated for 3 h at 37 °C and 5% CO₂. Resazurin is a blue, non-fluorescent sodium salt, which is converted to resorufin by metabolically active cells. Resorufin is a pink, fluorescent sodium salt that accumulates outside the cells. This reduction process requires functional mitochondrial activity which is inactivated immediately after cell death. Fluorescence spectra were measured using a 96-microwell plate reader connected to a Fluorolog®

BLOQUE IV. ESTUDIOS TOXICOLÓGICOS DE NANOPARTÍCULAS

spectrofluorometer (Jovin Yvon) at an excitation wavelength of 560 nm. The emission was recorded in the range of 572-650 nm with 1 nm resolution and a slit of 5 nm. Firstly, the mean of the intensities of the emission spectra of the duplicates was calculated and then, the maximum intensity values found in the range 578-585 nm were also averaged. The mean background signal (640-650 nm) was subtracted from the mean maximum emission values and subsequently normalized with the maximum fluorescence value obtained. The maximum fluorescence value corresponded not always to the untreated cells, probably due to the formation of hydroresorufin, a transparent non-fluorescent product which is formed upon further reduction of resorufin by viable cells. The means of the normalized fluorescence intensity values of the three experiments were plotted against the different concentrations of Ag. A sigmoidal distribution was obtained and fitted with the function of a logistic dose response curve, which enabled us calculating the Ag concentration yielding 50% cell death (LD_{50}). According to the results obtained by measuring the resorufin formation by living cells, the different sources for Ag exhibited increased toxicity (mean LD_{50} values). The data of one experiment, together with the corresponding fit are shown in Figure SI-12.



IV.1. Toxicity of silver nanoparticles depends on their surface chemistry



BLOQUE IV. ESTUDIOS TOXICOLÓGICOS DE NANOPARTÍCULAS

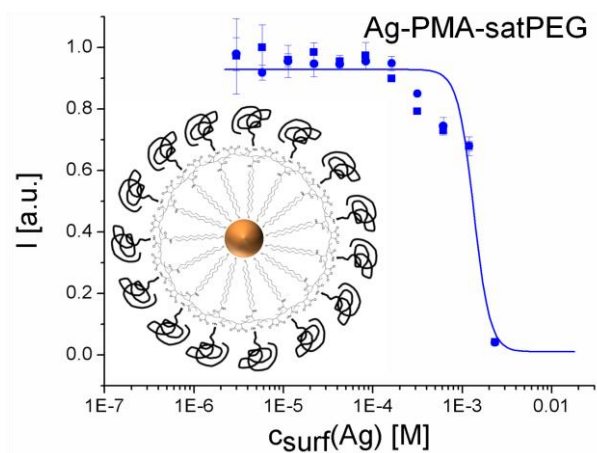


Figure SI-12. Resazurin-based viability test of 3T3 fibroblasts which had been incubated for 24 hours with Ag NPs. Onset of fluorescence (as quantified by the measured intensity I), is an indicator for viability of cells. The amount of Ag is quantified in the amount of Ag atoms which are present on the NP surface ($c_{\text{surf}}(\text{Ag})$). In case of AgNO_3 as silver source concentrations are given in terms of total amount of Ag $c(\text{Ag})$. In each graph two independent sets of data are shown with each data point of each set corresponding to the mean value \pm the standard deviation.

IV.1. Toxicity of silver nanoparticles depends on their surface chemistry

References

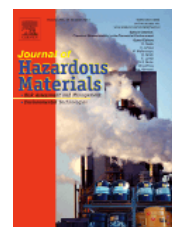
- [1] A. Mari, P. Imperatori, G. Marchegiani, L. Pilloni, A. Mezzi, S. Kaciulis, C. Cannas, C. Meneghini, S. Mobilio, L. Suber, *Langmuir* 2010, 26, 15561.
- [2] Y. Sun, *Chem. Soc. Rev.* 2013, 42, 2497.
- [3] R. A. Sperling, T. Liedl, S. Duhr, S. Kudera, M. Zanella, C.-A. J. Lin, W. H. Chang, D. Braun, W. J. Parak, *Journal of Physical Chemistry C* 2007, 111, 11552.
- [4] J. Yguerabide, E. E. Yguerabide, *Anal. Biochem.* 1998, 262, 137; J. Yguerabide, E. E. Yguerabide, *Anal. Biochem.* 1998, 262, 157.
- [5] G. T. Hermanson, *Bioconjugate Techniques*, Academic Press, San Diego 2008.
- [6] C.-A. J. Lin, R. A. Sperling, J. K. Li, T.-Y. Yang, P.-Y. Li, M. Zanella, W. H. Chang, W. J. Parak, *Small* 2008, 4, 334.
- [7] R. A. Sperling, T. Pellegrino, J. K. Li, W. H. Chang, W. J. Parak, *Adv. Funct. Mater.* 2006, 16, 943.
- [8] T. Pellegrino, L. Manna, S. Kudera, T. Liedl, D. Koktysh, A. L. Rogach, S. Keller, J. Rädler, G. Natile, W. J. Parak, *Nano Lett.* 2004, 4, 703.
- [9] M. T. Fernández-Argüelles, A. Yakovlev, R. A. Sperling, C. Luccardini, S. Gaillard, A. S. Medel, J.-M. Mallet, J.-C. Brochon, A. Feltz, M. Oheim, W. J. Parak, *NanoLetters* 2007, 7, 2613.
- [10] W. J. Parak, D. Gerion, D. Zanchet, A. S. Woerz, T. Pellegrino, C. Micheel, S. C. Williams, M. Seitz, R. E. Bruehl, Z. Bryant, C. Bustamante, C. R. Bertozzi, A. P. Alivisatos, *Chem. Mater.* 2002, 14, 2113; W. J. Parak, T. Pellegrino, C. M. Micheel, D. Gerion, S. C. Williams, A. P. Alivisatos, *Nanoletters* 2003, 3, 33.
- [11] T. Pellegrino, R. A. Sperling, A. P. Alivisatos, W. J. Parak, *Journal of Biomedicine and Biotechnology* 2007, 2007, article ID 26796.
- [12] T. Pellegrino, S. Kudera, T. Liedl, A. M. Javier, L. Manna, W. J. Parak, *Small* 2005, 1, 48; S. K. Basiruddin, A. Saha, N. Pradhan, N. R. Jana, *Journal of Physical Chemistry C* 2010, 114, 11009.
- [13] D. Lin, X. Tian, F. Wu, B. Xing, *Journal of Environmental Quality* 2010, 39, 1896.
- [14] F. Laborda, J. Jimenez-Lamana, E. Bolea, J. R. Castillo, *J. Anal. At. Spectrom.* 2011, 26, 1362.

IV.2. Effects of interaction of SWCNTs with nonylphenol on their toxicity

Submitted to Journal of Hazardous Materials

ELSEVIER

Journal of Hazardous Materials



Effects of the interaction of single-walled carbon nanotubes with 4-nonylphenol on their *in vitro* toxicity

Encarnación Caballero-Díaz¹, Rocío Guzmán-Ruiz², María del Mar Malagón²,
Bartolome Simonet¹, Miguel Valcárcel¹

¹Department of Analytical Chemistry, Campus de Rabanales, University of Córdoba, Córdoba, Spain.

²Department of Cell Biology, Physiology and Immunology, Instituto Maimónides de Investigaciones Biomédicas de Córdoba (IMIBIC)/Reina Sofia University Hospital, University of Córdoba, Córdoba, Spain.

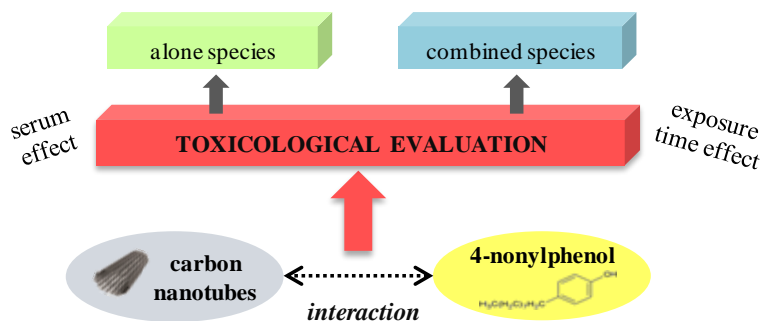
ABSTRACT

The aim of this study was to assess the toxicological risks arising from the coexistence of polyethylene glycol coated single-walled carbon nanotubes (SWCNTs-PEG) and a known environmental contaminant: 4-nonylphenol (NP). To this end, *in vitro* toxicity assays involving exposure of 3T3-L1 cells (mouse embryonic fibroblasts) to SWCNTs-PEG, alone or in combination with NP, for 24 or 48 h were performed. Experimental treatments were conducted in both presence and absence of serum (10%) in order to assess its influence on the toxicity of SWCNTs-PEG. Although the results provided no unambiguous evidences of synergistic toxicity between SWCNTs-PEG and NP, some specific treatments with mixtures

BLOQUE IV. ESTUDIOS TOXICOLÓGICOS DE NANOPARTÍCULAS

(SWCNTs-PEG+NP) resulted in an unexpected combined toxicity in relation to the individual treatments. Only in those few cases did the interaction between SWCNTs-PEG and NP had a synergistic effect on the resulting toxicity. The addition of 10% serum increased the stability of SWCNTs-PEG in the culture medium —possibly by effect of steric interactions— and reduced the toxicity of the nanoparticles as a result. Overall, the serum had a “protective effect” on cells against all treatments with SWCNTs-PEG, NP or their mixtures (SWCNTs-PEG+NP). Raman spectroscopy allowed the intracellular distribution of SWCNTs-PEG to be elucidated.

GRAPHICAL ABSTRACT



1. INTRODUCTION

By virtue of their extremely small size, nanoparticles possess unique physicochemical properties such as a high specific surface area and increased reactivity [1]. Carbon nanotubes (CNTs) are nanoparticles consisting of a variable number of graphene layers rolled into cylindrical tubes [2]. CNTs can be classified according to the number of graphene layers they contain as single-walled carbon nanotubes, double-walled carbon nanotubes or multi-walled carbon nanotubes [3]. These nanoparticles have proved useful in a wide range of fields including electronics [4], composite materials [5], coatings and films [6], catalysts support [7], energy storage [8], desalination and water purification [9], medicine [10], sensors [11], and sample treatment [12]. The increasing production and use of CNTs lead to their continuous release into the environment, where they can easily interact with other compounds thanks to their excellent sorption capacity. Besides, interactions given between CNTs and pesticides [13,14], pharmaceuticals [15,16], phthalate esters [17] and phenolic compounds [18,19] have been exploited in many analytical applications. These facts led us to examine the effect of the coexistence of CNTs with other environmental pollutants with a view to establishing more realistic scenarios for their toxicological evaluation.

4-nonylphenol (NP) is the degradation end-product of alkylphenol polyethoxylates, which are extensively used as nonionic surfactants in cleaning and personal-care products, plastics, paints, textiles, pesticides and many other synthetic products [20,21]. It is estimated that 60–65% of the overall production of these compounds ends in the aquatic environment [22]; this has fostered research into their potential toxicological effects. NP is considered an environmental endocrine disruptor and known to cause morphological changes, oxidative stress and apoptosis in various cell lines [23–25]. Also, its adverse effects on reproduction in vertebrates have been examined [26].

The widespread use of CNTs and NP, together with the fact that contaminants are not isolated in the environment, increases the likelihood of interaction between both species. Even though the toxicity of the individual compounds is well-known, their mixtures may induce unexpected toxic effects [27]. The combined toxicity of mixtures of nanoparticles with other environmental pollutants has already been the subject of several studies [27–35]. As can be seen from Table 1, some studies have exposed marked synergistic and antagonistic effects, whereas others have provided no unambiguous evidences in this respect. Very little is currently known about the combined toxicity of CNTs and NP despite the fact that interactions between the two are more than likely and have provided the basis for analytical methods using CNTs to extract NP from various types of matrices [18,36].

The primary purpose of this work was to evaluate for the first time the toxicological risks associated with the presence of polyethylene glycol coated single-walled carbon nanotubes (SWCNTs-PEG) in combination with a known endocrine disruptor: 4-nonylphenol (NP). *In vitro* toxicity was examined in methyl thiazolyl tetrazolium (MTT) assays where 3T3-L1 mouse embryonic fibroblasts were exposed to both species alone or in combination. Treatments were conducted at variable exposure times and concentrations of NP and SWCNTs-PEG. The influence of the presence of serum (10%) in the culture medium on the stability of SWCNTs-PEG —and hence on the global toxicity— was also evaluated. The agglomeration state of nanoparticle dispersions was examined by transmission electron microscopy (TEM) and their intracellular distribution elucidated by Raman spectroscopy.

IV.2. Effects of interaction of SWCNTs with nonylphenol on their toxicity

Table 1. *Published research on toxicity of binary mixtures composed of nanoparticles and other compounds.*

Nanoparticles	Compound	Observations in binary mixtures	Reference
Titanium dioxide (TiO ₂)	Bisphenol A	Small synergistic effects.	[27]
	Tributyltin	Nanoparticles increased the toxicity of tributyltin up to 20 fold compared with single compound.	[28]
	Lead acetate	No evidences of a synergistic acute toxicity although lead acetate may increase in some degree the toxicity of nanoparticles.	[29]
	As (V)	The toxicity of As (V) increased significantly in presence of low concentrations of nanoparticles.	[30]
	Dichlorodiphenyltrichloroethane (DDT)	The mixture caused a dose-dependent synergistic genotoxicity.	[31]
Aluminum oxide (Al ₂ O ₃)	As (V)	Enhanced toxic effect caused by a greater uptake of As (V)-loaded nano-Al ₂ O ₃ by organism.	[32]
Ferroferric oxide (Fe ₃ O ₄)	As (V)	Antagonistic effect since nanoparticles significantly reduced the toxicity of As (V).	[33]
Quantum dots (CdSe)	Cu ²⁺	Synergistic toxic effects since nanoparticles favoured a greater cell internalization of Cu ²⁺ into organism.	[34]
Gold and silver (Au, Ag)	Phenolic uncoupler 2,4-dinitrophenol (DNP)	Dose-dependent synergistic effects were found for mixtures of AgNPs and DNP. Only, weak synergistic effects and at low DNP concentrations were found for mixtures of AuNPs and DNP.	[35]

2. EXPERIMENTAL

2.1. Chemicals and reagents

Single-walled carbon nanotubes 0.5-0.6 μm in length and 4-5 nm in diameter coated with polyethylene glycol (SWCNTs-PEG) were obtained from Sigma-Aldrich (St. Louis, MO, USA). According to the manufacturer, their carbon basis is $\geq 80\%$ and their content in trace metals about 4-5%. Stock dispersions of SWCNTs-PEG at a concentration of 0.26 mg mL^{-1} were freshly prepared in 10% serum-containing and serum-free culture media, and homogenized by sonication with a VibracellTM 75041 ultrasonic probe (750 W, 20 KHz, Bioblock Scientific, Illkirch, France) with a diameter of 3 mm and an amplitude of 30% (225 W). The resulting dispersions were then autoclaved and stored until needed.

4-nonylphenol (NP), which was used as a model environmental contaminant, was purchased from Sigma-Aldrich (Madrid, Spain). Stock solutions of NP were freshly prepared in dimethyl sulfoxide (DMSO, $\geq 99.9\%$).

Binary mixtures (SWCNTs-PEG+NP) were prepared by blending the SWCNTs-PEG dispersion with the NP solution and allowing them to stand for 1 h before incubation with cells. The final concentration of DMSO in treatments was always below 0.1%, so, based on previous reports [27], it had no effect on cell viability.

2.2. Cell culture and treatment

3T3-L1 cells obtained from the American Type Culture Collection (Manassas, VA, USA) were seeded onto 6- or 12-well plates at a density of 3000 cells/cm² and incubated in Dulbecco's low glucose modified Eagle's Medium

IV.2. Effects of interaction of SWCNTs with nonylphenol on their toxicity

(DMEM) containing 10% fetal bovine serum (FBS), 4 mM glutamine and 1% antibiotic–antimycotic solution at 37 °C in a humidified atmosphere with 5% CO₂. On day 3–4 of culture, the medium was removed and cells were exposed to variable concentrations of SWCNTs-PEG and NP alone or in combination, in 10% FBS containing or FBS-free DMEM for either 24 or 48 h. Control cells were cultured in parallel in medium containing 0.1% DMSO alone for 24 or 48 h. At the end of each experiment, the medium was removed, cells were rinsed with phosphate buffered saline (PBS) and cell viability was evaluated by using the MTT assay according to the manufacturer’s instructions.

2.3. TEM analysis

TEM images were obtained with a field emission JEM-2100F TEM (JEOL, Inc.) equipped with a CCD camera (SCAI, Córdoba, Spain), using an acceleration voltage of 100 kV. SWCNTs-PEG at a 0.26 mg/mL concentration were dispersed in serum-free DMEM and in PBS under sonication. TEM samples were prepared by directly depositing a droplet (10 µL) of each dispersion onto a copper grid coated with Formvar film. This was followed by drying and evacuation before analysis.

2.4. MTT cytotoxicity assays

Cell viability was assessed with the 3-(4,5-dimethyl-2-thiazolyl)-2,5-diphenyl-2H-tetrazolium bromide (MTT) assay after 24 or 48 h exposure to variable concentrations of SWCNTs-PEG, NP and SWCNTs-PEG+NP. The MTT assay is based on the conversion of yellow MTT tetrazolium salt to dark blue formazan crystals by the action of mitochondrial succinate dehydrogenase in living cells. After DMSO is added to dissolve the crystals, the concentration of formazan per well is quantified by measuring the absorbance at 570 nm [7]. Briefly, 1 mL of MTT solution at a 0.1 mg/mL concentration in culture medium

was added to each well and incubated at 37 °C for 5 h. After removing the supernatant, the cells were rinsed twice with PBS and then supplied with 1 mL of DMSO to dissolve the formazan. The absorbance values obtained at 570 nm were directly proportional to the number of viable cells present in the samples. The untreated cells are used as control (100% viable) and cell viability values from treatments are expressed as a percentage relative to the control.

2.5. Raman Imaging

Raman spectra and images were obtained with an alpha500 R Confocal Raman Microscope equipped with a frequency doubled NdYAG laser with 532 nm excitation. A WITec UHTS 300 spectrometer and a DU970N-BV (EMCCD) camera (16×16 μm pixel size, 1600×200 pixels) were additionally connected to the microscope. WITec Project Plus software was used for advanced data evaluation.

For analysis, 3T3-L1 cells were seeded at a density of 3000 cells/cm² onto 0.1 mg/mL poly-L-lysine coated round cover slips in DMEM. Cells were exposed for 24 h to SWCNTs-PEG samples prepared in 10% FBS-containing DMEM. 3T3-L1 cells incubated in medium alone (without SWCNTs-PEG) were used as control. Treated cells were rinsed twice with PBS and then fixed with 4% paraformaldehyde for 15 min. After washing with PBS three times, the cover slips were placed on top of 22×22 mm, 0.16–0.19 mm thick glass slides from Emsdiasum (Hatfield, UK). Adherent cells on the slips were brought into focus in order to record Raman spectra and images.

2.6. Statistical analysis

Cell viability was expressed as a mean ± standard error. Experiments were repeated at least three times on different cell preparations, and a

IV.2. Effects of interaction of SWCNTs with nonylphenol on their toxicity

minimum of three replicate wells per treatment were tested in each experiment. Samples from all groups within an experiment were processed simultaneously. A paired Student's *t*-test was used to compare treatments. Statistical significance was set at $P < 0.05$. Statistical analyses were performed by using the software SPSS v. 13.0 (IBM, Chicago, IL).

3. RESULTS

SWCNTs and NP were selected as target substances to evaluate the toxicological effects of their interaction for two main reasons. On the one hand, both are present in numerous consumer products, which confers them ubiquity and a high likelihood of coming into contact with living organisms; on the other, the two species can be expected to interact owing to the exceptional sorption capacity of CNTs which has been exploited in numerous analytical methodologies [18,19]. Although the individual toxicity of each species is well-known, the toxicological consequences of their coexistence and interaction warrant investigation.

SWCNTs, like all other CNTs, are intrinsically insoluble and tend to agglomerate in water. The dispersion status of nanoparticles is a key factor influencing their interaction with cells —and hence, their toxicity. In this work, we initially chose commercial SWCNTs coated with polyethylene glycol as target nanoparticles in order to prepare more stable aqueous dispersions than those obtained with uncoated nanoparticles. The greater stability of SWCNTs-PEG in aqueous solutions may be explained by enhanced electrostatic and steric repulsion forces between adjacent nanoparticles [3].

3.1. TEM analysis

Characterizing nanoparticles is a crucial pre-requisite for assessing their toxicity. Detailed information about SWCNTs-PEG was obtained from the manufacturer (Sigma-Aldrich) and is given in Section 2.1. Fig. 1 shows TEM images obtained from dispersions of SWCNTs-PEG prepared in PBS and serum-free medium. The images revealed the widespread presence of SWCNTs-PEG bundles/aggregates of varying length and diameter forming a dense network of nanofibers. In general, nanoparticles tended to aggregate in both media (PBS and culture medium), albeit to a slightly greater extent in serum-free medium.

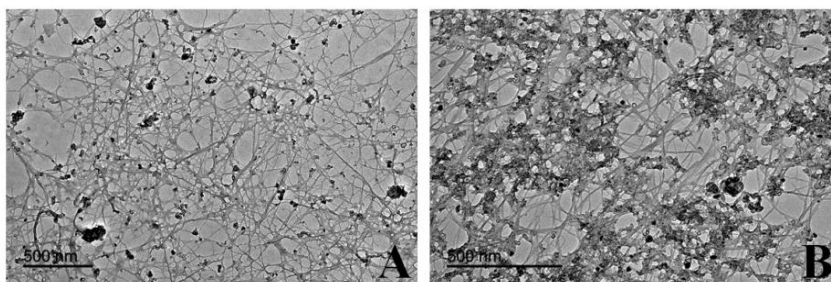


Figure 1. Transmission electron microscopy (TEM) images of SWCNTs-PEG dispersed in (A) PBS and (B) serum-free culture medium.

3.2. Toxicity of SWCNTs-PEG, NP and their mixtures on 3T3-L1 cells

3.2.1. 24 h exposure tests

The combined toxicity of SWCNTs-PEG and NP was examined in preliminary assays conducted at two different concentrations of NP (0.1 and 1 mg/L), both alone and in combination with 24 mg/L SWCNTs-PEG. As can be seen from Fig. 2, increasing the NP concentration from 0.1 to 1 mg/L led to a significant decrease ($P > 0.05$) in cell viability relative to untreated cell cultures. Also, exposure to SWCNTs-PEG alone (24 mg/L) resulted in the highest cell

IV.2. Effects of interaction of SWCNTs with nonylphenol on their toxicity

mortality rate found ($\approx 48\%$). However, the toxicity of binary mixtures of NP and SWCNTs-PEG was strongly dependent on that of the more cytotoxic species present (viz., SWCNTs-PEG) and roughly independent of the NP concentration added. No conclusive results were obtained from these experiments, consequently, a second series was conducted with higher NP concentrations (2, 5 and 10 mg/L), either alone or in combination with SWCNTs-PEG (2.6 and 13 mg/L) (see Fig. 3). In addition, we investigated whether the presence of serum in the culture medium affected the response of cells to NP and/or SWCNTs-PEG. Serum proteins are known to be able to coat CNTs and provide them steric stabilization thereby, reducing their tendency to agglomerating and their toxicity in biological environments [37,38]. It should be noted that strong interactions between SWCNTs and FBS were previously reported: serum proteins were found to attenuate the inherent toxicity of these nanoparticles and influence their uptake by cells [39–41].

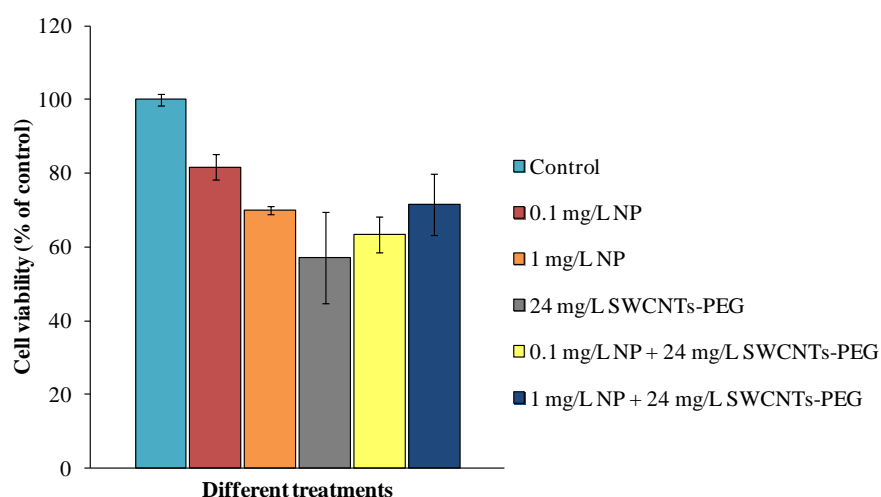


Figure 2. Cell viability data measured after treatments with NP (0.1 and 1 mg/L), SWCNTs-PEG (24 mg/L) and their mixtures. The results were obtained by using the MTT assay after 24 h exposure in FBS-free culture media and are expressed as mean \pm standard error for at least three independent experiments.

BLOQUE IV. ESTUDIOS TOXICOLÓGICOS DE NANOPARTÍCULAS

Fig. 3 shows the viability of 3T3-L1 cells exposed to different individual treatments with NP (2, 5 and 10 mg/L) and SWCNTs-PEG (2.6 and 13 mg/L), as well as their binary mixtures, for 24 h. Experiments were conducted in both 10% FBS-containing and serum-free media. In contrast to 24 mg/L concentration, 2.6 and 13 mg/L concentrations of SWCNTs-PEG in either culture media (with or without FBS) had no toxic effect on the cells. However, 3T3-L1 cell viability was greatly decreased by all concentrations of NP (2, 5 and 10 mg/L), whether alone or in combination with SWCNTs-PEG, in serum-free media. Interestingly, 3T3-L1 cell viability in 10% FBS-containing media was only reduced by the highest NP concentration used (10 mg/L), both alone and in combination with SWCNTs-PEG; nevertheless this cytotoxic effect remained lower in magnitude than that exerted by this same concentration of NP in serum-free media.

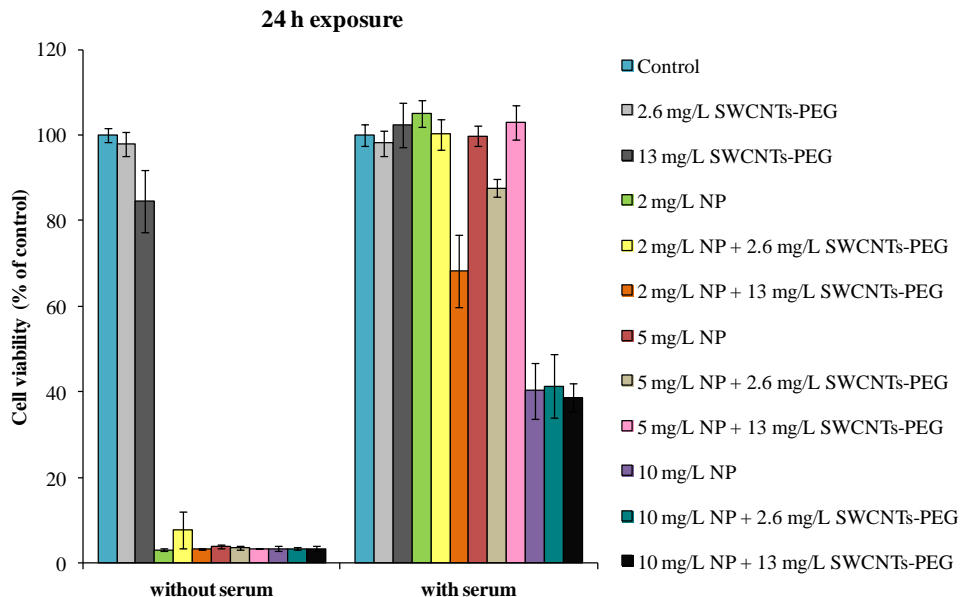


Figure 3. Cell viability percentages of 3T3-L1 cells exposed to variable concentrations of NP (2, 5 and 10 mg/L), SWCNTs-PEG (2.6 and 13 mg/L) and mixtures, in 10% serum-containing and serum-free culture media for 24 h. All results are expressed as mean \pm standard error for at least three independent experiments.

IV.2. Effects of interaction of SWCNTs with nonylphenol on their toxicity

These results confirm that the presence of serum increases the tolerance of cells to all treatments with NP, SWCNTs-PEG and their mixtures. Overall, no synergistic toxic effects from the mixtures of NP and SWCNTs-PEGs in either culture medium (with or without FBS) were observed. In the presence of serum, however, the mixture consisting of 2 mg/L NP and 13 mg/L SWCNTs-PEG, and that containing 5 mg/L NP and 2.6 mg/L SWCNTs, led to higher mortality rates than when SWCNTs-PEG and NP were tested individually at those same concentrations. Consequently, for those cases the unexpected toxicity of the mixtures can be ascribed to a synergistic action of SWCNTs-PEG and NP. Table 2 provides comprehensive information about cell viability as measured in the 24 h experiments.

Table 2. Viability of 3T3-L1 cells exposed to NP and/or SWCNTs-PEG in serum free (A) and 10% FBS containing media (B) for 24 h. Data are presented as mean \pm standard error for at least three independent experiments.

A)

24h exposure in FBS free media

NP (mg/L)	SWCNTs-PEG (mg/L)			
	0	2.6	13	24
0	100.0 \pm 1.5	97.9 \pm 2.7	84.5 \pm 7.3	57.2 \pm 12.4
0.1	81.7 \pm 3.5	n.a	n.a	63.3 \pm 4.8
1	70.0 \pm 1.2	n.a	n.a	71.7 \pm 8.3
2	3.2 \pm 0.2	7.8 \pm 4.4	3.4 \pm 0.2	n.a
5	4.0 \pm 0.4	3.6 \pm 0.4	3.5 \pm 0.1	n.a
10	3.4 \pm 0.6	3.5 \pm 0.3	3.5 \pm 0.6	n.a

n.a: no available information

B)

24h exposure in 10 % FBS containing media

NP (mg/L)	SWCNTs-PEG (mg/L)		
	0	2.6	13
0	100.0 \pm 2.4	98.1 \pm 3.0	102.5 \pm 5.2
2	105.1 \pm 3.1	100.2 \pm 3.5	68.2 \pm 8.5
5	99.8 \pm 2.3	87.7 \pm 2.0	103.0 \pm 4.0
10	40.3 \pm 6.5	41.4 \pm 7.4	38.7 \pm 3.3

3.2.2. 48 h exposure tests

The above-described study was expanded by increasing the exposure time from 24 to 48 h. Only SWCNTs-PEG was tested in serum-free media, given the high toxicity of NP observed in the previous 24 h experiments. Intriguingly, the presence or absence of serum in culture medium conditioned that 13 mg/L of SWCNTs-PEG showed or not cytotoxicity on cells (89.9 ± 3.8 vs 44.3 ± 4.2 ; Table 3). This result is consistent with previous findings where the addition of serum significantly altered the toxicity of nanoparticles [41].

All other 48 h treatments were conducted in 10% FBS-containing culture media. The treatments with 2 and 5 mg/L NP led to near 100% cell viability, whereas 10 mg/L NP caused high cell mortality. The combination of SWCNTs-PEG with 2 mg/L or 5 mg/L NP slightly reduced cell viability relative to NP alone, the reduction being independent of the concentration of SWCNTs-PEG added. For most experiments, the cytotoxicity of the mixtures was strongly influenced by the cytotoxicity of the more toxic species (i.e., SWCNTs-PEG); also, because both concentrations of SWCNTs-PEG (2.6 and 13 mg/L) led to identical cell viability percentages, the corresponding mixtures with NP also resulted in similar cell mortality rates. Only the combination of 5 mg/L NP and 13 mg/L SWCNTs-PEG resulted in increased cell mortality despite the absence of toxic effects observed for individual treatments with SWCNTs-PEG and NP at those same concentrations. This suggests a potential synergistic effect. No evidence of combined toxic effects was found with 10 mg/L NP, however.

IV.2. Effects of interaction of SWCNTs with nonylphenol on their toxicity

Table 3. Viability of 3T3-L1 cells exposed to NP and/or SWCNTs-PEG in serum free (A) and 10% FBS containing media (B) for 48 h. Data are presented as mean \pm standard error for at least three independent experiments.

A)

48h exposure in FBS free media

NP (mg/L)	SWCNTs-PEG (mg/L)		
	0	2.6	13
0	100.0 \pm 2.5	133.1 \pm 23.0	44.3 \pm 4.2

B)

48h exposure in 10 % FBS containing media

NP (mg/L)	SWCNTs-PEG (mg/L)		
	0	2.6	13
0	99.3 \pm 1.6	89.1 \pm 4.2	89.9 \pm 3.8
2	101.5 \pm 2.1	94.2 \pm 2.2	94.0 \pm 3.6
5	112.2 \pm 12.3	86.4 \pm 6.6	77.7 \pm 5.9
10	7.4 \pm 1.8	10.5 \pm 3.2	7.2 \pm 3.2

Fig. 4 compares the results of the 24 h and 48 h experiments in 10% FBS-containing culture media.

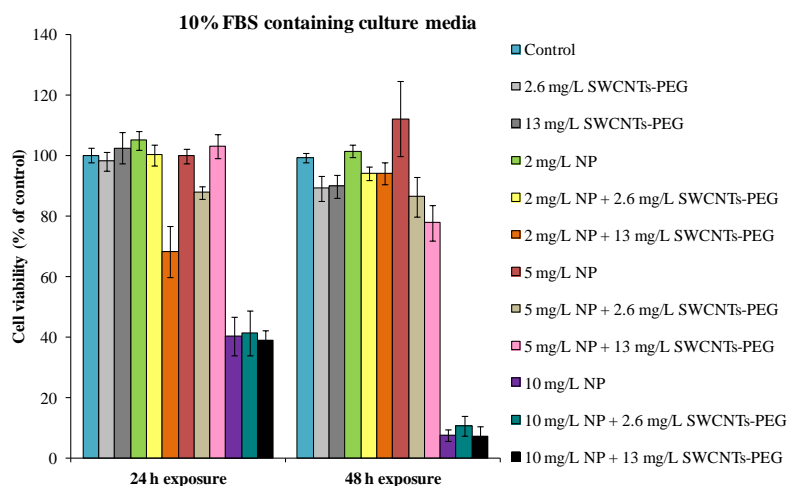


Figure 4. Cell viability percentages of 3T3-L1 cells exposed to variable concentrations of NP (2, 5 and 10 mg/L), SWCNTs-PEG (2.6 and 13 mg/L) and SWCNTs-PEG+NP in 10% serum-containing media for 24/48 h. All results are expressed as mean \pm standard error for at least three independent experiments.

Overall, increasing the exposure time had no substantial effect on cell viability. By exception, the highest NP concentration (10 mg/L) increased cell mortality in a time-dependent manner, but no appreciable differences between individual treatments or mixtures were observed.

3.3. Raman Imaging

The use of Raman Spectroscopy for imaging living cells is fairly recent [42–47]. Raman spectra exhibit narrow spectral peaks that allow distinct chemical species in complex cellular environments to be measured with the added advantage of obtaining comprehensive molecular information about single cells [42,43]. In Raman microscopy, the spectral distribution of bands is determined, and the intensity of each band mapped, to construct a Raman image [43]. Finally, there will be as many Raman images as peaks of interest previously set. An overlay image is constructed by assigning different color channels to the different Raman images obtained from a sample. In this work, the Raman peaks were assigned according to literature reports [3,44]. Fig. 5 shows an optical image (100x) and the Raman spectrum for SWCNTs-PEG.

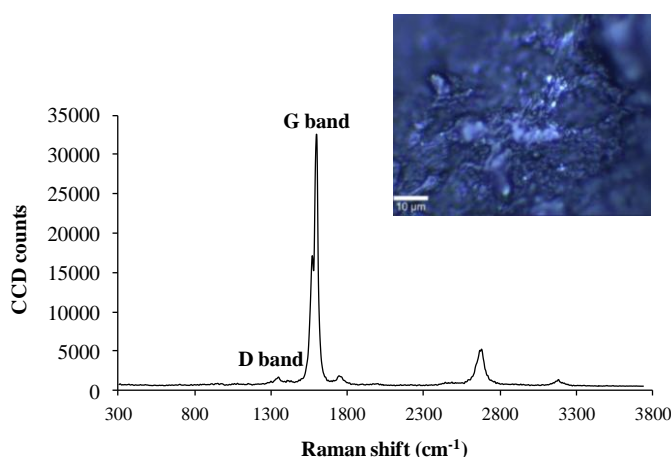


Figure 5. Optical image (100x) and Raman spectrum for SWCNTs-PEG.

IV.2. Effects of interaction of SWCNTs with nonylphenol on their toxicity

The D and G bands in the spectrum (1316 and 1595 cm^{-1} , respectively) are typical of graphitic carbon structures such as SWCNTs. The D band is sensitive to defects in the graphitic structure, whereas the G band corresponds to E_{2g} modes (stretching vibrations) [3]. As can be seen, the D band was barely visible, which suggests a lack of structural defects in the SWCNTs-PEG. Consequently, we selected the G band (peak at 1595 cm^{-1}) to identify the presence of these nanoparticles in biological samples. For cells, we selected the band at $2800\text{--}3000\text{ cm}^{-1}$ (peak at 2936 cm^{-1}), which usually corresponds to symmetric and asymmetric stretching of CH , CH_2 and CH_3 [44].

The Raman images for 3T3-L1 cells cultured in the absence of SWCNTs-PEG were constructed from the band $2800\text{--}3000\text{ cm}^{-1}$, typical of cells (see Fig. 6).

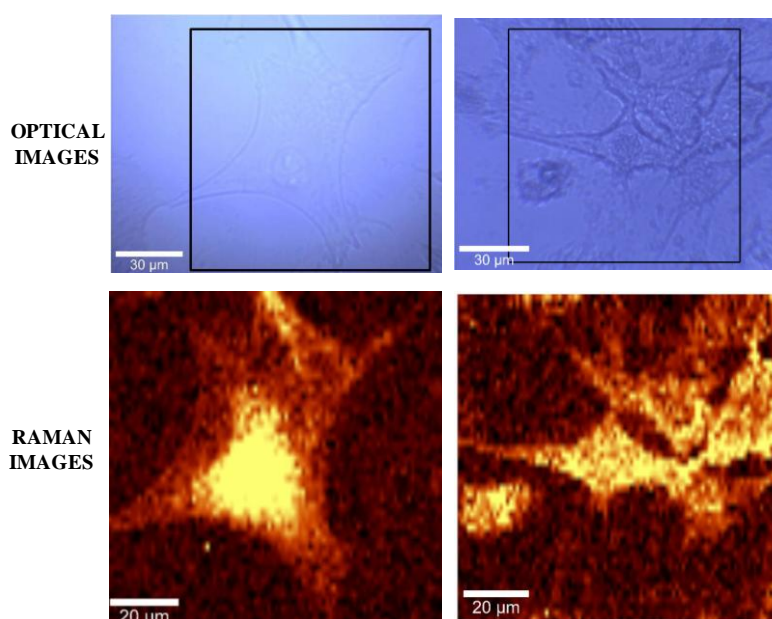


Figure 6. Optical images (50x) of mapped areas and Raman images of cells ($2800\text{--}3000\text{ cm}^{-1}$).

Further analyses were conducted on 3T3-L1 cells incubated with 13 mg/L SWCNTs-PEG for 24 h. Fig. 7 shows the Raman images and spectra obtained for a single cell.

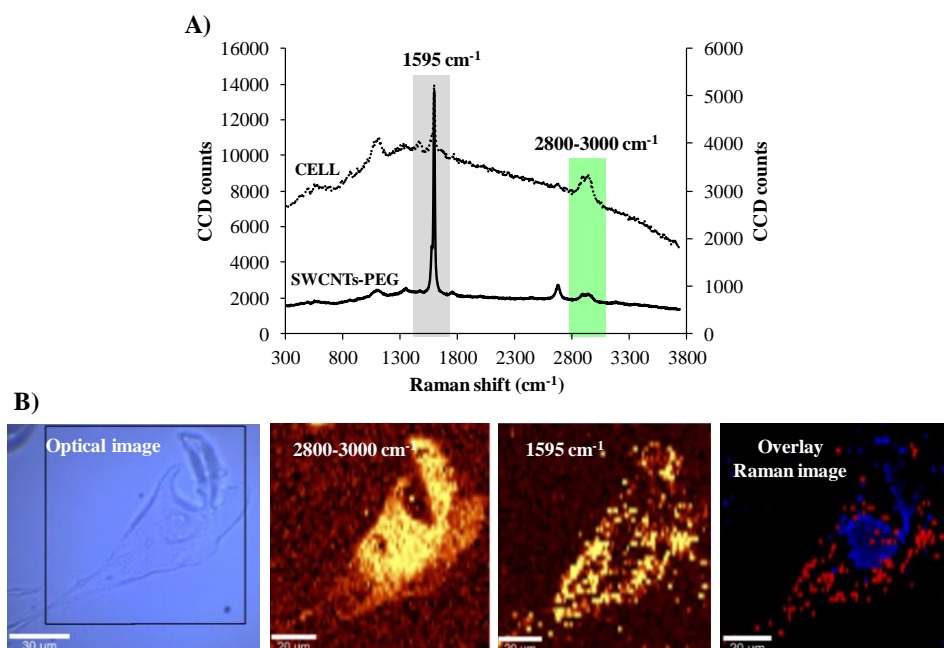


Figure 7. Imaging of the cellular distribution of SWCNTs-PEG in a 3T3-L1 cell after 24 h exposure to a 13 mg/L concentration of SWCNTs-PEG. (A) Average Raman spectra for SWCNTs-PEG and 3T3-L1 cells obtained from each Raman image. (B) Optical image (100x) of mapped area, and Raman images of cell (2800–3000 cm^{-1}) and SWCNTs-PEG (1595 cm^{-1}). The overlay Raman image was obtained by assigning different color channels to each Raman image (blue for cell and red for SWCNTs-PEG).

As can be seen, the Raman signal for SWCNTs-PEG clearly reflected the intracellular distribution of the nanoparticles and confirmed that they accumulated extensively into cells upon exposure. Moreover, the presence of the Raman band for cells in the SWCNTS-PEG spectrum and *viceversa* confirms the interaction between cells and nanoparticles. Regarding intracellular distribution, SWCNTs-PEG distributed throughout each cell —nucleus excepted.

IV.2. Effects of interaction of SWCNTs with nonylphenol on their toxicity

SWCNTs have a tubular shape that facilitates penetration of different types of membranes, uptake by cells and strong interactions with various protein systems; this property is referred to as the “snaking effect” [48]. To date, two main mechanisms have been used to explain the uptake of nanomaterials by cells. One is endocytosis/phagocytosis, which is an active process by which a cell engulfs extracellular particles by forming a vesicle that is integrated into the cell. The other is nanopenetration, which is a passive process that allows nanoparticles to diffuse directly across cell membranes [2]. Based on previous findings with PC12 and A549 cells, SWCNTs tend to accumulate on cell membranes or even be encapsulated inside endosomes in cytoplasm [3,49].

4. DISCUSSION

The most outstanding conclusions derived from these experiments are as follows: *(i)* the presence of 10% FBS in the culture medium had a “protective effect” on cells and considerably reduced cell mortality in the treatments with SWCNTs-PEG, whether alone or in combination with NP; *(ii)* the serum helped stabilize nanoparticles in the culture medium —the resulting dispersions were visibly more stable—; *(iii)* differences in agglomeration state of SWCNTs-PEG due to the presence or absence of serum marked differences in toxicity for individual treatments with SWCNTs-PEG in the 48 h experiments; *(iv)* increasing the time of exposure to the test substances had no substantial effect on cell viability except with the treatments using the highest NP concentration; *(v)* an excessively toxic concentration of either component precluded observation of their potential combined toxic effects; *(vi)* toxicological responses to the mixtures varied with the exposure conditions, which confirms the complexity of toxicological evaluation in scenarios involving nanoparticles; *(vii)* in some cases, the interaction between SWCNTs-PEG and NP had no effect on their global toxicity, which was influenced by the more toxic species only;

and (viii) while no general synergistic effects were observed under most of the experimental conditions studied, the interaction between SWCNTs-PEG and NP reflected isolated instances of synergy on 3T3-L1 cells exposed to both species jointly.

We chose to use the MTT based cytotoxicity assay here because it is deemed an especially sensitive evaluation method and had been used extensively to assess toxicity of CNTs [3,38,50]. At this point, it should be noted that interferences between multi-walled carbon nanotubes (MWCNTs) and MTT dye arising from the ability of the nanoparticles to reduce MTT to its formazan form in the absence of cells or enzymes were observed in previous literature [2,3,51,52]. Also, MWCNTs may bind to formazan crystals and stabilize their chemical structure, thereby preventing their solubilization [49]. To avoid potential interferences, we replaced the old culture medium containing SWCNTs-PEG with fresh medium immediately before adding the MTT dye, following an experimental protocol already described [38]. To the best of our knowledge, the PEG coating modifies the surface chemistry of SWCNTs and prevents binding of formazan crystals, which considerably reduces ambiguity in the results.

5. CONCLUSIONS

The interaction between SWCNTs-PEG and NP had no significant toxicological consequences. Cytotoxicity assays with 3T3-L1 cells revealed no general evidence of combined toxicity of SWCNTs-PEG and NP under most of the exposure conditions used. In most cases, the overall toxicity was only influenced by the more toxic species present. However, isolated synergistic effects from specific treatments were observed where the mixtures increased cell mortality with respect to the individual treatments even though identical concentrations of the individual species exhibited no toxic effects. These results

IV.2. Effects of interaction of SWCNTs with nonylphenol on their toxicity

testify to the difficulty of identifying a general tendency when so many influential factors come into play. Consequently, considering the coexistence of several species in the same environment can open up new research avenues leading to more realistic toxicological evaluation. This, however, will require much research effort. The presence of serum in the culture medium was found to have a protective effect against all treatments. Nanoparticles were better stabilized in FBS-containing media by effect of proteins coating the nanoparticles, and further stabilizing them by steric hindrance as a result. This in turn altered their interaction with cells and reduced their toxicity. Finally, Raman Spectroscopy proved useful to image single cells and identify SWCNTs-PEG in them. In fact, nanoparticles accumulated inside cells and distributed throughout —nucleus excepted— after 24 h exposure. As has been confirmed, the fairly recent use of the Raman technique in the biological field provides new approaches to cell analysis.

Acknowledgments

The authors would like to express their gratitude to Spain's Ministry of Economy and Competitiveness (MINECO/FEDER) for funding Projects CTQ2011-23790 and BFU2010-17116, and to Junta de Andalucía/FEDER for supporting Projects FQM-4801 and CTS-6606. E. Caballero-Díaz also wishes to thank MINECO for the award of a Research Training Fellowship (Grant AP2008-02955).

The authors declare no competing financial interest.

References

- [1] J.L. Luque-Garcia, R. Sanchez-Diaz, I. Lopez-Heras, P. Martin, C. Camara, Bioanalytical strategies for *in-vitro* and *in-vivo* evaluation of the toxicity induced by metallic nanoparticles, *TrAC* 43 (2013) 254–268.
- [2] X. Zhao, R. Liu, Recent progress and perspectives on the toxicity of carbon nanotubes at organism, organ, cell and biomacromolecule levels, *Environ. Int.* 40 (2012) 244–255.
- [3] Y. Zhang, Y. Xu, Z. Li, T. Chen, S.M. Lantz, P.C. Howard, M.G. Paule, W. Slikker, F. Watanabe, T. Mustafa, A.S. Biris, S.F. Ali, Mechanistic toxicity evaluation of uncoated and PEGylated single-walled carbon nanotubes in neuronal PC12 cells, *ACS Nano* 5 (2011) 7020–7033.
- [4] G. Y. Wang, Investigation progress on microelectronic materials: Carbon nanotube and graphene, *Adv. Mat. Res.* 531 (2012) 165–167.
- [5] C. Fu, L. Gu, Composite fibers from poly(vinyl alcohol) and poly(vinyl alcohol)-functionalized multiwalled carbon nanotubes, *J. Appl. Polym. Sci.* 128 (2013) 1044–1053.
- [6] F. Branzoi, V. Branzoi, A. Musina, Coatings based on conducting polymers and functionalized carbon nanotubes obtained by electropolymerization, *Prog. Org. Coat.* 76 (2013) 632–638.
- [7] G. Yang, X. Yang, M. Xu, C. Min, H. Xiao, K. Jiang, L. Chen, G. Wang, Multi-walled carbon nanotube modified with methylene blue under ultraviolet irradiation as a platinum catalyst support for methanol oxidation, *J. Power Sources* 222 (2013) 340–343.
- [8] D. Ahn, X. Xiao, Y. Li, A.K. Sachdev, H.W. Park, A. Yu, Z. Chen, Applying functionalized carbon nanotubes to enhance electrochemical performances of tin oxide composite electrodes for Li-ion battery, *J. Power Sources* 212 (2012) 66–72.
- [9] S. Kar, R.C. Bindal, P. K. Tewari, Carbon nanotube membranes for desalination and water purification: Challenges and opportunities, *Nano Today* 7 (2012) 385–389.
- [10] S. Parveen, R. Misra, S.K. Sahoo, Nanoparticles: A boon to drug delivery, therapeutics, diagnostics and imaging, *Nanomed–Nanotechnol.* 8 (2012) 147–166.
- [11] Y. Tong, H. Li, H. Guan, J. Zhao, S. Majeed, S. Anjum, F. Liang, G. Xu, Electrochemical cholesterol sensor based on carbon nanotube@molecularly imprinted polymer modified ceramic carbon electrode, *Biosens. Bioelectron.* 47 (2013) 553–558.
- [12] R. Lucena, B.M. Simonet, S. Cárdenas, M. Valcárcel, Potential of nanoparticles in sample preparation, *J Chromatogr A.* 1218 (2011) 620–637.

IV.2. Effects of interaction of SWCNTs with nonylphenol on their toxicity

- [13] Q. Zhou, J. Xiao, W. Wang, G. Liu, Q. Shi, J. Wang, Determination of atrazine and simazine in environmental water samples using multiwalled carbon nanotubes as the adsorbents for preconcentration prior to high performance liquid chromatography with diode array detector, *Talanta* 68 (2006) 1309–1315.
- [14] Q. Zhou, W. Wang, J. Xiao, Preconcentration and determination of nicosulfuron, thifensulfuron-methyl and metsulfuron-methyl in water samples using carbon nanotubes packed cartridge in combination with high performance liquid chromatography, *Anal. Chim. Acta* 559 (2006) 200–206.
- [15] G.Z. Fang, J.X. He, S. Wang, Multiwalled carbon nanotubes as sorbent for on-line coupling of solid phase extraction to high-performance liquid chromatography, *J Chromatogr A* 1127 (2006) 12–17.
- [16] B. Suárez, B. Santos, B.M. Simonet, S. Cárdenas, M. Valcárcel, Solid-phase extraction-capillary electrophoresis–mass spectrometry for the determination of tetracyclines residues in surface water by using carbon nanotubes as sorbent material, *J. Chromatogr. A* 1175 (2007) 127–132.
- [17] N. Rastkari, R. Ahmadkhaniha, Magnetic solid-phase extraction based on magnetic multi-walled carbon nanotubes for the determination of phthalate monoesters in urine samples, *J. Chromatogr. A* 1286 (2013) 22–28.
- [18] Y. Cai, G. Jiang, J. Liu, Q. Zhou, Multiwalled carbon nanotubes as a solid-phase extraction adsorbent for the determination of bisphenol A, 4-*n*-nonylphenol and 4-*tert*-octylphenol, *Anal. Chem.* 75 (2003) 2517–2521.
- [19] H.Y. Niu, Y.Q. Cai, Y.L. Shi, F.S. Wei, J.M. Liu, G.B. Jiang, A new solid-phase extraction disk based on a sheet of single-walled carbon nanotubes, *Anal. Bioanal. Chem.* 392 (2008) 927–935.
- [20] S. Lee, M. Cha, C. Kang, E.-T. Sohn, H. Lee, A. Munawir, J.-S. Kim, E. Kim, Mutual synergistic toxicity between environmental toxicants: A study of mercury chloride and 4-nonylphenol, *Environ. Toxicol. Pharmacol.* 27 (2009) 90–95.
- [21] Y. Hu, D.-M. Li, X.-D. Han, Analysis of combined effects of nonylphenol and monobutyl phthalate on rat Sertoli cells applying two mathematical models, *Food Chem. Toxicol.* 50 (2012) 457–563.
- [22] T. Vega, M.E. Torres, Z. Sosa, J.J. Santana, Determination of alkylphenol ethoxylated and their degradation products in liquid and solid samples, *TrAC* 28 (2009) 1186–1200.
- [23] Y. Gong, X.D. Han, Nonylphenol-induced oxidative stress and cytotoxicity in testicular Sertoli cells, *Reprod. Toxicol.* 22 (2006) 623–630.
- [24] Y. Gong, J. Wu, Y. Huang, S. Shen, X. Han, Nonylphenol induces apoptosis in rat testicular Sertoli cells via endoplasmic reticulum stress, *Toxicol. Lett.* 186 (2009) 84–95.

BLOQUE IV. ESTUDIOS TOXICOLÓGICOS DE NANOPARTÍCULAS

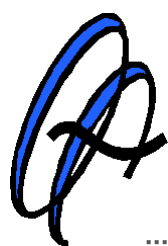
- [25] Q. Xiao, D. Li, H. Liu, A flounder (*Paralichthys olivaceus*) gill cell line as in vitro acute assay system of nonylphenol cytotoxicity, *Environ. Monit. Assess.* 175 (2011) 315–319.
- [26] X.D. Han, Z.G. Tu, Y. Gong, S.N. Shen, X.Y. Wang, L.N. Kang, Y.Y. Hou, J.X. Chen, The toxic effects of nonylphenol on the reproductive system of male rats, *Reprod. Toxicol.* 19 (2004) 215–221.
- [27] D. Zheng, N. Wang, X. Wang, Y. Tang, L. Zhu, Z. Huang, H. Tang, Y. Shi, Y. Wu, M. Zhang, B. Lu, Effects of the interaction of TiO₂ nanoparticles with bisphenol A on their physicochemical properties and in vitro toxicity, *J. Hazard. Mater.* 199–200 (2012) 426–432.
- [28] X. Zhu, J. Zhou, Z. Cai, TiO₂ nanoparticles in the marine environment: impact on the toxicity of tributyltin to abalone (*Haliotis diversicolor supertexta*) embryos, *Environ. Sci. Technol.* 45 (2011) 3753–3758.
- [29] R. Zhang, Y. Niu, Y. Li, C. Zhao, B. Song, Y. Li, Y. Zhou, Acute toxicity study of the interaction between titanium dioxide nanoparticles and lead acetate in mice, *Environ. Toxicol. Pharmacol.* 30 (2010) 52–60.
- [30] D. Wang, J. Hu, D.R. Irons, J. Wang, Synergistic toxic effect of nano-TiO₂ and As(V) on *Ceriodaphnia dubia*, *Sci. Total Environ.* 409 (2011) 1351–1356.
- [31] Y. Shi, J.-H. Zhang, M. Jiang, L.-H. Zhu, H.-Q. Tan, B. Lu, Synergistic genotoxicity caused by low concentration of titanium dioxide nanoparticles and p,p'-DDT in human hepatocytes, *Environ. Mol. Mutagen.* 51 (2010) 192–204.
- [32] D. Wang, J. Hu, B.E. Forthaus, J. Wang, Synergistic toxic effect of nano-Al₂O₃ and As(V) on *Ceriodaphnia dubia*, *Environ. Pollut.* 159 (2011) 3003–3008.
- [33] X.Y. Zou, B. Xu, C.P. Yu, H.W. Zhang, Combined toxicity of ferroferric oxide nanoparticles and arsenic to the ciliated protozoa *Tetrahymena pyriformis*, *Aquat. Toxicol.* 134–135 (2013) 66–73.
- [34] W. Zhang, X. Sun, L. Chen, K.F. Lin, Q.X. Dong, C.J. Huang, R.B. Fu, J. Zhu, Toxicological effect of joint cadmium selenium quantum dots and copper ion exposure on zebrafish, *Environ. Toxicol. Chem.* 31 (2012) 2117–2123.
- [35] A. Funfak, J. Cao, A. Knauer, K. Martin, J.M. Köhler, Synergistic effects of metal nanoparticles and a phenolic uncoupler using microdroplet-based two-dimensional approach, *J. Environ. Monit.* 13 (2011) 410–415.
- [36] X. Li, H. Zhao, X. Quan, S. Chen, Y. Zhang, H. Yu, Adsorption of ionizable organic contaminants on multi-walled carbon nanotubes with different oxygen contents, *J. Hazard. Mater.* 186 (2011) 407–415.
- [37] A. Dhawan, V. Sharma, Toxicity assessment of nanomaterials: methods and challenges, *Anal. Bioanal. Chem.* 398 (2010) 589–605.

IV.2. Effects of interaction of SWCNTs with nonylphenol on their toxicity

- [38] E. Heister, C. Lamprecht, V. Neves, C. Tilmaciu, L. Datas, E. Flahaut, B. Soula, P. Hinterdorfer, H.M. Coley, S.R.P. Silva, J. McFadden, Higher dispersion efficacy of functionalized carbon nanotubes in chemical and biological environments, *ACS Nano* 4 (2010) 2615–2626.
- [39] M. Davoren, E. Herzog, A. Casey, B. Cottineau, G. Chambers, In vitro toxicity evaluation of single walled carbon nanotubes on human A549 lung cells, *Toxicol. In Vitro* 21 (2007) 438–448.
- [40] A. Casey, M. Davoren, E. Herzog, F.M. Lyng, H.J. Byrne, G. Chambers, Probing the interaction of single walled carbon nanotubes within cell culture medium as a precursor to toxicity testing, *Carbon* 45 (2007) 34–40.
- [41] Y. Zhu, W. Li, Q. Li, Y. Li, X. Zhang, Q. Huang, Effects of serum proteins on intracellular uptake and cytotoxicity of carbon nanoparticles, *Carbon* 47 (2009) 1351–1358.
- [42] A.S. Stender, K. Marchuk, C. Liu, S. Sander, M.W. Meyer, E.A. Smith, B. Neuphane, G. Wang, J. Li, J.X. Cheng, B. Huang, N. Fang, Single cell optical imaging and spectroscopy, *Chem. Rev.* 113 (2013) 2469–2527.
- [43] A.F. Palonpon, M. Sodeoka, K. Fujita, Molecular imaging of live cells by Raman microscopy, *Curr. Opin. Chem. Biol.* 17 (2013) 708–715.
- [44] Z. Movasaghi, Raman spectroscopy of biological tissues, *Appl. Spectrosc. Rev.* 42 (2007) 493–541.
- [45] M. Li, J. Xu, M. Romero-Gonzalez, S.A. Banwart, W.E. Huang, Single cell Raman spectroscopy for cell sorting and imaging, *Curr. Opin. Biotechnol.* 23 (2012) 56–63.
- [46] M.A. Calin, S.V. Parasca, R. Savastru, M.R. Calin, S. Dontu, Optical techniques for the noninvasive diagnosis of skin cancer, *J. Cancer Res. Clin. Oncol.* 139 (2013) 1083–1104.
- [47] Y.S. Guo, X.M. Li, S.J. Ye, S.S. Zhang, Modern optical techniques provide a bright outlook for cell analysis, *TrAC* 42 (2013) 168–185.
- [48] Y. Zhang, S.F. Ali, E. Dervishi, Y. Xu, Z. Li, D. Casciano, A.S. Biris, Cytotoxicity effects of graphene and single-wall carbon nanotubes in neural pheochromocytoma-derived PC12 cells, *ACS Nano* 4 (2010) 3181–3186.
- [49] J.M. Wörle-Knirsch, K. Pulskamp, H.F. Krug, Oops they did it again! Carbon nanotubes hoax scientists in viability assays, *Nano Lett.* 6 (2006) 1261–1268.
- [50] G. Fotakis, J.A. Timbrell, In vitro cytotoxicity assays: Comparison of LDH, neutral red, MTT and protein assay in hepatoma cell lines following exposure to cadmium chloride, *Toxicol. Lett.* 160 (2006) 171–177.
- [51] R. Brayner, The toxicological impact of nanoparticles, *Nanotoday* 3 (2008) 48–55.

BLOQUE IV. ESTUDIOS TOXICOLÓGICOS DE NANOPARTÍCULAS

[52] N.A. Monteiro-Riviere, A.O. Inman, L.W. Zhang, Limitations and relative utility of screening assays to assess engineered nanoparticle toxicity in a human cell line, *Toxicol. Appl. Pharmacol.* 234 (2009) 222–235.



BLOQUE V

Resultados y Discusión

V.1. Contextualización general de la investigación planteada	344
V.2. Discusión específica de los resultados	348
- <i>Nanopartículas como herramientas de análisis ambiental</i>	348
- Nanopartículas en el tratamiento de muestra	
- Valoración general de las nanopartículas en el tratamiento de muestra	
- Valoración general de los métodos de extracción	
- Nanopartículas en la etapa de detección	
- <i>Nanopartículas como objetos de evaluación toxicológica</i>	376
- Influencia de la química superficial	
- Influencia de la presencia de otra especie química	
- Valoración general de los estudios de toxicidad	

Una vez finalizada la exposición de los trabajos científicos desarrollados durante la fase experimental de la Tesis Doctoral (*anteriores Bloques III y IV*), se procederá a discutir los resultados más significativos derivados de los mismos. Éstos se expondrán en dos grandes bloques temáticos:

➤ **Nanopartículas como herramientas de análisis ambiental.**

En este apartado abordaremos el empleo de NPs como herramientas en las etapas de tratamiento de muestra (técnicas de extracción) y detección dentro del procedimiento analítico.

➤ **Nanopartículas como objetos de evaluación toxicológica.**

En este apartado se describirán los resultados derivados de los estudios toxicológicos desarrollados. Éstos tuvieron como principales objetivos, evaluar la influencia de la química superficial de las NPs de plata sobre su citotoxicidad, y predecir posibles mecanismos de toxicidad combinada entre nanotubos de carbono y un conocido contaminante ambiental.

Con el fin de facilitar la lectura y reflexión de lo que se va a exponer, estos dos grandes apartados se dividirán a su vez en subapartados más específicos.

V.1. Contextualización general de la investigación planteada

La Figura V.I.1 esquematiza los dos grandes bloques temáticos en los que se enmarca la labor investigadora desarrollada, así como los apartados más específicos en los que pueden dividirse.

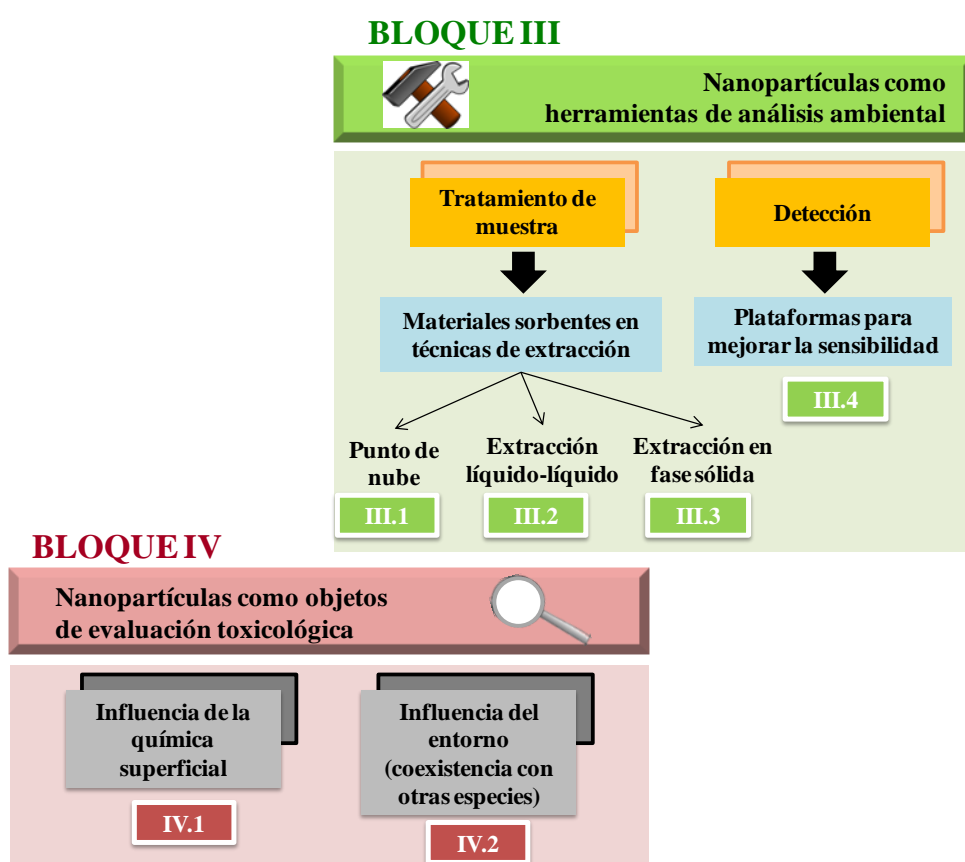


Figura V.1.1. Visión global de los bloques temáticos y apartados más específicos en los que puede encuadrarse la investigación desarrollada.

Como ya se ha comentado anteriormente, la investigación estuvo enfocada a profundizar en dos vertientes de conocimiento dentro de la *Nanociencia*; por un lado, la búsqueda de aplicaciones analíticas; y por otro lado, indagar en la toxicidad asociada a las NPs.

➤ *Nanopartículas como herramientas de análisis ambiental*

Las excelentes propiedades que exhiben las NPs, incluyendo su elevada área superficial específica y habilidad de adsorción, las convierten en candidatos muy atractivos para su uso en el ámbito de la Química Analítica.

A lo largo del desarrollo de esta Tesis se diseñaron varios métodos de tratamiento de muestra basados en el empleo de NPs, ya sea como fase extractante adicional o como única fase extractante presente. En el primer caso, las NPs fueron evaluadas como fases adicionales introducidas en los esquemas convencionales de extracción punto de nube (CPE) y extracción líquido-líquido (LLE). En esos casos, se investigó el papel que desempeñaban las NPs en combinación con las fases extractantes originales de las técnicas de extracción, es decir, surfactante para CPE y disolvente orgánico para LLE. Por otro lado, las NPs fueron propuestas como única fase extractante presente en un sistema de extracción en fase sólida (SPE).

Además del tratamiento de muestra, las NPs también presentan un gran potencial para su empleo en la etapa de detección del procedimiento analítico. Como aportación científica a este ámbito, desarrollamos un procedimiento analítico que constaba de dos etapas. Una primera etapa de tratamiento de muestra basada en el empleo de un sistema de microextracción en fase sólida disponible comercialmente, y una segunda etapa de detección por espectroscopía Raman en la que NPs de plata (AgNPs) fueron utilizadas como plataformas o sustratos para incrementar la sensibilidad de la técnica a través del conocido efecto SERS.

➤ ***Nanopartículas como objetos de evaluación toxicológica***

La investigación centrada en la aplicabilidad de las NPs ha sido mucho más notable que aquella dirigida a evaluar los posibles efectos toxicológicos de estos nanomateriales. Mientras que la búsqueda de nuevas y originales aplicaciones ha ocupado gran parte de la investigación en *Nanociencia*, la evaluación sistemática de los riesgos asociados ha quedado en un segundo plano. Esto unido a las carencias propias de los métodos de evaluación actuales, hace que los avances en este ámbito de estudio sean rigurosamente necesarios.

Uno de los principales retos en la evaluación toxicológica de las NPs es tener en cuenta los numerosos factores influyentes que entran en juego. En este sentido, las propiedades fisicoquímicas de las NPs incluyendo su forma, tamaño y química superficial, condicionan su diferente interacción con las células y consecuentemente, su toxicidad. Como principal aportación a este ámbito de estudio, se evaluó la toxicidad *in vitro* de AgNPs sintetizadas experimentalmente a partir del mismo núcleo de plata pero con diferentes agentes superficiales. La finalidad perseguida fue investigar la influencia de la química superficial de las NPs sobre su grado de oxidación, estabilidad coloidal e internalización celular, que son factores que repercuten directamente sobre su citotoxicidad.

Otro factor determinante, aparte de las características intrínsecas de las NPs, es su interacción con el entorno. Fluctuaciones de pH o en el contenido salino pueden determinar un diferente grado de toxicidad para NPs idénticas. En este punto, conviene hacer la siguiente reflexión. Los contaminantes ambientales no se encuentran aislados en el medio ambiente, sino que dada la ubicuidad de algunos de ellos es más que probable que puedan entrar en contacto con otras especies. Además, las NPs son extremadamente reactivas en superficie y tienen una habilidad excepcional para interaccionar con multitud

de compuestos tanto orgánicos como inorgánicos. Todo esto nos lleva a plantearnos los posibles riesgos toxicológicos derivados de la interacción entre las NPs y otros contaminantes ambientales comunes. A este respecto, efectos tóxicos aditivos, sinérgicos o antagónicos ya se han descrito en bibliografía, y son prueba irrefutable de la existencia de mecanismos de toxicidad combinada cuando las NPs coexisten con otras especies químicas. Nuestro trabajo estuvo dirigido a investigar por primera vez las consecuencias toxicológicas derivadas de la interacción de nanotubos de carbono (CNTs) con un conocido disruptor endocrino (4-nonilfenol).

V.2. Discusión específica de los resultados**NANOPARTÍCULAS COMO HERRAMIENTAS DE ANÁLISIS AMBIENTAL****Nanopartículas en el tratamiento de muestra**

En este apartado abordaremos los principales resultados derivados del empleo de NPs en los procesos de tratamiento de muestra. En primer lugar, se discutirán los hallazgos derivados de aquellas técnicas de extracción convencionales que fueron modificadas con la inclusión de NPs como fase adicional (ver *apartados III.1 y III.2*). Por último, se hará referencia a las principales aportaciones del método de SPE desarrollado con el uso de CNTs como únicas fases sorbentes (ver *apartado III.3*).

▪ *Nanopartículas como fase adicional en la extracción punto de nube (CPE)*

El término “*química verde*” se acuñó por primera vez en 1991 y engloba de forma generalizada la síntesis, manipulación y uso de compuestos químicos que reducen los riesgos para el ser humano y el medio ambiente. La presencia de contaminantes a bajas concentraciones y en matrices complejas hace necesaria una etapa de tratamiento de muestra previa a la detección. Esta etapa se considera la más contaminante dentro del procedimiento analítico puesto que implica el empleo de disolventes orgánicos. Las técnicas de extracción comúnmente utilizadas en el tratamiento de muestra son SPE y LLE, sin embargo, existen otras alternativas “*más verdes*” que reemplazan los disolventes orgánicos por surfactantes de menor toxicidad, y que son por tanto más respetuosas con el medio ambiente.

La técnica de extracción punto de nube o CPE, se encuadra dentro de estas alternativas “*verdes*” y se basa en la separación y preconcentración de

especies polares y apolares empleando disoluciones acuosas de surfactante. El fundamento de la separación radica en la formación de dos fases isotrópicas (fase acuosa y fase enriquecida en surfactante) a partir de una única fase acuosa micelar homogénea. La fase acuosa de mayor volumen contiene la matriz acuosa libre de analito y surfactante a una concentración inferior a su concentración micelar crítica (CMC), que es la concentración por encima de la cual los monómeros de surfactante se agregan formando estructuras micelares. La otra fase, de menor volumen, está enriquecida en complejos micelares que contienen el analito.

Se necesitan dos requisitos para que se produzca la separación en dos fases. Por un lado, la concentración de surfactante en la disolución acuosa inicial debe exceder su CMC para asegurar la formación de agregados micelares. Por otro lado, las condiciones experimentales iniciales tales como presión, temperatura o fuerza iónica deben verse alteradas de algún modo. Cuando se cumplen estos dos requisitos, la disolución acuosa micelar inicial se enturbia (enturbiamiento o *clouding*) y se produce la separación en dos fases.

Se han descrito diferentes mecanismos para justificar el fenómeno de separación en dos fases. La principal hipótesis se basa en la deshidratación de las moléculas de surfactante, lo que hace que éstas se aglomeren y se enturbie la disolución. Esta deshidratación puede producirse por un incremento de T^a o bien por el efecto *salting out* en presencia de una concentración elevada de electrolito (es decir, las moléculas de agua que rodean y estabilizan las micelas, pasan a solvatar los iones de la sal por su mayor afinidad hacia ellos). De cualquier forma, la solubilidad del surfactante en agua disminuye y como resultado, se forman dos fases claramente distinguibles.

Las hipótesis iniciales que nos guiaron a proponer un procedimiento analítico que combinaba NPs con un esquema CPE convencional fueron dos

BLOQUE V

principalmente. Por un lado, las NPs presentan una habilidad excepcional de adsorción y por tanto su presencia podría reforzar de algún modo la extracción de analito en un sistema que a su vez presenta surfactante como fase extractante. Por otro lado, el empleo de una dispersión de nanopartículas de carbono (CNPs) en un medio acuoso micelar como fase extractante en CPE no ha sido investigado hasta la fecha, y por consiguiente, su efecto sobre la eficiencia de extracción del proceso es aún desconocido.

En nuestro trabajo concretamente, las CNPs fueron añadidas en combinación con el surfactante dodecilsulfato de sodio (SDS). El analito modelo, fluorantreno, fue seleccionado en base a su importancia como contaminante ambiental, ya que está catalogado como contaminante prioritario según la Agencia de Protección Ambiental de los Estados Unidos (EPA). Asimismo, su estructura aromática y naturaleza apolar favorecen su interacción con las NPs (mediante interacciones hidrofóbicas y de tipo π - π), y con el surfactante (a través de interacciones hidrofóbicas con las cadenas apolares). Muestras ambientales de agua de río fueron utilizadas para validar el método de extracción desarrollado. La Tabla V.2.1 resume todos los parámetros experimentales estudiados así como el valor óptimo finalmente seleccionado.

Tabla V.2.1. Resumen de variables experimentales optimizadas en el procedimiento CPE modificado, así como valores finalmente seleccionados.

VARIABLES ESTUDIADAS	VALOR ÓPTIMO
Concentración de NaCl (mol L ⁻¹)	0.25
Concentración de SDS (mol L ⁻¹)	0.1
T ^a del proceso	T ^a ambiente
Tiempo interacción nanopartículas con SDS (min)	30
Tiempo interacción con analito (min)	10
Tiempo en contacto con NaCl (min)	60
Tipo de nanopartícula	nanodiamantes
Concentración de nanodiamantes (mg mL ⁻¹)	6
Eluyente	acetoniitrilo
Volumen de eluyente (mL)	1.5

La presencia del surfactante es imprescindible para que se produzca la formación de dos fases en cualquier CPE. En nuestro caso, posibilita además la estabilización de las CNPs en el medio acuoso lo que permite maximizar su superficie de interacción con las especies en disolución. Las concentraciones de SDS investigadas fueron siempre superiores a su CMC (8 mM a 25 °C), para así asegurar la presencia de agregados micelares en la disolución. Los estudios de optimización de la concentración de surfactante revelaron que 0.1 mol L⁻¹ de SDS fue la concentración óptima, ya que la señal analítica correspondiente al fluorantreno extraído se redujo a concentraciones superiores de SDS. Esto podría ser justificado de la siguiente manera. Por lo general, al incrementar la concentración de surfactante, también aumenta el factor de preconcentración ya que se favorece la formación de una fase enriquecida de mayor viscosidad y menor volumen. Sin embargo, en nuestro caso específico, tenemos que tener en cuenta el efecto de la inclusión de CNPs en el sistema. La superficie de las CNPs interacciona con las cadenas apolares del SDS a través de fuerzas hidrofóbicas. Las moléculas de SDS se van colocando de forma aleatoria sobre la superficie de las CNPs formando capas de recubrimiento. Cuando la concentración de SDS aumenta progresivamente para una cantidad constante de CNPs, el recubrimiento se va haciendo de mayor espesor hasta que llega un punto en el que las moléculas superficiales de SDS de CNPs adyacentes comienzan a interactuar entre sí a través de sus respectivas cadenas hidrocarbonadas. Esta interacción hace que las CNPs se aglomeren progresivamente reduciendo así su superficie de interacción con las especies en disolución y por tanto, su eficiencia en la extracción del analito. Este mecanismo podría justificar los peores resultados obtenidos a concentraciones de SDS superiores a 0.1 mol L⁻¹.

El cloruro de sodio (NaCl) fue seleccionado como electrolito del proceso. El incremento de la fuerza iónica del medio acuoso puede promover la separación de fases por el conocido fenómeno *salting out* (reducción de la solubilidad del surfactante por la presencia de sales) comentado anteriormente.

BLOQUE V

Asimismo puede incrementar la viscosidad y reducir el volumen de la fase enriquecida, lo que se traduce finalmente en un mayor factor de preconcentración. Esta mayor viscosidad facilita a su vez la manipulación de la fase enriquecida y su separación de la fase acuosa. Los resultados obtenidos mostraron que fue necesaria una concentración de 0.25 mol L^{-1} de NaCl para maximizar la extracción de fluorantreno de la matriz acuosa bajo las condiciones experimentales establecidas.

Diferentes CNPs fueron evaluadas como fase adicional en la técnica CPE (ver Figura V.2.1). Para realizar el estudio comparativo, el procedimiento fue conducido bajo condiciones experimentales constantes (0.1 mol L^{-1} de SDS; 0.25 mol L^{-1} de NaCl; 0.33 mg mL^{-1} de CNPs; T^a ambiente) exceptuando el tipo de CNPs. Nanodiamantes (NDs) y nanotubos de carbono multicapa (MWCNTs) fueron adquiridos comercialmente. Adicionalmente, los MWCNTs fueron sometidos experimentalmente a un proceso de oxidación para así obtener MWCNTs oxidados. Nanopartículas híbridas (NDs-MWCNTs) fueron sintetizadas experimentalmente a partir de la combinación de NDs y MWCNTs, y también fueron sometidas a estudio.

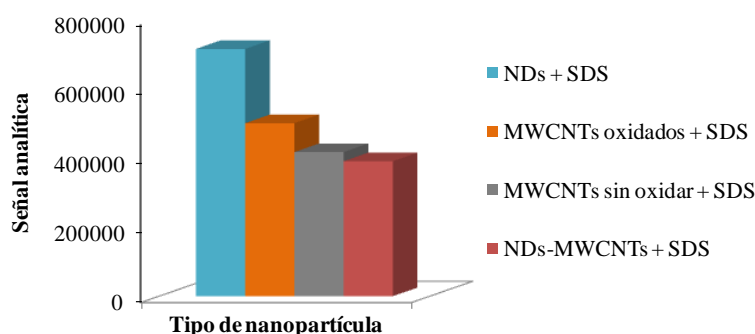


Figura V.2.1 Comparación de resultados obtenidos empleando distintas CNPs en el procedimiento CPE con SDS.

Los resultados obtenidos por comparación de las intensidades de fluorescencia pertenecientes a fluorantreno obtenidas tras la extracción, concluyeron que los NDs en combinación con el SDS proporcionaron una mayor extracción cuantitativa de analito. Teniendo en cuenta el reducido tamaño de estas NPs (3.2 nm de diámetro medio) respecto a los MWCNTs (140 nm de diámetro medio), para una cantidad fija de CNPs presentes, cabe esperar un mayor número de NDs que de MWCNTs y NDs-MWCNTs en disolución. Este mayor número de NPs presentes incrementa la relación área superficial/volumen, de forma que habrá una mayor superficie de NPs disponible para establecer interacciones con el fluorantreno o los complejos micelares (micela-analito). Esto podría explicar la mayor extracción de fluorantreno conseguida con NDs.

Los MWCNTs oxidados permitieron una extracción cuantitativa de analito moderadamente superior a aquella obtenida para las mismas NPs sin oxidar. Esto podría ser justificado por la mayor compatibilidad de los MWCNTs oxidados con el medio acuoso donde se lleva a cabo la extracción, gracias a la presencia de grupos funcionales sobre su superficie (tipo carboxílico o hidroxilo). Además, la oxidación de los CNTs supone el acortamiento de los mismos, de forma que para una misma cantidad de CNTs, cabe esperar un mayor número de MWCNTs cortos (oxidados) que largos (sin oxidar). El mayor número de NPs en disolución favorece un mayor grado de interacción con las especies presentes, tal y como hemos comentado anteriormente para el caso de los NDs. NDs-MWCNTs no reportaron beneficios adicionales a la extracción respecto a NDs y MWCNTs por separado, y por esa razón estas NPs híbridas fueron descartadas.

Uno de los aspectos más destacables es que aquellos experimentos que se realizaron en ausencia de CNPs no condujeron a la extracción de fluorantreno en tanto en cuanto no se apreciaron dos fases claramente distinguibles en el

sistema. La adición del electrolito a la disolución acuosa micelar hizo disminuir la solubilidad del SDS como consecuencia del efecto *salting out*, provocando así el enturbiamiento de la disolución. Este efecto podría por si solo conllevar a la formación de dos fases diferenciables, si bien ese no fue nuestro caso. Y es que bajo las condiciones experimentales estudiadas en este trabajo, la simple adición de NaCl, en ausencia de NPs y a T^a ambiente, no fue suficiente para que se apreciaran dos fases visiblemente diferentes. Por tanto podemos concluir que la presencia de CNPs resultó indispensable para conducir las extracciones.

En este punto, conviene reflexionar sobre el papel que desempeñaron las CNPs introducidas en el sistema. Las moléculas de SDS (surfactante aniónico) rodearon la superficie de las CNPs y les confirieron carga superficial negativa, lo que permitió su estabilidad en disolución a través de repulsiones electrostáticas. Sin embargo, cuando se añadió NaCl, aumentó la concentración iónica de Na⁺ presente lo que hizo que la superficie negativa del sistema formado por CNP-SDS se fuese neutralizando gradualmente. Esto hizo que las CNPs adyacentes comenzasen a interactuar a través de fuerzas de van der Waals provocando su desestabilización y aglomeración progresiva. Los agregados de CNPs se depositaron finalmente en la fase inferior (fase enriquecida). Esta retirada de CNPs de la fase acuosa también supuso la retirada de las estructuras micelares que se encontraban sobre su superficie. Este hecho provocó un enriquecimiento adicional de la fase inferior en moléculas de surfactante lo que pudo condicionar la formación de una fase enriquecida, esta vez sí, distinguible de la acuosa.

En resumen, aunque el incremento de la fuerza iónica de la disolución contribuyó directamente a la pérdida de estabilidad del surfactante en la fase acuosa y a la formación de la fase enriquecida, los efectos derivados de la inclusión de CNPs en el sistema y su interacción con las estructuras micelares

fueron determinantes para que las dos fases fuesen visiblemente diferenciables tras la adición del electrolito.

El método analítico desarrollado no presenta requerimientos especiales de T^a y el tiempo de extracción es aceptable. Estas características simplifican enormemente el procedimiento de análisis y lo hacen adecuado para la extracción de analitos termolábiles. Además, evaluar la influencia de la introducción de CNPs en combinación con la fase extractante micelar en CPE no ha sido considerado hasta la fecha, lo que le confiere a este trabajo un valor añadido por profundizar en el conocimiento del potencial de estas NPs en nuevos campos de aplicación dentro de la Química Analítica. El método analítico propuesto fue bastante reproducible y tuvo un límite de detección de $17 \mu\text{g L}^{-1}$. Su aplicación en último término a la determinación de fluorantreno en agua de río proporcionó resultados bastante satisfactorios.

▪ *Nanopartículas como interfase en la extracción líquido-líquido (LLE)*

La contribución de las NPs como fases sorbentes en combinación con la fase extractante originaria fue también investigada en la técnica LLE. En un esquema experimental que constaba de dos fases, una fase acuosa donadora y una fase orgánica aceptora, introducimos una interfase de CNPs estabilizadas en disolvente orgánico, con el objetivo de evaluar su efecto sobre la extracción cuantitativa del analito seleccionado.

El fundamento de este sistema de extracción de tres fases es similar a aquel que rige la LLE en combinación con membranas. En esos casos, las fases acuosa y orgánica entran en contacto en una membrana, generalmente polimérica, a través de la cual el analito difunde de una fase a otra. Las limitaciones de las membranas poliméricas convencionales se relacionan con

sus bajas selectividad, permeabilidad, resistencias química y térmica, y con su susceptibilidad a la obstrucción.

El empleo de membranas nanoestructuradas, que son aquellas que incorporan NPs a un soporte polimérico (principalmente polipropileno), ha tenido una gran acogida en el ámbito de la Química Analítica. Su reducido espesor, elevada área superficial y porosidad, son aspectos clave que favorecen un mayor flujo de analito a través de ellas. Las principales desventajas de las membranas modificadas con CNTs son consecuencia de la pérdida de área superficial específica de las NPs cuando son embebidas dentro de la matriz polimérica. Asimismo, se precisa llevar a cabo la síntesis del composite constituido por NPs y polímero.

La finalidad del trabajo de investigación planteado fue modificar la LLE convencional mediante la incorporación de una pseudofase de CNPs que actuase como membrana entre la fase acuosa donadora y la fase orgánica aceptora, eliminando el soporte polimérico para maximizar así la superficie de NPs disponible para interactuar con el analito.

La Figura V.2.2 representa esquemáticamente las fases de un sistema de LLE convencional (fase acuosa y fase orgánica), y del procedimiento experimental propuesto derivado de aquellos basados en el empleo de membranas (fase acuosa, interfase de CNPs y fase orgánica).

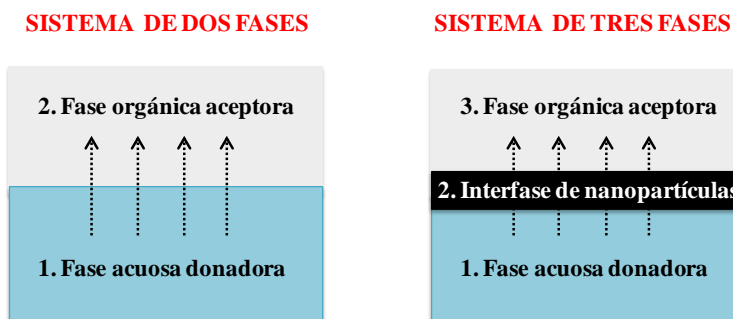


Figura V.2.2. Esquema de las fases que componen el sistema de LLE convencional (derecha) y el propuesto (izquierda).

La preparación de la interfase de CNPs fue bastante simple como puede apreciarse en la Figura V.2.3. Básicamente consistió en la homogeneización de una mezcla de CNPs y etilacetato con el uso de un mortero.



Figura V.2.3. Procedimiento de preparación de la interfase de CNPs.

El analito objeto de determinación fue atrazina, un herbicida perteneciente a la familia de las triazinas que es empleado de forma extensiva en la agricultura para controlar las malas hierbas. Este herbicida se aplica directamente sobre el suelo con lo cual puede generar lixiviaciones y también contaminar las aguas subterráneas y superficiales.

El potencial de diferentes CNPs para conformar la interfase en este esquema de extracción fue investigado. Nanodiamantes obtenidos por procesos

BLOQUE V

de detonación con un diámetro de 3.2 nm (NDs) y nanotubos de carbono multicapa con un diámetro entre 110-170 nm (MWCNTs) fueron estudiados al igual que para la técnica CPE comentada en el apartado anterior. A diferencia de entonces, aquí no se consideró sintetizar y estudiar el potencial de NPs híbridas (NDs-MWCNTs). En su lugar, nanotubos de carbono monocapa (SWCNTs) con un diámetro inferior a 2 nm, y nanodiamantes con carácter oleofílico (ND_o) y con un tamaño medio entre 4-15 nm, fueron sometidos a evaluación. La Figura V.2.4 muestra los resultados obtenidos en el estudio comparativo de diferentes CNPs como constituyentes de la interfase.

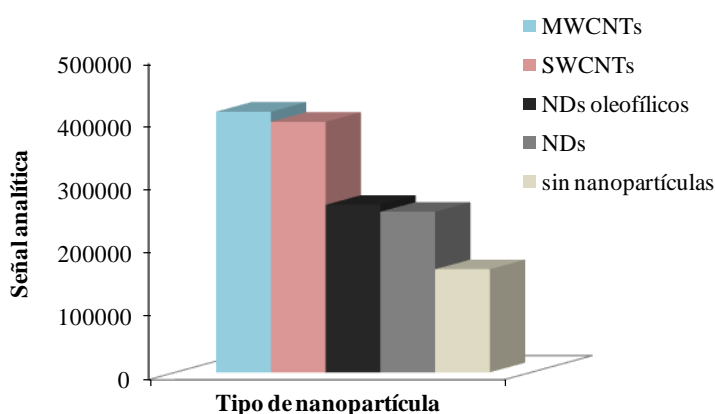


Figura V.2.4. Resultados comparativos según el tipo de CNP empleada en la interfase.

Debería puntualizarse que la inclusión de CNPs como interfase reforzó la extracción de atrazina de muestras acuosas en comparación a aquellas extracciones conducidas solo con dos fases (sin NPs). Estos resultados confirman que las CNPs proporcionaron vías adicionales de transporte para el soluto. Las NPs actuaron como extractantes en fase sólida sobre los que se adsorbieron las moléculas de analito, para después desorberse en la fase orgánica aceptora, a través de mecanismos consecutivos de adsorción-desorción. La eficiencia de extracción de atrazina empleando solo etilacetato fue por tanto mejorada por la presencia de CNPs con una proporción elevada de

sitios de adsorción accesibles. La extracción se condujo por lo tanto por una combinación de mecanismos de extracción en fase sólida (CNPs) y en fase líquida (etilacetato).

Los dos tipos de nanodiamantes investigados (NDs y ND_{oi}), exhibieron un comportamiento similar en la extracción. Su área superficial específica similar (≈ 282 m²/gramo; información proporcionada por el fabricante), la misma estructura de carbono con hibridaciones sp² y sp³, y sus dimensiones aproximadas, podrían justificar estos resultados. La mayor pureza de NDs (>98%) frente a ND_{oi} (55-75%) o el carácter oleofílico de estos últimos, no marcaron diferencias en cuanto a eficiencias de extracción para estas NPs.

En términos generales, los nanotubos de carbono (CNTs) promovieron una mayor transferencia de soluto de la fase donadora a la aceptora que los nanodiamantes. La mayor área superficial de los SWCNTs (400-700 m²/gramo; información proporcionada por el fabricante) en comparación con los dos tipos de nanodiamantes (≈ 282 m²/gramo) podría explicar los mejores resultados de extracción obtenidos cuando la interfase fue preparada con SWCNTs. Esto se debe a que el área superficial es una variable especialmente influyente en un sistema de extracción basado en membranas, ya que determina el flujo de soluto de una fase a otra. Adicionalmente, las interacciones de tipo π - π dadas entre sistemas aromáticos de CNTs y atrazina fomentaron una mayor extracción.

Partiendo del hecho de que el sistema de anillos aromáticos de MWCNTs formado por varias capas de grafeno enrolladas refuerza y favorece considerablemente las interacciones con analitos que muestren estructura aromática, podemos explicar los resultados similares obtenidos para MWCNTs y SWCNTs estableciendo las siguientes conjeturas sin entrar en información detallada.

El área superficial específica de un CNT depende de su diámetro, pero en mayor medida, del número de láminas de grafeno que lo constituyen. Así, al aumentar el número de capas de grafeno, el peso del CNT incrementa mucho más que su superficie, y consecuentemente esto se traduce en una menor área superficial específica. Por lo tanto, cabe suponer que los SWCNTs tendrán un área superficial específica superior a los MWCNTs y por tanto, mayor potencial de interacción con el soluto.

Asimismo, el acusado mayor tamaño de MWCNTs frente a SWCNTs conlleva la formación de una interfase con poros de mayor tamaño que favorecen el flujo de analito de la fase acuosa a la orgánica. En contraposición, el mayor tamaño de MWCNTs frente a SWCNTs hace que para una cantidad constante de NPs en la interfase, el número de SWCNTs sea mayor al número de MWCNTs, con la consecuente relación área superficial/volumen incrementada. Otros factores como la diferente estabilidad de las NPs en el disolvente de la interfase y su tendencia a la agregación pueden condicionar un comportamiento diferente.

Finalmente, aún cuando el mayor número de láminas de grafeno parezca indicar inicialmente una mayor capacidad de adsorción para MWCNTs que para SWCNTs, la influencia de los otros factores antes comentados determinó un comportamiento de extracción similar para ambas NPs.

El procedimiento de extracción para la determinación de atrazina en muestras acuosas, consistió en la preparación previa de la interfase con 5 mg de MWCNTs y 1 mL de etilacetato. Esta interfase se añadió posteriormente a 20 mL de muestra acuosa. A continuación, 3 mL de etilacetato fueron añadidos, y la mezcla se agitó manualmente con la finalidad de favorecer el contacto entre las fases. Tras 15 minutos de reposo, se separó la fase orgánica, se centrifugó y se

tomaron 1.4 mL de la misma para su evaporación. La reconstitución con 100 μ L de medio de inyección (2:8 etanol:agua) fue previa al análisis por CE (222 nm).

La principal matriz ambiental empleada para la validación del método analítico fue agua de río aunque también se realizaron estudios preliminares en suelo agrícola dado que éstos constituyen las primeras vías de entrada de este contaminante en el medio ambiente. El procedimiento para matrices de suelo no fue reoptimizado sino simplemente evaluado a modo de prueba. En este caso, la interfase constituida por 2 mg de MWCNTs y 1 mL de etilacetato fue añadida a una suspensión acuosa de 200 mg de suelo. La Figura V.2.5 muestra a modo de ejemplo dos electroferogramas obtenidos tras el análisis en agua de río y suelo.

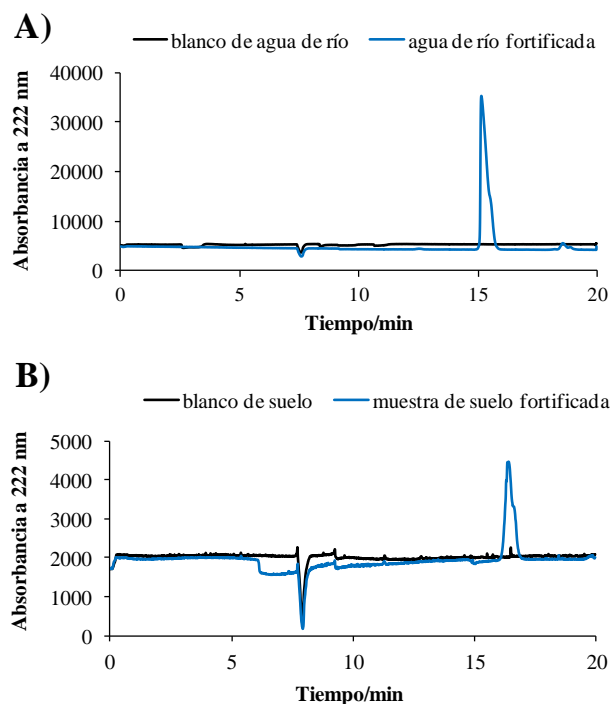


Figura V.2.5. Electroferogramas para (A) agua de río fortificada con 5 mg L⁻¹; y (B) suelo fortificado con 1 mg L⁻¹. Cada electroferograma de muestra fortificada va acompañado del blanco correspondiente (muestra sin fortificar).

Aquí se ha propuesto un método de extracción alternativo que explota la capacidad de adsorción de las CNPs mediante la formación de una interfase que refuerza el flujo de analito de la fase donadora a la aceptora en un esquema LLE convencional. El método tuvo una reproducibilidad aceptable ($\approx 11\%$) y valores de recuperación bastante buenos en muestras de agua de río ($>87.0\%$). Su versatilidad de aplicación a diferentes matrices ambientales le confiere un valor añadido si bien es cierto que serían necesarios más estudios con vistas a aplicaciones futuras en este sentido.

▪ *Nanopartículas como sólidos sorbentes en extracción en fase sólida (SPE)*

A diferencia de los trabajos de investigación anteriores, en este caso se consideró la técnica SPE como referente y se emplearon CNPs como únicas fases sorbentes para desarrollar un procedimiento analítico simple y de bajo coste. Con objeto de enfocar el procedimiento de extracción al análisis ambiental, el analito seleccionado fue el ácido salicílico (SA), un compuesto farmacéutico generado por la degradación del ácido acetilsalicílico. SA se considera un contaminante ambiental emergente dado su carácter ubicuo debido a la ineficacia en su eliminación de las plantas de tratamiento de aguas residuales. Además, gracias a la presencia de un anillo aromático en su estructura, cabría esperar una interacción favorecida con los CNTs.

El empleo de CNTs como materiales sorbentes fue evaluado en la modalidad de cartuchos empaquetados. La Tabla V.2.2 resume las diferentes variables experimentales optimizadas en este trabajo así como el valor óptimo seleccionado por favorecer una mayor extracción cuantitativa de SA.

Tabla V.2.2. Resumen de variables experimentales estudiadas empleando CNTs como sorbentes de SPE, así como valores finalmente seleccionados.

VARIABLES ESTUDIADAS	VALOR ÓPTIMO
Volumen de muestra (mL)	10
pH de muestra	2.0
Tipo de CNTs	MWCNTs-2 (nanocyl)
Cantidad de CNTs (mg)	15
Flujo de muestra (mL min ⁻¹)	0.19
Eluyente	acetona

Los resultados obtenidos del estudio del pH concluyeron que la interacción entre SA y CNTs estuvo gobernada mayoritariamente por interacciones π - π entre estructuras aromáticas, y no por fuerzas electrostáticas entre especies cargadas. Esto se debe a que cuando el analito estaba presente en su forma protonada o neutra (pH 2.0) la extracción cuantitativa fue mayor que cuando se encontraba parcial o completamente desprotonado (pH 3.7 y 9.9, respectivamente). Consecuentemente, la acidificación previa de las muestras fue necesaria para potenciar la interacción entre SA y NPs.

La Figura V.2.6 muestra los resultados del estudio comparativo entre tres tipos de CNTs como fases sorbentes; dos tipos de MWCNTs proporcionados por casas comerciales diferentes, y también SWCNTs.

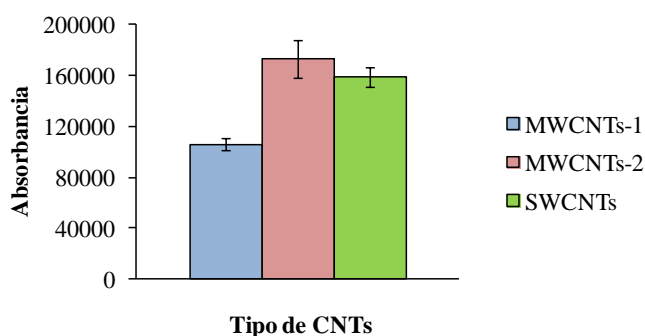


Figura V.2.6. Optimización del tipo de CNTs. MWCNTs-1 y MWCNTs-2 fueron obtenidos de Bayer y Nanocyl, respectivamente.

Tal y como se aprecia en la Figura V.2.6, MWCNTs proporcionados por distintas casas comerciales exhibieron comportamientos muy diferentes en la extracción de SA. Factores como la existencia de imperfecciones estructurales, o la presencia de impurezas o grupos funcionales superficiales derivados del proceso de síntesis, hacen que la superficie de los CNTs sea extremadamente compleja y variable lo que podría justificar su diferente comportamiento.

Por otro lado, los resultados confirmaron que no siempre el mayor número de láminas de grafeno presentes en la estructura de los CNTs contribuye positivamente a una mayor interacción con el analito, ya que en nuestro caso MWCNTs-2 si proporcionaron una extracción ligeramente mayor a SWCNTs, pero no MWCNTs-1. La existencia de numerosos factores influyentes así como la combinación de los mismos en diferente grado, explicarían la respuesta observada para los CNTs estudiados.

Las siguientes justificaciones podrían explicar los mejores resultados obtenidos con SWCNTs en comparación a MWCNTs-1. El mayor número de láminas de grafeno de MWCNTs-1, se traduce en una menor área superficial específica para estas NPs respecto a SWCNTs. Este hecho afecta negativamente a su capacidad de extracción, en tanto en cuanto la superficie de NPs disponible para adsorber el analito es inferior. Además, para una cantidad constante de NPs dentro del cartucho de SPE, el número de SWCNTs presentes será superior a MWCNTs como consecuencia de su menor tamaño; este mayor número de NPs incrementa la densidad de poros intersticiales por donde la muestra conteniendo el analito fluye y consecuentemente, la interacción entre el SA y CNTs se ve reforzada.

Solo ligeras diferencias en eficacia de extracción fueron encontradas entre SWCNTs y MWCNTs-2 debido posiblemente a que en este caso la contribución de un mayor número de láminas de grafeno para MWCNTs-2 compensó los

efectos negativos derivados de su menor área superficial específica y densidad de poros intersticiales respecto a SWCNTs.

La consecución de todos los estudios de optimización nos permitió definir finalmente el siguiente protocolo experimental. En un primer lugar, el cartucho fue preparado por empaquetar 15 mg de CNTs (MWCNTs-2). A continuación, 10 mL de muestra acuosa, previamente acidificada a pH 2, pasaron a través del cartucho a una tasa de flujo de 0.19 mL min^{-1} . El cartucho se secó pasando aire a través de él y finalmente, 1 mL de acetona fue empleado para llevar a cabo la elución previa al análisis por CE monitorizando la absorbancia a 200 nm.

Como ventaja del método SPE-CE desarrollado, habría que destacar la completa automatización de la etapa de carga de muestra en el cartucho, lo que simplificó considerablemente todo el proceso. La Figura V.2.7 ilustra a modo de ejemplo algunos electroferogramas obtenidos en la validación del método SPE-CE por su aplicación a muestras de agua de río.

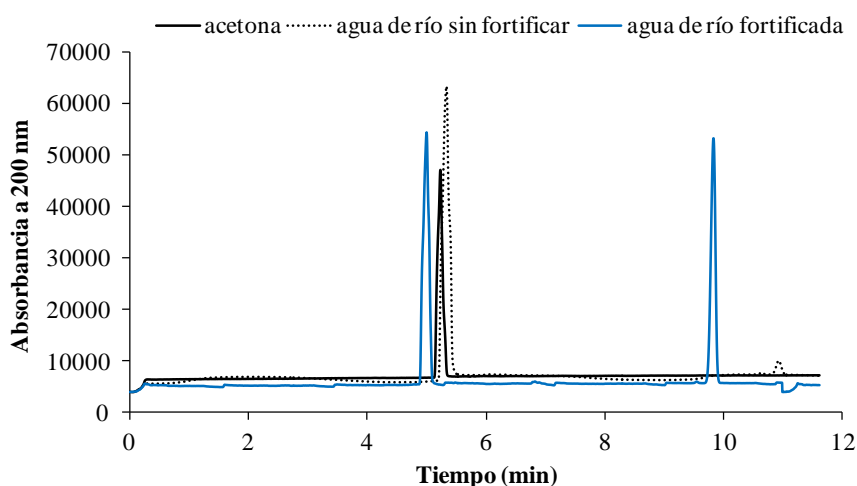


Figura V.2.7. Electroferogramas obtenidos de una muestra de agua de río fortificada con 6 mg L^{-1} y sin fortificar (blanco), ambas sometidas al procedimiento SPE-CE propuesto. El electroferograma del disolvente acetona también se presenta para identificar la señal encontrada en torno a los 5 minutos de análisis.

BLOQUE V

La línea base de los electroferogramas fue muy estable y el tiempo de análisis inferior a 12 minutos. El método SPE-CE fue bastante reproducible (<8.2%) y permitió extraer SA de muestras fortificadas con una cantidad mínima de material sorbente (15 mg de CNTs). Los valores de recuperación estuvieron en el rango 76-102%. La sencillez, el bajo coste y la rapidez del análisis por CE hacen que este método analítico pueda ser aplicado a laboratorios de análisis de rutina.

Valoración general de las nanopartículas en el tratamiento de muestra

A lo largo de la investigación comentada en los apartados anteriores, se evaluó el potencial de diferentes CNPs en tres técnicas de extracción distintas (CPE, LLE y SPE). Las NPs elegidas fueron nanodiamantes de elevada pureza (NDs), nanodiamantes con carácter oleofílico (ND_{ol}), nanotubos de carbono multicapa (MWCNTs), nanotubos de carbono monocapa (SWCNTs), nanotubos de carbono oxidados (MWCNT_{s_{ox}}) y NPs híbridas (NDs-MWCNTs). Las especificaciones proporcionadas por el fabricante se muestran en la Tabla V.2.3. Las NPs sintetizadas experimentalmente (es decir, MWCNT_{s_{ox}} y NDs-MWCNTs) no han sido incluidas en la misma.

Tabla V.2.3. Características de las CNPs adquiridas comercialmente para su uso en los métodos de extracción propuestos.

CNPs	Diámetro (nm)	Pureza (%)	Longitud (µm)	Área superficial (m ² /g)	Casa comercial
NDs	3.2	>98	-	≈282.8	NaBond
ND _{ol}	4-15	>55-75	-	≈287.9	NaBond
MWCNTs-1	5-20	>95	1-10	-	Bayer
MWCNTs-2	9.5	≈90	1.5	-	Nanocyl
MWCNTs-3	110-170	>90	5-9	-	MER
SWCNTs	<2	>90	5-15	400-700	Shenzhen Nanotech Port (NTP)

Las conclusiones más importantes que podemos resaltar en cuanto al potencial de todas las NPs estudiadas en los métodos de extracción son:

➤ SWCNTs mostraron por lo general un comportamiento de extracción muy similar a MWCNTs. Solo para el caso de MWCNTs-1 (Bayer), los SWCNTs proporcionaron eficiencias de extracción significativamente mayores.

➤ Los NDs mostraron una excelente respuesta en la técnica CPE, si bien no lo hicieron en el procedimiento de LLE. Diferentes mecanismos implicados en la extracción del analito en cada caso marcaron diferencias en el comportamiento de estas NPs. Además, la capacidad de extracción de un soluto no solo depende de las propiedades de los adsorbentes, sino también de las características de ese soluto y el tipo de interacciones que establece con la fase extractante. Teniendo en cuenta que la superficie de los NDs obtenidos mediante procesos de detonación es extremadamente compleja, pudiendo presentar de 10-15 grupos funcionales, cabe la posibilidad de que prevalezcan un tipo de interacciones sobre otras en función del analito a extraer. Asimismo, la influencia de otros factores, como la estabilidad de las NPs en el medio de extracción (acuoso micelar para CPE, y orgánico para LLE), el número de partículas presentes para una cantidad fija de NPs, o aspectos relacionados con el área superficial disponible para la interacción con el analito, pudieron condicionar el comportamiento variable de estas NPs según el esquema de extracción considerado.

➤ El carácter más oleofílico de algunos nanodiamantes (ND₀₁) así como la oxidación de los MWCNTs no afectaron de forma significativa a la eficiencia de extracción del analito en comparación con las mismas NPs sin modificar.

➤ Las NPs híbridas resultado de la combinación de NDs y MWCNTs no reforzaron la extracción del analito frente a MWCNTs y NDs por separado.

BLOQUE V

➤ En ausencia de NPs solo el procedimiento de LLE podría llevarse a cabo aunque obteniendo peores extracciones cuantitativas de analito. En los otros dos métodos de extracción propuestos (CPE y SPE), las NPs resultan indispensables para conducir la extracción.

Valoración general de los métodos de extracción

La Tabla V.2.4 hace una comparativa entre los métodos de extracción haciendo referencia a aspectos tales como la cantidad de muestra requerida (mL para muestras acuosas o mg para muestras de suelo), cantidad y tipo de NPs utilizadas, presencia de una fase extractante adicional, tiempo total del procedimiento de extracción y consumo de disolvente orgánico.

Tabla V.2.4. Comparativa entre parámetros experimentales de los tres métodos de extracción propuestos.

Método	Cantidad muestra	Cantidad y tipo de CNPs	Fase adicional	Tiempo extracción (min)	Consumo disolvente (mL)
CPE	6 mL	36 mg de NDs	sí	≈120	4 + 1.5
LLE	20 mL (agua)	5 mg de MWCNTs-3 (agua)	sí	>30 (agua)	4 (agua)
	200 mg (suelo)	2 mg de MWCNTs-3 (suelo)		≈100 (suelo)	2 (suelo)
SPE	10 mL	15 mg de MWCNTs-2	no	≈60	1

Mientras que el método de CPE precisó menor cantidad de muestra, su duración así como el consumo de disolvente orgánico fueron superiores que para los otros métodos. La mayor proporción de disolvente orgánico se empleó en la purificación de los NDs previa a las extracciones.

El método de LLE conllevó el mayor requerimiento de muestra. En contraposición, el tiempo de extracción para muestras acuosas y también la cantidad de NPs empleadas fueron mínimas con respecto a los demás métodos.

El método de SPE supuso el menor consumo de disolvente orgánico y solo en este caso, no hubo presente ninguna fase extractante adicional en el sistema.

Cabe decir que los métodos de extracción desarrollados mostraron diferencias en términos de reproducibilidad, límites de detección y valores de recuperación en muestras reales. El método más sensible y reproducible fue el método de CPE, aunque sus valores de recuperación fueron los más reducidos. Los métodos de LLE y SPE mostraron límites de detección similares entre sí, aunque la reproducibilidad y porcentajes de recuperación fueron superiores para el método de SPE.

Por último, la Tabla V.2.5 resume las fortalezas y debilidades asociadas a cada método de extracción.

Tabla V.2.5. Fortalezas y debilidades de los métodos de extracción propuestos.

Método	Fortalezas	Debilidades
CPE con nanodiamantes	<ul style="list-style-type: none"> - Bajos límites de detección. - Buena reproducibilidad. - Empleo de surfactante como fase extractante de menor toxicidad que los disolventes orgánicos. - El empleo de nanodiamantes no supone un coste superior al de otras nanopartículas. 	<ul style="list-style-type: none"> - Baja recuperación en muestras reales. - La elución y manejo de la fase enriquecida requiere cierta habilidad. - Complejidad del procedimiento por el número de etapas que lo componen. - La purificación de nanodiamantes ralentiza el procedimiento e incrementa el consumo de disolvente.
LLE con interfase de nanotubos de carbono multicapa	<ul style="list-style-type: none"> - Buenos valores de recuperación. - Tiempo de extracción reducido en matrices acuosas. - Electroferogramas con líneas de base muy estables y corta duración. - Versatilidad del método para su futura aplicación a matrices de suelo. 	<ul style="list-style-type: none"> - Bajos factores de preconcentración. - Mayor consumo de disolvente orgánico lo que se traduce en un mayor coste y toxicidad. - La recuperación de la fase orgánica requiere cierta habilidad. - Problemas de interferencias en matrices de suelo hacen necesarios nuevos estudios en este sentido.
SPE con nanotubos de carbono multicapa	<ul style="list-style-type: none"> - Procedimiento simple y de bajo coste. - Buenos valores de recuperación. - Automatización de la etapa de carga de muestra en el cartucho. - Bajo consumo de disolvente orgánico. - Electroferogramas con líneas de base muy estables y corta duración. - No se requiere evaporación. 	<ul style="list-style-type: none"> - El empaquetamiento manual de las nanopartículas en el cartucho puede ser fuente de irreproducibilidad. - No se estudió la reusabilidad del cartucho. - La baja relación entre volumen de muestra y volumen de eluyente hace que el factor de preconcentración, aunque maximizado, no sea muy elevado.

Nanopartículas en la etapa de detección

El empleo de la Espectroscopía Raman Amplificada por Superficie (SERS) como técnica de detección ha experimentado un incremento considerable desde la década de los ochenta, acentuándose en mayor medida a partir del año 2004. La Figura V.2.8 representa la evolución en el número de publicaciones científicas dedicadas a esta técnica de detección desde 1980 hasta la actualidad.

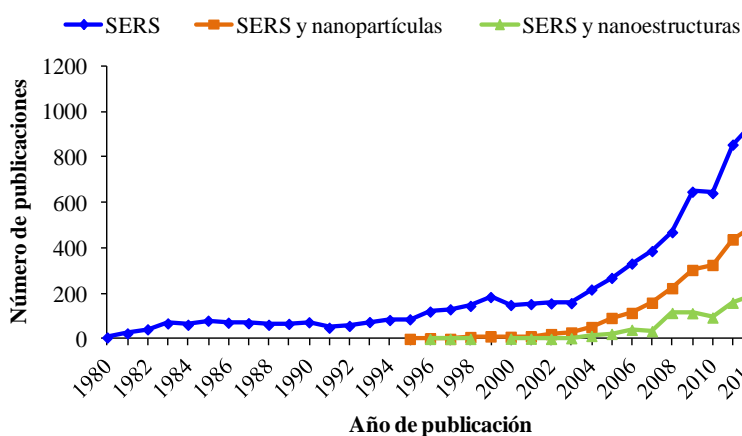


Figura V.2.8. Número de artículos científicos que contienen alguna de las siguientes palabras clave: “SERS”, “SERS y nanopartículas”, o “SERS y nanoestructuras” (Fuente bibliográfica: SCOPUS).

El efecto SERS se basa en el aumento de la difusión inelástica (señal Raman) de determinadas moléculas por un factor de 10^4 - 10^6 gracias a la presencia de nanoestructuras metálicas rugosas. Este incremento es consecuencia de la combinación de dos mecanismos principales; *i) mecanismo electromagnético*, se relaciona con la presencia de rugosidades en la superficie metálica y depende principalmente de la distancia existente entre el metal y el analito. Se trata por tanto de un mecanismo no selectivo al tipo de molécula analizada; *ii) mecanismo químico*, provocado por procesos de transferencia de carga que se activan como consecuencia de la quimiadsorción de las moléculas

de analito sobre la superficie metálica. A diferencia del anterior, este mecanismo si es selectivo al tipo de molécula analizada. Aunque parece ser que la combinación de ambos mecanismos resulta en la generación del efecto SERS, el mecanismo electromagnético contribuye en mayor grado al incremento de la señal.

Las NPs metálicas exhiben una habilidad excepcional para su empleo como soportes o plataformas SERS. Su elevada área superficial y compleja química superficial justifican en parte su empleo en esta técnica de detección. Las NPs de plata (AgNPs) son más eficientes en SERS que las NPs de oro, proporcionando factores de incremento de señal del orden de 10-100 veces superiores, sin embargo, muestran algunas desventajas como su mayor tendencia a la oxidación.

La aplicabilidad analítica del método planteado al control ambiental, estuvo enfocada a la determinación de almizcle de cetona (MK) en agua de río. Se trata de un compuesto sintético de estructura nitroaromática que se emplea en numerosos productos de cuidado personal como sustituto de las fragancias naturales que son extremadamente caras y difíciles de obtener. Dado su uso extendido y ubicuidad, ha sido catalogado recientemente como contaminante emergente. Su naturaleza hidrofóbica y baja tasa de degradación hacen que se encuentre en diversos compartimentos ambientales y de ahí el interés en su monitorización en este tipo de matrices.

El procedimiento analítico constó de dos etapas. Una primera etapa de tratamiento de muestra en la modalidad de microextracción con adsorbentes empaquetados (MEPS). En esta etapa, 500 μL de muestra acuosa se hicieron pasar a través de un cartucho MEPS con sorbente C18 previamente acondicionado. A continuación, la elución se realizó con tan solo 10 μL de metanol, y el extracto fue depositado y evaporado sobre un cristal de fluoruro

de calcio (CaF_2). La segunda etapa de detección fue realizada directamente sobre el extracto de elución (señal Raman) o bien añadiendo encima 6 μL de AgNPs (señal SERS). Las AgNPs fueron sintetizadas mediante la reducción del nitrato de plata por clorhidrato de hidroxilamina a T^a ambiente. La síntesis resultó ser muy simple y duró poco más de 10 minutos.

Los estudios de optimización de la etapa de detección se centraron en investigar el orden de deposición de MK y AgNPs sobre el soporte de CaF_2 así como el volumen de AgNPs, más adecuados para maximizar el efecto SERS. Los resultados mostraron que al añadir las AgNPs en último lugar, el efecto de incremento de señal generado fue más significativo lo que se puede correlacionar con el hecho de que en este caso las AgNPs no fueron arrastradas al añadir el extracto de MK encima. Se favoreció por tanto una interacción mejorada entre MK y la superficie del metal. En cuanto al volumen de AgNPs, 6 μL fue seleccionado como volumen óptimo. Alícuotas de mayor volumen formaron gotas demasiado grandes que hicieron que las AgNPs se extendiesen por un área mayor del soporte y se acumulasen preferentemente en los bordes de la gota. Este hecho dificultó la interacción entre AgNPs y MK, y también tuvo efectos negativos sobre la reproducibilidad del método.

VARIABLES EXPERIMENTALES COMO EL VOLUMEN DE MUESTRA ACUOSA, EL TIPO DE ELUYENTE, Y EL VOLUMEN DE DISOLVENTE DE LAVADO ENTRE EXTRACCIONES, FUERON CONSIDERADAS EN LOS ESTUDIOS DE OPTIMIZACIÓN DE LA ETAPA DE TRATAMIENTO DE MUESTRA CON MEPS.

La Figura V.2.9 muestra a modo de ejemplo un espectro Raman obtenido a partir de una disolución de MK en metanol (1000 mg L^{-1}) depositada y evaporada sobre el soporte de CaF_2 . El espectro SERS fue medido después de añadir 6 μL de AgNPs sobre una disolución de MK preparada en metanol a 0.1 mg L^{-1} .

BLOQUE V

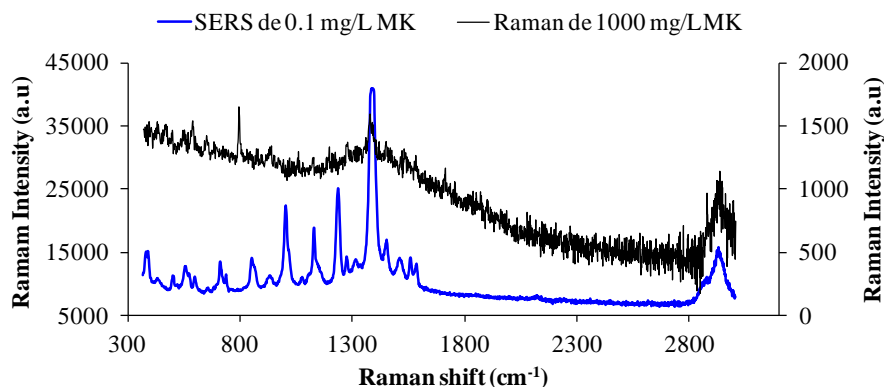


Figura V.2.9. Espectros Raman y SERS obtenidos de 1000 mg L⁻¹ y 0.1 mg L⁻¹ de MK, respectivamente.

Varios picos Raman definen el espectro característico de MK. El más prominente lo encontramos a 1390 cm⁻¹ que corresponde a la vibración de estiramiento del grupo NO₂. El pico a 713 cm⁻¹ podría asignarse a la flexión simétrica en el plano (“*tijera*”) del grupo nitro. Y las bandas a 1004 cm⁻¹ y 1276 cm⁻¹ podrían ser asociadas a la vibración del anillo aromático y de la cadena alifática, respectivamente. El factor de incremento de señal por efecto SERS fue del orden de 9.3×10^5 tomando como referencia el pico a 1390 cm⁻¹.

El método MEPS-SERS optimizado tuvo un límite de detección de 20 µg L⁻¹ y unos valores de recuperación en agua de río en el rango 47-63%. La Figura V.2.10 presenta a modo de ejemplo un espectro SERS obtenido tras aplicar el método MEPS-SERS a muestras de agua de río previamente fortificadas.

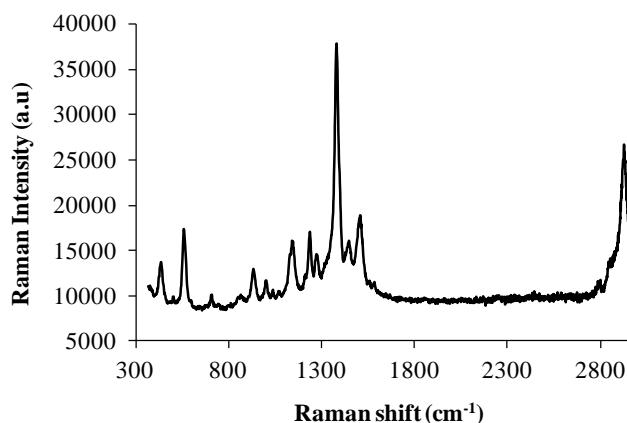


Figura V.2.10. Espectro SERS obtenido tras llevar a cabo el procedimiento MEPS-SERS con una muestra de agua de río fortificada con 0.2 mg L^{-1} de MK.

A continuación, se exponen las principales fortalezas y debilidades encontradas tras analizar el procedimiento MEPS-SERS propuesto:

▪ *Fortalezas*

- ✓ El procedimiento es simple y económico.
- ✓ El tiempo total es reducido.
- ✓ La síntesis de AgNPs es sencilla y requiere poco tiempo.
- ✓ La cantidad de muestra acuosa necesaria es mínima ($500 \mu\text{L}$).
- ✓ El consumo total de disolvente orgánico es muy reducido (1 mL).
- ✓ El factor de incremento de señal Raman fue del orden de 10^5 .
- ✓ La portabilidad del espectrómetro Raman así como del sistema MEPS abre la posibilidad a la realización de estudios *in situ*.

▪ *Debilidades*

- ✗ Las AgNPs tienden a oxidarse con facilidad y por ello hay que sintetizarlas con frecuencia.

- ✘ La irreproducibilidad asociada a la deposición del sustrato activo en SERS es un factor limitante.
- ✘ Los valores de recuperación en agua de río no fueron excepcionalmente buenos.

NANOPARTÍCULAS COMO OBJETOS DE EVALUACIÓN TOXICOLÓGICA

Las mismas propiedades que hacen que las NPs sean muy explotadas en el ámbito analítico, convierten a su vez su evaluación toxicológica en una temática de estudio obligatoria.

La *Nanotoxicidad* engloba el estudio de los posibles impactos tóxicos de las NPs sobre los sistemas biológicos y ecológicos. El protocolo de evaluación consiste primero en la realización de ensayos *in vitro* con líneas celulares aisladas de organismos vivos. A continuación, y una vez definidos los efectos a nivel celular, se lleva a cabo una evaluación toxicológica más específica sobre organismos vivos (principalmente vertebrados) a través de la realización de ensayos *in vivo*.

Los estudios toxicológicos que se desempeñaron durante la Tesis Doctoral permitieron indagar en los efectos citotóxicos causados por diferentes tipos de NPs sobre fibroblastos de embriones de ratón (líneas celulares NIH/3T3 y 3T3-L1). Los estudios de toxicidad *in vitro* fueron planteados de acuerdo a dos objetivos de partida. Por un lado, evaluar la influencia de las propiedades fisicoquímicas de las NPs, en concreto su química superficial, sobre su toxicidad asociada. Para ello se estudió en qué grado la diferente funcionalización superficial de unas mismas AgNPs podría afectar a su capacidad de internalización celular, estabilidad coloidal, tasa de oxidación, y en último término, a su citotoxicidad. Por otro lado, se pretendía investigar la influencia del entorno sobre la toxicidad de las NPs. En este sentido, se evaluó el

riesgo toxicológico asociado a la presencia simultánea de nanotubos de carbono con un contaminante ambiental (4-nonilfenol) teniendo en cuenta las posibles interacciones dadas entre ambas especies.

Influencia de la química superficial de las nanopartículas de plata sobre su toxicidad

Para conducir este trabajo de investigación, se sintetizaron en primer lugar AgNPs hidrofóbicas recubiertas de dodeciltiol. A partir de éstas, se sintetizaron posteriormente cuatro tipos de AgNPs hidrofílicas por aplicar diferente funcionalización superficial a los núcleos de plata originales. Las AgNPs hidrofílicas obtenidas fueron las siguientes:

- AgNPs recubiertas de ácido mercaptoundecanoico (AgNPs-MUA).
- AgNPs recubiertas de polímero anhídrido maleico de poliisobutileno modificado con dodecilamina (AgNPs-PMA).
- AgNPs-PMA fueron a su vez recubiertas con polietilenglicol de 10 KDa (PEG) en superficie. Cuando solo se unió una molécula de PEG en superficie se consiguieron AgNPs-PMA-1PEG. Sin embargo, cuando la superficie se saturó con PEG se obtuvieron AgNPs-PMA-satPEG.

Las AgNPs fueron sintetizadas en etapas consecutivas de menor a mayor grado de funcionalización superficial. Posteriormente, fueron sometidas a una caracterización exhaustiva que consistió en determinar su diámetro hidrodinámico (d_h), potencial zeta, y estabilidad en disoluciones con concentraciones variables de NaCl.

BLOQUE V

Los estudios de caracterización revelaron que el recubrimiento con PEG incrementó efectivamente el d_h de las AgNPs. Los valores del potencial zeta nos permitieron clarificar que la estabilidad coloidal estuvo gobernada por repulsiones electrostáticas para AgNPs-MUA y AgNPs-PMA (debido a su carga superficial negativa), y por repulsiones estéricas para AgNPs-PMA-satPEG.

La Figura V.2.11 muestra los resultados de los estudios de estabilidad en disoluciones con concentraciones crecientes de NaCl.

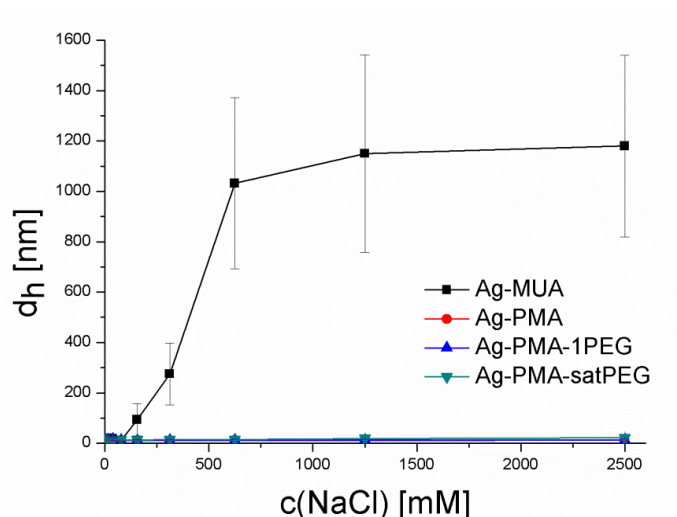


Figura V.2.11. Estudio de estabilidad coloidal. Cambios en el diámetro hidrodinámico (d_h) de los cuatro tipos de AgNPs sometidas a concentraciones variables de NaCl.

Tal y como se puede deducir del incremento de d_h a concentraciones crecientes de NaCl, AgNPs-MUA se aglomeraron completamente, mientras que el resto de AgNPs mantuvieron un d_h más o menos constante. La menor estabilidad (por repulsiones electrostáticas) de AgNPs-MUA respecto a AgNPs-PMA se explica por su menor potencial zeta negativo (-24.9 ± 1.7 vs -31.0 ± 1.3). En cuanto a las AgNPs con PEG, su estabilidad definida por repulsiones estéricas compensó los efectos negativos derivados de la adición de NaCl.

La oxidación de las AgNPs con la consecuente liberación de iones Ag^+ al medio se considera una de las principales causas de su toxicidad. Teniendo en cuenta que la tasa de oxidación de las AgNPs puede variar según el tiempo de incubación y el pH del medio, se llevaron a cabo estudios incubando los cuatro tipos de AgNPs a diferentes tiempos y condiciones de pH. Los resultados obtenidos por ultracentrifugación de las disoluciones y análisis por ICP-MS se presentan en la Tabla V.2.6.

Tabla V.2.6. Cantidad de Ag^+ liberada, expresada como porcentaje respecto a la concentración total de plata presente según el tiempo de incubación y el pH.

Nanopartículas	Incubación a pH 7.0		
	Día 0	Día 7	Día 14
AgNPs-MUA	<0.0015	<0.0015	<0.0015
AgNPs-PMA	<0.0015	<0.0015	0.146±0.001
AgNPs-PMA-satPEG	<0.0015	<0.0015	<0.0015
Nanopartículas	Incubación a pH 3.0		
	Día 0	Día 7	Día 14
AgNPs-MUA	0.781±0.002	1.316±0.002	-
AgNPs-PMA	1.120±0.004	1.390±0.003	-
AgNPs-PMA-satPEG	0.701±0.001	0.735±0.001	-

Los resultados evidenciaron que incluso en el peor de los casos (pH 3.0 y 7 días de incubación) la tasa de oxidación estuvo en torno al 1%, lo que confirma que las AgNPs no se disolvieron completamente como podría esperarse. Además, la oxidación se acentuó a pH ácido lo que supone que dentro de los compartimentos intracelulares de tipo endosomas o lisosomas (con $\text{pH} \approx 4-5$) la oxidación de las AgNPs se verá favorecida.

El diferente recubrimiento superficial de las AgNPs no afectó a la liberación de iones Ag^+ ya que no se encontraron diferencias notables en la oxidación sufrida por los cuatro tipos de AgNPs. Esto podría justificarse por el hecho de que el recubrimiento inicial más cercano al núcleo fueron cadenas hidrocarbonadas de longitud parecida para todas las AgNPs investigadas. El

BLOQUE V

recubrimiento adicional con PEG no ejerció por tanto ningún efecto sobre la oxidación de las AgNPs.

Para conducir los estudios de internalización celular y ensayos de citotoxicidad se emplearon células NIH/3T3. Para los primeros, las células fueron expuestas durante 15 horas a AgNPs-PMA y AgNPs-PMA-satPEG modificadas con el fluoróforo DY-636. Se ha descrito que la presencia de moléculas PEG en la superficie de las NPs reduce su habilidad de penetración celular con respecto a las mismas NPs sin recubrir. Por lo tanto, si exponemos las células a las mismas cantidades de plata en forma de AgNPs-PMA y de AgNPs-PMA-satPEG, estaremos considerando la misma cantidad de plata pero con diferente grado de internalización celular. Las imágenes de microscopía confocal obtenidas se muestran en la Figura V.2.12. Éstas confirmaron que la saturación de la superficie con PEG redujo enormemente la internalización celular de las AgNPs.

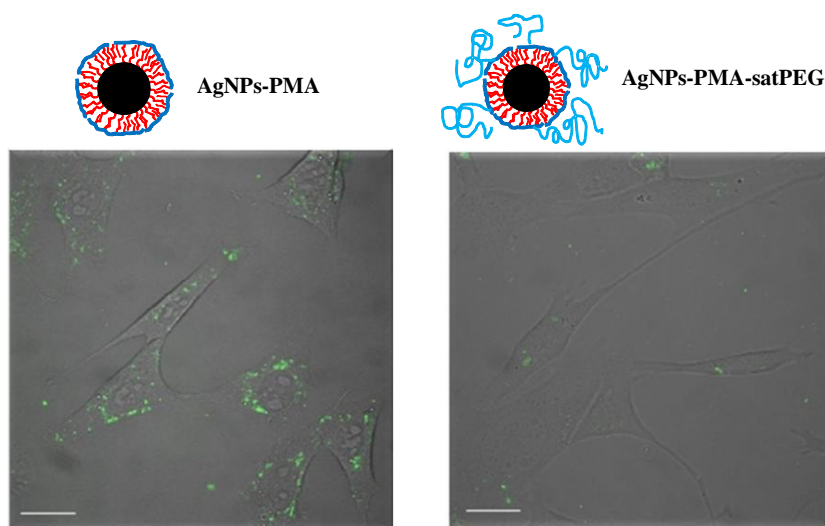


Figura V.2.12. Imágenes de fluorescencia de células que han sido expuestas durante 15 horas a AgNPs-PMA y AgNPs-PMA-satPEG marcadas superficialmente con DY-636. Las imágenes son el resultado de la superposición del canal de transmisión y el de fluorescencia. La barra de escala equivale a 20 μm .

El ensayo Azul Alamar o de la resazurina fue tomado como protocolo experimental para evaluar la citotoxicidad asociada a las diferentes AgNPs investigadas. Esta ensayo mide el potencial que presentan las células vivas para reducir un colorante no fluorescente (resazurina) a un producto fluorescente (resorufina) mediante la acción de sus enzimas mitocondriales. Las células fueron incubadas durante 24 horas con las diferentes AgNPs. El incremento de fluorescencia observado (λ_{exc} 560nm; rango emisión 572-650nm) fue directamente proporcional a la viabilidad celular de las muestras. La Figura V.2.13 muestra las curvas dosis-respuesta obtenidas para los cuatro tipos de AgNPs. El valor de dosis letal media (LD_{50}) se considera el punto de inflexión de la curva y equivale a la concentración que causa una mortalidad celular del 50%.

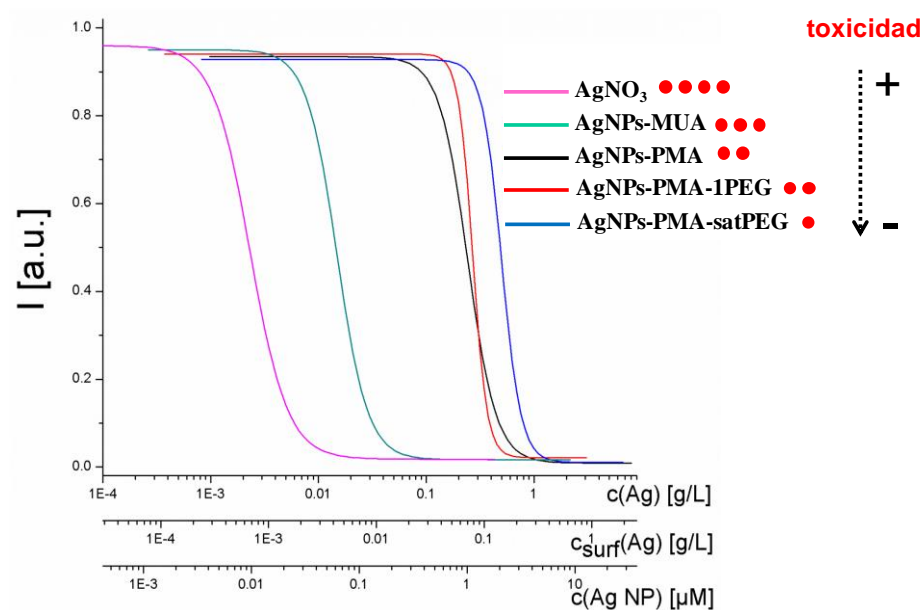


Figura V.2.13. Curvas dosis-respuesta obtenidas a partir del ensayo de la resazurina con células NIH/3T3 expuestas durante 24 horas a diferentes AgNPs. $AgNO_3$ fue el control positivo del ensayo.

BLOQUE V

La cantidad de plata es expresada de tres formas distintas: *i*) cantidad de plata total [$c(\text{Ag})$]; *ii*) molaridad de AgNPs presentes [$c(\text{AgNP})$]; y *iii*) cantidad de plata en la superficie de las AgNPs [$c_{\text{surf}}(\text{Ag})$]. Esta triple escala nos permite comparar la citotoxicidad de una misma cantidad de plata en forma de iones (AgNO_3), o en forma de NPs (AgNPs). Las principales conclusiones derivadas de los ensayos de citotoxicidad, así como del resto de estudios desarrollados se esquematizan en la Figura V.2.14.

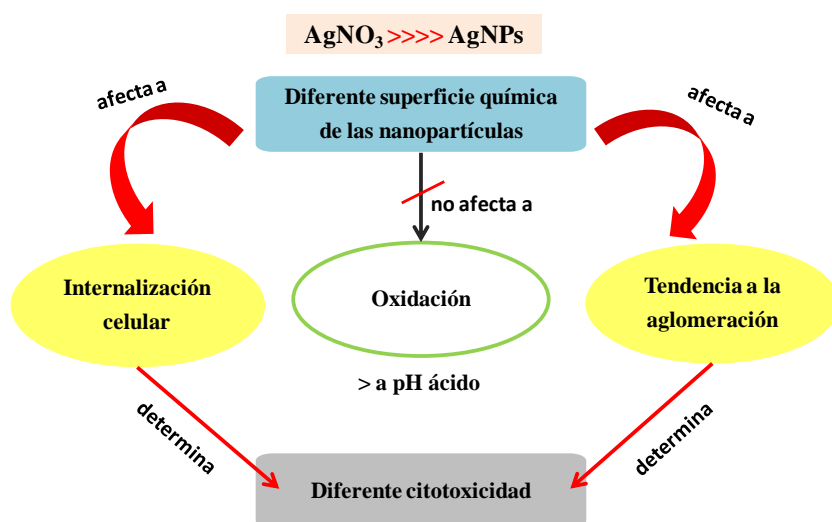


Figura V.2.14. Conclusiones más significativas derivadas del trabajo sobre toxicidad de AgNPs con diferente química superficial.

Como se puede inferir de la Figura V.2.14:

- Todas las AgNPs mostraron una toxicidad inferior a AgNO_3 al normalizar a cantidad de plata presente [eje $c(\text{Ag})$].
- Los diferentes recubrimientos (MUA y PMA, con o sin PEG) no marcaron diferencias notables en la oxidación del núcleo de plata. La oxidación de las AgNPs solo estuvo influenciada por el pH del entorno,

de forma que a pH ácido la oxidación fue superior a aquella observada a pH neutro. Esto confirma que dentro de los compartimentos intracelulares como endosomas/lisosomas se espera que la oxidación sea más acentuada que en el medio extracelular.

- A pesar de presentar igual grado de oxidación, AgNPs-MUA resultaron ser bastante más tóxicas que AgNPs-PMA lo que se explica por su peor estabilidad en medios salinos.
- La saturación de la superficie de AgNPs-PMA con moléculas de PEG redujo su internalización celular y esto se tradujo en una menor toxicidad (valores de LD₅₀ superiores). Con lo cual podemos concluir que para cantidades equivalentes de Ag, la Ag intracelular (AgNPs-PMA) es más tóxica que aquella presente en el medio extracelular (AgNPs-PMA-satPEG).
- La inclusión de una única molécula de PEG sobre la superficie no ocasionó cambios en la toxicidad de AgNPs-PMA.

Influencia de la presencia de otra especie química sobre la toxicidad de los nanotubos de carbono

La influencia del entorno es un aspecto clave en la evaluación de los efectos toxicológicos de las NPs. Diferente contenido salino o la presencia de proteínas pueden alterar la estabilidad de las NPs en disolución. Asimismo fluctuaciones en el pH del entorno influyen en el grado de oxidación de algunas NPs, como ya vimos para las AgNPs. Todos estos factores pueden modular finalmente la toxicidad derivada de las NPs.

Sin embargo, hay un aspecto que no se tiene en cuenta en la mayoría de estudios de toxicidad actuales, y es el efecto de la coexistencia de las NPs con otras especies. La elevada área superficial específica y reactividad química de las NPs, hacen que su interacción con otras especies sea más que probable cuando entren en contacto. A pesar de este hecho, los riesgos toxicológicos derivados de esta interacción han sido muy poco investigados. En algunos trabajos ya publicados, efectos tóxicos aditivos, sinérgicos o antagónicos fueron observados tras la exposición de las células a mezclas de NPs con otros compuestos. Esto sugiere que la toxicidad resultante de una mezcla puede ser impredecible aún conociendo la toxicidad de las especies individuales que la componen.

El trabajo de investigación desarrollado evalúa por primera vez, los riesgos toxicológicos asociados a la presencia simultánea de nanotubos de carbono monocapa recubiertos con PEG (SWCNTs-PEG) y un conocido contaminante ambiental. SWCNTs-PEG fueron seleccionados por su mayor biocompatibilidad y solubilidad en medios acuosos en comparación a esas mismas NPs sin recubrimiento. 4-nonilfenol (NP) fue elegido por su relevancia ambiental ya que es un contaminante ubicuo que actúa como disruptor endocrino. Además, la estructura del NP con un anillo aromático y una larga cadena hidrocarbonada favorecería su interacción con los SWCNTs-PEG.

Los estudios toxicológicos *in vitro* fueron conducidos con células 3T3-L1. La actividad metabólica de células expuestas durante 24/48 h a tratamientos con SWCNTs-PEG y NP, solos o en combinación, fue evaluada mediante el ensayo de citotoxicidad del MTT. En este caso la viabilidad celular presente en las muestras es proporcional a la absorbancia de un producto fluorescente (formazán) que es generado como consecuencia de la actividad metabólica de células vivas.

La Figura V.2.15 muestra los porcentajes de viabilidad celular obtenidos de células expuestas durante 24 h a tratamientos individuales con (A) SWCNTs-PEG y (B) NP, en medios de incubación sin suero.

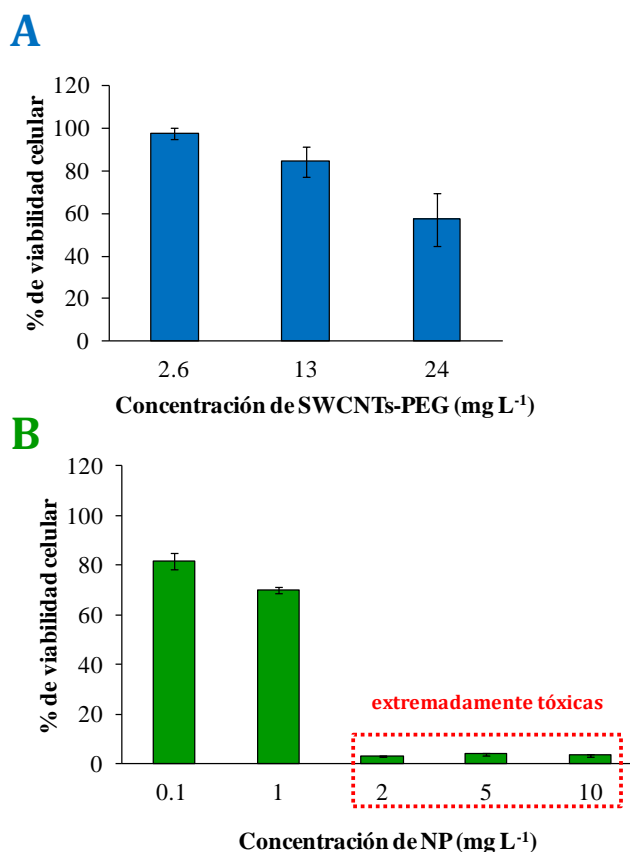


Figura V.2.15. Viabilidad celular (respecto al control) de células expuestas durante 24 horas a (A) SWCNTs-PEG y (B) NP, en estudios separados.

Como se observa en los resultados derivados de los estudios con SWCNTs-PEG (Figura V.2.15 A), solo el tratamiento con 24 mg L⁻¹ tuvo efectos negativos considerables sobre la viabilidad celular. En cuanto a los tratamientos con NP (Figura V.2.15 B), dosis de 2, 5 y 10 mg L⁻¹ de NP provocaron una mortalidad celular extremadamente elevada.

BLOQUE V

La presencia de suero en el medio de cultivo quiso ser investigada por su efecto sobre la estabilidad de los SWCNTs-PEG, ya que se ha descrito que las proteínas del suero rodean las NPs y les confieren una mayor estabilización en ambientes biológicos a través de repulsiones estéricas. La Figura V.2.16 muestra los porcentajes de viabilidad celular obtenidos de células expuestas durante 24 horas a tratamientos individuales con SWCNTs-PEG (2.6 y 13 mg L⁻¹) y NP (2, 5 y 10 mg L⁻¹) en medios de cultivo sin suero y en otros conteniendo un 10% de suero fetal bovino (FBS).

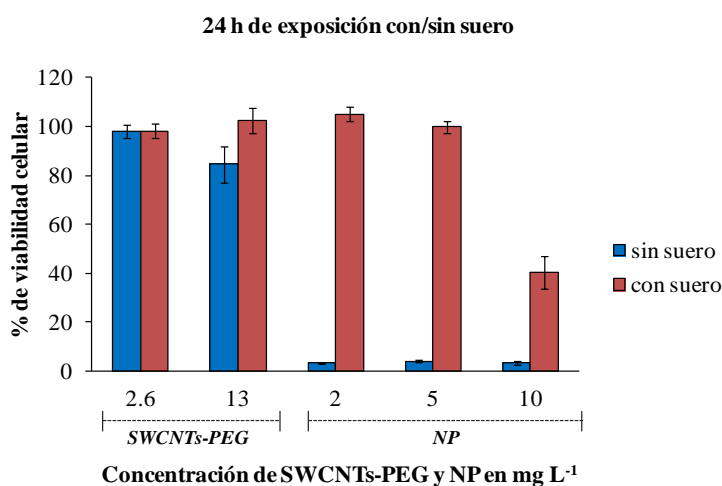


Figura V.2.16. Efecto de la presencia de suero sobre la toxicidad de SWCNTs-PEG y NP para exposiciones de 24 horas.

El suero aumentó la tolerancia de las células hacia todos los tratamientos individuales, ejerciendo un efecto “*protector*” sobre las mismas. Este efecto fue mucho más notable para los tratamientos con NP, aunque también se observó en menor grado para los tratamientos con SWCNTs-PEG. El suero mejoró la estabilidad de los SWCNTs-PEG en el medio de cultivo, ya que permitió la preparación de dispersiones visiblemente más estables. Esta mayor estabilidad se tradujo en una menor toxicidad (ver tratamientos con 13 mg L⁻¹ de SWCNTs-PEG).

Una vez concluidos los ensayos con NP y SWCNTs-PEG por separado, las células fueron expuestas durante 24 horas a mezclas de estas dos especies en medios con o sin suero. La elevada toxicidad asociada a NP en medios sin suero impidió investigar posibles efectos tóxicos combinados en las mezclas con SWCNTs-PEG.

Por lo general, los ensayos en los que las células fueron expuestas a NP y SWCNTs-PEG simultáneamente, no revelaron evidencias claras de toxicidad combinada (adición, sinergia, o antagonismo) entre SWCNTs-PEG y NP, sino que la toxicidad resultante de la exposición a las mezclas quedó definida por aquella asociada a la especie más tóxica presente. No obstante, se registraron algunos casos puntuales en los que la combinación de SWCNTs-PEG y NP redujo la viabilidad celular aún cuando a esas mismas concentraciones y por separado, ni SWCNTs-PEG ni NP tuvieron efectos citotóxicos sobre las células. La Figura V.2.17 representa los porcentajes de viabilidad celular para aquellos casos (A y B) que sugieren mecanismos de toxicidad sinérgica entre SWCNTs-PEG y NP. Se presentan los porcentajes de viabilidad celular obtenidos para los tratamientos con SWCNTs-PEG y NP por separado, y en combinación.

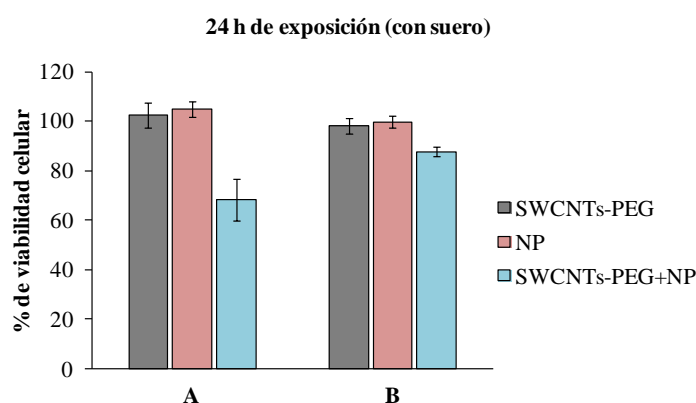


Figura V.2.17. Tratamientos individuales y con mezclas que sugieren posibles efectos citotóxicos sinérgicos; **A** (2 mg L^{-1} de NP; 13 mg L^{-1} de SWCNTs-PEG; y sus mezclas); **B** (5 mg L^{-1} de NP; 2.6 mg L^{-1} de SWCNTs-PEG; y sus mezclas).

BLOQUE V

El **caso A** refleja un efecto sinérgico más notable. Como se puede apreciar, cuando las células fueron expuestas a SWCNTs-PEG y NP por separado, no se observaron efectos citotóxicos (viabilidad celular del 100%), pero cuando fueron incubadas con las mezclas (SWCNTs-PEG + NP) la tasa de mortalidad celular alcanzó valores en torno al 32%.

En el **caso B**, el incremento de toxicidad por exposiciones a mezclas de SWCNTs-PEG y NP respecto a los tratamientos individuales, fue tan solo del 12% pero aún así, la tendencia observada en este caso fue diferente al resto de tratamientos con mezclas y por eso hemos considerado mencionarlo en este punto.

La influencia del tiempo de exposición fue también examinada realizando estudios a 48 horas. Los resultados no mostraron diferencias significativas con las exposiciones de 24 horas, salvo para los tratamientos con la concentración más elevada de NP (10 mg L⁻¹). Igualmente en estos estudios se observó que el suero tuvo un efecto “*protector*” sobre las células para tratamientos con SWCNTs-PEG (13 mg L⁻¹), de forma que la toxicidad se redujo notablemente de un 90% a un 44%. Esto se podría correlacionar con el hecho de que las proteínas confieren una mayor estabilidad a las NPs en medios biológicos y esto en nuestro caso parece reducir su toxicidad inherente. Por lo general, no se observaron evidencias de toxicidad combinada entre SWCNTs-PEG y NP, exceptuando un caso puntual en el que la toxicidad obtenida tras la exposición a las mezclas (SWCNTs-PEG + NP) superó en un 10% a aquella observada para los tratamientos individuales.

Con carácter innovador, el potencial de la Espectroscopía Raman para conocer la distribución intracelular de los SWCNTs-PEG se puso en práctica. En primer lugar, se seleccionaron aquellas regiones Raman características de células y SWCNTs-PEG que permitirían su identificación posterior en muestras

biológicas (*regiones de huellas digitales*). Para ello se analizaron independientemente células y SWCNTs-PEG, y se obtuvieron los espectros Raman que se muestran en la Figura V.2.18.

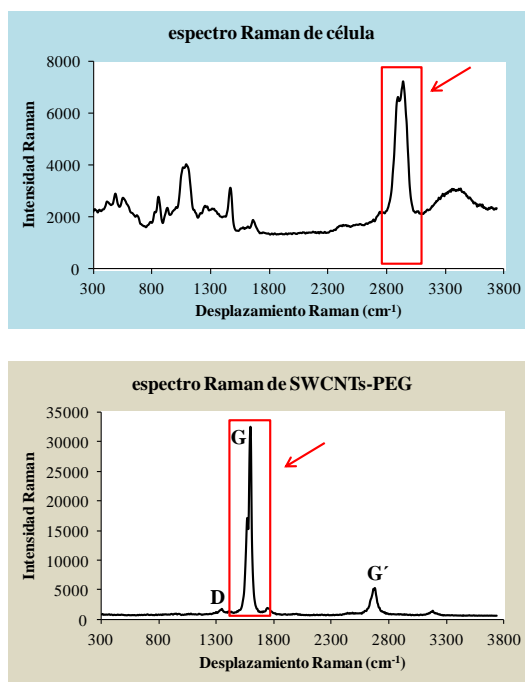


Figura V.2.18. Espectros Raman característicos de células 3T3-L1 y SWCNTs-PEG.

La banda localizada en el rango 2800-3000 cm^{-1} (pico a 2936 cm^{-1}) fue seleccionada como región espectral característica, o *huella digital*, de las células. Asumimos que esta banda corresponde en términos generales al estiramiento simétrico y asimétrico de los grupos CH , CH_2 y CH_3 .

En el espectro de los SWCNTs-PEG distinguimos tres bandas Raman características de las estructuras de grafito. La banda D (1316 cm^{-1}) se relaciona con los defectos presentes en la estructura del grafito, y puesto que es casi imperceptible para SWCNTs-PEG, esto es indicativo de la falta de defectos en su estructura. La banda G (1595 cm^{-1}) corresponde a la vibración fundamental

BLOQUE V

(primer orden) de elongación tangencial. La banda G se asocia a un sobretono (segundo orden). Nosotros seleccionamos la banda G de mayor intensidad como *huella digital* de los SWCNTs-PEG para identificar su localización dentro de las muestras biológicas.

Una vez seleccionadas las *huellas digitales*, se procedió al análisis de muestras biológicas con células 3T3-L1 que fueron previamente expuestas durante 24 horas a SWCNTs-PEG (13 mg L^{-1}). La Figura V.2.19 muestra el análisis Raman llevado a cabo.

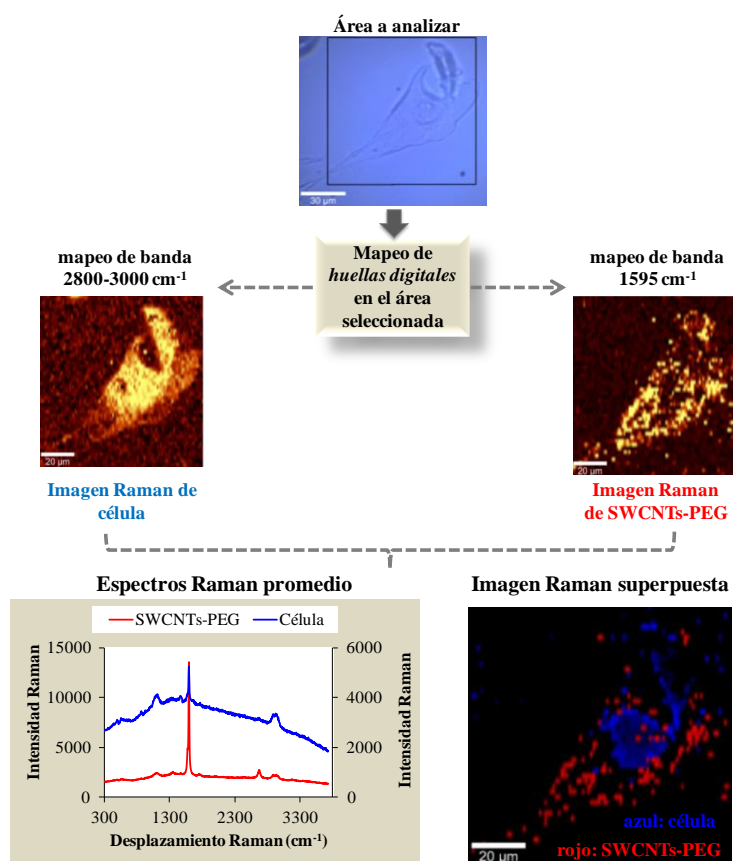


Figura V.2.19. Análisis Raman de una célula 3T3-L1 después de su exposición durante 24 h a 13 mg L^{-1} de SWCNTs-PEG. La imagen superpuesta obtenida por asignar diferentes colores a las imágenes Raman de la célula (azul) y los SWCNTs-PEG (rojo). Los espectros Raman promedio del área analizada también son presentados.

Tal y como puede verse en la imagen Raman superpuesta, los SWCNTs-PEG se acumularon en las células después de la exposición. Además, la presencia de la región característica de las células en el espectro de los SWCNTs-PEG y *viceversa*, confirma la interacción producida entre ambos. Los SWCNTs-PEG se distribuyeron de forma generalizada por toda la célula, si bien hay que decir que apenas se observaron en la zona del núcleo. Esto concuerda con la mayoría de publicaciones relacionadas en las que las NPs se distribuyen por las zonas cercanas a la membrana o en compartimentos intracelulares (endosomas o lisosomas) pero rara vez en el núcleo.

Valoración general de los estudios de toxicidad

La evaluación toxicológica llevada a cabo en los dos trabajos de investigación anteriormente discutidos, se realizó mediante ensayos *in vitro* que tuvieron un fundamento similar. En ambos casos, la viabilidad celular de las muestras fue calculada en base a la formación de un producto como consecuencia de la actividad metabólica de células vivas. Este producto fue fluorescente para el ensayo Azul Alamar o de la resazurina (detección por fluorimetría) o coloreado para el ensayo MTT (detección por espectrofotometría). Asimismo, las células pertenecientes a la misma tipología, fibroblastos de origen embrionario de ratón, fueron expuestas durante 24/48h a tratamientos con las NPs con el objetivo de clarificar, o bien los efectos de su química superficial, o aquellos derivados de su interacción con otro contaminante ambiental bastante común.

La Tabla V.2.7 resume y compara los estudios toxicológicos realizados.

Tabla V.2.7. Características y conclusiones derivadas de los estudios toxicológicos realizados.

Ensayo <i>in vitro</i>	Línea celular empleada	Tipo de nanopartícula y factor a considerar	Parámetros a estudiar	Conclusiones
Resazurina	NIH/3T3 (fibroblastos de embriones de ratón)	<ul style="list-style-type: none"> -Nanopartículas de plata con diferentes recubrimientos superficiales. - Influencia de la química superficial de las nanopartículas. 	<ul style="list-style-type: none"> -Tasa de oxidación en función del pH. -Estabilidad coloidal en medios salinos. - Grado de internalización celular. 	<ul style="list-style-type: none"> -La Ag en forma de nanopartículas fue menos tóxica que como iones libres (AgNO₃). -El recubrimiento no afectó a la tasa de oxidación, aunque si lo hizo el pH. -El recubrimiento influyó en la estabilidad coloidal de las nanopartículas y en su internalización celular, factores que alteraron la toxicidad.
MTT	3T3-L1 (fibroblastos de embriones de ratón preadipocitos)	<ul style="list-style-type: none"> -Nanotubos de carbono monocapa modificados con polietilenglicol. - Influencia de la coexistencia con otro contaminante ambiental. 	<ul style="list-style-type: none"> -Toxicidad de especies por separado y en combinación. - Toxicidad en presencia o ausencia de suero. - Tiempo de exposición. 	<ul style="list-style-type: none"> -El suero ejerció un efecto protector contra todos los tratamientos e incrementó la estabilidad de las nanopartículas disminuyendo su toxicidad. -El tiempo de exposición no afectó de forma significativa. -No se observaron evidencias claras de toxicidad combinada.



CONCLUSIONES

CONCLUSIONS

Esta Memoria consta de dos grandes bloques temáticos. Un primer bloque (*Bloque III*) centrado en el desarrollo de nuevas metodologías analíticas basadas en el empleo de NPs y aplicadas al control medioambiental. Y un segundo bloque (*Bloque IV*) cuya finalidad fue investigar la toxicidad de varios tipos de NPs dando prioridad a diferentes factores influyentes en la misma, como la química superficial, o la presencia e interacción con otras especies químicas.

En esta sección se expondrán las principales conclusiones derivadas de la investigación desarrollada durante la Tesis Doctoral en función del bloque temático al que pertenecen.

Para aquellos trabajos sobre aplicaciones analíticas, destacamos que:

✓ El rol de las CNPs como tercera fase dentro de un esquema convencional de CPE fue evaluado por primera vez. La introducción de NPs en el sistema, así como los efectos derivados de su interacción con las estructuras micelares presentes, facilitaron la formación de dos fases distinguibles y por tanto permitieron la consecución de la extracción.

✓ La capacidad de las CNPs para mejorar la eficiencia de extracción fue investigada en un sistema de LLE asistido por una interfase de CNPs. La membrana formada por CNPs estabilizadas reforzó el transporte de soluto de la fase acuosa a la orgánica.

✓ Un procedimiento analítico muy simple y de bajo coste fue propuesto para la determinación de un compuesto farmacéutico mediante el empleo de tan solo 15 mg de CNTs como fase sorbente en la etapa de tratamiento de muestra.

Conclusiones

✓ Las propiedades fisicoquímicas de las NPs junto con su interacción con el medio, condicionaron su diferente comportamiento de extracción. El estado de aglomeración, el tamaño, los grupos funcionales superficiales derivados de su síntesis, el área superficial específica y el tipo de interacciones que establecen con el medio y las especies presentes en él, conforman un escenario bastante complejo para justificar el comportamiento de las NPs. Además, tanto el analito como los mecanismos que sustentan la extracción en cada caso, influyen en la idoneidad de las NPs para los diferentes procedimientos planteados.

✓ La habilidad de las AgNPs para mejorar la señal de detección Raman a través del efecto SERS quedó demostrada al obtenerse factores de incremento de la señal del orden de 10^5 respecto a aquella obtenida en ausencia de estas NPs.

En cuanto a los estudios de toxicidad conviene señalar que:

✓ La diferente funcionalización superficial de las AgNPs afectó a su estabilidad coloidal en disoluciones salinas, y por lo tanto, también afectó a su toxicidad. Las NPs menos estables provocaron una mayor mortalidad celular.

✓ El grado de internalización celular de las NPs puede ser alterado en función del recubrimiento superficial que presenten. Este hecho se correlaciona con la diferente toxicidad observada para las NPs internalizadas en diferente grado. Por consiguiente, la química superficial influye en la toxicidad de las NPs por condicionar su diferente habilidad de penetración celular.

✓ La oxidación de las AgNPs, si bien es una de sus principales causas de toxicidad, no se vio alterada por el diferente recubrimiento superficial, sino más bien por el pH del medio.

✓ La oxidación de las AgNPs se favoreció en ambientes ácidos, por lo tanto cuando estas NPs se encuentren dentro de los compartimentos intracelulares de tipo endosomas/lisosomas (con un $\text{pH} \approx 4-5$), cabe esperar una tasa de oxidación superior a aquella producida en el medio extracelular neutro.

✓ La misma cantidad de plata resultó ser menos tóxica en forma de NPs que en forma de iones de Ag^+ (AgNO_3).

✓ Los estudios de interacción entre SWCNTs-PEG y 4-nonilfenol no revelaron evidencias claras de toxicidad combinada (adición, sinergia o antagonismo) pese a la interacción esperada entre ambas especies.

✓ El suero ejerció un efecto “*protector*” sobre las células ya que incrementó la tolerancia de las mismas a todos los tratamientos con SWCNTs-PEG y 4-nonilfenol. Las proteínas del suero mejoraron la estabilidad de las NPs en el medio de cultivo, y esto se tradujo en una menor mortalidad celular.

✓ El empleo de la Espectroscopía Raman permitió conocer la distribución intracelular de los SWCNTs-PEG, una vez fueron definidas las regiones Raman características o huellas digitales. Indudablemente, esta técnica proporciona nuevas oportunidades para el *imaging* de las células a pesar del hecho de que su aplicación en este ámbito se encuentra todavía en sus primeras fases.

Conclusions

This Report is consisted of two principal thematic blocks. A first block (Block III), about the development of new analytical methodologies based on the use of NPs and applied to the environmental control. And a second block (Block IV), focused on examining the toxicity of several types of NPs giving priority to different influential factors, such as the surface chemistry, or the presence and interaction with other chemical compounds.

In this section, the main conclusions derived from the research developed during the Doctoral Thesis will be presented according to the block they belong to.

For those research works devoted to the development of new analytical applications, we highlight that:

✓ *The role of CNPs as third phase in the conventional CPE technique has been investigated for the first time. The inclusion of NPs in the aqueous system and the effects arising from their interaction with the micellar aggregates, favored the formation of two clearly discernible phases that allowed performing the extraction.*

✓ *The potential of CNPs as pseudophase in the conventional LLE technique was demonstrated in terms of enhanced extraction efficiency in comparison to the classical technique without NPs. The membrane composed of stabilized CNPs, located between the aqueous and organic phases, favored the extraction by providing additional avenues for solute transport.*

✓ *An extremely simple and low cost analytical procedure has been developed for determining a pharmaceutical compound by using only 15 mg of CNTs as sorbent phase in the sample treatment step.*

✓ *The physicochemical properties of NPs along with their interaction with the medium determine their different extraction behavior. The agglomeration state, size, residual surface groups resulting from synthesis process, specific surface area, and type of interactions established with the extraction medium and their components, constitute a complex scenario for warranting the behavior observed for all NPs investigated. Additionally, the target analyte and the mechanisms that support the extraction in each case, affect the suitability of the NPs for the different procedures proposed.*

✓ *The ability of AgNPs to improve the Raman signal by SERS effect has been proved. A 10^5 -fold enhancement factor of Raman signal was achieved thanks to the presence of these NPs.*

Regarding toxicity studies, it should be pointed that:

✓ *The different surface functionalization of AgNPs affected their colloidal stability in saline solutions and consequently, their toxicity. Less stable NPs provoked a greater cell mortality.*

✓ *The uptake of NPs by cells can be modulated by their surface coating. This fact is correlated with the distinct toxicity observed for NPs internalized in different degree. Thus, the surface chemistry influences the toxicity of NPs by altering their uptake by cells.*

✓ *While the oxidation rate of AgNPs is one of the most important toxicity mechanisms associated to these NPs, no variations were reported depending on their surface coating. In contrast, the pH was a very influential factor.*

✓ *The oxidation of AgNPs is favored in acidic environments, therefore, once these NPs are internalized inside intracellular compartments of*

Conclusions

endosomal/lysosomal type (with $pH \approx 4-5$), a higher oxidation rate than in the neutral extracellular medium is expected.

✓ *The same amount of silver turned out to be less harmful in form of NPs than as Ag^+ ions ($AgNO_3$).*

✓ *The studies of interaction of SWCNTs-PEG with 4-nonylphenol revealed no clear evidences of combined toxicity (addition, synergy, antagonism) despite the interaction expected between both species.*

✓ *The serum had a “protective” effect on cells since increased their tolerance to all treatments with SWCNTs-PEG and 4-nonylphenol. Serum proteins enhanced the stability of NPs in culture medium and this fact led to lower cell mortality rates.*

✓ *The potential of Raman spectroscopy to examine the distribution of SWCNTs-PEG inside biological samples has been confirmed. The analysis of Raman spectroscopic fingerprints (characteristic Raman regions) for cells and CNTs allowed elucidating their location within samples. Undoubtedly, Raman technique provides new opportunities for cell imaging despite the fact that its application to that field is still in its early stage.*



AUTOEVALUACIÓN

SELF-ASSESSMENT

Además de las aportaciones más relevantes que se han expuesto en la sección anterior, también convendría mencionar aquellas carencias o dificultades encontradas en el desarrollo de la fase experimental, para así poder definir las líneas futuras de investigación necesarias en este sentido.

A continuación se describen las principales limitaciones de la investigación desarrollada durante la Tesis Doctoral.

- ✘ El diferente comportamiento de extracción de las NPs habría sido mejor justificado con la ayuda de estudios de caracterización de las NPs implicadas, en especial, aquellas sintetizadas experimentalmente.

- ✘ Los bajos factores de preconcentración obtenidos en algunos casos podrían haber sido mejorados al incluir una nueva o más eficiente etapa de evaporación dentro del procedimiento analítico.

- ✘ Los métodos analíticos desarrollados fueron en todos los casos aplicados a la determinación de un único analito, por lo tanto, sería conveniente que, una vez optimizado el protocolo experimental, se llevasen a cabo estudios para la determinación simultánea de varios analitos presentes en una misma muestra.

- ✘ La reutilización del cartucho con CNTs en el procedimiento de SPE nos habría permitido simplificar en mayor grado la etapa de extracción, mejorar la reproducibilidad, y reducir el coste y consumo de NPs.

- ✘ En cuanto a los estudios toxicológicos, éstos podrían haber sido conducidos por diferentes ensayos *in vitro* que permitiesen contrastar los resultados obtenidos, no necesariamente en términos cuantitativos de

Autoevaluación

viabilidad celular pero sí en información cualitativa. Experimentos paralelos con diferentes ensayos habrían mejorado la fiabilidad de los resultados.

✘ Los efectos citotóxicos observados corresponden a un tipo concreto de NPs y sobre una línea celular específica. Esto impide extrapolar los resultados a otras condiciones experimentales, y por tanto, establecer conclusiones generalizadas.

✘ La investigación sobre los mecanismos generadores de toxicidad de las NPs, tales como la formación de ROS o las alteraciones morfológicas, habría enriquecido y complementado la evaluación toxicológica realizada.

✘ Una evaluación más completa (en términos de citotoxicidad) considerando más concentraciones de 4-nonilfenol y SWCNTs-PEG, separados o en mezclas, nos habría permitido construir las curvas de dosis respuesta correspondientes a las especies solas y en combinación. Esta información habría arrojado más luz sobre los posibles efectos de toxicidad combinada teniendo en cuenta un abanico más amplio de condiciones de estudio. Además, la comparación en términos de LD_{50} para las especies solas y en combinación habría sido más representativa de la tendencia general observada.

In addition to the most relevant contributions that were exposed in the previous section, it should be also noted those shortcomings found throughout the development of experimental phase, with the purpose of defining future research lines needed to overcome them.

Below, the most important limitations of the research performed during the Doctoral Thesis are mentioned.

✘ The different behavior exhibited by NPs in the proposed extraction schemes could have been better warranted with the help of characterization studies for all the NPs investigated, especially those synthesized experimentally.

✘ The low preconcentration factors obtained in some cases could have been enhanced by including an additional or more efficient evaporation step within the analytical procedure.

✘ All analytical methodologies were applied to the determination of one analyte consequently, it would be convenient that once the experimental protocol was optimized, further studies were aimed to analyze several analytes from a same sample.

✘ The reuse of the SPE cartridges prepared with packed CNTs would have allowed us to simplify to a greater extent the extraction step, improving the reproducibility, and reducing the cost and consumption of NPs.

✘ Regarding toxicological studies, different cytotoxicity assays could have been performed in order to contrast the results, no necessarily in terms of percentages of cell viability but in qualitative information. Parallel experiments with different assays would have increased the reliability of the results obtained.

Self-assessment

✘ *Outcomes arising from toxicological studies are related to the cytotoxic effects caused by a type of NPs and on a particular cell line. This fact prevents from extrapolating the results to other experimental conditions and thus, establishing generalized conclusions on the effects observed.*

✘ *Further research on mechanisms of toxicity of NPs including the generation of ROS or the analysis of morphological alterations would enrich and complement the toxicological evaluation carried out.*

✘ *A more exhaustive evaluation (in terms of cytotoxicity) for further concentrations of 4-nonylphenol and SWCNTs-PEG, alone or in combination, would have allowed us to plot the dose response curves corresponding to single compounds and mixtures. This information would have shed light on potential effects of combined toxicity considering a broader range of incubation conditions. The comparison in terms of LD₅₀ for single compounds and mixtures would have been more representative of the general tendency observed.*

ANEXOS
 **PRODUCCIÓN**
CIENTÍFICA

Anexo A
Publicaciones científicas

1. **Nanodiamonds assisted-cloud point extraction for the determination of fluoranthene in river water.**

E. Caballero-Díaz, B.M. Simonet, M. Valcárcel, *Analytical Methods* 5 (2013) 3864-3871.

2. **Liquid-liquid extraction assisted by a carbon nanoparticles interface. Electrophoretic determination of atrazine in environmental samples.**

E. Caballero-Díaz, B. Simonet, M. Valcárcel, *Analyst* 138 (2013) 5913-5919.

3. **Microextraction by packed sorbents combined with surface-enhanced Raman spectroscopy for determination of musk ketone in river water.**

E. Caballero-Díaz, B.M. Simonet, M. Valcárcel, *Analytical and Bioanalytical Chemistry* 405 (2013) 7251-7257.

4. **The toxicity of silver nanoparticles depends on their uptake by cells and thus on their surface chemistry.**

E. Caballero-Díaz, C. Pfeiffer, L. Kastl, P. Rivera-Gil, B. Simonet, M. Valcárcel, J. Jiménez-Lamana, F. Laborda, W.J. Parak, *Particle and Particle Systems Characterization* 30 (2013) 1079-1085.

5. **The social responsibility of Nanoscience and Nanotechnology: an integral approach.**

E. Caballero-Díaz, B.M. Simonet, M. Valcárcel, *Journal of Nanoparticle Research* 15 (2013) 1534-1546.

6. Multiplexed sensing and imaging with colloidal nano- and microparticles.

S. Carregal-Romero, E. Caballero-Díaz, L. Beqa, A.M. Abdelmonem, M. Ochs, D. Hühn, B. Simonet, M. Valcárcel, W.J. Parak, *Annual Review of Analytical Chemistry* 6 (2013) 53-81.

7. Carbon nanotubes as solid-phase extraction sorbents for extraction of salicylic acid from river water.

E. Caballero-Díaz, M. Valcárcel, *Journal of Separation Science*
DOI 10.1002/jssc.201301204

8. Effect of the interaction of single-walled carbon nanotubes with 4-nonylphenol on their *in vitro* toxicity.

E. Caballero-Díaz, R. Guzmán-Ruiz, M.M. Malagón, B.M. Simonet, M. Valcárcel, submitted to *Journal of Hazardous Materials*.

Nanodiamonds assisted-cloud point extraction for the determination of fluoranthene in river water

Cite this: *Anal. Methods*, 2013, 5, 3864

Encarnación Caballero-Díaz, Bartolomé M. Simonet and Miguel Valcárcel*

The classic cloud point extraction has been modified by the inclusion of nanodiamonds and applied to the extraction–preconcentration of fluoranthene from river water. The effects of ionic strength and surfactant concentration, process temperature, incubation time, nanoparticle type and concentration and elution conditions were investigated in depth. The effect of the carbon nanoparticles (CNPs) on the performance of the conventional cloud point scheme enabled the formation of two phases in a relatively short time and without temperature requirements. Experiments carried out under optimized conditions but in absence of nanoparticles were unsuccessful in terms of phase separation and consequently, the nanoparticles are indispensable to the analytical performance. The work developed here, confirms the versatility of the CNPs to be introduced in diverse sample treatment processes, resulting very interesting to investigate in each case their impact on the performance of the process. The application of the proposed method followed by fluorimetric detection enabled the determination of fluoranthene in spiked river water providing a good relative standard deviation (RSD) (6.6%, $n = 3$) and acceptable recovery values (>65%).

Received 1st April 2013
Accepted 15th May 2013

DOI: 10.1039/c3ay40541a

www.rsc.org/methods

1 Introduction

Analytical methods with high sensitivity, selectivity and resolution are required in order to determine analytes at trace concentration levels in complex matrices. Extraction–separation techniques overcome this problem since they isolate analytes from the matrix, thereby reducing, controlling or eliminating the interferences originally present, and additionally, preconcentrate and determine the analytes at very low concentrations.¹ Conventional extraction techniques such as liquid–liquid or solid–phase extraction (LLE, SPE) and liquid–phase or solid–phase microextraction (LPME, SPME) are relatively expensive, tedious and consume large amounts of organic solvents.²

Cloud point extraction (CPE) has become one of the most outstanding extraction techniques. This technique is based on the separation of a homogeneous micellar aqueous solution into two isotropic liquid phases. One of them, the smaller-volume surfactant-rich phase, contains the surfactant interacting with the analyte molecules at a concentration above its critical micellar concentration (CMC), that is the surfactant concentration above which the surfactant molecules aggregate to form micelles. The other larger-volume aqueous phase is only composed of surfactant molecules at a concentration close to the CMC. In comparison to the above mentioned extraction

techniques CPE shows remarkable advantages such as, versatility for extracting and preconcentrating analytes of different nature, variable preconcentration factors depending on the amount of surfactant added, lower loss of analyte since it is not necessary to evaporate the solvent, low cost and no toxicological effects thanks to the use of biodegradable surfactants. The limitations are mainly related to the high background absorbance of the surfactants in the UV region and to the handling of the surfactant-rich phase since this is too viscous to be directly injected into conventional analytical instruments, and therefore a previous dilution or clean up step is usually necessary before detection.^{1–3} In order to ensure that separation into two phases occurs, two conditions are required. The first is that the surfactant concentration must exceed the CMC for the formation of micelles. The second is that the experimental conditions such as temperature, pressure and ionic strength must be altered. When separation into two phases takes place, the solution becomes turbid due to the diminished solubility of the surfactant in water. However, this phenomenon is reversible when the experimental conditions return to their initial point. The cloud point temperature (CPT), temperature at which the solution becomes turbid, plays an important role in the formation of the two phases when nonionic or zwitterionic surfactants are used. The mechanism by which two phases are formed is still subject of controversy. However, it may be attributed to the competition between the entropy (which promotes the solubility of the micelles in water) and enthalpy (which promotes the separation of the micelles from water) when the temperature of the system increases.⁴ The water

Department of Analytical Chemistry, Marie Curie Building (Annex), Campus de Rabanales, University of Córdoba, E-14071 Córdoba, Spain. E-mail: qatmeobj@uco.es; Fax: +34 957 218616; Tel: +34 957 218616

Liquid–liquid extraction assisted by a carbon nanoparticles interface. Electrophoretic determination of atrazine in environmental samples

Cite this: *Analyst*, 2013, 138, 5913

Encarnación Caballero-Díaz,^a Bartolomé Simonet^b and Miguel Valcárcel^{*a}

A novel method for the determination of atrazine, using liquid–liquid extraction assisted by a nanoparticles film formed *in situ* and composed of organic solvent stabilized-carbon nanoparticles, is described. The presence of nanoparticles located at the liquid–liquid interface reinforced the extraction of analyte from matrix prior to capillary electrophoresis (CE) analysis. Some influential experimental variables were optimized in order to enhance the extraction efficiency. The developed procedure confirmed that carbon nanoparticles, especially multi-walled carbon nanotubes, are suitable to be used in sample treatment processes introducing new mechanisms of interaction with the analyte. The application of the proposed preconcentration method followed by CE detection enabled the determination of atrazine in spiked river water providing acceptable RSD values (11.6%) and good recoveries (about 87.0–92.0%). Additionally, a similar extraction scheme was tested in soil matrices with a view to further applications in real soil samples.

Received 4th March 2013

Accepted 15th July 2013

DOI: 10.1039/c3an00439b

www.rsc.org/analyst

1 Introduction

The excessive and uncontrolled use of herbicides in agriculture crops causes the contamination of soils, and due to their persistence and mobility, the surface and ground waters are also affected by mechanisms such as the leaching or runoff of these compounds.

Atrazine (2-chloro-4-ethylamino-6-isopropylamino-1,3,5-triazine) is a herbicide belonging to the triazines family and it is widely used for broadleaf and grassy weed control. Among its known toxic effects, its estrogenic activity should be pointed out since this herbicide acts as environmental endocrine disruptor resulting in high toxicity.¹ As a consequence, atrazine has been already determined in different kinds of environmental matrices such as, soils,² groundwater,³ surface waters⁴ and atmosphere.⁵ The analytical techniques frequently reported in the detection of this herbicide focus on liquid or gas chromatography optionally coupled with mass spectrometry,^{6,7} although to a lesser extent, capillary electrophoresis,⁸ immunoassay,⁹ voltammetry¹⁰ and spectrophotometry,¹¹ among others techniques, have been also used with this same purpose. In most cases, a preconcentration step prior to analytical detection is necessary since herbicides are usually found at low concentrations in waters. Liquid–liquid extraction (LLE),¹²

solid-phase extraction (SPE),¹³ solid phase microextraction (SPME)¹⁴ and liquid phase microextraction (LPME)¹⁵ have been reported as sample treatment techniques in order to extract atrazine from different matrices, SPE being the most widely described technique to date.

The use of nanoparticles as components of the extracting phase in liquid extraction procedures has gained importance. Carbon nanotubes (CNTs) are considered as excellent sorbents for organic compounds due to their large adsorption surface and high affinity for these compounds.¹⁶ Nanodiamonds (NDs), carbon nanoparticles with a truncated octahedral architecture, have also been extensively investigated because of their high adsorption capacity and specific surface area, however their applications in sample treatment processes are still reduced. Their sorption properties make carbon nanoparticles potentially useful in membrane extraction processes. The limitations of conventional polymeric membranes used for water purification¹⁶ and gas separation¹⁷ lie in their low selectivity, permeability, susceptibility to the obstruction or fouling (what results in a reduced diffusion flux) as well as low chemical and thermal resistance. The use of CNT-based membranes has considerably increased in these application fields and offers possibilities to improve the extraction efficiency by adding new channels to mass transfer. These membranes consist of CNTs embedded in a polymer matrix, so that the selectivity and permeability of analytes are improved in comparison to those for non-modified membranes.¹⁸ These membranes have been fabricated using different polymeric matrices such as polyethersulfone (PES),¹⁹ poly(bisphenol A-co-4-nitrophthalic anhydride-co-1,3-phenylenediamine) (PBNPI),²⁰ polysulfone (PSF)²¹ or polyamide.²² This

^aDepartment of Analytical Chemistry, Marie Curie Building (Annex), Campus de Rabanales, University of Córdoba, E-14071 Córdoba, Spain. E-mail: qa1meohj@uco.es; Fax: +34 957 218616; Tel: +34 957 218616

^bCarbures Europe company, Bahía de Cádiz Technopark, El Puerto de Santa María, E-11500 Cádiz, Spain

Anal Bioanal Chem (2013) 405:7251–7257
DOI 10.1007/s00216-013-7185-6

RESEARCH PAPER

Microextraction by packed sorbents combined with surface-enhanced Raman spectroscopy for determination of musk ketone in river water

Encarnación Caballero-Díaz · Bartolomé M. Simonet · Miguel Valcárcel

Received: 9 April 2013 / Revised: 29 May 2013 / Accepted: 26 June 2013 / Published online: 11 August 2013
© Springer-Verlag Berlin Heidelberg 2013

Abstract Microextraction by packed sorbents (MEPS) combined with Surface-enhanced Raman spectroscopy (SERS) was investigated, and applied to the determination of musk ketone (MK) in river water samples. The full MEPS–SERS method includes analyte enrichment by MEPS preconcentration with C₁₈ sorbent followed by SERS detection supported by silver nanoparticles. An eluent drop containing the analyte is deposited directly from the MEPS syringe on a CaF₂ glass plate. When the drop has dried, a specific volume of silver nanoparticles solution is added on it before each SERS measurement. Several experimental variables were studied in depth; under the optimum experimental conditions MK can be extracted from a 500 µL sample with recoveries in the range 47–63 %. The limit of detection was 0.02 mg L⁻¹ and the relative standard deviation 15.2 % (*n*=4). Although not investigated in this work, the proposed method might be suitable for in-situ monitoring, because of the portability of the Raman spectrometer used.

Keywords Microextraction by packed sorbents (MEPS) · Surface-enhanced Raman spectroscopy (SERS) · Musk ketone (MK) · Silver nanoparticles · River water

Introduction

Currently, there is an increasing attention on musks compounds because they are common additives in numerous

consumer products, for example detergents, cosmetics, and other personal care products [1]. Because of their widespread use, musk products have become ubiquitous emerging contaminants that can be found in different environmental matrices near wastewater discharge urban areas [1]. Synthetic musks can be classified into three families: polycyclic musks, nitromusks, and macrocyclic musks, being the first of them the most commonly used. The nitromusk family includes five compounds: musk ambrette, musk moskene, musk tibetene, musk xylene (MX), and musk ketone (MK); although only the last two are permitted [2]. Permitted maximum concentrations (*w/v*, %) for MX and MK are, respectively, 1.0 % and 1.4 % in fine fragrances, 0.4 % and 0.5 % in eau de toilette, and 0.03 % and 0.04 % in other products [3, 4].

The effect of musk compounds on biota and ecosystems has become an emerging research area. Polycyclic musks and nitromusks are lipophilic in nature; this results in slow biodegradation and a tendency to bioaccumulate in different environmental compartments, for example sediments [5, 6], sludge [7, 8], and biota [9, 10]. Although MK is suspected of increasing the carcinogenic effects of other substances, few related toxicological studies have been conducted. Comutagenic effects between benzo[*a*]pyrene and MK have been described in human derived hepatoma cell lines, because MK amplifies the genotoxicity of that carcinogen [11]. Furthermore, recent in-vitro studies have confirmed that some polycyclic musks bind weakly to estrogen, androgen, or progesterin receptors, and thus have endocrine-disrupting properties [12].

Determination of musk compounds in environmental samples has already been performed by different analytical techniques. A preconcentration step is usually required because of the low concentrations at which these compounds are found. Solid-phase microextraction (SPME) is a solventless preconcentration technique that consists of extracting

E. Caballero-Díaz · B. M. Simonet · M. Valcárcel (✉)
Department of Analytical Chemistry, Marie Curie Building
(Annex), Campus de Rabanales, University of Córdoba,
14071 Córdoba, Spain
e-mail: qa1meobj@uco.es

The Toxicity of Silver Nanoparticles Depends on Their Uptake by Cells and Thus on Their Surface Chemistry

Encarnación Caballero-Díaz, Christian Pfeiffer, Lena Kastl, Pilar Rivera-Gil, Bartolome Simonet, Miguel Valcárcel, Javier Jiménez-Lamana, Francisco Laborda, and Wolfgang J. Parak*

A set of three types of silver nanoparticles (Ag NPs) are prepared, which have the same Ag cores, but different surface chemistry. Ag cores are stabilized with mercaptoundecanoic acid (MUA) or with a polymer shell [poly(isobutylene-alt-maleic anhydride) (PMA)]. In order to reduce cellular uptake, the polymer-coated Ag NPs are additionally modified with polyethylene glycol (PEG). Corrosion (oxidation) of the NPs is quantified and their colloidal stability is investigated. MUA-coated NPs have a much lower colloidal stability than PMA-coated NPs and are largely agglomerated. All Ag NPs corrode faster in an acidic environment and thus more Ag(I) ions are released inside endosomal/lysosomal compartments. PMA coating does not reduce leaching of Ag(I) ions compared with MUA coating. PEGylation reduces NP cellular uptake and also the toxicity. PMA-coated NPs have reduced toxicity compared with MUA-coated NPs. All studied Ag NPs were less toxic than free Ag(I) ions. All in all, the cytotoxicity of Ag NPs is correlated on their uptake by cells and agglomeration behavior.

1. Introduction

Silver nanoparticles (Ag NPs) are frequently used in industry, mainly because of their antimicrobial properties,^[1] with applications in an increasing number of medical and consumer products. However, their antibacterial features and extremely small size, which makes them to have a high surface area and to be more reactive, also suggest a toxicological risk when these

NPs come into contact with biological systems.^[2] Countless toxicological studies involving Ag NPs have already been carried out in different organisms ranging from bacteria to humans.^[3–5] Although it is generally known that corrosion (oxidation) and subsequent release of Ag(I) ions is a major source of toxicity,^[6,7] there is still a lack of detailed general knowledge concerning the origin of the Ag NPs' toxicity. Most important shortcomings are that individual studies are often based on different NPs, and also on different types of cells, which complicate the comparison and extrapolation of results. In some studies, the final toxicity resulted to be an unclear combination of effects among the Ag NPs and their released Ag(I) ions, whereas in other works the Ag(I) ions showed a greater (or even the only) contribution to the toxicity than the Ag NPs *per se*.^[3,7–9] Several studies describe the release of Ag(I) ions upon NP oxidation and subsequent partial dissolution of the Ag NPs over time as amplification of the toxicity of the (undissolved) Ag NPs, which can cause intracellular reactions, as, for example, in the mitochondria.^[5] Other studies even claim that the only effect originates from Ag ions, which acts on the cell membrane, whereas under the same conditions Ag NPs had no effect.^[9] Studies indicate that toxicity depends on size,^[10] shape,^[11] charge,^[12] and colloidal stability^[13] of the Ag NPs.

Although correlation of the physicochemical properties of NPs to their interaction with cells is attempted by a large-body research studies, a comprehensive picture is still missing (not only for Ag NPs but in general) albeit many effects are well established. This is partly due to the fact that not all physicochemical properties are easy to be determined experimentally, and most of them are entangled (e.g., loss in colloidal stability/reduced dispersion also increases the effective hydrodynamic diameter of the NPs).^[14] The interaction of NPs with cells is not only governed directly but also it is strongly influenced by interplay with the medium. Salt can reduce colloidal stability, and the NP surface will be covered with a corona of proteins, which provides signature to the NP surface.^[15] This interaction is not static, but rather dynamic and may change with time.^[16] Although this already gives a complex scenario for the NP–medium interaction, modern techniques such as fluorescence correlation spectroscopy (FCS) allow for detailed

E. Caballero-Díaz, C. Pfeiffer, L. Kastl,
Dr. P. Rivera-Gil, Prof. W. J. Parak
Fachbereich Physik
Philipps Universität Marburg
Marburg, Germany
E-mail: wolfgang.parak@physik.uni-marburg.de
E. Caballero-Díaz, Dr. B. Simonet, Prof. M. Valcárcel
Department of Analytical Chemistry
University of Cordoba
Córdoba, Spain
J. Jiménez-Lamana, Prof. F. Laborda
Group of Analytical Spectroscopy and Sensors (GEAS)
Institute of Environmental Sciences (IUCA)
University of Zaragoza
Zaragoza, Spain
Prof. W. J. Parak
CIC Biomagune
San Sebastian, Spain



DOI: 10.1002/ppsc.201300215

J Nanopart Res (2013) 15:1534
 DOI 10.1007/s11051-013-1534-4

REVIEW

The social responsibility of Nanoscience and Nanotechnology: an integral approach

Encarnación Caballero-Díaz ·
 Bartolomé M. Simonet · Miguel Valcárcel

Received: 11 September 2012 / Accepted: 22 February 2013 / Published online: 10 March 2013
 © Springer Science+Business Media Dordrecht 2013

Abstract The concept of social responsibility provides the ideal framework for raising awareness and arousing reflection on the social and environmental impact of nanoparticles in the range of 1–100 nm generated from research activities in nanoscience and production-related activities in nanotechnology. The model proposed here relates the essential aspects of these concepts by connecting the classical sequence Research–Development–Innovation (R&D&I) to nanoscience and nanotechnology (N&N) and social responsibility (SR). This paper identifies the stakeholders of the process and provides an extensive definition of Social Responsibility and related concepts. In addition, it describes the internal and external connotations of the implementation of SR at research centers and nanotechnological industries, and discusses the social implications of nanoscience and nanotechnology with provision for subjects such as nanoethics, nanotoxicity, and nanomedicine, which have emerged from the widespread use of nanomaterials by today's society.

Keywords Nanoscience and nanotechnology · Social responsibility · Corporate social responsibility · Stakeholders · Integral model · Social and environmental impacts

E. Caballero-Díaz · B. M. Simonet · M. Valcárcel (✉)
 Department of Analytical Chemistry, University of
 Cordoba, Campus de Rabanales, 14071 Cordoba, Spain
 e-mail: qalvacam@uco.es

Abbreviations

AENOR	Spanish association for standardization and certification
CSR	Corporate social responsibility
CSP	Corporate social performance
FECYT	Spanish foundation for science and technology
ILO	International labour organization
ISO	International organization for standardization
IUPAC	International union of pure and applied chemistry
N&N	Nanoscience & nanotechnology
OECD	Organization for economic cooperation and development
R&D	Research & development
R&D&I	Research & development & innovation
SR	Social responsibility
UN	United Nations

Introduction

Nanotechnology has been deemed as a key emerging technology for fulfilling the “Grand Challenges of our Time” in areas such as health care, energy production, environmental protection (climate change and remediation), and potable water procurement (Lund Declaration 2009).

Like other highly promising technologies such as nuclear engineering and biotechnology, nanotechnology possesses two contradictory connotations, namely: the



Multiplexed Sensing and Imaging with Colloidal Nano- and Microparticles

Susana Carregal-Romero,^{1,2}
Encarnación Caballero-Díaz,^{1,3} Lule Beqa,¹
Abuelmagd M. Abdelmonem,¹ Markus Ochs,¹
Dominik Hühn,¹ Bartolome Simonet Suau,³
Miguel Valcarcel,³ and Wolfgang J. Parak¹

¹Fachbereich Physik and WZMW, Philipps Universität Marburg, Marburg 35043, Germany; email: susana.carregal@physik.uni-marburg.de, wolfgang.parak@physik.uni-marburg.de

²BIONAND, Centro Andaluz de Nanomedicina y Biotecnología, Málaga 29590, Spain

³Department of Analytical Chemistry, Campus de Rabanales, University of Córdoba, Córdoba 14071, Spain

Annu. Rev. Anal. Chem. 2013. 6:53–81

First published online as a Review in Advance on February 28, 2013

The *Annual Review of Analytical Chemistry* is online at anchem.annualreviews.org

This article's doi:
10.1146/annurev-anchem-062012-092621

Copyright © 2013 by Annual Reviews.
All rights reserved

Keywords

multifunctional colloidal nanoparticles, analyte recognition, bar-coding, multiplexing

Abstract

Sensing and imaging with fluorescent, plasmonic, and magnetic colloidal nano- and microparticles have improved during the past decade. In this review, we describe the concepts and applications of how these techniques can be used in the multiplexed mode, that is, sensing of several analytes in parallel or imaging of several labels in parallel.



Accepted in Journal of Separation Science

Carbon nanotubes as SPE sorbents for extraction of salicylic acid from river water

Encarnación Caballero-Díaz, Miguel Valcárcel, DOI 10.1002/jssc.201301204

ELSEVIER

Journal of Hazardous Materials



Submitted to Journal of Hazardous Materials

Effects of the interaction of single-walled carbon nanotubes with 4-nonylphenol on their *in vitro* toxicity

Encarnación Caballero-Díaz, Rocío Guzmán-Ruiz, María del Mar Malagón, Bartolome Simonet, Miguel Valcárcel

ANEXOS
**PRODUCCIÓN**
CIENTÍFICA

Anexo B
Comunicaciones en congresos

III Workshop de Nanociencia y Nanotecnología (Oviedo, 2009).

- Comunicación oral y póster titulados “Nanodiamantes para la purificación y preconcentración de analitos”.

E. Caballero-Díaz, B.M. Simonet, M. Valcárcel.

I Congreso Científico de Investigadores en Formación (Córdoba, 2009).

- Comunicación oral titulada “Nanopartículas como objetos y herramientas analíticas en la monitorización ambiental”.

E. Caballero-Díaz, B.M. Simonet, M. Valcárcel.

XII Reunión del Grupo Regional Andaluz de la Sociedad Española de Química Analítica, GRASEQA (Córdoba, 2010).

- Póster titulado “Empleo de nanopartículas de carbono para la preconcentración de medios micelares”.

E. Caballero-Díaz, B.M. Simonet, M. Valcárcel.

IV Workshop de Nanociencia y Nanotecnología (Zaragoza, 2010).

- Póster titulado “Nanodiamantes: Propiedades y Aplicaciones”.

E. Caballero-Díaz, B.M. Simonet, M. Valcárcel.

- Comunicación oral flash y póster titulados “Empleo de nanopartículas de carbono para la preconcentración de medios micelares”.

E. Caballero-Díaz, B.M. Simonet, M. Valcárcel.

III Encuentro NANOUCO sobre Nanociencia y Nanotecnología de Investigadores y Tecnólogos Andaluces (Córdoba, 2011).

- Póster titulado “Estudio de la capacidad de nanopartículas de carbono para la preconcentración de micelas aniónicas y neutras”.

E. Caballero-Díaz, B.M. Simonet, M. Valcárcel.

- Póster titulado “Extracción de atrazina en muestras medioambientales mediante films de nanopartículas de carbono situados en interfases líquido-líquido”.

E. Caballero-Díaz, B.M. Simonet, M. Valcárcel.

International Conference NaNaX5 (Nanoscience with Nanocrystals) (Fuengirola, 2012).

- Póster titulado “Nanotoxicity studies of four synthesized silver nanoparticles complexes for future biological applications”.

E. Caballero-Díaz, C. Pfeiffer, L. Kastl, P. Rivera-Gil, B.M. Simonet, M. Valcárcel, W.J. Parak.

XXIII Reunión Nacional de Espectroscopía. VII Congreso Ibérico de Espectroscopía (Córdoba, 2012).

- Póster titulado “Nanotoxicity studies of silver nanoparticles with different superficial coatings for future biological applications”.

E. Caballero-Díaz, C. Pfeiffer, L. Kastl, B.M. Simonet, M. Valcárcel, P. Rivera, W.J. Parak.

IV Encuentro NANOUCO sobre Nanociencia y Nanotecnología de Investigadores y Tecnólogos Andaluces (Córdoba, 2013).

- Póster titulado “A synergistic combination of MEPS-preconcentration and Surface Enhanced Raman Spectroscopy for the determination of musk ketone in river water”.

E. Caballero-Díaz, B.M. Simonet, M. Valcárcel.

VI Workshop de Nanociencia y Nanotecnología (Alcalá de Henares, 2013).

- Comunicación oral flash y póster titulados “The toxicity of silver nanoparticles depends on their uptake by cells and thus on their surface chemistry”.

E. Caballero-Díaz, C. Pfeiffer, L. Kastl, P. Rivera-Gil, B. Simonet, M. Valcárcel, J. Jiménez-Lamana, F. Laborda, W.J. Parak.

ANEXOS
 **PRODUCCIÓN**
CIENTÍFICA

Anexo C
Pósters

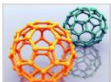


Empleo de nanopartículas de carbono para la preconcentración de medios micelares

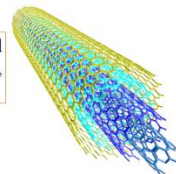
E. Caballero-Díaz, B.M. Simón, M. Valcárcel
Departamento de Química Analítica, Universidad de Córdoba, Edificio Anexo C3, Campus de Rabanales, 14071 Córdoba.
E-mail: qa1meobj@uco.es



OBJETIVO

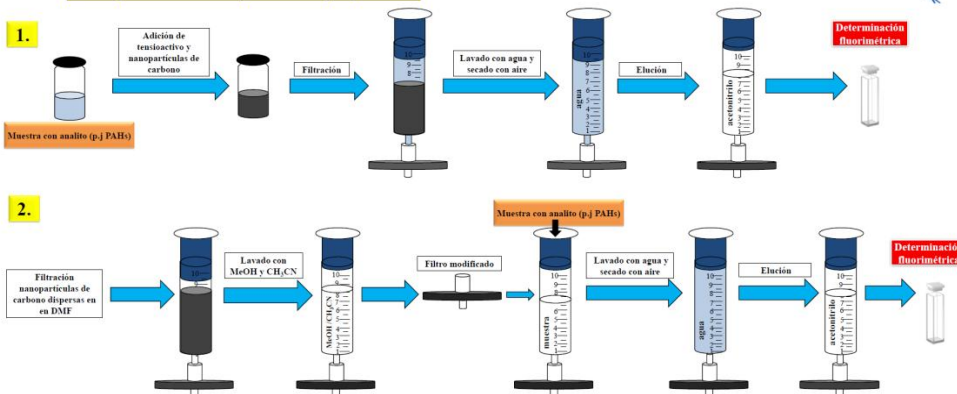


Evaluar la capacidad de diferentes nanopartículas de carbono para simplificar el proceso de extracción con medios micelares, reduciendo el tiempo de extracción, y evitando el calentamiento del sistema o la adición de sal.



SECCIÓN EXPERIMENTAL

Dos procedimientos experimentales propuestos



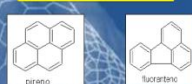
Nanopartículas estudiadas

Grafito sp^2 — Grafeno — **Nanotubos de carbono** — **Fullerenos (C60)** — **Nanodiamantes (ND)** — Diamante sp^3

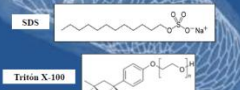
Grado de hibridación sp^2/sp^3

	MWCNTs	SWCNTs	Fullerenos	Nanodiamantes
Longitud	7 +/- 2 μ m	5-15 μ m		4-6 nm
Díametro	140 +/- 30 nm	1-2 nm	7.9 Å	
Características	CNTs de pared múltiple. Pureza >90 %.	CNTs de pared simple. Pureza >77%	Estructura polidéica de elevada estabilidad. Pureza del 99 %.	Obtenidos por proceso de detonación. Pureza del 98-99%

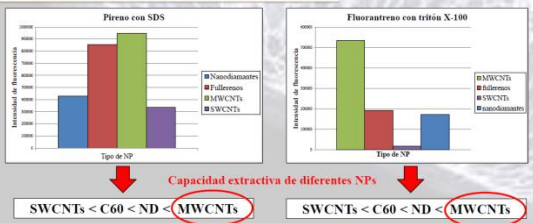
Analitos modelo



Tensioactivos evaluados



RESULTADOS Y DISCUSIÓN



• El procedimiento experimental 1 resultó más adecuado para la preconcentración de analitos que el 2 por favorecer una mayor interacción entre micelas y nanopartículas de carbono, siendo finalmente seleccionado para el estudio del comportamiento de preconcentración de diferentes nanopartículas de carbono.

• El procedimiento analítico desarrollado presenta una menor duración, complejidad y coste en comparación con otros procesos de extracción con medios micelares obteniéndose una reproducibilidad similar.

• Los MWCNTs mostraron mejor preconcentración que el resto de nanopartículas estudiadas para los dos tensioactivos empleados.

• Se ha podido demostrar como los SWCNTs presentan una interacción elevada con las micelas de tensioactivo en el caso de sodio dodecilsulfato (SDS) mientras que esa interacción es prácticamente inexistente para el caso del triton X-100.



Empleo de nanopartículas de carbono para la preconcentración de medios micelares

E. Caballero-Díaz, B.M. Simonet, M. Valcárcel

Departamento de Química Analítica, Universidad de Córdoba. Edificio Anexo C3, Campus de Rabanales, 14071 Córdoba.

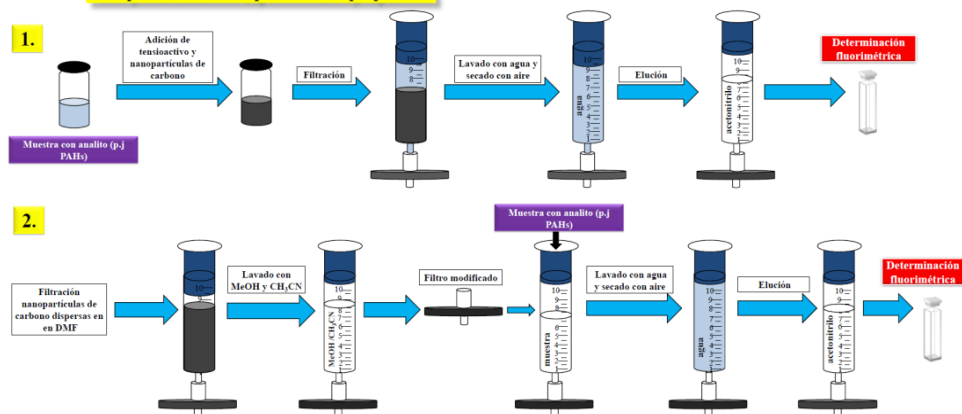
E-mail: ga1meobj@uco.es

OBJETIVO

Evaluar la capacidad de diferentes nanopartículas de carbono para simplificar el proceso de extracción con medios micelares, reduciendo el tiempo de extracción, y evitando el calentamiento del sistema o la adición de sal para la obtención de pseudofases.

SECCIÓN EXPERIMENTAL

Dos procedimientos experimentales propuestos

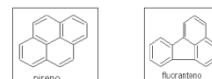


Nanopartículas estudiadas

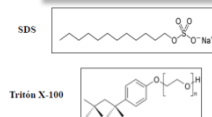


	Graphite	Nanotubos de carbono	Fullerenos (C60)	Nanodiamantes (ND)	Diamante
Grado de hibridación sp ² /sp ³	sp ²	sp ²	sp ²	sp ³	sp ³
Longitud		7 +/- 2 µm	5-15 µm		4-6 nm
Diámetro		140 +/- 30 nm	1-2 nm	7-9 Å	
Características		CNTs de pared múltiple. Pureza >90 %.	CNTs de pared simple. Pureza >77%	Estructura polidéica de elevada estabilidad. Pureza del 99 %.	Obtenidos por proceso de detonación. Pureza del 98-99%

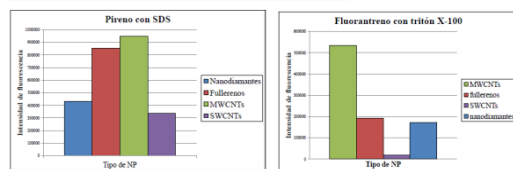
Analitos modelo



Tensioactivos evaluados



RESULTADOS Y DISCUSIÓN



Capacidad extractiva de diferentes NPs

SWCNTs < C60 < ND < MWCNTs SWCNTs < C60 < ND < MWCNTs

• El procedimiento experimental 1 resultó más adecuado para la preconcentración de analitos que el 2 por favorecer una mayor interacción entre micelas y nanopartículas de carbono, siendo finalmente seleccionado para el estudio del comportamiento de preconcentración de diferentes nanopartículas de carbono.

• El procedimiento analítico desarrollado presenta una menor duración, complejidad y coste en comparación con otros procesos de extracción con medios micelares obteniéndose una reproducibilidad similar.

• Los MWCNTs mostraron mejor preconcentración que el resto de nanopartículas estudiadas para los dos tensioactivos empleados.

• Se ha podido demostrar como los SWCNTs presentan una interacción elevada con las micelas de tensioactivo en el caso de sodio dodecilsulfato (SDS) mientras que esa interacción es prácticamente inexistente para el caso del triton X-100.



NANODIAMANTES: PROPIEDADES Y APLICACIONES

E. Caballero-Díaz, B.M. Simonet, M. Valcárcel

Departamento de Química Analítica, Universidad de Córdoba. Edificio Anexo C3, Campus de Rabanales, 14071 Córdoba.

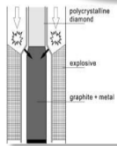
E-mail: qa1meobj@uco.es

Los nanodiamantes (NDs) son formas alotrópicas del carbono con hibridación sp^3 que se encuentran reducidas a escala nanométrica, es decir, se trata de materia particulada que como mínimo posee una dimensión menor de 100 nm.



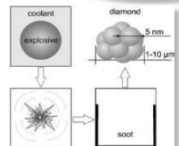
MÉTODOS DE SÍNTESIS

Descarga de ondas (Shock Waves)



Transformación de grafito a diamante en condiciones de alta presión y temperatura, generadas en una explosión.

Detonación



La fuente de carbono es el propio explosivo. La combustión es incompleta debido a la falta de oxígeno y se generan impurezas.

Otros

1. Deposición de vapor químico (CVD).
2. Molienda de microdiamantes.

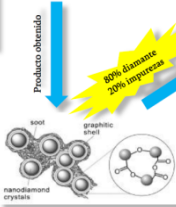
Es necesario un procedimiento de purificación...

1. Tratamiento mecánico.
2. Tratamiento con ácidos.
3. Tratamiento térmico en presencia de argón.

PROPIEDADES

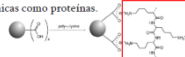
En función del método de síntesis...

Elevada dureza, alta conductividad térmica, amplia transparencia óptica, fotoestable, estabilidad química, posibilidad de funcionalización superficial, biocompatibilidad, fluorescencia intrínseca característica superior a algunos fluoróforos convencionales, y elevada capacidad de adsorción asociada a su gran área superficial específica (300-400 m^2/g).



FUNCIONALIZACIÓN (cambia las propiedades de las nanopartículas)

- COVALENTE Enlaces C-C entre NDs hidrogenados/carboxilados y compuestos orgánicos mediante reacciones fotoquímicas, electroquímicas y radicales. Unión de grupos funcionales perfluorocetilos, grupos superficiales silano, fabricación de fluoro-nanodiamantes, unión de cloruros de ácidos carboxílicos, unión de alcoholes de largas cadenas, ...
- NO COVALENTE Enlaces de H y otras interacciones polares entre NDs oxidados/carboxilados y moléculas orgánicas como proteínas.
- ADSORCIÓN Adsorción física de biomoléculas como lisozimas.



Las biomoléculas ancladas en la superficie conservan su actividad

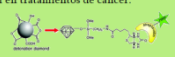
APLICACIONES Los nanodiamantes funcionalizados superficialmente se pueden emplear para ...

Aplicaciones Analíticas

- Captura y preconcentración de péptidos y proteínas (presentan una elevada afinidad por estas moléculas). Aplicable a procesos de purificación de la muestra previos al análisis.
- Mejora de la selectividad y sensibilidad en el análisis de ADN y péptidos multifosforilados (unión específica o inespecífica con proteínas o ácidos nucleicos).
- Soportes para la digestión proteolítica de proteínas ancladas sobre la superficie. Soportes para la síntesis de aminoácidos y oligopéptidos sobre la superficie.
- Preconcentración de hidrocarburos aromáticos policíclicos mediante la técnica de extracción punto de nube.
- Catalizadores heterogéneos enantioselectivos.
- Desarrollo de sensores ópticos.

Aplicaciones Médicas

- Vehículo para liberación de drogas, genes y anticuerpos en el organismo. Aplicación en tratamientos de cáncer.
- Soporte de moléculas bioactivas que interaccionan con componentes intracelulares como ADN o proteínas para su marcaje fluorescente. "Nanobiosensores"
- Sorbente para la eliminación de toxinas en el organismo.



Otras aplicaciones

- Pulido de superficie.
- Recubrimiento de superficies (proporcionan mayor dureza y tiempo de vida) en composites o de electrodos.
- Lubricante en aceites de motor.

RETOS

- Producción de muestras homogéneas de NDs con una estrecha distribución de tamaño.
- Estabilización de NDs funcionalizados en medios fisiológicos. Control de la aglomeración de estas nanopartículas en muestras. Mejoras en la funcionalización superficial de los NDs. Funcionalización 1:1
- Funcionalización superficial homogénea. Reducción de grupos carbonilos superficiales con borano
- Estudios de biocompatibilidad.

TOXICIDAD



III Encuentro NANOUCO

Extracción de atrazina en muestras medioambientales mediante films de nanopartículas de carbono situados en interfases líquido-líquido

E. Caballero-Díaz, B.M. Simonet, M. Valcárcel

Departamento de Química Analítica, Universidad de Córdoba. Edificio Anexo C3, Campus de Rabanales, 14071 Córdoba.

E-mail: qa1meobj@uco.es

ANTECEDENTES

• La atrazina 6 [2-Cloro-4-etilamino-6-isopropilamino-1,3,5-triazina] es una herbicida ampliamente usado en la agricultura que se encuentra a niveles traza contaminando el medio ambiente. Su determinación requiere un procedimiento de tratamiento de muestra debido a su baja concentración en muestras ambientales.

• Las nanopartículas de carbono han despertado un reciente interés en procesos de tratamiento de muestras debido a sus excelentes propiedades, lo que les hace ser excelentes transportadores y buenos sorbentes.

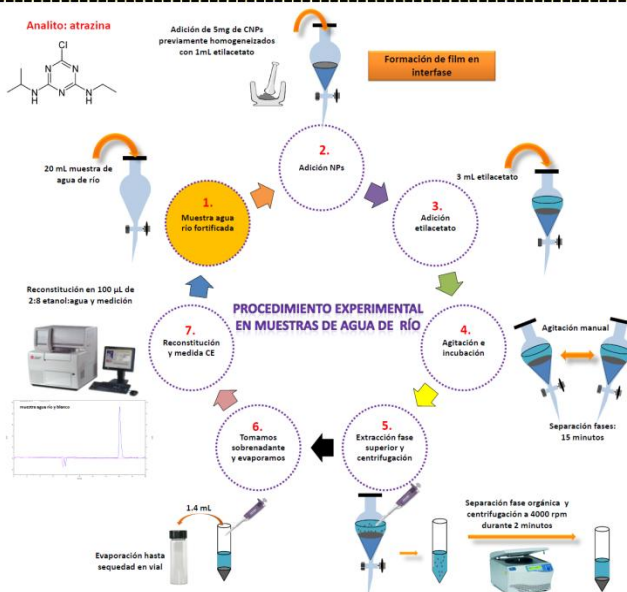
• Han sido descritos sistemas de membranas modificadas con nanotubos de carbono (CNTs) que ofrecen ventajas respecto a la técnica convencional de microextracción líquido-líquido, ya que los CNTs **aumentan el flujo de analito** de la fase donadora a la fase aceptora por un incremento en el área superficial efectiva, y actúan como **canales de transporte adicionales** de analito de una fase a otra.

• También se ha descrito que los CNTs pueden formar un film entre dos fases inmiscibles en la extracción líquido-líquido de proteínas.

OBJETIVOS

• Estudiar la extracción de atrazina a través de un film de nanopartículas de carbono (CNPs) formado en la interfase líquido-líquido. En este trabajo se presentan los resultados del análisis de muestras medioambientales.

• Comparar la efectividad de diferentes nanopartículas de carbono para formar el film y extraer atrazina de muestras reales.



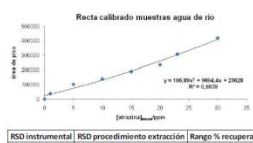
La inclusión de nanopartículas de carbono en una interfase entre la fase acuosa (donadora) y la fase orgánica (aceptora) cambia el mecanismo de transporte de atrazina de una fase a otra:

1. Canales adicionales de transporte de soluto.
2. Medio de adsorción de soluto para su después desorción en la fase aceptora.
3. Combinación de extracción en fase sólida y en fase líquida.
4. Mayor permeabilidad y mayor coeficiente de partición de soluto.

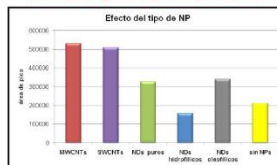
PROCEDIMIENTO EXPERIMENTAL EN SUELO



RESULTADOS Y DISCUSIÓN



Evaluación del tipo de nanopartícula para formar el film



Análisis de muestras fortificadas de suelo el cual no contenía el analito previamente



Estudio de variables para la optimización del procedimiento en agua de río



CONCLUSIONES:

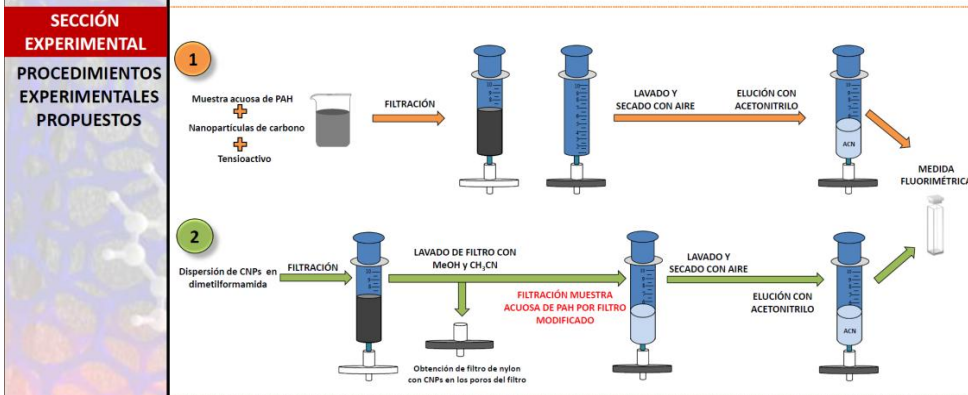
- La extracción con film de nanopartículas favorece una mayor extracción de atrazina de la matriz o fase donadora, en comparación con el estudio realizado sin nanopartículas. Este aumento de extracción se ha relacionado con el aporte de transportes adicionales que ofrecen los CNTs y que facilitan el paso de analito de una fase a otra.
- Con MWCNTs obtuvimos mejores resultados de extracción de atrazina en comparación con el resto de CNPs estudiadas. Los nanodiamantes presentaron menor capacidad de extracción de atrazina respecto a los nanotubos de carbono de pared múltiple (MWCNTs) y simple (SWCNTs) pese a tener una mayor área superficial específica.

III Encuentro **NANOUCO**

Estudio de la capacidad de nanopartículas de carbono para la preconcentración de micelas aniónicas y neutras

E. Caballero-Díaz, B.M. Simonet, M. Valcárcel
 Departamento de Química Analítica, Universidad de Córdoba. Edificio Anexo C3, Campus de Rabanales, 14071 Córdoba.
 E-mail: qa1meobj@uco.es

OBJETIVO
 Evaluar la capacidad de diferentes nanopartículas de carbono (CNPs) para simplificar el proceso de extracción con medios micelares, reduciendo el tiempo de extracción, y evitando el calentamiento del sistema o la adición de sal para la obtención de pseudofases. Esta simplificación es derivada de la elevada capacidad de las nanopartículas de quimiosorber compuestos sobre su superficie.

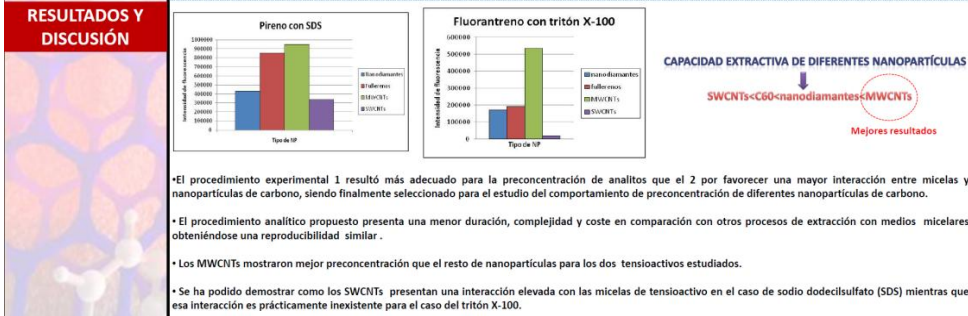


NANOPARTÍCULAS, TENSOACTIVOS Y ANALITOS

Nanopartículas estudiadas

	Grado de hibridación sp ² /sp ³			
	Grafeno	Nanotubos de carbono	Fullerenos (C60)	Nanodiamantes (ND)
Longitud	7 +/- 2 µm	5-15 µm		4-6 nm
Diámetro	140 +/- 30 nm	1-2 nm	7-9 Å	
Características	CNTs de pared múltiple. Pureza >90 %	CNTs de pared simple. Pureza >77%		Obtenidos por proceso de detonación. Pureza del 98-99%

Analitos estudiados: PIRENO, FLUORANTRENO, Tensoactivos estudiados: SDS, TRITÓN X-100



Nanotoxicity studies of four synthesized silver nanoparticles complexes for future biological applications

E. Caballero-Díaz^{a,b}, Christian Pfeiffer^b, Lena Kastl^b, Pilar Rivera Gil^b, Wolfgang J. Parak^b, Bartolome M. Simonet^a, Miguel Valcárcel^a

^aDepartment of Analytical Chemistry, Campus de Rabanales, University of Córdoba, 14071 Córdoba, Spain
^bFachbereich Physik, Philipps Universität Marburg, 35037 Marburg, Germany



INTRODUCTION

Due to their antimicrobial properties the silver nanoparticles (AgNPs) are the most widely used nanoparticles in cosmetics and as bactericides in fabrics and other consumer products. For their wide field of application, these nanoparticles require clear and full elucidations of their potential toxicity. Until now, numerous toxicity studies focusing on AgNP have been carried out on cell lines including mouse fibroblast, rat liver, human hepatocellular carcinoma and human skin carcinoma cells. All of these studies show that both concentration and surface coatings nature are key factors to determine the toxicity of these metallic nanoparticles [1,2].

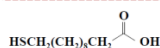
OBJECTIVE

Study the cytotoxicity of four different silver nanoparticles complexes incubated with NIH/3T3 cells for 24 hours. All the complexes were prepared from a same silver core that was modified with different superficial coatings in order to increase the stability of nanoparticles in solution and to prevent the release of harmful potentially silver ions.

EXPERIMENTAL SECTION

All of the silver nanoparticles were covered firstly with an amphiphilic polymer [poly(maleic anhydride)+alkylamine] to make them soluble in aqueous solution. Afterwards, they were modified with an additional superficial agent:

11-mercaptoundecanoic acid



Poly (ethylene glycol) (PEG-amine) (10KDa)



Finally, four silver complexes were studied:

1. AgNPs with amphiphilic polymer.
2. AgNPs with amphiphilic polymer and one superficial PEG molecule.
3. AgNPs with amphiphilic polymer and saturated with PEG.
4. AgNPs with amphiphilic polymer and 11-mercaptoundecanoic acid.

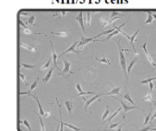
The study was completed comparing with the toxicity of silver ions (using AgNO_3 as a source).

Resazurin based cell viability assay:

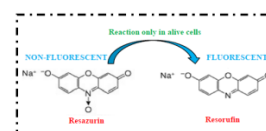
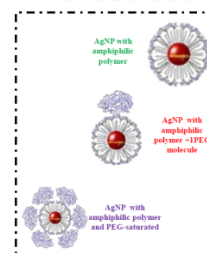
This nanotoxicological study is based in the reducing power of living cells to convert resazurin, a non-fluorescent dye and cell permeable compound, to resorufin which produces very bright fluorescent. In this way, we can evaluate quantitatively the cell viability after 24 hours of incubation with nanoparticles depending on the fluorescence observed.

We incubated the NIH/3T3 cells in a 96-wells plate with the test substances for 24 hours at different concentrations. After 24 h, the cells were washed with PBS and 100 μL of growth medium solution containing 10% resazurin were added and incubated for the next three hours. Finally, the fluorescence signal was collected at an excitation wavelength of 560 nm.

NIH/3T3 cells



MOLECULAR ASSEMBLY

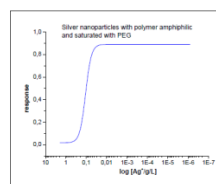


RESULTS AND CONCLUSIONS

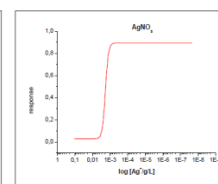
The LD 50 results showed differences in the cytotoxicity depending on the superficial coating of silver nanoparticles since the different molecular assembly on a same silver core affects to both the stability of the nanoparticles in solution and the internalization of the nanoparticles into the cells. The data are showed in the table.

Silver nanoparticles complexes	LD50 in g Ag ⁺ /L
AgNPs with amphiphilic polymer and saturated with PEG.	0.1081
AgNPs with amphiphilic polymer and 11-mercaptoundecanoic acid.	0.1015
AgNPs with amphiphilic polymer.	0.0307
AgNPs with amphiphilic polymer and one superficial PEG molecule.	0.0217
AgNO₃	0.0020

^aCC50 values calculated from the average of the results obtained in two cytotoxicity tests for each studied silver nanoparticle complex.



Example of dose-response curve obtained for silver nanoparticles with amphiphilic polymer and saturated with PEG.

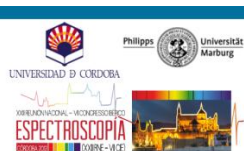


Example of dose-response curve obtained for silver nitrate.

While the silver nitrate showed the highest cytotoxicity, silver nanoparticles with amphiphilic polymer and saturated with PEG in surface showed the lowest cytotoxicity what can attribute to a reduction of the release of silver ions to the medium thanks to the protective coatings as well as a lower internalization of the nanoparticles into the cells due to their larger size.

REFERENCES:

- [1] L. Yilmirer, N.T.K. Thanh, M.Lotzidou, A.M.Sefilian, *Toxicological considerations of clinically applicable nanoparticles*, *Nano Today* (2011) 6, pp.585-607.
[2] A.J.Huh, Y.J.Kwon, "Nanomedicines": A new paradigm for treating infectious diseases using nanomaterials in the antibiotics resistant era, *Journal of Controlled Release* 156 (2011) pp. 128-145.



XXIII REUNIÓN NACIONAL DE ESPECTROSCOPIA VII CONGRESO IBERICO DE ESPECTROSCOPIA - CORDOBA 2012 - 17-20 Septiembre 2012

Nanotoxicity studies of silver nanoparticles with different superficial coatings for future biological applications

E.Caballero^a, C. Pfeiffer^a, L. Kast^b, P.Rivera^a, W. J. Parak^b, B. M. Simonet^a, M. Valcarcel^a

^aDepartment of Analytical Chemistry, Campus de Rabanales, University of Córdoba, 14071 Córdoba, Spain
^bFachbereich Physik, Philipps Universität Marburg, 35037 Marburg, Germany

INTRODUCTION

Due to their antimicrobial properties the silver nanoparticles (AgNPs) are the most widely used nanoparticles in cosmetics and as bactericides in fabrics and other consumer products. For their wide field of application, these nanoparticles require clear and full elucidations of their potential toxicity. Until now, numerous toxicity studies focusing on AgNP have been carried out on cell lines including mouse fibroblast, rat liver, human hepatocellular carcinoma and human skin carcinoma cells. All of these studies show that both concentration and surface coatings nature are key factors to determine the toxicity of these metallic nanoparticles [1,2].

OBJECTIVE

Study the cytotoxicity of four different silver nanoparticles complexes incubated with NIH/3T3 cells for 24 hours. All the complexes were prepared from a same silver core that was modified with different superficial coatings in order to increase the stability of nanoparticles in solution and to prevent the release of harmful potentially silver ions.

EXPERIMENTAL SECTION

All of the silver nanoparticles were covered firstly with an amphiphilic polymer [poly(maleic anhydride)+alkylamine] to make them soluble in aqueous solution. Afterwards, they were modified with an additional superficial agent:

11-mercaptoundecanoic acid



Poly (ethylene glycol) (PEG-amine) (10KDa)



Finally, four silver complexes were studied:

1. AgNPs with amphiphilic polymer.
2. AgNPs with amphiphilic polymer and one superficial PEG molecule.
3. AgNPs with amphiphilic polymer and saturated with PEG.
4. AgNPs with amphiphilic polymer and 11-mercaptoundecanoic acid.

The study was completed comparing with the toxicity of silver ions (using AgNO₃ as a source).

Resazurin based cell viability assay:

This nanotoxicological study is based in the reducing power of living cells to convert resazurin, a non-fluorescent dye and cell permeable compound, to resorufin which produces very bright fluorescent. In this way, we can evaluate quantitatively the cell viability after 24 hours of incubation with nanoparticles depending on the fluorescence observed.

We incubated the NIH/3T3 cells in a 96-wells plate with the test substances for 24 hours at different concentrations. After 24 h, the cells were washed with PBS and 100 µL of growth medium solution containing 10% resazurin were added and incubated for the next three hours. Finally, the fluorescence signal was collected at an excitation wavelength of 560 nm.

RESULTS AND CONCLUSIONS

The LD 50 results showed differences in the cytotoxicity depending on the superficial coating of silver nanoparticles since the different molecular assembly on a same silver core affects to both the stability of the nanoparticles in solution and the internalization of the nanoparticles into the cells. The data are showed in the table.

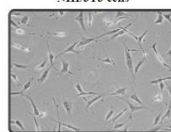
Silver nanoparticles complexes	LD50 in g Ag ⁺ /L
AgNPs with amphiphilic polymer and saturated with PEG.	0,1081
AgNPs with amphiphilic polymer and 11-mercaptoundecanoic acid.	0,1015
AgNPs with amphiphilic polymer.	0,0307
AgNPs with amphiphilic polymer and one superficial PEG molecule.	0,0217
AgNO ₃	0,0020

^aLD50 values calculated from the average of the results obtained in two cytotoxicity tests for each studied silver nanoparticles complex

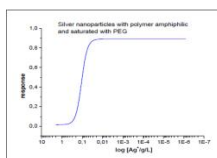
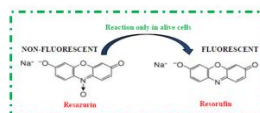
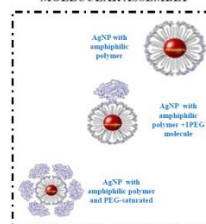
References:

- [1] L. Vidali, N.T.K. Thanh, M.L. Rodríguez, A.M. Sillido, *Toxicological considerations of clinically applicable nanoparticles*, *Nano Today* (2012) 6, pp.585-607.
- [2] A.J.Huh, Y.J.Kwon, "Nanocoatings", *A new paradigm for treating infectious diseases using nanomaterials in the antibiotics resistant era*, *Journal of Controlled Release* 156 (2011) pp. 128-145.

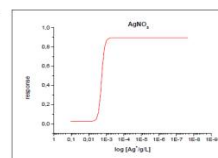
NIH/3T3 cells



MOLECULAR ASSEMBLY



Example of dose-response curve obtained for silver nanoparticles with amphiphilic polymer and saturated with PEG



Example of dose-response curve obtained for silver nitrate

While the silver nitrate showed the highest cytotoxicity, silver nanoparticles with amphiphilic polymer and saturated with PEG in surface showed the lowest cytotoxicity what can attribute to a reduction of the release of silver ions to the medium thanks to the protective coatings as well as a lower internalization of the nanoparticles into the cells due to their larger size.

IV Workshop
NANOUCO
A synergistic combination of MEPS-preconcentration and Surface Enhanced Raman Spectroscopy for the determination of musk ketone in river water
 E.Caballero-Díaz^a, B.M.Simonet^a, M.Valcárcel^a
^aDepartamento de Química Analítica, Universidad de Córdoba, Edificio Anexo C3, Campus de Rabanales, 14071 Córdoba
 Teléfono: 957 218616 E-mail: qa1mcoj@uco.es



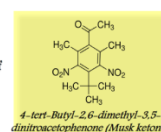
INTRODUCTION

Synthetic musk compounds are frequently used as fragrances in a wide range of pharmaceuticals and personal care products. Their development was aimed at replacing those extremely expensive natural musks, but their wide variety of applications and high production have become them in emerging contaminants that are ultimately released into the environment through discharges of domestic wastewater.

There are three different families of musks compounds, polycyclic musks, macrocyclic musks and nitro musks. Musk ketone is included in the last family and together with musk xylene are the most widely used nitro musks although with some restrictions related to their still unclear toxic effects.

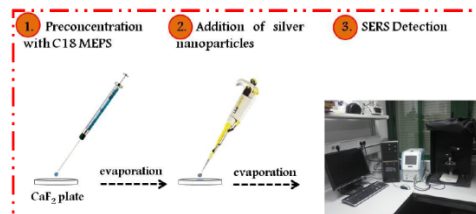
OBJECTIVE

The main objective of this work was to determine musk ketone in river water by a combined experimental procedure consisting of Microextraction by Packed Sorbents (MEPS) followed by Surface Enhanced Raman Spectroscopy (SERS) detection.

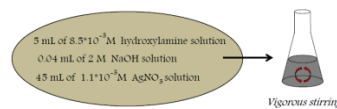


EXPERIMENTAL SECTION

1. Conditioning of C18 MEPS syringe with methanol and milli-Q water.
2. Passing a spiked water sample through the C18 MEPS cartridge
3. Passing air in order to remove water traces in the sorbent.
4. Eluting the analyte with 10 µL of methanol that are directly deposited on a CaF₂ glass.
5. Evaporating the drop of analyte and depositing 6 µL of silver nanoparticles (AgNPs) solution above it.
6. Evaporating to dryness and measuring Raman/SERS spectra.



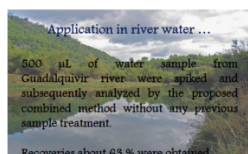
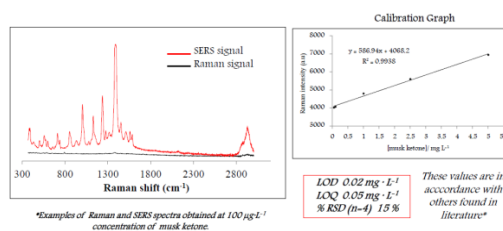
Silver nanoparticles (AgNPs) were previously synthesized according to the following procedure.



RESULTS AND DISCUSSION

Variables in SERS detection	Studied values	Optimized variable
Deposition order of analyte and AgNPs	•Analyte drop deposited on AgNPs. •AgNPs deposited on analyte drop.	AgNPs deposited on an evaporated drop of analyte
Silver nanoparticles solution volume (µL)	2, 6, 20, 40, 70	6

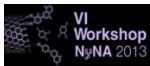
Variables in MEPS preconcentration	Studied values	Optimized variable
sample volume (µL)	50, 200, 500, 1000	500
sample pH	3, 6, 9	6
elution solvent	Methanol, acetonitrile	methanol



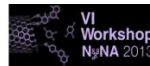
CONCLUSIONS

In this work a MEPS-SERS method has been developed to determine an emerging contaminant in river water samples. Musk ketone was selected as analyte due to its ubiquity in numerous personal care products what becomes it in a contaminant of growing interest. The developed method resulted in a low detection limit and acceptable values of relative standard deviation taking into account the values found in literature about nanoparticles modified-substrates as SERS supports for the determination of compounds. Other significant advantages are the simplicity of the experimental procedure, a reduce analysis time and the portable nature of the detection system.

^a Prochazka, M.; Simunkova, P.; Hajdinkova-Smilova, N. *Colloid Surf., A: Physicochem. Eng. Aspects* 2012, 402, 24



The toxicity of silver nanoparticles depends on their uptake by cells and thus on their surface chemistry



E.Caballero-Díaz^a, Christian Pfeiffer^b, Lena Kastl^b, Pilar Rivera Gil^b, Wolfgang J. Parak^b, Bartolome M. Simonet^a, Miguel Valcarol^a

^a Department of Analytical Chemistry, Campus de Rabanales, University of Córdoba, 14071 Córdoba, Spain
^b Fachbereich Physik, Philipps Universität Marburg, 35037 Marburg, Germany



INTRODUCTION

Due to their antimicrobial properties the silver nanoparticles (AgNPs) are the most widely used nanoparticles in cosmetics and as bactericides in fabrics and other consumer products. For their wide field of application, these nanoparticles require clear and full elucidations of their potential toxicity. Until now, numerous toxicity studies focusing on AgNP have been carried out on cell lines including mouse fibroblast, rat liver, human hepatocellular carcinoma and human skin carcinoma cells. All of these studies show that both concentration and surface coatings nature are key factors to determine the toxicity of these metallic nanoparticles [1,2].

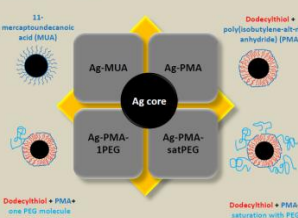
AIMS OF THE WORK

Synthesize four different silver nanoparticles prepared from a same silver core and different superficial coatings.

Assess the importance of surface chemistry of AgNPs on their cell uptake, oxidation rate and toxicity on NIH/3T3 embryonic fibroblasts.

EXPERIMENTAL SECTION

Four different AgNPs were synthesized from a same silver core but with different coating agents:



All synthesised AgNPs were subjected to different studies:

- Colloidal properties**
 - Hydrodynamic diameter
 - Zeta potential
 - Stability in solutions with increasing salt content
- Oxidation rate**
 - Release of Ag⁺ in aqueous solutions at two different pH (acidic and neutral pH)
- Uptake by cells**
 - Cell internalization of Ag-PMA and Ag-PMA-satPEG modified superficially with DY636
- Cytotoxicity test**
 - Assessment of toxicity for all AgNPs synthesized by resazurin assay using NIH/3T3 embryonic fibroblasts as cell line

RESULTS AND DISCUSSION / CONCLUSIONS

CHARACTERIZATION OF COLLOIDAL FEATURES

Hydrodynamic diameter (d_h)
 PEGylation increased the d_h of AgNPs

Zeta potential
 MUA and PMA provided negative charge to nanoparticles and consequently the stability in solution was governed by electrostatic repulsions. PEG saturation reduced the negative charge but allowed the stabilization by steric repulsions.

Stability in NaCl containing solutions
 Ag-MUA increased their d_h with the increase in NaCl content while the rest of AgNPs remained with a practically constant d_h. Therefore, Ag-PMA are much more stable in solution than Ag-MUA.

OXIDATION RATE

Under acidic conditions (simulating conditions inside endo/lysosomal compartments) the percentage of Ag⁺ released was greater than at neutral pH (around 1%).

Even after seven days in incubation, the amount of Ag⁺ released was below the limit of detection (<0.0015%).

pH=3 pH=7

Differences in the Ag⁺ release only were observed for different pH not for different types of AgNPs. These results lead us to the following conclusions. On the one hand, the release of Ag⁺ is more prominent at acidic pH what could be extrapolated to a greater ions release rate in endo/lysosomal acidic compartments than in extracellular neutral environments. On the other hand, the fact of not finding differences among different AgNPs demonstrates that modifications on surface coating do not affected to the oxidation rate of the AgNPs studied.

UPTAKE BY CELLS

The saturation of the nanoparticles surface with PEG molecules reduced significantly the cell internalization for Ag-PMA-satPEG. A greater degree of cell uptake was observed by those nanoparticles that had only a polymeric coating (Ag-PMA). Only qualitative results were obtained by this study although these clearly elucidated that the surface coating is a key factor that determines the uptake of AgNPs by 3T3 cells.

RESAZURIN CYTOTOXICITY TEST

Ag⁺ ions (AgNO₃, as source) resulted to be more toxic than all AgNPs studied. PMA coating reduced the toxicity of AgNPs in comparison to MUA coating. Among AgNPs modified with PMA, those saturated with PEG molecules (Ag-PMA-satPEG) showed the lowest toxicity. This result is in accordance with the lower cell internalization observed for these same nanoparticles.

[1] L. Yildirim, N.T.K. Thanh, M. Loizidou, A.M. Sathian, Toxicological considerations of clinically applicable nanoparticles, *Nano Today* (2011) 6, pp 585-607.
 [2] L.L. Huh, Y.L. Kwon, "Nanomedicines": A new paradigm for treating infectious diseases using nanomaterials in the antibiotic resistant era, *Journal of Controlled Release* 156 (2011) pp. 128-145.

